

**Characterization of the Two Isoforms of
*cbb*₃-Type Cytochrome *c* Oxidase
from *Pseudomonas stutzeri* ZoBell**

Dissertation
zur Erlangung des Doktorgrades
der Naturwissenschaften

vorgelegt beim Fachbereich 14
Biochemie, Chemie und Pharmazie
der Johann Wolfgang Goethe Universität
in Frankfurt am Main, Deutschland

von
Hao XIE
aus Tianjin, China

Frankfurt am Main (2014)
(D30)

vom Fachbereich Biochemie, Chemie und Pharmazie der Johann Wolfgang Goethe
Universität als Dissertation angenommen.

Dekan: Prof. Dr. Thomas Prisner

1. Gutachter: Prof. Dr. Bernd Ludwig
2. Gutachter: Prof. Dr. Hartmut Michel

Datum der Disputation:

Die Doktorarbeit wurde vom März 2010 bis zum Februar 2014 unter Leitung von Prof. Dr. Hartmut Michel in der Abteilung für Molekulare Membranbiologie am Max-Planck-Institut für Biophysik in Frankfurt am Main durchgeführt.

Eidesstattliche Erklärung

Hiermit versichere ich, dass ich die vorliegende Arbeit selbstständig angefertigt habe und keine weiteren Hilfsmittel und Quellen als die hier aufgeführten verwendet habe.

Hao XIE

Frankfurt am Main, den

Publications

H. Xie, S. Buschmann, J. D. Langer, B. Ludwig, H. Michel, Biochemical and biophysical characterization of the two isoforms of *cbb*₃-type cytochrome *c* oxidase from *Pseudomonas stutzeri*. *J Bacteriol* 196, 472 (2014).

S. Buschmann, E. Warkentin, **H. Xie**, J. D. Langer, U. Ermler, H. Michel, The structure of *cbb*₃ cytochrome oxidase provides insights into proton pumping. *Science* 329, 327 (2010).

Table of Contents

Table of Contents	i
List of Figures.....	v
List of Tables.....	vii
Zusammenfassung	ix
Summary.....	xvii
Kurzzusammenfassung.....	xxiii
Abstract.....	xxv
Abbreviations and Symbols.....	xxvii

1 Introduction 1

1.1 Oxidative phosphorylation and electron transport.....	1
1.1.1 ATP and oxidative phosphorylation	1
1.1.2 The electron transport chain.....	2
1.2 Heme-copper terminal oxidases	5
1.2.1 Classification of heme-copper terminal oxidases	5
1.2.2 Evolutionary origins of heme-copper terminal oxidases	7
1.2.3 Structure of heme-copper terminal oxidases.....	8
1.3 The <i>aa₃</i> -type cytochrome <i>c</i> oxidase.....	12
1.3.1 The catalytic reaction cycle	12
1.3.2 Electron transfer process.....	14
1.3.3 Proton pathway and proton pumping.....	15
1.4 The <i>cbb₃</i> -type cytochrome <i>c</i> oxidase	16
1.4.1 Distribution of <i>cbb₃</i> -CcOs.....	16
1.4.2 Subunit composition and structure of <i>cbb₃</i> -CcOs	17
1.4.3 Functional studies of <i>cbb₃</i> -CcOs.....	22
1.4.4 Regulation and expression of <i>cbb₃</i> -CcOs.....	24
1.4.5 Assembly of <i>cbb₃</i> -CcOs	26
1.5 <i>Pseudomonas stutzeri</i>	28
1.5.1 Respiration in <i>Pseudomonas stutzeri</i> ZoBell.....	29
1.6 Aim of this work.....	31

2 Materials and Methods 33

2.1 Materials	33
2.1.1 Chemicals.....	33
2.1.2 Bacterial strains.....	33
2.1.3 Plasmids	34
2.1.4 Microbial media and supplements	37
2.1.5 Buffers and solutions	38

2.1.6	Enzymes, proteins, markers and kits	38
2.1.7	Databases, servers and software	39
2.2	Methods	41
2.2.1	Molecular biological methods	41
2.2.2	Biochemical methods	47
2.2.3	Biophysical methods	57
3	Results.....	63
3.1	Identification of the two <i>cbb</i> ₃ -operons	63
3.2	Microbiological characterization of <i>P. stutzeri</i> ZoBell	64
3.2.1	Growth of <i>P. stutzeri</i> ZoBell	64
3.2.2	Relationship between cell number and optical density	65
3.2.3	Antibiotic resistance analysis	65
3.3	Construction of <i>ccoNO(Q)P</i> knock-out strains	66
3.3.1	Transformation of <i>P. stutzeri</i> ZoBell	66
3.3.2	Maintenance of plasmids in <i>P. stutzeri</i> ZoBell	67
3.3.3	Construction of suicide plasmids and gene deletion	68
3.3.4	Verification of deletion strains	70
3.4	Construction and purification of the tagged <i>cbb</i> ₃ -CcOs	72
3.4.1	Construction of the expression vectors	72
3.4.2	Expression screening of Strep- and His ₆ -tagged <i>cbb</i> ₃ -CcOs	73
3.4.3	Large-scale purification of Strep-tagged <i>cbb</i> ₃ -CcOs	75
3.4.4	Control of the expression of two <i>cbb</i> ₃ -isoforms	77
3.4.5	SDS-PAGE analysis of Cbb ₃ -1 and Cbb ₃ -2	79
3.4.6	Determination of the oligomeric state of Cbb ₃ -1 and Cbb ₃ -2	80
3.4.7	Subunit composition of both <i>cbb</i> ₃ -isoforms	80
3.5	Characterization of Cbb ₃ -1 and Cbb ₃ -2	83
3.5.1	UV/Vis spectra of <i>cbb</i> ₃ -CcO	83
3.5.2	Circular dichroism spectra of <i>cbb</i> ₃ -CcO	84
3.5.3	Thermal stability of <i>cbb</i> ₃ -CcO	85
3.5.4	Fourier transform infrared spectra of <i>cbb</i> ₃ -CcO	87
3.5.5	Electrochemical measurement of <i>cbb</i> ₃ -CcO	88
3.5.6	Determination of the oxygen reductase activity	89
3.5.7	Determination of the catalase activity	92
3.5.8	The redox active tyrosine residue	93
3.5.9	Variants of Glu323	95
3.6	Identification and characterization of the natural electron donor of <i>cbb</i> ₃ -CcO	96
3.6.1	Prediction of <i>c</i> -type cytochromes of <i>P. stutzeri</i>	96
3.6.2	Construction of expression vectors for cytochromes <i>c</i>	96
3.6.3	Cell growth and small-scale expression of cytochromes <i>c</i>	97
3.6.4	Purification of recombinant cytochromes <i>c</i>	99
3.6.5	UV/Vis spectra of recombinant cytochromes <i>c</i>	102
3.6.6	Electrochemical measurement of recombinant cytochromes <i>c</i>	104

3.6.7	Determination of the natural electron donor of <i>cbb</i> ₃ -CcOs	105
4	Discussion	111
4.1	The presence of the two <i>cbb</i> ₃ -CcOs in <i>P. stutzeri</i>	111
4.2	The presence of multiple <i>cbb</i> ₃ -CcOs in proteobacteria	112
4.3	Construction of a homologous expression system to produce both <i>cbb</i> ₃ -isoforms from <i>P. stutzeri</i>	113
4.3.1	Homologous vs. heterologous protein expression	113
4.3.2	Construction of the <i>cbb</i> ₃ -knockout strains	114
4.3.3	Purification of the wild-type <i>cbb</i> ₃ -CcOs	117
4.3.4	Design of expression vectors for recombinant <i>cbb</i> ₃ -CcOs	118
4.3.5	Isolation of the individual recombinant <i>cbb</i> ₃ -isoforms	119
4.4	Characterization of the two <i>cbb</i> ₃ -isoforms	120
4.4.1	Regulation of the expression of both <i>cbb</i> ₃ -isoforms	120
4.4.2	The role of the CcoQ subunit	122
4.4.3	Identification of an unknown transmembrane helix in the crystal structure of Cbb ₃ -1	122
4.4.4	Both <i>cbb</i> ₃ -isoforms share high levels of similarity	123
4.4.5	The thermal stability of both <i>cbb</i> ₃ -isoforms	124
4.4.6	Oxygen reductase activity of the two <i>cbb</i> ₃ -isoforms using an artificial electron donor	125
4.4.7	Catalase activity of the two <i>cbb</i> ₃ -isoforms	127
4.4.8	Electrochemical properties of the redox cofactors	128
4.5	The physiological electron donor for the <i>cbb</i> ₃ -CcO	129
4.5.1	The presence of <i>c</i> -type cytochromes in <i>P. stutzeri</i>	129
4.5.2	Production of the <i>P. stutzeri</i> cytochromes <i>c</i> in <i>E. coli</i>	130
4.5.3	The natural electron donor for the <i>P. stutzeri</i> <i>cbb</i> ₃ -CcOs	131
4.5.4	Substrate specificity of both <i>cbb</i> ₃ -isoforms	132
5	References	135
6	Appendix	157
	Acknowledgments	189
	Curriculum Vitae	191

List of Figures

Figure 1-1:	Schematic diagram of the electron transport chain within the mitochondrial inner membrane.	3
Figure 1-2:	Classification of the heme-copper oxidase superfamily.	5
Figure 1-3:	X-ray structures of different types of HCOs and NORs.	9
Figure 1-4:	Simplified schematic representation of the oxygen reduction reaction at the heme a_3 -Cu _B binuclear center.	13
Figure 1-5:	Crystal structure of <i>cbb</i> ₃ -CcO from <i>P. stutzeri</i> ZoBell.	18
Figure 1-6:	A close-up view of heme <i>b</i> and heme b_3 -Cu _B binuclear center.	19
Figure 1-7:	Comparison of a copper-coordinated His-Tyr cross-link between <i>cbb</i> ₃ - and <i>aa</i> ₃ -CcO.	20
Figure 1-8:	Regulation of <i>cbb</i> ₃ -gene (<i>ccoNOQP</i>) expression.	25
Figure 1-9:	Schema of the assembly process for <i>cbb</i> ₃ -CcO in <i>R. capsulatus</i>	27
Figure 1-10:	Schematic representation of the branched respiratory pathway of <i>P. stutzeri</i> ZoBell.	30
Figure 2-1:	Plasmid map of pXH22.	36
Figure 2-2:	Plasmid map of pXH39.	37
Figure 3-1:	Schematic representation of the organization of two <i>cbb</i> ₃ -operons and the <i>ccoGHIS</i> gene cluster on the <i>P. stutzeri</i> ZoBell chromosome.	63
Figure 3-2:	Growth of wild-type <i>P. stutzeri</i> ZoBell in LB and asparagine medium.	64
Figure 3-3:	Schematic representation of the construction of the suicide plasmids.	69
Figure 3-4:	Genetic maps of two <i>cbb</i> ₃ -CcO deletion strains.	70
Figure 3-5:	Qualitative PCR analysis of the deletion of <i>cbb</i> ₃ -CcO loci.	71
Figure 3-6:	A schematic summary of the constructed expression vectors for both <i>cbb</i> ₃ -CcOs.	73
Figure 3-7:	SDS-PAGE gels of the small-scale expression and purification of Strep-tagged <i>cbb</i> ₃ -CcOs.	74
Figure 3-8:	SDS-PAGE gels of the small-scale expression and purification of His ₆ -tagged Cbb ₃ -2.	75
Figure 3-9:	SDS-PAGE gels of the two-step purification of recombinant Cbb ₃ -1.	76
Figure 3-10:	Elution profiles of the purification of recombinant Cbb ₃ -1.	77
Figure 3-11:	Structure of the promoter region of the gene <i>ccoN</i>	78
Figure 3-12:	SDS-PAGE gels of both purified recombinant Cbb ₃ -1 and Cbb ₃ -2.	79
Figure 3-13:	BN-PAGE gels of purified recombinant <i>cbb</i> ₃ -isoforms.	80
Figure 3-14:	Peptide mass fingerprinting analysis of two <i>cbb</i> ₃ -isoforms (Cbb ₃ -1 and Cbb ₃ -2).	81
Figure 3-15:	The sequence coverage obtained by peptide mass fingerprinting analysis for the assembly protein CcoH.	82
Figure 3-16:	UV/Vis spectra of wild-type Cbb ₃ -1.	83
Figure 3-17:	UV/Vis spectra of both recombinant <i>cbb</i> ₃ -isoforms.	84
Figure 3-18:	Far-UV circular dichroism spectra of <i>cbb</i> ₃ -CcOs.	85
Figure 3-19:	Differential scanning calorimetry curves of <i>cbb</i> ₃ -CcOs.	86

Figure 3-20:	Oxidized-minus-reduced FTIR difference spectra of two recombinant <i>cbb</i> ₃ -isoforms from <i>P. stutzeri</i>	87
Figure 3-21:	Potentiometric titration of recombinant Cbb ₃ -1.	88
Figure 3-22:	Potentiometric titration of recombinant Cbb ₃ -2.	88
Figure 3-23:	Measurements of oxygen reductase activity of wild-type Cbb ₃ -1.	89
Figure 3-24:	Optimization of the conditions for activity assay of <i>cbb</i> ₃ -CcO.	90
Figure 3-25:	Dependence of the <i>cbb</i> ₃ -CcO activity on the concentration of TMPD.	91
Figure 3-26:	Comparison of the oxygen reductase activity between wild-type Cbb ₃ -1, recombinant Cbb ₃ -1 and Cbb ₃ -2.	92
Figure 3-27:	Comparison of the catalase activity between wild-type Cbb ₃ -1, recombinant Cbb ₃ -1 and Cbb ₃ -2.	93
Figure 3-28:	The His-Tyr cross-link in <i>cbb</i> ₃ -CcO and the location of the selected residues for site-directed mutagenesis studies.	93
Figure 3-29:	The reduced-minus-oxidized difference spectra of wild-type Cbb ₃ -1 and four variants.	94
Figure 3-30:	The active site of <i>cbb</i> ₃ -CcO of <i>P. stutzeri</i>	95
Figure 3-31:	Comparison of uninduced and IPTG-induced cells containing the expression vector with the gene encoding cytochrome <i>c</i>	97
Figure 3-32:	SDS-PAGE gels of small-scale expression of recombinant cytochromes <i>c</i>	98
Figure 3-33:	Purification of recombinant cytochrome <i>c</i> ₄	99
Figure 3-34:	Purification of recombinant cytochrome <i>c</i> ₅	100
Figure 3-35:	Purification of recombinant cytochrome <i>c</i> ₅₅₁	101
Figure 3-36:	UV/Vis spectra of recombinant cytochrome <i>c</i> ₄	102
Figure 3-37:	UV/Vis spectra of recombinant cytochrome <i>c</i> ₅	103
Figure 3-38:	UV/Vis spectra of recombinant cytochrome <i>c</i> ₅₅₁	103
Figure 3-39:	Cyclic voltammetry of three recombinant cytochromes <i>c</i>	104
Figure 3-40:	Potentiometric titration of recombinant cytochromes <i>c</i>	105
Figure 3-41:	Inhibition of the oxidase activity by KCN.	106
Figure 3-42:	Dependence of the cytochrome <i>c</i> -mediated oxygen reductase activity of <i>cbb</i> ₃ -CcO on the ionic strength.	106
Figure 3-43:	A comparison between the wild-type and the recombinant cytochrome <i>c</i> ₅₅₁	107
Figure 3-44:	Oxygen reductase activity of wild-type Cbb ₃ -1.	107
Figure 3-45:	Oxygen reductase activity of recombinant Cbb ₃ -1.	108
Figure 3-46:	Oxygen reductase activity of recombinant Cbb ₃ -2.	109
Figure 3-47:	Comparison of the oxidase activity between wild-type Cbb ₃ -1 and recombinant Cbb ₃ -1 and Cbb ₃ -2.	110
Figure 4-1:	Organization of the <i>ccoNOQP</i> genes in proteobacteria.	112
Figure 4-2:	Selection of allelic exchange mutant using one-step selection strategy based on the EGFP-based suicide plasmid.	116
Figure 4-3:	Location of the both N- and C-termini of the three subunits CcoNOP.	119
Figure 4-4:	Comparison of the electrostatic surface potentials of both <i>cbb</i> ₃ -isoforms.	133

List of Tables

Table 2-1:	List of bacterial strains.....	33
Table 2-2:	List of plasmids.....	34
Table 2-3:	Location of pXH22 features.....	36
Table 2-4:	Location of pXH39 features.....	37
Table 2-5:	List of microbial media.....	37
Table 2-6:	List of medium supplements.....	38
Table 2-7:	List of enzymes, proteins, markers and kits.....	38
Table 2-8:	List of databases and servers.....	39
Table 2-9:	List of software.....	40
Table 2-10:	List of buffers and solution for DNA electrophoresis.....	42
Table 2-11:	PCR master mix.....	43
Table 2-12:	Reaction mixture for a typical PCR amplification.....	43
Table 2-13:	PCR cycling programs.....	44
Table 2-14:	Components of 12.5% and 15% Tris-glycine gels for SDS-PAGE analysis.....	53
Table 2-15:	List of buffers and solutions for SDS-PAGE.....	54
Table 2-16:	List of buffers for BN-PAGE.....	54
Table 2-17:	List of solutions for heme staining.....	55
Table 2-18:	List of buffers and solution for Western blot.....	56
Table 2-19:	List of used extinction coefficients.....	57
Table 2-20:	List of crystallization screens.....	61
Table 3-1:	Correlation between cell number and optical density.....	65
Table 3-2:	Antibiotic sensitivities of wild-type <i>P. stutzeri</i> ZoBell.....	65
Table 3-3:	Transformation efficiency of electrocompetent cells.....	66
Table 3-4:	Maintenance of a variety of plasmids in <i>P. stutzeri</i> ZoBell.....	67
Table 3-5:	Primer pairs used to verify the deletion of <i>cbb₃-CcOs</i> loci.....	71
Table 3-6:	Summary of eight expression vectors.....	75
Table 3-7:	Purification of Strep-tagged Cbb ₃ -1.....	77
Table 3-8:	A summary of typical protein yields of <i>cbb₃-CcOs</i>	79
Table 3-9:	Thermodynamic parameters for the thermal denaturation of <i>cbb₃-CcOs</i>	86
Table 3-10:	Summary of midpoint redox potentials of heme cofactors of <i>cbb₃-CcOs</i>	89
Table 3-11:	Comparison of activities of wild type and variants.....	94
Table 3-12:	Variants of Glu323.....	95
Table 3-13:	Selected cytochromes <i>c</i> of <i>P. stutzeri</i>	96
Table 3-14:	The predicted signal peptides of 4 selected cytochromes.....	97
Table 3-15:	Summary of typical protein yields of recombinant cytochromes <i>c</i>	102
Table 3-16:	Summary of midpoint redox potentials of heme <i>c</i>	105
Table 4-1:	Summary of the midpoint redox potentials of five heme cofactors in <i>cbb₃-CcOs</i>	128

Zusammenfassung

Die Cytochrom-c-Oxidase (CcO) gehört der Superfamilie der Häm-Kupfer-Oxidase an und ist das terminale Enzym der mitochondrialen und prokaryotischen Atmungskette. Cytochrom-c-Oxidase katalysieren, in einer gekoppelten Reaktion, die exotherme Reduktion von molekularem Sauerstoff zu Wasser und den Transport von Protonen über die innere Mitochondrien- oder Zellmembran. Der durch diesen Prozess generierte elektrochemische Protonengradient wird von der F₀F₁-ATP Synthase für die Synthese von ATP aus ADP und anorganischem Phosphat verwendet.

Die Superfamilie der Häm-Kupfer-Oxidase wird auf Grund der Ergebnisse phylogenetischer Studien in drei Familien (A, B und C) unterteilt. Die A-Familie der Häm-Kupfer-Oxidase wird durch die gut charakterisierten aa₃-Typ Cytochrom-c-Oxidase repräsentiert, welche sowohl in Mitochondrien als auch in vielen Bakterienstämmen vorkommen. In der B-Familie findet sich eine Vielzahl bakterieller und archaealer terminaler Oxidase. Die cbb₃-Typ Cytochrom-c-Oxidase (cbb₃-CcO) bilden die C-Familie. Sie sind am weitesten entfernte Verwandte der Oxidase aus der mitochondrialen Atmungskette.

Die cbb₃-Oxidase kommen ausschließlich im Bakterienreich vor, wo sie weit verbreitet sind. Besonders häufig werden sie jedoch in Proteobakterien gefunden. Sie bestehen aus vier Transmembranunterheiten (CcoN, CcoO, CcoQ und CcoP), welche erstmals als Genprodukte des *ccoNOQP* (*fixNOQP*) Operons in symbiotischen stickstofffixierenden Bakterien identifiziert wurden. Cbb₃-Oxidase werden hauptsächlich bei niedrigen Sauerstoffkonzentrationen beobachtet. Aufgrund ihrer hohen Affinität für Sauerstoff haben diese Oxidase wichtige Funktionen in vielen anaeroben Prozessen, wie z.B. bei der Stickstofffixierung oder bei der anoxygenen Photosynthese. Als einzige terminale Oxidase einiger krankheitserregenden Bakterienstämme, wie z.B. *Helicobacter pylori* und *Neisseria meningitidis*, kommt der cbb₃-Oxidase eine essentielle Bedeutung für die Kolonisierung von sauerstoffarmen Geweben zu. Sie repräsentiert daher möglicherweise einen spezifischen Faktor für die bakterielle Pathogenität.

Der Schwerpunkt dieser Arbeit liegt auf der Untersuchung der cbb₃-CcO aus *Pseudomonas stutzeri* ZoBell, einem nicht-fluoreszierenden stickstofffixierenden Bakterium, welches sowohl in wässrigen als auch ländlichen Habitaten weit verbreitet ist. Entgegen früheren Analysen wurde in dieser Arbeit gezeigt, dass dieser Stamm zwei cbb₃-Operons (*ccoNOP-1* und *ccoNOQP-2*) besitzt. Das Cbb₃-1 Wildtypenzym konnte aus nativen Membranen aufgereinigt und seine Struktur mit

einer Auflösung von 3,2 Å gelöst werden. Die Struktur zeigt, dass die katalytische Untereinheit der *cbb*₃-CcO Ähnlichkeiten zur denen der A- und B-Familien aufweist. Signifikante Unterschiede wurden in Bezug auf Elektronentransfer und Protonentranslokation gefunden. *Cbb*₃-Oxidasen wurden bereits in vielen gram-negativen Bakterien untersucht, jedoch wurde bisher wenig Augenmerk auf die isoformspezifischen Unterschiede gerichtet. In dieser Arbeit wurde deshalb solchen isoformspezifischen Unterschieden am Beispiel der *cbb*₃-Oxidasen aus *P. stutzeri* besondere Beachtung geschenkt: (i) ein homologes Expressionssystem für die zwei *cbb*₃-Isoformen von *P. stutzeri* wurde etabliert; (ii) beide Isoformen wurden biochemisch und biophysikalisch charakterisiert; (iii) die natürlichen Elektronendonoren der beiden *cbb*₃-Isoformen wurden ermittelt.

(i) Etablierung eines homologen Expressionssystems zur separaten Isolierung beider *cbb*₃-Isoformen von *P. stutzeri* ZoBell.

Das Genom von *P. stutzeri* ZoBell war zu Beginn dieser Arbeit nicht sequenziert. Zur Bestimmung der eigentlichen Nukleotidsequenz des *cbb*₃-Operons wurde deshalb eine Serie von *Primern* entworfen. Die Sequenz der *Primer* entsprach hoch konservierten Regionen anderer verwandter *Pseudomonas*-Stämme, deren Genomsequenz bekannt war. Die Ergebnisse zeigten, dass *P. stutzeri* ZoBell zwei unabhängige *cbb*₃-Operons besitzt, die im Genom in einer Tandem-Anordnung vorliegen. Beide *cbb*₃-Operons beinhalten die drei strukturellen Gene für die Untereinheiten CcoN, CcoO und CcoP; zusätzlich besitzt das zweite *cbb*₃-Operon das Gen *ccoQ*. Die Sequenz-Identitäten der zwei *cbb*₃-Isoformen sind mit 87% für die Untereinheit CcoN, 97% für Untereinheit CcoO und 63% für Untereinheit CcoP sehr hoch. Aufgrund der hohen Sequenzhomologie zwischen *Cbb*₃-1 und *Cbb*₃-2 liegen beide Isoformen während des chromatographischen Aufreinigungsprozesses für gewöhnlich als Mischung vor. Mithilfe von vier chromatographischen Aufreinigungsschritten gelang es jedoch, die native *Cbb*₃-1 aus Membranen von *P. stutzeri* homogen zu isolieren. Die homogene Aufreinigung der nativen Isoform *Cbb*₃-2 gelang bis zum jetzigen Zeitpunkt nicht.

Zum detaillierten Studium und zum Vergleich der beiden *cbb*₃-Isoformen von *P. stutzeri* wurde in dieser Arbeit ein homologes Expressionssystem entwickelt. Ein homologes Expressionssystem ist aufgrund des Vorhandenseins von verschiedenen Proteinen welche, u.a. in den Assemblierungsprozess der *cbb*₃-CcO involviert sind, von großem Vorteil. Die Etablierung eines solchen Systems stellte aufgrund des Mangels an physiologischem und mikrobiologischem Wissen über *P. stutzeri* ZoBell und des Fehlens geeigneter Mittel zur genetischen Manipulation ein sehr herausforderndes Projekt dar. Trotz dieser Schwierigkeiten gelang es, mittels homologer Rekombination und der Verwendung eines neuen „Suicide-Plasmids“, zwei Deletionsstämme zu

kreieren (ΔCbb_3-1 and ΔCbb_3-2). Eine spezifische Besonderheit des „Suicide-Plasmids“ war dabei die Einbringung eines grün-fluoreszierenden Proteins als zusätzlichen Selektionsmarker, wodurch der Auswahlprozess deutlich vereinfacht wurde. Für die rekombinante Expression wurde eine Serie von pBBR-basierenden Expressionsvektoren konstruiert und getestet. Diese Vektoren unterschieden sich hinsichtlich der Platzierung des Affinitätsanhängsels, der regulatorischen Elemente und der kodierten Isoformen. Da eine voneinander unabhängige Expression der beiden Isoformen nicht möglich war, wurde jede der beiden rekombinanten *cbb*₃-Isoformen im entsprechenden Deletionsstamm exprimiert, so dass sich jeweils ein *cbb*₃-Operon im Genom und eines auf dem Plasmid befanden. Die Isolierung der jeweiligen *cbb*₃-Isoformen wurde mittels Affinitätschromatographie erreicht. Eine homogene Aufreinigung konnte mit Hilfe dreier aufeinanderfolgenden chromatographischen Schritten erreicht werden. Mittels Promotoraustausch gelang es, das Expressionsniveau der *Cbb*₃-2-Isoform zu erhöhen. Für gewöhnlich lag die Ausbeute von beiden rekombinant aufgereinigten *cbb*₃-Isoformen bei 2-4 mg pro Liter Kulturmedium. Die Identität beider *cbb*₃-Isoformen wurde mittels Peptidmassenfingerprint von Trypsin/Chymotrypsin-verdauten Proben bestätigt. Des Weiteren konnte durch die massenspektrometrischen Messungen das Vorliegen von chimären *cbb*₃-CcO-Formen ausgeschlossen werden.

(ii) Charakterisierung beider *cbb*₃-isoformen.

Die Ergebnisse dieser Arbeit zeigen, dass beide *cbb*₃-Isoformen ein hohes Maß an biochemischen und biophysikalischen Gemeinsamkeiten aufweisen.

Der oligomere Zustand der beiden aufgereinigten rekombinanten *cbb*₃-Isoformen wurde mittels „Blauer Nativer Polyacrylamid-Gelelektrophorese“ ermittelt. Beide Isoformen treten als einzelne Banden bei einem Molekulargewicht von 165 kDa auf, was darauf hinweist, dass beide *cbb*₃-Isoformen als Monomere vorliegen. UV/Vis Spektroskopie wurde verwendet, um die Kofaktoren der *cbb*₃-Oxidase zu untersuchen. Die Differenzspektren beider Isoformen stimmen mit dem Spektren der Wildtyp-*Cbb*₃-1 überein, woraus auf eine korrekte Assemblierung der Häm- und Metallzentren geschlossen werden kann. Die Sekundärstrukturen beider *cbb*₃-Isoformen wurde mittels Circular dichroismus-Spektroskopie (CD) verglichen. Beide *cbb*₃-Isoformen zeigen identische CD-Spektren. Zusätzlich wurde Fourier-Transform-Infrarotspektroskopie (FTIR) verwendet, um die rekombinanten *cbb*₃-Oxidasen zu charakterisieren. Auch hier weisen beide Isoformen ähnliche spektroskopische Charakteristika auf.

Die Sauerstoffreduktase-Aktivität beider *cbb*₃-Isoformen wurde polarographisch mittels einer Clark-Typ Sauerstoffelektrode und eines artifiziellen Elektronendonorsystems (Na-Ascorbat und

N,N,N',N'-Tetramethyl-*p*-phenylendiamin [TMPD]) gemessen. Nach Optimierung der Bedingungen für den pH-Wert, die Ionenstärke und das molare Verhältnis von Na-Ascorbat zu TMPD konnten für die aufgereinigten rekombinanten Proteine Cbb₃-1 und Cbb₃-2 Sauerstoffreduktase-Aktivitäten gemessen werden, welche ähnlich wie die des Wildtyp-Cbb₃-1 sind. Dadurch wurde nachgewiesen, dass beide rekombinanten Enzyme vollständig aktiv sind. Des Weiteren konnte eine nichtlineare Abhängigkeit der *cbb*₃-CcO Enzymaktivität von der Konzentration von TMPD beobachtet werden. Die Raten der Sauerstoffreduktion folgen einer Michaelis-Menten-Kinetik mit einem V_{\max} -Wert von ca. 4000 e⁻/s und einem K_m von 3.6 mM. Beide Werte wurden bei nicht eindeutiger Sättigung ermittelt und sind ungewöhnlich hoch. Möglicherweise geben sie nicht die tatsächlichen kinetischen Parameter wieder. Nichtsdestotrotz kann mit Sicherheit gesagt werden, dass die *cbb*₃-Oxidasen aus *P. stutzeri* die Reduktion von Sauerstoff mit mindestens 2000 e⁻/s katalysieren können. Dies ist die höchste Aktivität, die jemals für eine *cbb*₃-CcO gemessen wurde. Eine solch hohe Aktivität ist vermutlich auf die drei *c*-Typ Häme in den Untereinheiten CcoO und CcoP zurückzuführen, welche mehrere Eintrittsstellen für Elektronen bieten und gleichzeitig mit TMPD reagieren könnten. Möglicherweise ist unter den gegebenen Bedingungen auch der Elektronentransfer in der *cbb*₃-CcO effizienter als in der *aa*₃-CcO. Zusätzlich zur Sauerstoffreduktase-Aktivität wurde die Aktivität der Katalase-Nebenreaktion gemessen. Es konnten keine signifikanten Unterschiede in der Katalase-Aktivität zwischen der Wildtyp-Cbb₃-1 und den rekombinanten Proteinen Cbb₃-1 und Cbb₃-2 nachgewiesen werden. Die Katalase-Aktivität der *cbb*₃-CcO ist ähnlich wie die der Wildtyp-*aa*₃-CcO aus *Paracoccus denitrificans*.

UV/Vis-Redox titrationen wurden durchgeführt, um das Redoxpotential der Häm-Kofaktoren in den beiden *cbb*₃-Isoformen zu ermitteln und so zu einem besseren Verständnis des Elektronentransfers in der *cbb*₃-CcO beizutragen. Da jedoch die Redoxpotentiale der *c*-Typ Häme zu dicht beieinander liegen, um sie unterscheiden zu können, konnte nur ein Wert für beide *cbb*₃-Isoformen ermittelt werden (155 mV for Cbb₃-1 und 185 mV für Cbb₃-2). Diese Ergebnisse lassen darauf schließen, dass die drei *c*-Typ Häme durch His/Met-Ligandenpaare axial koordiniert werden. Das höchste Redoxpotential wurde für das *low-spin* Häm *b* (+262 mV für Cbb₃-1 und +278 mV für Cbb₃-2) ermittelt. Das *high-spin* Häm *b*₃ besitzt ein niedriges Potential (+132 mV für Cbb₃-1 und +158 mV für Cbb₃-2).

Ungeachtet der hohen Ähnlichkeit zwischen den beiden *cbb*₃-Isoformen wurden auch einige signifikante Unterschiede beobachtet. Die DNA-Sequenzanalysen zeigten, dass die Promotoren der beiden *cbb*₃-Operons verschiedene regulatorische Elemente enthalten. Eine ANR (Arginin-Nitrate-Regulation)-Bindungsstelle ist nur im Promotor des Operons *ccoNOP-1*

vorhanden. Unter mikroaeroben Wachstumsbedingungen, war die Ausbeute an Cbb₃-1, welche unter Kontrolle des ANR-abhängigen Promotors exprimiert wurde, um das 6-8 fache höher als die von Cbb₃-2. Diese Ergebnisse weisen darauf hin, dass beide *cbb*₃-Isoformen verschiedene energetische und regulatorische Funktionen haben. Ein weiterer Unterschied besteht in der Untereinhenzuzusammensetzung der beiden *cbb*₃-Isoformen hinsichtlich der An-/Abwesenheit der CcoQ-Untereinheit. Eine massenspektrometrische Analyse zeigte, dass CcoQ eine Untereinheit der Cbb₃-2 ist. Die Abwesenheit von CcoQ in Cbb₃-1 ist möglicherweise dadurch bedingt, dass Cbb₃-1 hauptsächlich bei niedrigen Sauerstoffkonzentrationen exprimiert wird, wenn ein Schutz der CcoP-Untereinheit gegen proteolytischen Abbau unter aeroben Bedingungen nicht notwendig ist. Ein deutlicher Unterschied zwischen beiden *cbb*₃-Isoformen liegt in ihrer thermischen Stabilität. Die Ergebnisse der dynamischen Differenzkalorimetrie (DSC) zeigen, dass Cbb₃-1 stabiler ist als Cbb₃-2. Die gesamte kalorimetrische Enthalpieänderung der rekombinanten Cbb₃-1 (2,016 kJ mol⁻¹) ist höher als die der Cbb₃-2 (1.556 kJ mol⁻¹). Des Weiteren denaturiert Cbb₃-2 im Vergleich zur rekombinanten Cbb₃-1 10°C früher.

Mutagenese-Studien wurden durchgeführt, um die funktionelle Bedeutung zweier hoch konservierter Aminosäuren in der Nähe des aktiven Zentrums zu untersuchen: Y251 und E323. Es ist bekannt, dass das redoxaktive Tyrosin kovalent mit einem der drei Histidin-Liganden des Cu_B verbunden ist. Es wurde bereits früher nachgewiesen, dass dieses Tyrosin eine wichtige Rolle für die katalytische Aktivität der Häm-Kupfer-Oxidasen spielt. Im Vergleich zu den A- und B-Typ-Oxidasen liegt dieses kritische Tyrosin (Y251) in den *cbb*₃-Oxidasen auf einer anderen Transmembranhelix. Die Varianten Y251F und Y251A wurden erstellt, um die enzymatische Bildung eines Tyrosinradikals zu verhindern. Die Doppel-Varianten Y251A/I252Y und Y251A/G211Y wurden konstruiert, um zu testen, ob es möglich ist die His-Tyr Verbindung an einer alternativen Stelle wiederherzustellen. Alle vier Varianten hatten ihre Sauerstoffreduktase-Aktivität verloren. Die Aminosäure E323 ist durch Wasserstoffbrückenbindung mit den Histidin-Liganden des Häm *b*₃ verknüpft. Es wurde nachgewiesen, dass die enzymatische Aktivität komplett aufgehoben wird, wenn E323 durch ein Alanin (E323A) oder ein Glutamin (E323Q) ersetzt wird. Die Variante E323D weist noch ca. 40% der Wildtyp-*cbb*₃-CcO Aktivität auf.

(iii) Identifizierung und Charakterisierung der natürlichen Elektronendonoren von *P. stutzeri cbb*₃-CcO .

Um die physiologische Bedeutung und die Unterschiede beider *cbb*₃-Isoformen zu verstehen, bedarf es der Identifizierung ihrer endogenen Elektronendonoren, die bis jetzt bei *P. stutzeri* unbekannt waren. Die Suche nach einem Häm-C Bindungsmotiv im Genom und Homologieanalysen ergaben das Vorkommen von 16 potenziellen Cytochrom-c-Proteinen. Vier

dieser Proteine (Cytochrom c_4 , c_5 , c_{551} , und c_{552}) wurden als angemessene Kandidaten angesehen, da sie in aerob wachsenden Zellen nachgewiesen und isoliert werden konnten. Die Gene der Cytochrome wurden aus dem Genom von *P. stutzeri* kloniert und heterolog in *Escherichia coli* exprimiert. Die Cytochrome c_4 , c_5 und c_{551} konnten in relativ großen Mengen exprimiert und in drei Aufreinigungsschritten bis zur Homogenität gereinigt werden. Anhand von UV/Vis-Spektroskopie und elektrochemischen Messungen wurde nachgewiesen, dass diese drei rekombinanten Proteine identische spektroskopische und elektrochemische Eigenschaften aufweisen wie die nativen Proteine.

Die drei rekombinanten Cytochrome c_4 , c_5 und c_{551} wurden auf ihre Eignung als natürliche Elektronendonoren der cbb_3 -Isoformen untersucht. Die Cytochrom-c abhängige Oxidaseaktivität wurde polarographisch in der Anwesenheit von reduziertem Cytochrom-c und Na-Ascorbat gemessen. Die Ergebnisse sind die folgenden: (i) Der Elektronentransfer von Cytochrom-c auf cbb_3 -CcO ist ionenstärkeabhängig. (ii) Alle drei Cytochrome dienen beiden cbb_3 -Isoformen als Elektronendonator, jedoch mit unterschiedlich hoher Effizienz. Die höchste Sauerstoffreduktase-Aktivität wurde mit 100 μ M reduziertem Cytochrom c_4 beobachtet (z.B. ca. 500 e^-/s für Wildtyp-Cbb₃-1). Die Umsatzraten von reduziertem c_{551} waren ähnlich hoch wie die von Cytochrom c_4 (80 bis 90%), wohingegen die Umsatzraten mit c_5 um ungefähr 80% reduziert waren. Diese Ergebnisse zeigen, dass die beiden Cytochrome c_4 und c_{551} als effiziente endogene Substrate für die cbb_3 -Oxidasen von *P. stutzeri* dienen, während Cytochrom c_5 ein schwacher Elektronendonator ist. Elektrochemische Messungen weisen darauf hin, dass die relativ hohen Reaktionsraten, welche mit Cytochrom c_4 and c_{551} beobachtet wurden, darauf zurückzuführen sind, dass beide Cytochrome mindestens ein *low-spin* Häm C enthalten. Im Vergleich dazu hat Cytochrom c_5 ein hohes Redoxpotential, welches möglicherweise einen Elektronentransfer zur cbb_3 -CcO verhindert. (iii) Eine Anpassung der Daten zeigte eine unerwartete lineare Abhängigkeit der Oxidase-Aktivität von der Konzentration der reduzierten *c*-Typ-Cytochrome (20 bis 100 mM). Aufgrund der fehlenden Sättigung konnten die tatsächlichen kinetischen Parameter nicht bestimmt werden. (iv) Messungen mit zwei verschiedenen eukaryotischen Cytochrome-c-Proteinen aus Hefe und aus Pferdeherz ergaben, dass beide Proteine keine effizienten Elektronendonoren für die zwei *P. stutzeri* cbb_3 -Oxidasen darstellen.

Zusätzlich zu den beobachteten Unterschieden in den Umsatzraten mit drei endogenen Cytochrome-c-Proteinen, wurden weitere signifikante Unterschiede zwischen beiden cbb_3 -Isoformen gefunden. Die katalytischen Aktivitäten, welche für die Cbb₃-2 gemessen wurden, sind im Vergleich zu Cbb₃-1 um 70% reduziert. Ein Modell der Cbb₃-2, welches unter Einbeziehung von Aminosäuresequenz und Oberflächenladung und Röntgenstruktur der Cbb₃-1

erstellt wurde, lässt potentielle Strukturveränderungen und Oberflächenladungsunterschiede im Vergleich zu Cbb₃-1 erkennen. Diese könnten die Grundlage für die verschiedenen Substratspezifitäten der beiden *cbb*₃-Isoformen bilden.

In dieser Arbeit wurden zum ersten Mal eine umfassende Charakterisierung und ein Vergleich der beiden *cbb*₃-Isoformen von *P. stutzeri* ZoBell vorgenommen. Die gereinigten *cbb*₃-Isoformen weisen ein hohes Maß an Gemeinsamkeiten in Bezug auf ihre biochemischen und biophysikalischen Eigenschaften auf. Unterschiede wurden bezüglich ihrer Untereinheitenzusammensetzung, der thermalen Stabilität, der Substratspezifität und der Expressionsregulierung beider *cbb*₃-Oxidase festgestellt. Diese Arbeit bietet sehr gute Perspektiven für weiterführende funktionelle und strukturelle Untersuchungen der beiden *cbb*₃-CcO Isoformen.

Summary

Heme-copper oxidases (HCOs) are the terminal enzymes of the aerobic respiratory chain in the inner mitochondrial membrane or the plasma membrane in many prokaryotes. These multi-subunit membrane protein complexes catalyze the reduction of oxygen to water, coupling this exothermic reaction to the establishment of an electrochemical proton gradient across the membrane in which they are embedded. The energy stored in the electrochemical proton gradient is used e.g. by the F_0F_1 -ATP synthase to generate ATP from ADP and inorganic phosphate.

The superfamily of HCOs is phylogenetically classified into three major families: A, B and C. The A-family HCOs, represented by the well-studied aa_3 -type cytochrome *c* oxidases (aa_3 -CcOs), are found in mitochondria and many bacteria. The B-family of HCOs contains a number of bacterial and archaeal oxidases. The C-family comprises only the cbb_3 -type cytochrome *c* oxidase (cbb_3 -CcO) and is most distantly related to the mitochondrial respiratory oxidases.

The cbb_3 -CcOs are widely distributed within the bacterial phyla but particularly abundant in proteobacteria. They are composed of four transmembrane subunits (CcoN, CcoO, CcoQ and CcoP), which were first identified as gene products of a *ccoNOQP* (*fixNOQP*) operon in the symbiotic diazotrophs. The cbb_3 -CcOs are predominantly observed under low oxygen tension and are characterized by a high apparent affinity for oxygen. As a consequence, they play an important role in the proper functioning of many anaerobic biological processes, e.g., nitrogen fixation or anoxygenic photosynthesis. In some pathogenic bacteria, e.g., *Helicobacter pylori* and *Neisseria meningitidis*, cbb_3 -CcO is the sole respiratory enzyme. This finding indicates that cbb_3 -CcO is essential for the colonization of host tissues and plays a specific role for bacterial pathogenicity.

In this work, we focus on the cbb_3 -CcOs of *Pseudomonas stutzeri* ZoBell, a non-fluorescent denitrifying bacterium widely distributed in aquatic and terrestrial habitats. It had previously been reported that this bacterium possesses only one *ccoNOQP* operon coding for cbb_3 -CcO. However, we showed that this strain actually possesses two cbb_3 -operons (*ccoNOP-1* and *ccoNOQP-2*), encoding isoforms of cbb_3 -CcO (Cbb₃-1 and Cbb₃-2). In 2010, the structure of wild-type Cbb₃-1 purified from the native membranes was solved in our laboratory at a resolution of 3.2 Å. It revealed that, although the catalytic subunit of cbb_3 -CcOs shares similar features to the A- and B-family HCOs, significant differences considering electron transfer and proton translocation processes exist between the HCO superfamilies. The characteristic features of cbb_3 -CcOs have been studied in several Gram-negative bacteria; however, less emphasis has been placed on the

isoform-specific differences. Therefore, the study in hand focuses on a detailed examination of isoform-specific properties of *cbb*₃-CcOs and pursues three major objectives: (i) to establish a homologous expression system for the two *P. stutzeri* *cbb*₃-isoforms; (ii) to characterize both isoenzymes by biochemical and biophysical analyses; (iii) to investigate the natural electron donor(s) of the two *cbb*₃-isoforms.

(i) Construction of a homologous expression system for the separate isolation of both *cbb*₃-isoforms from *P. stutzeri* ZoBell.

At the beginning of this work, no genome sequence data were available for *P. stutzeri* ZoBell. To determine the authentic nucleotide sequences of the *cbb*₃-operon, a series of primers was designed, which was based on the highly conserved regions identified by comparison of the published genome sequences from several related *Pseudomonas* species. The sequence data showed that *P. stutzeri* ZoBell possess two independent *cbb*₃-operons, and the two *cbb*₃-operons are tandemly arranged in a 7-kb segment of the genome. Both *cbb*₃-operons contain the three structural genes for the subunits CcoN, CcoO and CcoP, whereas the gene *ccoQ* is only present in the second *cbb*₃-operon. The amino acid sequence identities of the two *cbb*₃-isoforms are very high and amount to 87% for subunit CcoN, 97% for subunit CcoO and 63% for subunit CcoP. Due to the high homology between Cbb₃-1 and Cbb₃-2, both wild-type isoforms are usually found as a mixture in the same chromatographic fractions during the purification process. Although the wild-type Cbb₃-1 has been successfully purified to homogeneity from the native membranes of *P. stutzeri* by four chromatographic steps, the isolation of Cbb₃-2 from the protein mixture was not achieved.

To enable a detailed investigation and comparison of the two *cbb*₃-isoforms from *P. stutzeri*, a homologous expression system was developed in this work. A homologous expression would be preferable due to the availability of various proteins involved in the maturation and assembly of a fully functional *cbb*₃-CcO. However, the construction of such a system is quite challenging due to the lack of basic physiological and microbiological knowledge of *P. stutzeri* ZoBell and to the scarcity of appropriate tools for the genetic manipulation. Despite the difficulties, two deletion strains (Δ Cbb₃-1 and Δ Cbb₃-2) were constructed by double homologous recombination using a newly developed suicide plasmid. One unique feature of this suicide plasmid is the application of the enhanced green fluorescent protein as a second selection marker, which greatly simplifies the screening procedures. For recombinant expression, a series of pBBR-based expression vectors was constructed and tested. These vectors differ from each other in terms of location and type of tags, regulatory elements and isoforms. As the expression of the *cbb*₃-isoforms was found to be interdependent, the presence of both *cbb*₃-operons in the strain was necessary. Therefore, the

respective recombinant isoform was expressed from the corresponding *P. stutzeri* deletion strain, which contained one *cbb₃*-operon in the genome and the previously deleted operon on an expression vector with an additional affinity tag. Isolation of the individual *cbb₃*-isoforms was achieved by affinity chromatography, and both isoenzymes were purified to homogeneity by three chromatographic steps. Promoter replacement was used to increase the expression level of Cbb₃-2, and a typical yield of both purified recombinant *cbb₃*-isoforms was 2 to 4 mg per liter of culture medium. The identity of both *cbb₃*-isoforms was confirmed by peptide mass fingerprinting (PMF) of trypsin/chymotrypsin-digested *cbb₃*-CcO samples, using a combination of nLC-ESI- and nLC-MALDI-TOF mass spectrometry (MS). In addition, the MS data excluded the formation of a chimeric form of the *cbb₃*-CcO.

(ii) Characterization of the two *cbb₃*-isoforms.

The results obtained in this work show that the two *cbb₃*-isoforms share a very high degree of similarity in their biochemical and biophysical properties.

The oligomeric state of the two purified recombinant *cbb₃*-isoforms was evaluated by blue native polyacrylamide gel electrophoresis (BN-PAGE). Both isoforms appeared as a single band with an apparent size of 165 kDa, which suggested that the two *cbb₃*-isoforms are monomeric. Ultraviolet/visible (UV/Vis) spectroscopy was used to study the cofactors of *cbb₃*-CcOs. The oxidized, reduced and reduced-minus-oxidized difference spectra of both recombinant *cbb₃*-isoforms are well consistent with the results observed with the wild-type Cbb₃-1, which indicated a proper assembly of heme and metal centers. A comparison of the secondary structural content of the two *cbb₃*-isoforms was carried out by using circular dichroism (CD) spectroscopy, and identical CD spectra were obtained for both *cbb₃*-isoforms. Additionally, Fourier transform infrared (FTIR) spectroscopy was applied to characterize the recombinant *cbb₃*-CcOs. Both isoforms showed similar spectroscopic characteristics.

The oxygen reductase activity of both *cbb₃*-isoforms was measured polarographically with a Clark-type oxygen electrode and an artificial electron-donating system (ascorbate and *N,N,N',N'*-tetramethyl-*p*-phenylenediamine [TMPD]). Under conditions optimized for pH, ionic strength, and the molar ratio of ascorbate to TMPD, it was found that the purified recombinant Cbb₃-1 and Cbb₃-2 catalyze the reduction of oxygen at a rate comparable to the wild-type Cbb₃-1, which indicated that the recombinant proteins produced in this work are fully active. Moreover, a non-linear dependence of enzyme activity of *cbb₃*-CcO as a function of the concentration of TMPD was observed. The rates of oxygen reduction followed Michaelis-Menten kinetics with a V_{\max} value of about 4000 e⁻/s and a K_m of 3.6 mM. Both values, obtained in the absence of

well-defined saturation, are unusually high and may not represent true kinetic parameters. Nevertheless, it could be safely concluded that the *P. stutzeri* *cbb*₃-CcO can catalyze the reduction of oxygen at a rate of at least 2000 e⁻/s. To date, this is the highest activity reported for a *cbb*₃-CcO. Such a high activity may reflect that the three *c*-type hemes in the subunit CcoO and CcoP provide multiple electron entry sites and can react with TMPD. It also suggests that electron transfer in the *cbb*₃-CcO is more efficient than that in *aa*₃-CcO under these *in vitro* assay conditions. In addition to the oxygen reductase activity, the catalase side reaction of *cbb*₃-CcOs was measured. This assay shows no significant difference in catalase activity, neither between wild-type and recombinant proteins nor between Cbb₃-1 and Cbb₃-2. Furthermore, the observed catalase activity of *cbb*₃-CcO is comparable to that of the wild-type *aa*₃-CcO from *Paracoccus denitrificans*.

To contribute to a better understanding of the electron transfer processes in *cbb*₃-CcO, UV/Vis redox titrations were carried out to determine the midpoint redox potentials of heme cofactors in the two *cbb*₃-isoforms. For the three *c*-type hemes, the redox potentials are too close to be distinguished, therefore, only one value can be determined for each *cbb*₃-isoforms (155 mV for Cbb₃-1 and 185 mV for Cbb₃-2). These results imply that all three *c*-type hemes exhibit His/Met axial coordination. Among the five hemes of *cbb*₃-CcO, the highest redox potential was obtained for the low-spin heme *b* (+263 mV for Cbb₃-1 and +278 mV for Cbb₃-2). The high-spin heme *b*₃ has a low potential (+132 mV for Cbb₃-1 and +158 mV for Cbb₃-2).

A high similarity between two *cbb*₃-isoforms was experimentally confirmed; even so, a number of differences was observed. DNA sequence analysis revealed that the promoters of the two *cbb*₃-operons contain different regulatory elements. A consensus arginine nitrate regulation (ANR) binding site is only present in the promoter region of the operon *ccoNOP-1*. Under microaerobic growth conditions, the yield of Cbb₃-1, which is expressed under this ANR-dependent promoter, was 6- to 8-fold higher than that of Cbb₃-2. These results indicate that both *cbb*₃-isoforms have different energetic and regulatory roles. Another difference between both *cbb*₃-isoforms is the subunit composition concerning the presence/absence of the CcoQ subunit. PMF analysis revealed that CcoQ is associated with Cbb₃-2, yet not with Cbb₃-1. This absence of CcoQ in Cbb₃-1 might be a consequence of the fact that this isoform is mainly expressed at low oxygen tensions, i.e., CcoQ is not required to protect the core complex from the oxygen-induced instability and degradation. A significant difference regarding the thermal stability could be observed between both *cbb*₃-isoforms. Although for either *cbb*₃-isoform, a two-step temperature-dependent denaturation was observed using differential scanning calorimetry (DSC), the DSC results show that Cbb₃-1 is more stable than Cbb₃-2. The total calorimetric enthalpy change of recombinant

Cbb₃-1 (2,016 KJ mol⁻¹) is higher than that of Cbb₃-2 (1,556 KJ mol⁻¹). Furthermore, Cbb₃-2 denatures 10°C earlier in comparison to the recombinant Cbb₃-1.

Mutagenesis studies were performed to examine the functional importance of two highly conserved active-site residues: Y251 and E323. The redox active tyrosine (Y251) is known to be covalently linked to one of the three histidine ligands of Cu_B, and is considered to play an important role in the catalytic activities of CcOs. In the *cbb*₃-CcOs, this critical tyrosine (Y251) is located in a different helix compared with the A- and B-type CcOs. The variants Y251F and Y251A were created to prevent the enzymatic formation of the tyrosine radical, whereas the double variants Y251A/I252Y and Y251A/G211Y were designed to test the possibility that the His-Tyr cross-link could be restored if this tyrosine residue was present in an alternative location. All four variants were inactive in the oxygen reductase activity assay. E323 is a residue that forms hydrogen bonds to the histidine ligand of the heme *b*₃. It was found that the enzymatic activity was completely abolished when E323 was replaced by an alanine (E323A) or a glutamine (E323Q) residue, whereas the variant E323D retains about 40% of the wild-type oxidase activity.

(iii) Identification and characterization of the natural electron donor of *P. stutzeri cbb*₃-CcOs.

Understanding the physiological significance and differences of both *cbb*₃-isoforms requires the identification of their endogenous electron donor(s). In *P. stutzeri*, however, the endogenous electron donor was not known. Based on the search for the heme *c* binding motif and homology analyses, 16 proteins were predicted to be *c*-type cytochromes. Cytochromes *c*₄, *c*₅, *c*₅₅₁ and *c*₅₅₂ were considered as potential candidates because they could be detected and isolated from aerobically grown cells. They were cloned from the genome of *P. stutzeri*, and heterologously expressed in *Escherichia coli*. However, only cytochrome *c*₄, *c*₅, and *c*₅₅₁ could be successfully expressed at relatively high levels and were purified to homogeneity using three chromatographic steps. UV/Vis spectroscopy and electrochemical measurements were employed to show that these recombinant cytochromes *c* exhibit spectroscopic and electrochemical properties identical to the native proteins.

The three recombinant cytochromes *c* (*c*₄, *c*₅, and *c*₅₅₁) were tested for their ability to serve as natural electron donors for both *cbb*₃-isoforms. Therefore, cytochrome *c*-dependent oxidase activity was measured polarographically in the presence of reduced cytochrome *c* and ascorbate. Our results indicate the following significant findings: (i) Interaction between the *cbb*₃-CcO and cytochrome *c* is an ionic strength-dependent process. (ii) All three cytochromes can clearly donate electrons to the two *cbb*₃-isoforms, however, at different rates. The highest rate of oxygen

reduction was obtained when 100 μM reduced cytochrome c_4 was used (e.g., approx. 500 e^-/s for the wild-type Cbb₃-1). The turnover rates measured with cytochrome c_{551} are comparable to those found with cytochrome c_4 (80 to 90%), while the ones observed with cytochrome c_5 are reduced by about 80%. These results show that both cytochrome c_4 and c_{551} can serve as efficient endogenous substrates for the *cbb*₃-CcOs from *P. stutzeri*, whereas cytochrome c_5 is a poor electron donor. Furthermore, the results of electrochemical measurements suggest that the relatively high reaction rate observed with cytochrome c_4 and c_{551} may be attributed to the fact that both cytochromes harbor at least one low-potential heme c . In contrast, cytochrome c_5 has a high redox potential, which may hinder the electron transfer to the *cbb*₃-CcOs. (iii) The fit of the data shows an unexpected linear dependence of the oxidase activity on the concentration of reduced cytochromes c (20 to 100 mM). Due to the lack of saturation, the kinetic parameters could not be determined. (iv) Measurements performed with two eukaryotic cytochromes c (from yeast and horse heart) show that both proteins are not effective as electron donors for the two *P. stutzeri* *cbb*₃-CcOs.

In addition to the difference in turnover rates observed with three endogenous cytochromes c , significant differences between the two *cbb*₃-isoforms were also found. Catalytic activities measured for the Cbb₃-2 were reduced by about 70% when compared with Cbb₃-1. Inferring from the amino acid sequences and a surface charge calculation based on the X-ray structure of Cbb₃-1 as well as a model of Cbb₃-2, we propose that potential structural changes and surface charge differences, which occur in the solvent exposed domains of subunits CcoP-1 and CcoP-2, can be considered as a major factor responsible for the difference of substrate specificity between both *cbb*₃-isoforms.

In conclusion, this work, for the first time, gives a comprehensive characterization and comparison of the two isoforms of *cbb*₃-CcO from any bacterium, here from *P. stutzeri* ZoBell. The two purified *cbb*₃-isoforms share a high degree of similarity in terms of their biochemical and biophysical properties. On the other hand, differences were observed in respect to subunit composition, thermal stability, substrate specificity, and regulation of the expression of both *cbb*₃-CcOs. Certainly, this work offers perspectives for future functional and structural studies on the two isoforms of *cbb*₃-CcO.

Kurzzusammenfassung

Die *cbb*₃-Typ Cytochrom-c-Oxidase (*cbb*₃-CcOs) bilden die zweitgrößte Familie innerhalb der Häm-Kupfer-Oxidase-Superfamilie. Sie sind evolutionär am weitesten von den mitochondrialen *aa*₃-Oxidase entfernt. Sie sind im Bakterienreich weit verbreitet, kommen aber hauptsächlich in Proteobakterien vor. Die *cbb*₃-Oxidase katalysieren in einer gekoppelten Reaktion die Reduktion von molekularem Sauerstoff zu Wasser und den Transport von Protonen über die bakterielle Cytoplasmamembran. *Cbb*₃-Oxidase werden hauptsächlich bei niedrigen Sauerstoffkonzentrationen exprimiert und weisen eine hohe Affinität zu Sauerstoff auf. Bekannt ist die Bedeutung der *cbb*₃-Oxidase für Stickstoff fixierende Bakterien. Überdies kommt ihnen als einzige terminale Oxidase in einigen pathogenen Bakterien eine Schlüsselrolle bei der Besiedlung sauerstoffarmer Gewebe zu.

Entgegen früherer Studien wurde in dieser Arbeit gezeigt, dass das Gamma-Proteobakterium *Pseudomonas stutzeri* ZoBell zwei unabhängige *cbb*₃-Operons (*ccoNOP-1* und *ccoNOQP-2*) besitzt, die für zwei *cbb*₃-Isoformen (*Cbb*₃-1 und *Cbb*₃-2) kodieren. In der Abteilung Molekulare Membranbiologie des MPI für Biophysik konnte das *Cbb*₃-1 Wildtypenzym aus nativen Membranen aufgereinigt und die Struktur mit einer Auflösung von 3,2 Å bestimmt werden. Die Struktur offenbarte signifikante Unterschiede in Bezug auf Elektronentransfer und Protonentranslokation im Vergleich mit anderen Oxidase-Familien.

*Cbb*₃-Oxidase wurden bereits in verschiedenen Bakterien untersucht, jedoch wurde bis zum jetzigen Zeitpunkt wenig Augenmerk auf die isoformspezifischen Unterschiede gelegt. Bevor detaillierte Studien erfolgen konnten, mussten zuvor beide *cbb*₃-Isoformen getrennt voneinander isoliert werden können, was aufgrund der hohen Sequenzhomologie aus dem Wildtyp von *P. stutzeri* nicht möglich ist. In dieser Arbeit wurde ein homologes Expressionssystem in *P. stutzeri* ZoBell etabliert, das eine spezifische Isolierung beider Isoformen ermöglicht. Zur Deletion der beiden chromosomalen *cbb*₃-Operons durch homologe Rekombination wurde ein neues EGFP-basierendes „Suicide-Plasmid“ entwickelt. Die rekombinanten *cbb*₃-Isoformen konnten danach in dem jeweiligen Deletionsstamm mit einem Affinitätsanhänger homolog exprimiert werden. Die Identität beider *cbb*₃-Isoformen wurde mittels Peptidmassenfingerprint-Analyse bestätigt. Die funktionelle und strukturelle Charakterisierung der *cbb*₃-Isoformen erfolgte mithilfe von biochemischen und biophysikalischen Methoden, wie z.B. UV/Vis Spektroskopie, Circular dichroismus Spektroskopie, dynamischer Differenzkalorimetrie, Fourier-Transform-Infrarotspektroskopie, elektrochemischen Messungen sowie Sauerstoffreduktase- und Katalase-

Aktivitätsmessungen. Die Ergebnisse zeigten, dass die beiden *cbb*₃-Isoformen eine große Anzahl von Ähnlichkeiten aufweisen. Allerdings wurden auch einige Unterschiede in Bezug auf Untereinheitzusammensetzung, thermale Stabilität, Substratspezifität und Regulation der Expression zwischen beiden *cbb*₃-Oxidase festgestellt.

Die Sauerstoffreduktase-Aktivität der *cbb*₃-Isoformen wurde polarographisch mittels einer Sauerstoffelektrode und eines artifiziellen Elektronendonator-Systems (Na-Ascorbat und *N,N,N',N'*-Tetramethyl-*p*-phenylendiamin [TMPD]) gemessen. Nach Optimierung der Bedingungen für den pH-Wert, die Ionenstärke und das molare Verhältnis von Na-Ascorbat zu TMPD konnten für die aufgereinigten rekombinanten Proteine Cbb₃-1 und Cbb₃-2 Sauerstoffreduktase-Aktivitäten gemessen werden, welche denen der nativen Cbb₃-1 ähneln. Interessanterweise wurden eine hohe Umsatzrate von mindestens 2000 e⁻/s und eine hohe Michaelis-Menten-Konstante ($K_m \sim 3.6$ mM), für beide *cbb*₃-Oxidase ermittelt. Dies ist die höchste Aktivität, die bisher für eine *cbb*₃-CcO gemessen wurde. Zusätzlich zur Sauerstoffreduktase-Aktivität wurde die Aktivitätsmessung der Katalase-Nebenreaktion durchgeführt. Es konnten keine signifikanten Unterschiede in der Katalase-Aktivität zwischen der nativen Cbb₃-1 und den rekombinanten Proteinen Cbb₃-1 und Cbb₃-2 nachgewiesen werden.

Um die nativen Elektronendonoren der *cbb*₃-CcO zu untersuchen, wurden drei *c*-Typ Cytochrome *c*₄, *c*₅ und *c*₅₅₁ aus *P. stutzeri* kloniert und heterolog in *Escherichia coli* exprimiert. Die rekombinanten Cytochrome wurden bis zur Homogenität aufgereinigt und wiesen identische spektroskopische und elektrochemische Eigenschaften wie die entsprechenden Wildtyp-Proteine auf. Es konnte gezeigt werden, dass die Cytochrome *c*₄ und *c*₅₅₁ als effiziente native Substrate für die *cbb*₃-CcO dienen, während Cytochrom *c*₅ ein schwacher Elektronendonator ist. Dabei sind die katalytischen Aktivitäten, die für die rekombinante Cbb₃-2 gemessen wurden, im Vergleich zur rekombinanten Cbb₃-1 bis auf 30% reduziert. Diese Ergebnisse weisen auf unterschiedliche Substratspezifitäten beider *cbb*₃-Isoformen hin.

Mit dieser Arbeit ist erstmals eine umfangreiche Charakterisierung beider Isoformen der *cbb*₃-CcO von *P. stutzeri* ZoBell gelungen. Das etablierte Expressionssystem dient als grundlegende Basis für zukünftige funktionelle und strukturelle Studien.

Abstract

The *cbb*₃-type cytochrome *c* oxidases (*cbb*₃-CcOs) constitute the second most abundant family of the heme-copper terminal oxidases (HCOs) and are most distantly related to the mitochondrial *aa*₃-CcOs. They are found exclusively in bacteria, especially in proteobacteria. The *cbb*₃-CcOs catalyze the reduction of oxygen to water and couple this reaction to the generation of a proton electrochemical gradient across the bacterial cytoplasmic membrane. They are often expressed under low oxygen tension and have a high apparent affinity for oxygen. As a consequence, *cbb*₃-CcOs are required for diazotrophs to sustain nitrogen fixation and are crucial for the colonization of oxygen deficient tissues by many human pathogens.

It has previously been reported that the gamma-proteobacterium *Pseudomonas stutzeri* ZoBell possesses only one *ccoNOQP* operon coding for *cbb*₃-CcO. In this work, we showed that this strain actually possesses two independent *cbb*₃ operons encoding two isoforms of *cbb*₃-CcO (Cbb₃-1 and Cbb₃-2). In our laboratory, the wild-type Cbb₃-1 was purified from the native membranes and its structure was determined at 3.2 Å resolution. This structure revealed significant differences in the electron transfer and proton translocation processes among the three families of HCO.

Although *cbb*₃-CcOs have been studied functionally in several bacteria, less emphasis has been placed on the isoform-specific differences between the *cbb*₃-CcOs. As a prerequisite for a detailed investigation, both isoforms must be isolated separately. However, this is difficult due to the high homology between Cbb₃-1 and Cbb₃-2. Therefore, in this work, we established a homologous expression system in *P. stutzeri* ZoBell, which allows the specific isolation of each of the two *cbb*₃-isoforms. To delete each of the two chromosomal *cbb*₃ operons by homologous recombination, a novel EGFP-based suicide plasmid was constructed. Both recombinant *cbb*₃-isoforms were homologously expressed from a plasmid in the corresponding deletion strain and purified to homogeneity by affinity chromatography. The identity of both isoforms was confirmed by peptide mass fingerprinting analysis. Functional and structural characteristics of the two *cbb*₃-isoforms were carefully investigated by using different biochemical and biophysical techniques, including UV/Visible spectroscopy, circular dichroism spectroscopy, differential scanning calorimetry, Fourier transform infrared spectroscopy, electrochemical measurement as well as oxygen reductase and catalase activity measurements. Our data show that the two *cbb*₃-isoforms share a very high degree of similarity. On the other hand, differences were observed in respect to subunit composition, thermal stability, substrate specificity, and regulation of the

expression of both *cbb*₃-CcOs.

The oxygen reductase activity of both *cbb*₃-CcOs was first measured using an artificial electron-donating system (ascorbate and *N,N,N',N'*-tetramethyl-*p*-phenylenediamine [TMPD]). We found that TMPD can directly donate electrons to both *cbb*₃-CcOs, and both recombinant isoforms catalyze the reduction of oxygen at a rate similar to the wild-type Cbb₃-1. Interestingly, a surprisingly high turnover of at least 2,000 e⁻/s and a high Michaelis-Menten constant ($K_m \sim 3.6$ mM) were characteristic for both *cbb*₃-CcOs. To date, this is the highest activity reported for a *cbb*₃-CcO. In addition, the catalase side reaction of *cbb*₃-CcO was measured. This assay shows no significant difference, neither between wild-type and recombinant proteins nor between Cbb₃-1 and Cbb₃-2.

To investigate the natural electron donor(s) of *cbb*₃-CcOs, three cytochromes *c* (*c*₄, *c*₅ and *c*₅₅₁) from *P. stutzeri* were cloned and expressed heterologously in *Escherichia coli*. The recombinant cytochromes *c* were purified to homogeneity, and exhibited spectroscopic and electrochemical properties identical to the wild-type proteins. It could be shown that cytochrome *c*₄ and *c*₅₅₁ are very likely the natural substrates for both *cbb*₃-isoforms, whereas cytochrome *c*₅ is not a good substrate. In addition, these three endogenous cytochromes *c* can only support the activity of Cbb₃-2 to a level of 30%, when compared to the Cbb₃-1. This finding indicates that both *cbb*₃-isoforms exhibit differences in substrate specificity.

In conclusion, the results of this work provide, for the first time, a comprehensive characterization of the two isoforms of *cbb*₃-CcO from any bacterium, here from *P. stutzeri* ZoBell. The established expression system will also serve as a solid and convenient platform for future functional and structural studies.

Abbreviations and Symbols

In this work amino acids are abbreviated in one- or three-letter codes according to the IUPAC rules for the nomenclature. Other abbreviations and symbols that appear more than once are listed in the following table.

Table A: Chemical abbreviations.

Abbreviation	Name
AAs	amino acids
ADP	adenosine-5'-diphosphate
AP	alkaline phosphatase
APS	ammonium persulfate
ATP	adenosine-5'-triphosphate
BCA	bicinchoninic acid
BCIP	5-bromo-4-chloro-indolyl-phosphatase
ddH ₂ O	double-distilled water (=Milli-Q ultrapure water, Millipore)
dNTP	deoxyribonucleotide triphosphate
DDM (=LM)	n-dodecyl- β -D-maltoside
DMSO	dimethyl sulfoxide
DMF	<i>N,N</i> -dimethylformamide
DNA	deoxyribonucleic acid
EDTA	ethylenediaminetetracetic acid
EtBr	ethidium bromide
EtOH	ethanol
HABA	2-(4'-hydroxy-benzeneazo)-benzoic acid
HAc	acetic acid
HEPES	4-(2-hydroxyethyl)-piperazine-1-ethanesulfonic acid
IPTG	isopropyl β -D-1-thiogalactopyranoside
β -ME	2-mercaptoethanol
MeOH	methanol
MES	2-(<i>N</i> -morpholino)-ethanesulfonic acid
MOPS	3-(<i>N</i> -morpholino)-propanesulfonic acid
NADH	nicotinamide adenine dinucleotide
NBT	nitro blue tetrazolium
Ni-NTA	nickel nitrilotriacetic acid
Pefabloc (=AEBSF)	4-(2-aminoethyl)-benzenesulfonyl fluoride hydrochloride
PVDF	polyvinylidene difluoride
RNA	ribonucleic acid
SDS	sodium dodecyl sulfate
TEMED	<i>N,N,N',N'</i> -tetramethylethylenediamine
TMBZ	3,3',5,5'-tetramethylbenzidine

TMPD	<i>N,N,N',N'</i> -tetramethyl- <i>p</i> -phenylenediamine
Tris	tris-hydroxymethyl-aminomethane
X-Gal	5-bromo-4-chloro-3-indolyl β -D-galactopyranoside

Table B: Biological, biochemical and biophysical abbreviations.

Abbreviation	Name
AOX	alternative oxidase
A _{xxx}	absorbance at xxx nm
BN	blue-native
CcO (=COX)	cytochrome <i>c</i> oxidase
CD	circular dichroism
CFU	colony-forming unit
CMC	critical micelle concentration
CV	column volumes
ΔH	enthalpy change
DNase	deoxyribonuclease
DSC	differential scanning calorimetry
EGFP	enhanced green fluorescent protein
EPR	electron paramagnetic resonance
ESI	electrospray ionization
FTIR	fourier transform infrared spectroscopy
F _v	antibody variable domain fragment
Fw	forward (primer design)
HCO	heme-copper oxidase
HPLC	high-performance liquid chromatography
IMAC	immobilized-metal affinity chromatography
K_m	Michaelis–Menten constant
MALDI	matrix-assisted laser desorption/ionization
MS	mass spectroscopy
MW	molecular weight
MWCO (\approx NMWL)	molecular weight cut off (\approx nominal molecular weight limit)
nLC	nanoscale liquid chromatography
NOR	nitric oxide reductase
OD _{xxx}	optical density at xxx nm
ORF	open reading frame
ORI (ori)	origin of replication
RCF ($\times g$)	relative centrifugal force
rec.	recombinant
PAGE	polyacrylamide gel electrophoresis
PCR	polymerase chain reaction
pI	isoelectronic point
PMF	peptide mass fingerprint
QOX	quinol oxidase

rec.	recombinant
Rev	reverse (primer design)
RNase	ribonuclease
SHE	standard hydrogen electrode
T_m	transition temperature
TMH	transmembrane helix
TOF	time-of-flight
UQ	oxidized form of quinone
UQH ₂	reduced form of quinone, also hydroquinone or quinol
UV/Vis	ultraviolet/visible
V_{max}	the maximum reaction velocity
wt.	wildtype

Table C: Abbreviations of units and other general abbreviations.

Abbreviation/Symbol	Name
3D	three-dimensional
Å	angstrom
approx.	approximate
bp	base pair(s)
°C	degree celsius
conc.	concentration
ϵ	extinction coefficient
e.g.	exempli gratia (latin), for example (english)
<i>et al.</i>	et alii (latin), and others (english)
J	joule
l	liter
min	minute
Pa	Pascal
psi	pound per square inch
rpm	revolutions per minute
RT	room temperature
σ	standard deviation
sec	second
V	volt
vs.	versus (latin), against (english)
v/v	volume/volume
w/v	weight/volume
w/w	weight/weight

1 Introduction

All living organisms are open systems that require a continuous influx of free energy to maintain a highly ordered state. Phototrophs capture the light energy from the sun, whereas chemotrophs acquire their energy by oxidizing chemical substances. In cellular respiration, the heterotrophic nutrients are degraded into energy-depleted end products. During this catabolic process, the stored chemical energy can be released by oxidative metabolism in the form of adenosine-5'-triphosphate (ATP) that powers most of the energy-consuming cellular activities.

1.1 Oxidative phosphorylation and electron transport

1.1.1 ATP and oxidative phosphorylation

Adenosine-5'-triphosphate (ATP) is the primary energy carrier of life that couples endergonic and exergonic reactions in all known organisms. ATP can be hydrolyzed to adenosine-5'-diphosphate (ADP) and inorganic phosphate (P_i). The cleavage of the terminal phosphoanhydride bond is highly exergonic ($\Delta G^\circ \approx -30.5$ kJ/mol), because one hydrolysis product, the orthophosphate group (HPO_4^{2-}), is greatly resonance-stabilized and therefore contains less free energy than the reactant (ATP). During metabolic processes, ATP provides energy for most thermodynamically unfavorable reactions by the transfer of a phosphate-containing moiety (such as a phosphoryl group) to a substrate molecule, rather than by being directly hydrolyzed (Nelson and Cox 2000).

Since large amounts of ATP are required to maintain the metabolic activities, the limited stores of intracellular ATP must be replenished. In aerobic nonphotosynthetic organisms, generation of ATP is mainly accomplished through two types of processes: substrate-level phosphorylation and oxidative phosphorylation. The substrate-level phosphorylation is the synthesis of ATP by the direct transfer of a phosphoryl group from a phosphorylated reactive intermediate to ADP, which commonly occurs during the early stages of carbohydrate catabolism, including glycolysis and citric acid cycle. Production of ATP using energy from other high-energy compounds is less efficient.

In contrast, ATP is mainly produced by oxidative phosphorylation, which occurs in the last stage of aerobic cellular respiration. During oxidative phosphorylation, reduced electron carriers (NADH & $FADH_2$), which are produced predominantly by the citric acid cycle and the β -oxidation of fatty acids, are oxidized. The electrons are transferred through a series of redox active, membrane-integral protein complexes until they reach the ultimate electron acceptor, molecular

oxygen (O₂). In this process, electron transfer is coupled to proton (ion) translocation across the mitochondrial inner membrane or the bacterial cytoplasmic membrane. The free energy of substrate oxidation is sequentially released and stored in an electrochemical proton (ion) gradient, also known as the proton (ion)-motive force (*pmf* or *imf*). The *pmf* is then used by the F₀F₁-ATP-synthase to synthesize ATP from ADP and P_i. This conversion of redox energy into transmembrane electrical and proton gradients and finally into chemical energy stored in ATP was first postulated by Peter Mitchell in 1961, and is known as the chemiosmosis theory (Mitchell 1961).

1.1.2 The electron transport chain

The generalized model of the electron transport chain (ETC), also known as the respiratory chain, consists of four membrane-embedded protein complexes (complex I-IV) containing redox-active cofactors (Saraste 1999). Within the ETC, electrons flow stepwise from low redox potential donors (-320 mV for NADH/NAD⁺) to high redox potential acceptors (+815 mV for O₂/H₂O), which allows the free energy to be released continuously and in small increments. Among the four protein complexes, electron transport is mediated by two mobile electron carriers: a membrane-diffusible ubiquinone and a water-soluble cytochrome *c*.

Complex I (NADH:ubiquinone oxidoreductase or NADH dehydrogenase) is the electron entry point in the respiratory electron transport chain. It catalyzes the oxidation of NADH, transfers two electrons through flavin mononucleotide (FMN) and multiple iron-sulfur clusters to ubiquinone (Brandt 2006). The electron transfer is coupled to the pumping of protons with a stoichiometry of 3 to 4 H⁺/2 e⁻ (Wikström and Hummer 2012). Mitochondrial complex I is one of the largest known membrane protein assemblies and is comprised of 46 subunits with a molecular weight of approx. 1,000 kDa (Hirst *et al.*, 2003). It has an L-shaped structure formed by a peripheral arm containing all the prosthetic groups and a hydrophobic arm residing in the membrane (Efremov *et al.*, 2010; Hunte *et al.*, 2010). Recently, the structure of the whole complex I from *Thermus thermophilus* has become available (Baradaran *et al.*, 2013). However, the molecular mechanism whereby the redox reaction couples to proton pumping is still unknown (Hirst 2013).

Complex II (succinate:ubiquinone oxidoreductase or succinate dehydrogenase) is the only membrane-bound component of the citric acid cycle and forms a second electron entry point into the ETC. Complex II oxidizes succinate to fumarate while reducing ubiquinone to ubiquinol. The electrons are transferred first to flavin adenine dinucleotide (FAD), then through three iron-sulfur clusters to ubiquinone. In contrast to the other three complexes, complex II is not a proton pump (Cecchini 2003; Yankovskaya *et al.*, 2003; Maklashina and Cecchini 2010).

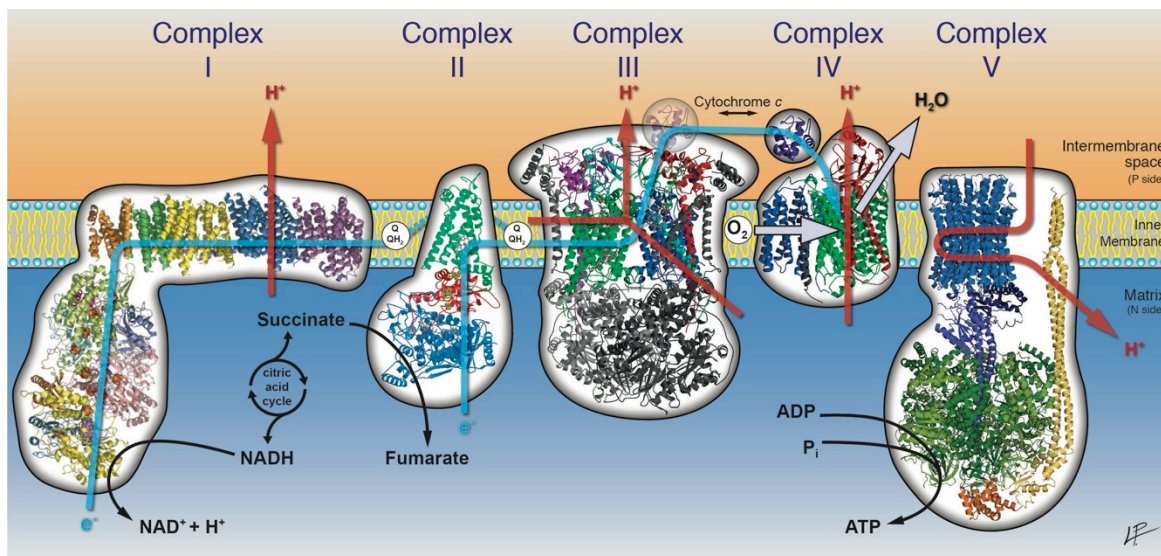
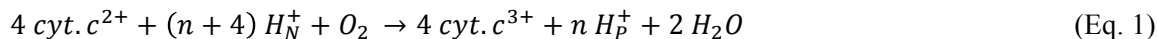


Figure 1-1: Schematic diagram of the electron transport chain within the mitochondrial inner membrane. The electron transport chain is composed of four redox-active membrane protein complexes (complex I-IV) that transfer electrons to the ultimate electron acceptor, molecular oxygen. Electron flow (blue arrows) is accompanied by proton pumping (red arrows) from matrix (N side) to intermembrane space (P side), generating an electrochemical gradient, which is utilized by F_0F_1 -ATP synthase (complex V) to generate ATP. Together with cytochrome *c*, ubiquinone (Q) and its reduced form (ubiquinol, QH_2) serve as mobile electron carriers. Structural representation of complex I-IV was generated using PDB entries 3M9S, 1NEK, 3CX5 and 1QLE, respectively. This figure was kindly provided by Paolo Lastrico (MPI of Biophysics, Frankfurt am Main).

Complex III (ubiquinone:cytochrome *c* oxidoreductase or bc_1 complex) is the third member of the electron transport chain and has a homodimeric structure (Xia *et al.*, 1997; Iwata *et al.*, 1998; Lange and Hunte 2002). It couples the transfer of electrons from ubiquinol to oxidized cytochrome *c* with proton pumping. According to the Q-cycle mechanism (Mitchell 1976), ubiquinol undergoes a two-cycle and bifurcated oxidation, in which two separate active sites (Q_o for the oxidation of ubiquinol and release of protons; Q_i for the reduction of ubiquinone) are involved. During one complete Q-cycle, two ubiquinols are oxidized and therefore donate four electrons to complex III. Two electrons are transferred to the “Rieske” $[2Fe-2S]$ center and from there via cytochrome c_1 to the final electron acceptor cytochrome *c*. The other two electrons are transferred through the low potential heme b_L to the high potential heme b_H , where one ubiquinol is regenerated by a two-step rereduction and protonation of ubiquinone (Trumpower 1999; Crofts 2004). In complex III, the reduction of cytochrome *c* and deprotonation of ubiquinol is accompanied by proton translocation. The stoichiometry is thermodynamically equivalent to $2 H^+ / 2 e^-$ (Hinkle *et al.*, 1991; Wikström and Hummer 2012).

Complex IV (cytochrome *c*:oxygen oxidoreductase or cytochrome *c* oxidase) is the terminal enzyme in the ETC. It catalyzes the four-electron reduction of O₂ to water and couples this reaction to the proton translocation across the membrane. In contrast to other members of ETC, complex IV does not generate any reactive oxygen species (ROS, including H₂O₂, O₂⁻ and [•]HO) (Ludwig *et al.*, 2001). The overall reaction is illustrated by the following equation:



These enzymes use O₂ as an electron sink. O₂ diffuses through the membrane to the catalytic center. During one catalytic cycle, four electrons are subsequently supplied by the reduced cytochromes *c*, which are located in the intermembrane space of mitochondria or bacterial periplasmic space (P side). Eight protons are taken from the mitochondrial matrix or bacterial cytoplasm (N side). Complex IV translocates eight charge equivalents across the membrane for the reduction of one molecule of O₂, giving a thermodynamic stoichiometry of 4 H⁺/2 e⁻ (Wikström 1977; Wikström 1984; Hinkle *et al.*, 1991). Complex IV is the main topic of this thesis. Therefore, more detailed aspects of the function and structure of this enzyme are shown in the following sections.

Among the members of the ETC, three protein complexes (I, III and IV) are involved in proton translocation across the membrane and therefore contribute to the formation of *pmf*. Over the past decade, the interaction between respiratory complexes has been studied using blue-native polyacrylamide gel electrophoresis (Schägger and Pfeiffer 2000) and electron microscopy (Schäfer *et al.*, 2007). Several supercomplex assemblies from different organisms have been characterized, e.g., bovine mitochondrial I₁III₂IV₁ (Althoff *et al.*, 2011) and plant mitochondrial I₁III₂ (Eubel *et al.*, 2004). The presence of the supercomplex organization of the respiratory enzymes supports the solid-state model (Chance and Williams 1955), which assumes a more efficient electron transfer than that suggested by the random collision model (Hackenbrock *et al.*, 1986). So far, no complex II has been found in the respiratory supercomplexes.

In contrast to eukaryotes, the ETCs in bacteria are highly variable (Unden and Bongaerts 1997; Richardson 2000; Zannoni 2010). Different types of dehydrogenases can pass electrons into the ETC at the level of ubiquinone. Moreover, different terminal oxidases with different affinities for O₂ are used to adapt to environmental changes.

1.2 Heme-copper terminal oxidases

1.2.1 Classification of heme-copper terminal oxidases

Heme-copper terminal oxidases (HCOs) are terminal enzymes of the aerobic respiratory chain. These enzymes catalyze the reduction of O₂ to water and generally contribute to energy conservation. HCOs are quite diverse in terms of subunit composition, electron donor, heme type and proton pathways (García-Horsman *et al.*, 1994; Hemp and Gennis 2008). According to their electron donors, they can be divided into two subgroups: the quinol oxidases (QOX) and cytochrome *c* oxidases (CcOs or COX). One major difference between QOX and CcOs is the lack of a Cu_A metal center in the hydrophilic domain of subunit II of QOX. In addition, QOX transfer electrons directly from ubiquinol to oxygen and therefore bypass complex III.

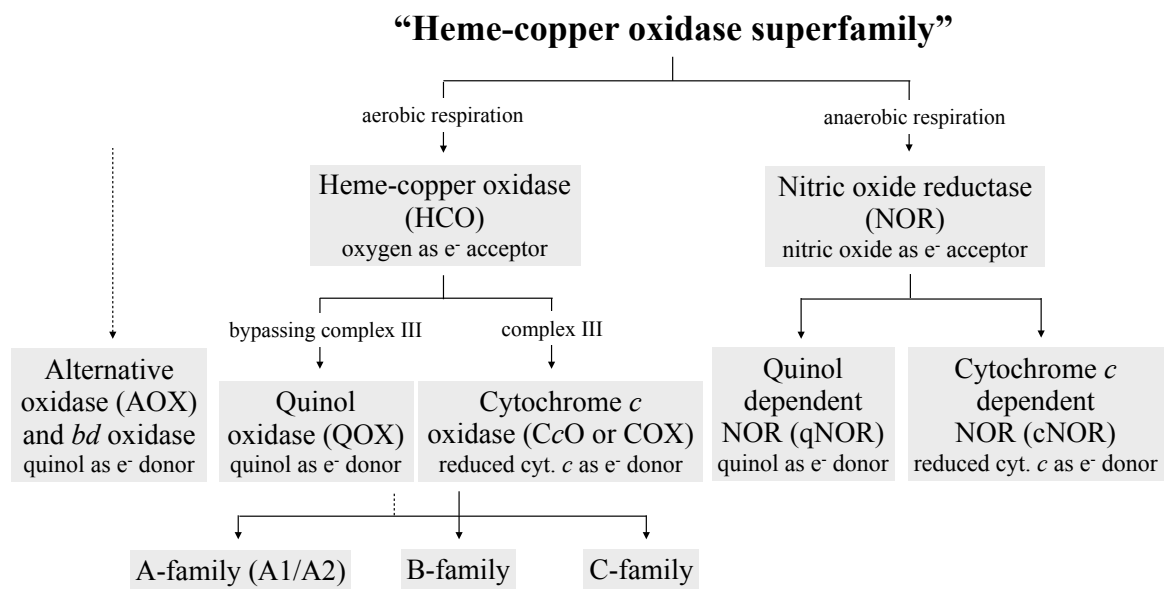


Figure 1-2: Classification of the heme-copper oxidase superfamily. The criteria used for the classification are indicated. Abbreviations are shown in parentheses. Alternative oxidases and *bd* oxidases are shown together because they are phylogenetically unrelated to the other members of heme-copper oxidase.

Despite the high diversity, HCOs are characterized by the presence of a transmembrane catalytic subunit, which contains a low-spin heme (*a* or *b*) and a binuclear center composed of a high spin heme (*a*₃, *b*₃ or *o*₃) and Cu_B. Six histidine residues, which are involved in the coordination of the three cofactors, are strictly conserved among the HCOs. Based on the similarity of amino acid sequences and constituents of the proton pathways in the core catalytic subunit, members of HCOs are phylogenetically classified into three major families: A-family (mitochondrial-like oxidases), B-family (*ba*₃-like oxidases) and C-family (*cbb*₃-like oxidases) (Pereira *et al.*, 2001; Sousa *et al.*,

2011; Sousa *et al.*, 2012).

Among the HCOs, the A-family is the largest one and contains the best-studied members of the HCOs. It comprises the enzymes found in mitochondria and many bacteria. This family is characterized by the presence of at least two proton pathways, the D- and K-pathway. Protons are transferred through both pathways that connect the protein surface on the N side of the membrane with the catalytic reaction center. Based on the presence or absence of a conserved glutamate residue in the D-pathway, the A-family can be further divided into the A1- and A2-type (Pereira *et al.*, 2001). A1-type HCOs are represented by the *aa*₃-CcO from bovine mitochondria and from the α -proteobacterium *Paracoccus denitrificans*. In both enzymes, the D-pathway contains several hydrophilic residues ending at Glu278 (*P. denitrificans* numbering), which is considered to be crucial for the conformational change associated with the proton gating mechanism (Michel 1998; Dürr *et al.*, 2008). Instead of this glutamate residue, the terminal end of the D-pathway in A2-type HCOs is functionally replaced by a so-called -YSHPXV- motif, which contains a conserved tyrosine and a conserved serine residue. Examples for the A2-type HCOs are the *caa*₃-CcOs from *Thermus thermophilus* and *Rhodothermus marinus* (Srinivasan *et al.*, 2005; Lyons *et al.*, 2012). In addition, *caa*₃-CcOs contain an extramembrane cytochrome *c* domain that is fused to its subunit II (van der Oost *et al.*, 1991; García-Horsman *et al.*, 1994). Despite the differences between A1 and A2, all members of the A-family HCOs are characterized by the presence of a redox-active tyrosine residue that is covalently cross-linked to one of the three-histidine ligands of Cu_B via a thioether bond, and by a proton-pumping stoichiometry of 1.0 H⁺/e⁻ (Pereira *et al.*, 2000; Brzezinski and Gennis 2008).

The B-family HCOs, represented by the *ba*₃-CcO from *T. thermophilus*, are found in archaea and bacteria. The members of this family have only one proton pathway (K-pathway analog), which is locationally similar to the K-pathway of A-family HCOs without sharing any sequence similarity (von Ballmoos *et al.*, 2011). They use one single pathway for the transfer of both substrate and pumped protons, and a reduced stoichiometry of 0.5 H⁺/e⁻ (Kannt *et al.*, 1998; Han *et al.*, 2011) compared to A-family HCOs was reported. The *ba*₃-CcOs also contain the primary electron acceptor Cu_A in the periplasmic domain of subunit II. Like A-family HCOs, both amino acids of the cross-linked tyrosine-histidine motif are located on the same α -helix (Buse *et al.*, 1999; Soulimane *et al.*, 2000). Besides the oxygen reductase activity, B-family enzymes can also reduce nitric oxide (NO) to nitrous oxide (N₂O) at low levels (Giuffrè *et al.*, 1999).

The C-family only comprises *cbb*₃-CcOs, which are found exclusively in bacteria, especially in proteobacteria. The *cbb*₃-CcOs differ from the other members of the HCO superfamily by having a distinctly different subunit composition and different redox centers. The *cbb*₃-CcOs are discussed in detail in Chapter 1.3.

Nitric oxide reductases (NORs) share structural similarity and some common features with HCOs, and are therefore considered to be included into the HCO superfamily (van der Oost *et al.*, 1994; Zumft 2005; Ducluzeau *et al.*, 2009; Matsumoto *et al.*, 2012). NORs can be divided into quinol dependent NOR (qNOR) and cytochrome *c* dependent (cNOR) with respect to their electron donor. Presently, there is no evidence that NORs can translocate protons across the membrane.

Apart from the HCOs, alternative oxidases (AOX), *bd* oxidases and their homologues (e.g., cyanide-insensitive oxidase [CIO] from *Pseudomonas aeruginosa*) are also part of the electron transport chain (Borisov *et al.*, 2011). AOX are significantly resistant to cyanide and found predominantly in mitochondria of higher plants and fungi (Vanlerberghe and McIntosh 1997). The *bd* oxidases are widely distributed prokaryotic quinol oxidases, which have a high affinity for oxygen (García-Horsman *et al.*, 1994; D'mello *et al.*, 1996). AOX and *bd* oxidases use ubiquinol as the electron donor to reduce molecular oxygen, and they do not pump protons. Since they show no sequence homology and structural relationship to each other nor to any members of the HCOs, they are not included in the taxonomic studies of HCOs.

1.2.2 Evolutionary origins of heme-copper terminal oxidases

To study the phylogenetic relationships among the members of HCOs, one of the most important considerations is the timing of transition from anoxic to oxic environments on Earth (around 2.5 billion years ago). The earliest opinion was that aerobic respiration appeared after oxygenic photosynthesis, and the latter was performed by the ancestors of the cyanobacteria (Dickerson *et al.*, 1976; Broda and Peschek 1979). This opinion was later revised, since the primitive HCOs are present in the common ancestors of archaea and bacteria, and the split between these two domains of life occurred before the development of the photosystem in cyanobacteria (Woese 1987; Castresana *et al.*, 1994; Castresana *et al.*, 1995; Castresana and Saraste 1995).

Among the HCOs, it was proposed that the C-family HCOs evolved much earlier than A- and B-family enzymes, since C-family HCOs share relatively high structural and functional similarity to the NORs. The speculation of early divergence of C-family HCOs was further supported by the following biochemical observation: (i) the *cbb₃*-CcOs are mainly expressed at low oxygen concentrations; (ii) they display higher NO reductase activity compared to the *caa₃*- and *ba₃*-CcOs (Giuffrè *et al.*, 1999; Forte *et al.*, 2001). In addition, the link between *cbb₃*-CcOs and NORs suggested a single phylogenetic origin of HCOs (Castresana *et al.*, 1994; García-Horsman *et al.*, 1994; Saraste and Castresana 1994).

Recently, this scenario was challenged after subsequent analyses of the available complete genomes (Ducluzeau *et al.*, 2008; Brochier-Armanet *et al.*, 2009). Conversely, it was suggested

that the A-family enzymes are the most ancient members of the HCOs. It was also proposed that members of HCOs have multiple independent origins (Pereira *et al.*, 2001). B-family enzymes likely originated from archaea and were transferred to bacteria by horizontal gene transfer (HGT), whereas *cbb₃*-CcOs have a proteobacterial origin and therefore are more recent than A- and B-family HCOs (Brochier-Armanet *et al.*, 2009).

1.2.3 Structure of heme-copper terminal oxidases

To date, crystal structures of all different types of HCOs are available, including cNOR and qNOR. A brief introduction to each representative is given in the following section.

In 1995, the crystal structure of the *aa₃*-CcO from *P. denitrificans* was first determined at 2.8 Å resolution (Iwata *et al.*, 1995), followed by the metal center structure (Tsukihara *et al.*, 1995) and the whole structure of the mitochondrial *aa₃*-CcO from bovine heart (Tsukihara *et al.*, 1996). Since then, several high-resolution structures have been published, which differ in terms of organism, redox-state, ligand binding and lipid binding (Ostermeier *et al.*, 1997; Yoshikawa *et al.*, 1998; Tsukihara *et al.*, 2003; Qin *et al.*, 2006; Koepke *et al.*, 2009). The *aa₃*-CcO from *P. denitrificans* is composed of four subunits, in which subunits I-III comprise the catalytic core and show functional and structural homology to the eukaryotic enzymes¹ (Figure 1-3 A). Subunit I contains twelve transmembrane helices (TMHs) with a threefold rotational symmetry. It has three redox active metal centers, a low-spin heme *a*, a high-spin heme *a₃* and Cu_B. Oxygen reduction occurs at the heme *a₃*-Cu_B binuclear center. There are two additional metal centers containing Mg²⁺ (or Mn²⁺) and Ca²⁺. The Mg²⁺/Mn²⁺ site is suggested to be involved in water exit from the reaction center and proton pumping (Schmidt *et al.*, 2003; Sharpe *et al.*, 2009), whereas the physiological function of the Ca²⁺ binding site is currently unclear (Pfitzner *et al.*, 1999; Lee *et al.*, 2002).

Subunit II consists of two TMHs and a C-terminal globular domain, which is located on the P side of the membrane. The large hydrophilic domain is characterized by a ten-stranded β-barrel and harbors a mixed valence dinuclear Cu_A center. The Cu_A center functions as the primary electron acceptor of *aa₃*-CcO that mediates the electron transfer from cytochrome *c* to the heme *a*. Several surface-exposed acidic residues near the Cu_A center are responsible for the electrostatic interactions forming the transient complex with cytochrome *c* (Witt *et al.*, 1998; Drosou *et al.*, 2002; Maneg *et al.*, 2004). Subunit III is composed of seven TMHs and does not contain any metal cofactors. The helices of subunit III are divided by a large V-shaped cleft into two bundles, and this cleft is occupied by lipid molecules (Michel *et al.*, 1998; Qin *et al.*, 2007). Subunit III might

¹ The eukaryotic *aa₃*-CcOs consist of three mitochondrially encoded core subunits (I, II and III) and up to ten nucleus-encoded subunits (10 in mammalian cells and up to 9 in yeasts).

be involved in the stabilization of the whole enzyme, and it is also proposed that the membrane-anchored cytochrome c_{552} might bind to the cleft (Iwata *et al.*, 1995). Subunit IV contains one TMH with unknown function. Deletion of this subunit has no effect on the stability and activity of the enzyme (Witt and Ludwig 1997).

The crystal structure of the caa_3 -CcO (A2-type HCO) (Figure 1-3 B) from *T. thermophilus* has been recently published (Lyons *et al.*, 2012). It is composed of three subunits, namely, I/III, IIc and IV. The overall architecture of the caa_3 -CcO is similar to that of the aa_3 -CcO. However, several significant features are present in the current structure: (i) The core catalytic subunit I/III is a fusion of the classical subunit I and III, which is comprised of 19 TMHs. It harbors three redox active metal centers and one conserved Mg^{2+} binding site. Compared to the aa_3 -CcO, both low- and high-spin hemes are a_s type, which have a hydroxyethylgeranylgeranyl group instead of the hydroxyethylfarnesyl side chain (Lubben and Morand 1994; Lyons *et al.*, 2012). (ii) Subunit IIc exists as a fusion of a cytochrome *c* domain and a classical subunit II containing the dinuclear Cu_A center (Mather *et al.*, 1993). The covalently bound heme *c* is proposed to be the initial electron entry and exit site of the caa_3 -CcO. (iii) The structure analysis also showed that caa_3 -CcO has a previously unknown subunit IV. It consists of two TMHs and is located in the hydrophobic interface of subunit I/III (Lyons *et al.*, 2012).

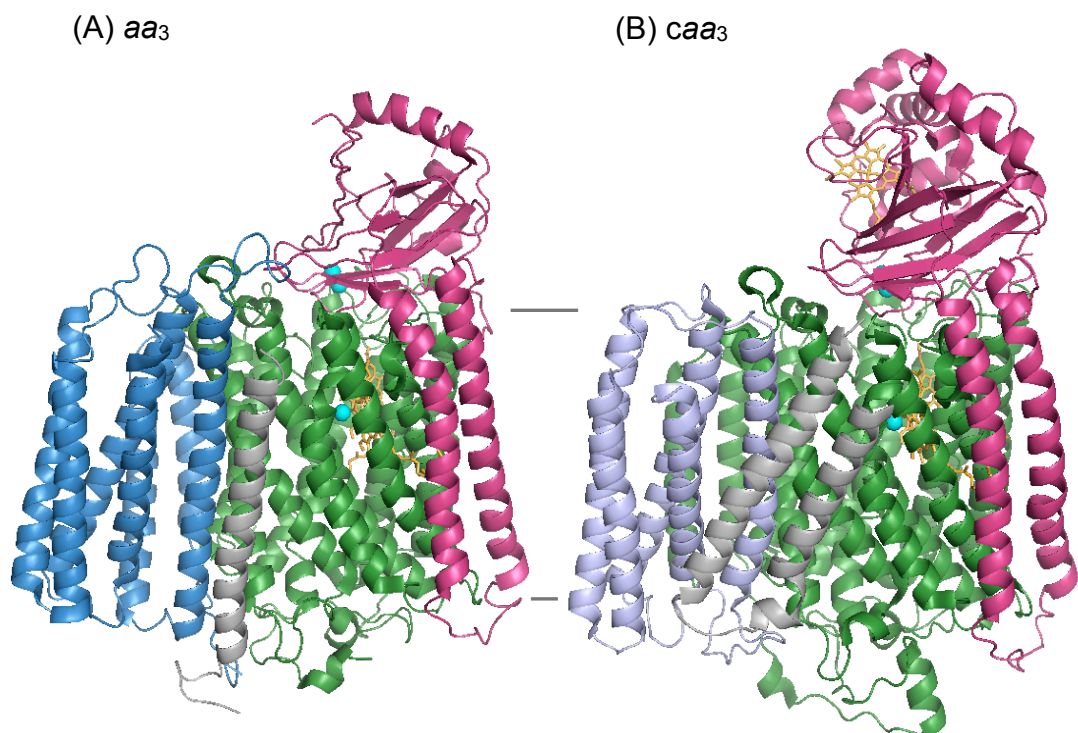


(Figure continued on next page)

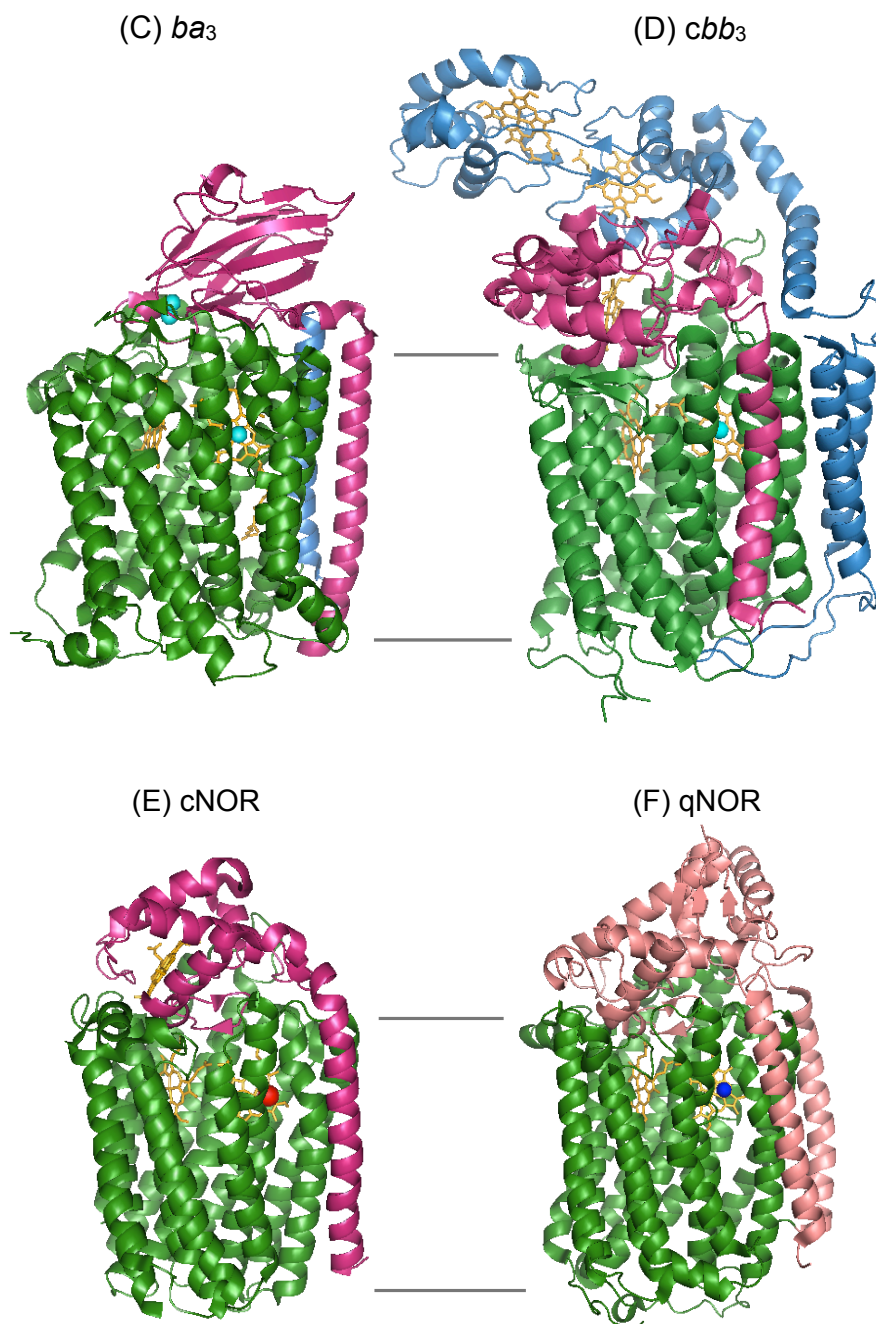


Figure 1-3: X-ray structures of different types of HCOs and NORs. (A) *aa*₃-CcO from *Paracoccus denitrificans*; (B) *caa*₃-CcO from *Thermus thermophilus*; (C) *ba*₃-CcO from *Thermus thermophilus*; (D) *cbb*₃-CcO from *Pseudomonas stutzeri*; (E) cNOR from *Pseudomonas aeruginosa*; (F) qNOR from *Geobacillus stearothermophilus*. The catalytic subunits of HCOs and NORs are shown in green. The catalytic subunit of *caa*₃-CcO is a fusion of a canonical subunit I (green) and subunit III (light blue). Additional subunits are presented in red and blue. Copper ions are shown as blue spheres and hemes are represented as yellow sticks. cNOR and qNOR contain an iron atom (Fe_B, red) and a zinc atom (Zn_B, dark blue) in the catalytic subunit instead of Cu_B, respectively. Coordinates were taken from PDB entries: 1QLE (*aa*₃), 2YEV (*caa*₃), 1XME (*ba*₃), 3MK7 (*cbb*₃), 3O0R (cNOR) and 3AYF (qNOR). 3D structural images were generated using the PyMOL software.

The crystal structure of *ba*₃-CcO (Figure 1-3 C) from *T. thermophilus* was first obtained at 2.4 Å (Soulimane *et al.*, 2000) and recently at 1.8 Å resolution (Tiefenbrunn *et al.*, 2011). The *ba*₃-CcO is composed of three subunits, I, II and IIa. Subunit I consists of thirteen TMHs, which is unique among the HCOs. The 13th helix does not superpose with any helix of the *aa*₃-CcOs. Subunit I binds a heme *b* and heme *a*₃₃-Cu_B binuclear center. Subunit II of *ba*₃-CcO has only one TMH, which corresponds to the second helix of subunit II of *aa*₃-CcO. The hydrophilic domain of subunit II also contains a dinuclear Cu_A center, which is the same as in the A-family HCOs. Subunit IIa is the smallest subunit with one TMH. This helix superposes with the first TMH of subunit II of *aa*₃-CcO (Soulimane *et al.*, 2000).

The X-ray structure of the C-family *cbb*₃-CcO (Figure 1-3 D) from *Pseudomonas stutzeri* was determined at 3.2 Å resolution in 2010, and shows significant structural differences to other HCOs (Buschmann *et al.*, 2010). Since the *cbb*₃-CcO is the major topic of this work, the structure of this enzyme is discussed in Section 1.4.2 in detail.

NOR is closely related to the *cbb*₃-CcOs. The first crystal structure of the bacterial cNOR (Figure 1-3 E) was recently determined consisting of a small NorC and a large NorB subunit (Hino *et al.*, 2010). The NorB catalytic subunit shows strong structural homology to the subunit I of all CcOs. It contains twelve TMHs, two *b*-type hemes and a non-heme iron Fe_B center. Heme *b*₃ and Fe_B form the binuclear active center where the reduction of NO takes place. In contrast to Cu_B of CcOs, Fe_B is coordinated not only by three histidine residues but also by a glutamate residue. The NorC subunit consists of one TMH and a globular hydrophilic domain, which contains a heme *c*. The proposed electron transfer pathway in cNOR from heme *c* to the active site is similar to the pathway of *cbb*₃-CcO, which also has a covalently bound heme *c* in its CcoO subunit. Neither the D- nor the K-proton pathway was found in cNOR (Hino *et al.*, 2010).

The overall structure of qNOR (Figure 1-3 F) is similar to that of cNOR (Matsumoto *et al.*, 2012). However, qNOR is a single-subunit enzyme consisting of fourteen TMHs and an α -helical hydrophilic domain that harbors no heme *c*. The qNOR has a potential hydrophilic channel delivering protons from the cytoplasm to the reaction center (Matsumoto *et al.*, 2012; Salomonsson *et al.*, 2012), whereas cNOR is thought to take the catalytic protons from the periplasmic side (Reimann *et al.*, 2007; Hino *et al.*, 2010).

It should also be noted that one calcium-binding site, which is coordinated by two propionates of heme *b* and *b*₃ in both cNOR and qNOR, is also characteristic for *cbb*₃-CcOs.

1.3 The aa_3 -type cytochrome c oxidase

Since the aa_3 -CcOs are the best-studied members of the HCOs, an introduction regarding the catalytic reaction cycle, electron transfer process and the proton translocation of the aa_3 -CcOs is given in the sections below (1.3.1 – 1.3.3). Unless otherwise mentioned, the numbering system of the aa_3 -CcO from *P. denitrificans* is used.

1.3.1 The catalytic reaction cycle

The aa_3 -CcOs catalyze the reduction of oxygen with a high turnover rate, normally in the range of 400 to 600 e^-/s . During one complete catalytic cycle, the binuclear metal center (heme a_3 iron and Cu_B) undergoes different redox state changes, involving several catalytic intermediates (Figure 1-4). Two of these intermediates, the P (“peroxy”) and F (ferryl) states, were first discovered by Wikström in 1981 by reversing the electron transfer in mitochondria (Wikström 1981). Based on these findings and the subsequent investigation of the proton pumping, the first model of the catalytic cycle was developed, in which proton pumping only occurs during the oxidative phase, i.e., during the transition from P to F and from F to O (oxidized) (Wikström 1989). This model suggested that the first two electron transfer steps (O to E [electronated] and E to O) are not coupled to any proton translocation across the membrane. In 1999, Michel proposed a modified model (Michel 1999) with consideration of the electroneutrality principle (Mitchell and Rich 1994; Rich 1995). By following this principle, each of the four electron transfer steps in the catalytic cycle is accompanied by the uptake of one proton. Moreover, this new model suggested that one proton is already pumped during the transition from O to E state.

Figure 1-4 shows a simplified catalytic reaction cycle of aa_3 -CcO based on Michel’s mechanistic model. In the **O state**, both metal ions in the binuclear center are oxidized and in a ferric/cupric (Fe^{3+}/Cu_B^{2+}) state. Based on the presence of a continuous electron density between both metal ions in the crystal structure of *Paracoccus aa_3-CcO* (Ostermeier *et al.*, 1997), it was proposed that Fe^{3+} and Cu_B^{2+} are coordinated by a water molecule and a hydroxide ion (OH^-), respectively (Michel 1999). A conserved tyrosine residue (Tyr280), which is covalently crosslinked to His276, is present in the protonated state. The one-electron-reduced **E state** is formed, when the first electron arrives in the binuclear center and subsequently reduces Cu_B . Reduction of Cu_B (Cu_B^{2+} to Cu_B^{1+}) is accompanied by the protonation of its bound OH^- ligand, forming a water molecule. After receiving a second electron, the heme a_3 iron is reduced, yielding the ferrous/cuprous (Fe^{2+}/Cu_B^{1+}) **R state**. The transition from E to R is coupled to the translocation of one proton across the membrane. In the following step, molecular oxygen binds to the two-electron reduced binuclear center, leading to the formation of the **A state**. The appearance of a ferrous-oxy adduct in this state

was confirmed by resonance Raman spectroscopy, since a $\text{Fe}^{2+}\text{-O}_2$ stretching band is similar to that observed for oxyhemoglobin and oxymyoglobin (Han *et al.*, 1990; Rousseau and Han 2002). During the binding of O_2 to the heme a_3 iron, two water molecules are released. The A state is unstable and spontaneously rearranges to the next reaction state.

The **P state** (P_M) was originally proposed to be a peroxy intermediate, in which two metal centers in the active site are bridged by a peroxide group (Wikström 1981). However, the P state was redefined as an oxoferryl state ($\text{Fe}^{4+}=\text{O}^{2-}$) with an OH^- bound to Cu_B , as revealed by resonance Raman spectroscopy (Proshlyakov *et al.*, 1996; Proshlyakov *et al.*, 1998). The presence of the oxoferryl species indicates that the dioxygen bond is already broken. This process requires four electrons and one proton; however, the transition from the A to the P state is not coupled to any proton uptake and electron transfer events. Two electrons are provided by the heme a_3 iron (Fe^{2+} to Fe^{4+}), while the third electron is derived from Cu_B (Cu_B^{1+} to Cu_B^{2+}). The fourth electron equivalent and one proton are thought to be donated by the nearby Tyr280, yielding a tyrosine radical. Electron paramagnetic resonance (EPR) studies have been used to support the existence of a free radical in this reaction step (MacMillan *et al.*, 1999), although the radical does not reside on

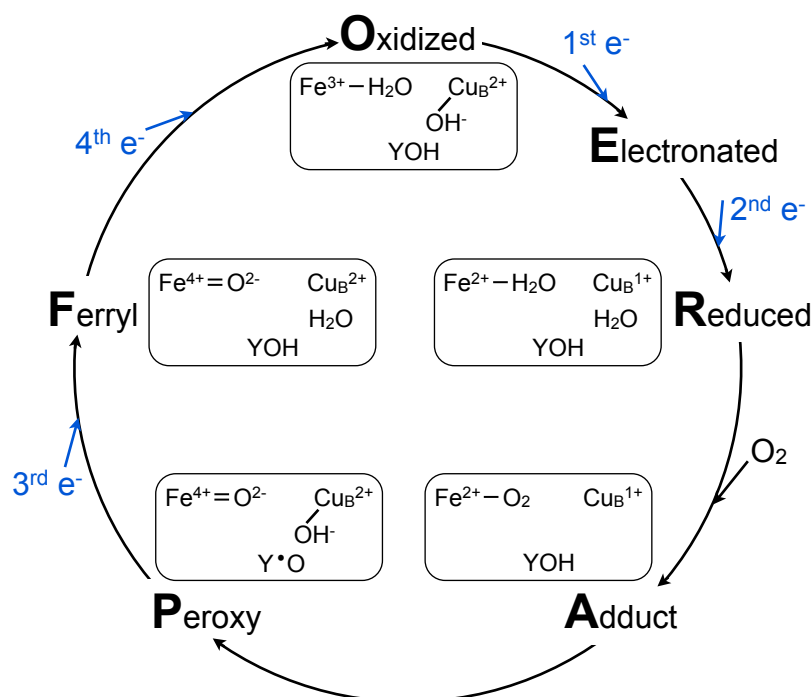


Figure 1-4: Simplified schematic representation of the oxygen reduction reaction at the heme a_3 - Cu_B binuclear center. Reaction intermediates are shown clockwise. The blue arrows indicate the electron input from the cytochromes c to the active site. The black boxes inside the reaction cycle show the detailed electronic state of heme a_3 iron (Fe) and Cu_B , as well as of the tyrosine residue (Y280). The tyrosine radical is indicated by a dot in the “peroxy” state (also called P_M state). Proton translocation and water release during the catalytic cycle are not shown for better clarity. This figure is drawn based on the reaction mechanism proposed by Michel and modified from von der Hocht *et al.*, 2011.

Tyr280 (Budiman *et al.*, 2004; Yu *et al.*, 2011). Because the transition from A to P state is a nonsequential and irreversible process, CcOs catalyze the reduction of oxygen without the formation of any ROS species. The P state can be artificially generated by various methods and has a characteristic absorption at around 610 nm in the P-minus-O difference spectrum (Chance *et al.*, 1975; Bickar *et al.*, 1982; von der Hocht *et al.*, 2011). The **F state** is formed upon the transfer of a third electron from an external electron donor to the active site, followed by the reduction of the tyrosine radical. The F state is also an oxoferryl intermediate with an absorption maximum at 580 nm in the F-minus-O difference spectrum. In Michel's scheme, the P to F transition is associated with pumping of two protons across the membrane. In the last step of the catalytic cycle, the transfer of the fourth electron leads to the resumption of the O state and to the pumping of one proton. Other cycles have been proposed, in which one proton is pumped upon each electron transfer to the active site (Bloch *et al.*, 2004; Wikström and Verkhovsky 2007).

1.3.2 Electron transfer process

The reduction of one molecule of oxygen to water requires four electrons. The electrons are transferred one at a time from cytochrome *c* to the initial electron acceptor (Cu_A) of $aa_3\text{-CcO}$. The rate-limiting step in the electron transfer process is the formation and dissociation of the cytochrome *c* and CcO complex (Antalis and Palmer 1982). The interaction between cytochrome *c* and CcO has been described to follow a two-step model (Maneg *et al.*, 2004; Richter and Ludwig 2009). In the first step, the electrostatic surface potential is responsible for the long-range recognition and orientation of both proteins. The subunit II of $aa_3\text{-CcO}$ has a set of acidic residues on the surface of its hydrophilic domain. Mutagenesis data indicated that these negatively charged residues are involved in initial docking by forming electrostatic interactions with positively charged residues on the surface of cytochrome *c* (Witt *et al.*, 1995; Witt *et al.*, 1998; Zhen *et al.*, 1999). In the second step, hydrophobic interactions play a major role in short-range optimization of the interaction geometry between both redox partners (Witt *et al.*, 1998). One tryptophan residue (Trp121) on the subunit II has been identified as the electron entry site in the $aa_3\text{-CcO}$ (Witt *et al.*, 1998; Drosou *et al.*, 2002). Once a stable complex is formed, an electron can be rapidly transferred from cytochrome *c* to Cu_A with a time constant of $\sim 15 \mu\text{s}$ (Hill 1991).

Subsequently, the electron is transferred from Cu_A to heme *a* at a distance of 19.5 Å. The intramolecular electron transfer rate between these two cofactors has been studied by using different electron injection techniques. It has been established that this process occurs with a time constant of $\sim 10 \mu\text{s}$ in bacterial CcOs (Konstantinov *et al.*, 1997; Zaslavsky *et al.*, 1998; Verkhovsky *et al.*, 2001) and about 50 to 100 μs in mitochondrial enzymes (Kobayashi *et al.*, 1989; Farver *et al.*, 2000). In the next stage, electron transfer between heme *a* and a_3 was shown to

have a time constant of about 3 μ s (Oliveberg and Malmström 1991; Verkhovsky *et al.*, 1992). However, this rate of electron transfer is much slower than that calculated from the edge-to-edge distance between two hemes (~ 5 Å) using electron tunneling theory in biomolecules (Page *et al.*, 1999). Furthermore, ultra-fast electron transfer from heme *a* to *a*₃ has been proposed (Verkhovsky *et al.*, 2001) and the rate was later determined to be 1.2 ns using femtosecond absorption spectroscopy (Pilet *et al.*, 2004). The last step of electron transfer is from heme *a*₃ to Cu_B. Since this step is coupled to proton translocation, it was shown that the electron transfer is in the range of several hundreds of microseconds (Belevich *et al.*, 2007).

1.3.3 Proton pathway and proton pumping

During one reaction cycle, four protons are consumed upon formation of two water molecules (chemical protons) and four additional protons are translocated from the N side to P side across the membrane (pumped protons). The proton transfer requires a hydrogen-bonded network within the hydrophobic interior of the CcOs. Previous mutagenesis studies suggested the presence of two independent proton pathways inside subunit I (Hosler *et al.*, 1993; Fetter *et al.*, 1995), which was confirmed later by the crystal structure of *aa*₃-CcOs. According to the Grotthuss mechanism (Grotthuss 1806), protons can rapidly move along the hydrogen-bonded chain of water molecules and amino acid residues within these proton channels (Nagle and Tristram-Nagle 1983).

The D-pathway is named after a highly conserved Asp124, which constitutes the cytoplasmic entry point of this pathway. A single mutation of this residue (D124N) strongly inhibits the activity and proton translocation (Fetter *et al.*, 1995; Pfitzner *et al.*, 1998). This pathway proceeds from Asp124 via a series of conserved polar residues (Asn113, Asn131, Asn199, Tyr35, Ser189 and Ser193) to highly conserved Glu278 (Pfitzner *et al.*, 2000). Inside the cavity between Asp124 and Glu278 up to eleven crystallographic water molecules have been observed (Qin *et al.*, 2006; Koepke *et al.*, 2009). Since the D-pathway is responsible for the translocation of all pumped protons and at least two chemical protons, the side chain of Glu278 was considered to be the branching point for the protons to be transferred either to the binuclear center or to the loading site for proton pumping (Wikström *et al.*, 2003). Mutagenesis studies on Glu278 confirmed its importance for the proton pumping (Svensson-Ek *et al.*, 1996; Ädelroth *et al.*, 1997; Verkhovskaya *et al.*, 1997). Interestingly, mutation of Asn131 to Asp produces an uncoupled variant, which retains its oxygen-reducing activity but loses the proton-pumping ability (Pfitzner *et al.*, 2000; Siletsky *et al.*, 2004). It has been shown that this variant (N131D) shows an increase in the p*K*_a of Glu278 from 9.4 to 11.0 (Namslauer *et al.*, 2003). In addition, a conformational change of the Glu278 side chain was also reported for this variant (Dürr *et al.*, 2008).

The K-pathway, named after an essential lysine residue (Lys354), leads directly to the binuclear center via the highly conserved residues Lys354, Thr351 and Tyr280. The K-pathway is shorter than the D-pathway, and only two internal water molecules are visible in the crystal structures (Koepke *et al.*, 2009). The importance of Lys354 is supported by the observation that mutation of this residue completely abolished the enzymatic activity (Hosler *et al.*, 1996; Konstantinov *et al.*, 1997). It has been concluded that at least one chemical proton is taken up by the K-pathway in the reductive phase of the reaction cycle, which is important for the initial reduction of the metal center and subsequent oxygen binding (Ruitenbergh *et al.*, 2000).

In addition to the D- and K-pathway, a third proton pathway (H-pathway) has been suggested based on the crystal structure of bovine mitochondrial *aa₃-CcO* (Yoshikawa *et al.*, 2006; Shimokata *et al.*, 2007). However, the existence of this alternative H-pathway has been excluded from the bacterial *aa₃-CcOs*, since mutations in this region showed no functional influence on proton translocation (Pfitzner *et al.*, 1998; Lee *et al.*, 2000).

1.4 The *cbb₃*-type cytochrome *c* oxidase

1.4.1 Distribution of *cbb₃-CcOs*

The *cbb₃-CcOs*, comprising more than 20% of the HCOs, are predominantly found in proteobacteria (Pitcher and Watmough 2004). The *cbb₃-CcO* was first identified as gene product of the *fixNOQP* (*ccoNOQP*) operon in the nitrogen-fixing bacteria *Bradyrhizobium japonicum* (Preisig *et al.*, 1993), *Sinorhizobium meliloti* (Kahn *et al.*, 1993) and *Azorhizobium caulinodans* (Mandon *et al.*, 1994). Four structural genes were initially designated as *fixNOQP* because expression of *cbb₃-CcO* was required for the nitrogen-fixing endosymbiosis with their host legumes under low oxygen conditions. They have been redefined as *ccoNOQP*, since further studies also confirmed the presence of this operon in the non-symbiotic purple photosynthetic bacteria *Rhodobacter capsulatus* (Gray *et al.*, 1994; Thöny-Meyer *et al.*, 1994) and *Rhodobacter sphaeroides* (García-Horsman *et al.*, 1994). Early studies reported that *cbb₃-CcOs* exist exclusively in proteobacteria (Myllykallio and Liebl 2000). More recently, due to a dramatic increase in the number of sequenced bacterial genomes, a detailed phylogenetic analysis showed that *cbb₃-CcOs* are found in almost all phyla of bacteria, with the exception of Thermotogales, Deinococcales and Firmicutes (Ducluzeau *et al.*, 2008). To date, no *cbb₃-CcO* was found in archaea (Ducluzeau *et al.*, 2008), which is consistent with the deficiency of enzymes required for the assembly of *cbb₃-CcO* in archaea (Hemp and Gennis 2008). No representatives of *cbb₃-CcO* are present in eukaryotes. But interestingly, three structural genes (*ccoNOP*) were found in the last

free-living mitochondrial ancestor *Midichloria mitochondrii*, however, its *ccoN* gene is split into two open reading frames (Sassera *et al.*, 2011).

Since the first *ccoNOQP* operon had been identified, *cbb₃-CcOs* from several species of Gram-negative bacteria, including *R. capsulatus*, *R. sphaeroides*, *P. denitrificans*, *B. japonicum*, *Helicobacter pylori*, *Campylobacter jejuni*, *Vibrio cholera* and *Pseudomonas stutzeri* (Pitcher and Watmough 2004; Chang *et al.*, 2010), were isolated and studied. In some human pathogens, e.g., *H. pylori* (Tomb *et al.*, 1997), *C. jejuni* (Parkhill *et al.*, 2000), *Neisseria meningitidis* (Deeudom *et al.*, 2006) and *Neisseria gonorrhoeae* (Chung *et al.*, 2008), *cbb₃-CcO* is the only HCO encoded by the genome. Due to its high affinity for oxygen, it has been suggested that the *cbb₃-CcO* is essential for pathogenic bacteria during the colonization of host tissues under oxygen limiting conditions. Since mammalian cells do not have any *cbb₃-CcO*, it becomes a potential drug target for these human pathogens.

1.4.2 Subunit composition and structure of *cbb₃-CcOs*

Compared to the A- and B-family HCOs, *cbb₃-CcOs* feature a distinctly different subunit composition. The canonical *cbb₃-CcO* is composed of four transmembrane subunits encoded by the *ccoNOQP* operon, namely, CcoN, CcoO, CcoQ and CcoP. CcoN is the catalytic subunit, which is homologous to subunit I of the A- and B-family HCOs. CcoO and CcoP are heme-containing subunits that are only found in *cbb₃-CcO*. CcoQ is a small, membrane-spanning subunit and its function is less characterized.

Recently, the crystal structure of *cbb₃-CcO* from *P. stutzeri* ZoBell has been determined at 3.2 Å resolution (Buschmann *et al.*, 2010). This structure revealed that although the catalytic subunit of *cbb₃-CcO* shares similar features to the A- and B-family HCOs, significant differences considering electron transfer and proton translocation were observed (Figure 1-5). So far, only the enzyme purified from the native membrane of *P. stutzeri* ZoBell has been reported to yield crystals (Urbani *et al.*, 2001; Buschmann *et al.*, 2010).

CcoN, the largest subunit with a molecular mass of 53 kDa, contains twelve TMHs, which span the periplasmic membrane with both N- and C-termini close to each other in the cytoplasm. The overall structure of CcoN follows the architecture of the catalytic subunits of other members among HCOs, although the sequence identity between CcoN and subunit I of A- and B-family enzymes is low (< 20%). CcoN contains a low spin heme *b* and a binuclear center formed by a high spin heme *b₃* and a copper (Cu_B) ion (Varotsis *et al.*, 1995; Pinakoulaki *et al.*, 2002). The center-to-center distance between the iron ions of adjacent hemes is 13.1 Å, while the edge-to-edge distance of both hemes is 3.6 Å. Both values are slightly less than those found in

other members of the HCOs². The distance between the iron ion of heme b_3 and Cu_B is 4.6 Å, which is similar to that observed in other enzymes. The six histidine residues involved in ligand binding of two hemes and Cu_B are conserved in all HCOs. The hexa-coordinated iron center in low spin heme b is axially ligated to His60 and His347³ and, additionally, the A- and D-propionates of heme b are stabilized by hydrogen-bonding interactions with Arg57 (Figure 1-6 B).

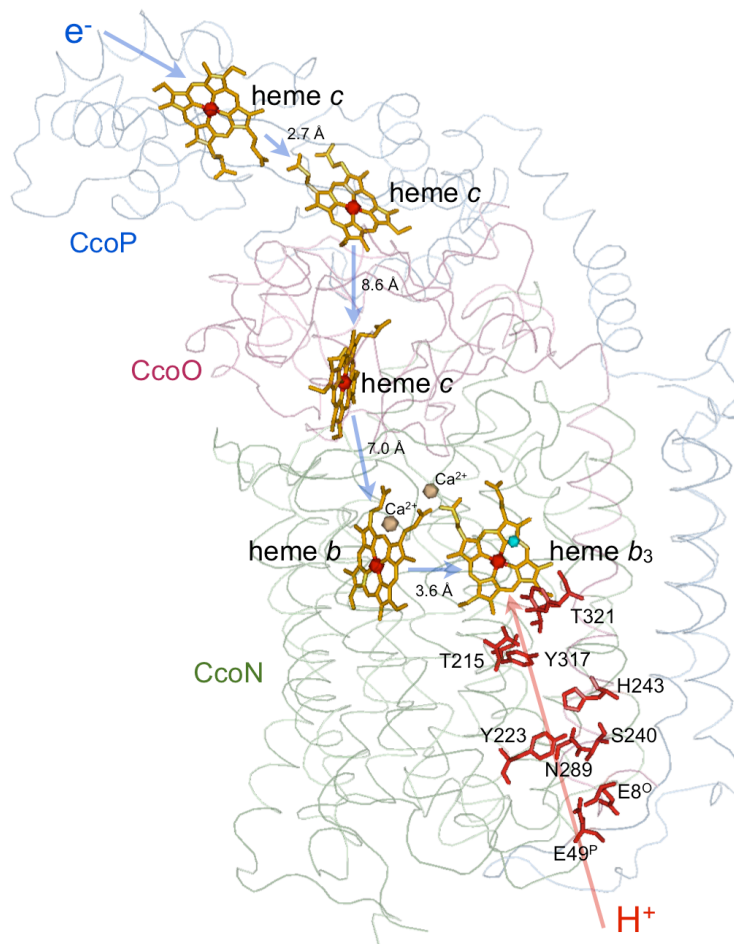


Figure 1-5: Crystal structure of cbb_3 -CcO from *P. stutzeri* ZoBell. Subunit CcoN (green), CcoO (red) and CcoP (blue) are shown in cartoon loop format. Hemes are represented as yellow sticks. Copper, iron and calcium ions are shown as cyan, red and wheat spheres. Electron transfer is indicated by blue arrows. Edge-to-edge distances between hemes are shown. Amino acid residues most likely involved in proton translocation (red arrow) are shown in red. Amino acid numbering refers to cbb_3 -CcO from *P. stutzeri* ZoBell. Coordinates were taken from PDB entry 3MK7. The 3D structural image was generated using PyMOL software.

² The center-to-center distances between two hemes are 13.2 Å for aa_3 -CcO, 13.9 Å for ba_3 -CcO, 14.1 Å for cNOR and 13.7 Å for qNOR. The edge-to-edge distances are 5.2 Å for aa_3 -CcO, 5.2 Å for ba_3 -CcO, 4.3 Å for cNOR and 3.8 Å for qNOR. Distances are measured from PDB entries: 1QLE (aa_3), 1XME (ba_3), 3OOR (cNOR) and 3AYF (qNOR).

³ In this chapter, unless otherwise stated, the residue numbering corresponds to the cbb_3 -CcO from *Pseudomonas stutzeri* ZoBell. Residues in CcoO and CcoP are indicated by superscript letters (O and P).

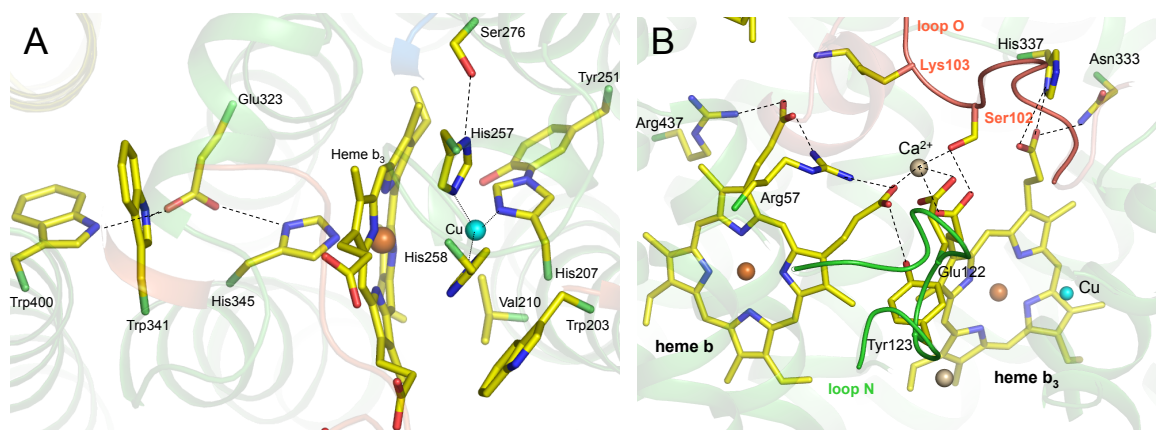


Figure 1-6: A close-up view of heme b and heme b_3 - Cu_B binuclear center. (A) The oxygen-binding site is composed of heme b_3 and Cu_B . At the distal side of heme b_3 , Cu_B is ligated to three histidines. His257 is hydrogen-bonded to Ser276, His207 is covalently cross-linked to Tyr251 and His258 is flanked by Trp203. At the proximal side, the axial ligand (His345) of the heme iron is hydrogen-bonded to Glu323. (B) Interactions between protein and propionate side chains of heme b and b_3 . Both hemes are associated with a Ca^{2+} ion. The A-propionate of heme b_3 is ligated to His337, and both A- and D-propionates of heme b are stabilized by hydrogen-bonding interactions with Arg57. This figure is taken from Buschmann *et al.*, 2010.

Structural analysis revealed several unique features of the binuclear center in *cbb3*-CcO (Figure 1-6). Compared with other active-site hemes of the A- and B-family HCOs, heme b_3 is in a more bent conformation, which might be induced by the absence of the hydroxyethyl farnesyl side chain of heme b_3 (Buschmann *et al.*, 2010). The penta-coordinated iron center of heme b_3 is ligated by His345 at its proximal site and has one coordination position available for the oxygen binding at its distal side. One unique hydrogen bond between the His345 ligand of heme b_3 and a conserved glutamate residue (Glu323) was first suggested by EPR and mutagenesis studies (Rauhamaäki *et al.*, 2009) and further confirmed by X-ray crystallography. This Glu-His-Fe interaction is only found in *cbb3*-CcO and is similar to the Asp-His-Fe triad at the active site of many metalloenzymes, e.g., cytochrome *c* peroxidase. Its function was believed to control the reduction potential of the active site heme (Goodin and McRee 1993; D'Antonio *et al.*, 2011). Another structural difference observed is the noncovalent fixation of D-propionates of heme b and b_3 by coordination to a Ca^{2+} ion in *cbb3*-CcO, whereas the D-propionates of both hemes in A- and B-family CcOs are bound to the positively charged guanidino groups of two conserved arginine residues via salt bridges (Qian *et al.*, 2004; Chang *et al.*, 2012). The presence of the Ca^{2+} ion suggests that it is unlikely that the D-propionates are proton-loading sites for proton pumping in *cbb3*-CcO. In addition, mutagenesis studies indicate that the Ca^{2+} ion is crucial for assembly of the fully functional *cbb3*-complex (Ouyang *et al.*, 2012). Interestingly, interactions between the Ca^{2+} ion and the D-propionates of heme b and b_3 are also observed in cNOR and qNOR (Hino *et al.*, 2010; Matsumoto *et al.*, 2012).

The Cu_B is ligated to three histidine residues (His207, His257 and His258). Like other members of

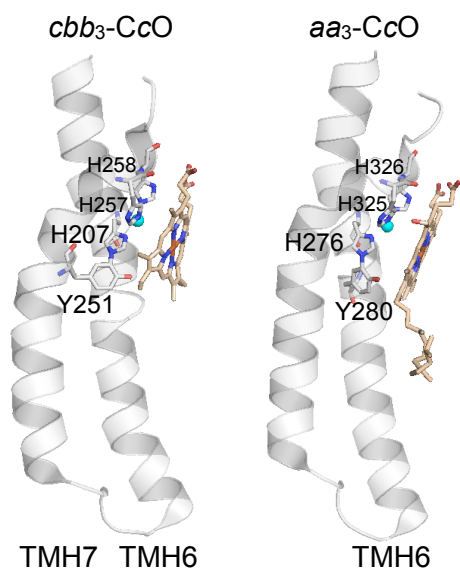


Figure 1-7: Comparison of a copper-coordinated His-Tyr cross-link between *cbb₃*- and *aa₃*-CcO. In *cbb₃*-CcO (left), Y251 and H207 derived from two transmembrane helices (TMH6 & TMH7), whereas Y280 and H276 (*P. denitrificans* numbering) in *aa₃*-CcO originate from the same TMH6.

HCOs, one of these three histidine ligands is cross-linked to a redox active tyrosine residue (Figure 1-7). In *aa₃*-CcOs, this copper-coordinated His-Tyr cross-link is located at the end of the K proton pathway and both residues originate from the same transmembrane helix (TMH6). The covalently modified tyrosine residue is considered to play an important role in the catalytic mechanism by donating a hydrogen atom from its hydroxyl group to the binuclear center (see 1.3.1). This process facilitates the cleavage of the O-O bond, resulting in the formation of a tyrosyl radical in the P_M intermediate (Buse *et al.*, 1999; MacMillan *et al.*, 1999). In *cbb₃*-CcO, this tyrosine is not present in TMH6. However, its functional role is adopted by Tyr251, which

originates from a different TMH and is crosslinked to H276 in TMH6 (Hemp *et al.*, 2005; Hemp *et al.*, 2006; Rauhamäki *et al.*, 2006; Buschmann *et al.*, 2010).

CcoN also contains the channels that are required for the proton and oxygen transfer. The presence of only one proton pathway in *cbb₃*-CcO has been first predicted using structure modeling (Sharma *et al.*, 2006; Sharma *et al.*, 2008) and was later thoroughly confirmed by mutagenesis studies (Hemp *et al.*, 2007) and structural analysis (Buschmann *et al.*, 2010). Like in B-family CcOs, this pathway is positioned analogous to the K-pathway in the A-family CcOs. The “K”-pathway in *cbb₃*-CcOs is composed of a series of ionizable residues that form a hydrogen-bonding network with water molecules (Figure 1-5). However, all essential residues involved in proton translocation are absent in A-family CcOs, and only two tyrosines (Tyr223 and Tyr317) can be found in B-family CcOs. Besides the proton pathway, a hydrophobic membrane cavity is present in the structure, which connects the membrane bilayer surface to the binuclear center. This internal cavity provides a possible pathway for oxygen molecules. Similar cavities are also found in A- and B-family CcOs and NORs (Luna *et al.*, 2008; Hino *et al.*, 2010; Matsumoto *et al.*, 2012). However, the hydrophobic cavity from *aa₃*-CcO is relatively small, which is thought to be

inefficient to mediate the oxygen transfer (Luna *et al.*, 2008).

CcoO is a membrane anchored mono *c*-type cytochrome with a molecular mass of 24 kDa. It consists of one TMH with an intracellular amino terminus and a hydrophilic domain on the periplasmic side of the inner membrane. In the soluble domain, a low spin heme *c* is covalently linked to the protein via thioether bonds and the heme iron is ligated to His69^O and Met137^O. CcoO has little homology to subunit II from other members of HCOs. However, it is structurally related to NORs, since the NorC subunit of cNOR also harbors a heme *c*. Based on the crystal structure, it was suggested that the heme *c* of CcoO mediates the electron transfer from CcoP to heme *b* of CcoN. The edge-to-edge distance between heme *c* and heme *b* is 7.0 Å, which is much shorter than the distance between Cu_A and heme *a* in *aa*₃-CcOs. The so-called loop O of CcoO has strong contacts with the first two α helices and several loops of CcoN. A conserved residue (Ser102^O) within loop O is ligated to the Ca²⁺ ion that coordinates both hemes *b* in CcoN (Figure 1-6 B). This serine residue is functionally replaced by a glycine residue in cNOR and qNOR. There is one hydrophilic cavity located at the periplasmic interface between CcoO and CcoN, which is hypothesized to provide a channel that allows protons and water molecules to leave the catalytic center. This cavity is however only found in *cbb*₃-CcO. CcoO and CcoN together are defined as core complex, since only these two subunits are strictly conserved in all *cbb*₃-CcOs (Ducluzeau *et al.*, 2008) and can form an assembly-intermediate complex (see 1.3.5 for details).

CcoP is composed of two N-terminal TMHs and a C-terminal globular domain, connected by a long helical linker. The molecular mass of CcoP is 35 kDa. Two TMHs of CcoP are linked to each other via a long loop that is in contact with the cytoplasmic region of CcoN. One glutamate residue (Glu49^P) in this loop has been suggested to be the entry of the proton pathway (Buschmann *et al.*, 2010; Lee *et al.*, 2011). In *Rhodobacter* species, the first N-terminal TMH was found to be absent based on the sequence alignment. The C-terminal globular domain contains two conserved CXXCH heme-binding motifs that provide one histidine ligand to the heme iron at its 5th coordination site each. A previous study suggested that one of the two hemes *c* in CcoP has a bis-histidine axial ligation based on spectroscopic analysis (Pitcher *et al.*, 2002). However, the current structure shows that the 6th coordination site of both hemes *c* is occupied by a methionine. Despite the differences in heme coordination, both hemes *c* are predicted to be involved in electron transfer processes. The distal heme *c* can accept an electron from the periplasmic electron donor and subsequently transfers the electron to the proximal heme *c*. Then the electron flows from the proximal heme *c* of CcoP to CcoO and from there to the active site of CcoN (Figure 1-5). In addition to electron binding, one heme *c* of CcoP was observed to bind carbon monoxide (CO) (Pitcher *et al.*, 2002; Pitcher *et al.*, 2003), which is not common in all hexacoordinated heme groups. Based on this phenomenon, CcoP has been proposed to serve as a gas-sensing element

(Pitcher and Watmough 2004) since heme-based-sensor proteins use heme prosthetic groups to perceive environmental gases (Gilles-Gonzalez and Gonzalez 2005). However, recent studies have shown that the binding of CO to CcoP could be an artifact from the solubilization and purification procedures (Huang *et al.*, 2010).

CcoQ is the smallest subunit of *cbb₃-CcO* with a calculated molecular mass of around 7 kDa. It consists of one N-terminal TMH with a hydrophilic stretch at the C-terminus protruding into the cytoplasm. CcoQ has no homology to proteins of known function and is not present in all *cbb₃-operons* (Cosseau and Batut 2004). It is also absent in the current crystal structure of *P. stutzeri cbb₃-CcO*. In *R. sphaeroides*, CcoQ has been proposed to be involved in the transduction of an inhibitory signal, which controls the expression of photosynthesis genes (Oh and Kaplan 1999; Eraso and Kaplan 2000). This hypothesis is however questionable since CcoQ does not contain any cofactors (Pitcher and Watmough 2004). Functional complementation and genetic deletion studies in *R. capsulatus* suggested that CcoQ is associated with CcoP, and is required to stabilize the interaction of CcoP with the CcoNO core complex (Peters *et al.*, 2008). In *R. sphaeroides*, CcoQ appears to protect the core complex from degradation in the presence of oxygen (Oh and Kaplan 2002). In contrast, the *B. japonicum* CcoQ has been reported not to be essential for the complex formation and stabilization (Zufferey *et al.*, 1996).

1.4.3 Functional studies of *cbb₃-CcOs*

In this section, a brief summary concerning functional studies of *cbb₃-CcOs* is given, regarding the following aspects: oxygen reduction activity and affinity for oxygen, NO reduction activity, native electron donors and proton-pumping stoichiometry.

In *P. stutzeri*, the detergent-solubilized *cbb₃-CcO* has been reported to have a turnover number in the range from 250 to 720 e⁻/s (Forte *et al.*, 2001; Urbani *et al.*, 2001; Pitcher *et al.*, 2002). Similar results were also observed from *R. sphaeroides cbb₃-CcO*, which has a turnover number of 200 to 600 e⁻/s (Sharma *et al.*, 2006; Huang *et al.*, 2008; Lee *et al.*, 2011). Although *cbb₃-CcOs* catalyze the reduction of O₂ with an activity comparable to the *aa₃-CcOs*, the *cbb₃-CcOs* exhibit a higher affinity for oxygen than *aa₃-CcO*. For the *cbb₃-CcO* from *B. japonicum*, the Michaelis-Menten constant (*K_m*) for O₂ has been experimentally determined to be 7 nM. This *K_m* value is in the range of the free O₂ concentration within the root nodules (~ 3 to 22 nM), where *B. japonicum* lives symbiotically with the legume host plant (Preisig *et al.*, 1996). The importance of *cbb₃-CcO* to the symbiotic nitrogen fixation has been also reported in other diazotrophs, e.g., *A. caulinodans* (Mandon *et al.*, 1994; Kaminski *et al.*, 1996). Despite the physiological role of *cbb₃-CcO* in the energy supply of cells, it was suggested that this enzyme could serve to protect the O₂-sensitive

nitrogenase by keeping the O_2 concentration at a very low level (Poole and Hill 1997; Bertsova and Bogachev 2002). The cbb_3 -CcOs are also found in many microaerophilic pathogenic bacteria. *C. jejuni*, a major cause of diarrhea and gastroenteritis, possesses two terminal oxidases, cbb_3 -CcO and CIO. The *Campylobacter cbb_3-CcO exhibits a high affinity for O_2 ($K_m = 40$ nM), whereas its CIO is a low affinity enzyme ($K_m = 800$ nM) (Jackson *et al.*, 2007). The presence of a high affinity cbb_3 -CcO may allow this pathogen to colonize the mucous layer of the intestine where the oxygen concentration is low.*

Besides the reduction of O_2 , the cbb_3 -CcOs are found to be able to reduce NO. It has been reported that the *P. stutzeri cbb_3-CcO performs NO reduction with a turnover number of $100 \text{ mol NO} \cdot \text{mol } cbb_3^{-1} \cdot \text{min}^{-1}$ ($\approx 1.7 \text{ e}^-/\text{s}$) and a K_m of $12 \text{ } \mu\text{M}$ (Forte *et al.*, 2001). The cbb_3 -CcO isolated from *R. sphaeroides* has a slightly higher NO reduction activity, which was measured to be between 2 and $10 \text{ e}^-/\text{s}$ (Huang *et al.*, 2008). The NO reduction activity of cbb_3 -CcO is much higher than that reported for other members of CcO and QOX ($0.05 \text{ e}^-/\text{s}$ and $0.5 \text{ e}^-/\text{s}$ for the ba_3 -CcO and caa_3 -CcO from *T. thermophilus*, respectively and $0.005 \text{ e}^-/\text{s}$ for the bo_3 -QOX from *E. coli*) (Giuffrè *et al.*, 1999; Butler *et al.*, 2002). Nevertheless, this activity is lower than that observed for the true NORs (20 to $50 \text{ e}^-/\text{s}$) (Zumft 1997), and this reaction does not lead to the generation of a transmembrane proton gradient across the membrane.*

The scientific finding concerning the physiological electron donors of cbb_3 -CcO is still fragmentary. It was suggested that cytochrome c_4 and c_5 are required for the transfer of electrons to cbb_3 -CcO in *Azotobacter vinelandii* (Rey and Maier 1997; Bertsova and Bogachev 2002) and in two *Neisseria* species (Deeudom *et al.*, 2008; Li *et al.*, 2010), although there are no direct measurements of electron transfer between both proteins. Recent studies performed in *V. cholera* have demonstrated that cytochrome c_4 can support the oxygen reduction activity of cbb_3 -CcO at a rate of at least $300 \text{ e}^-/\text{s}$, while cytochrome c_5 was excluded as electron donor. Due to the lack of saturation of activity as a function of the concentration of cytochrome c_4 , the affinity of this electron donor for its redox partner was not defined (Chang *et al.*, 2010). In *H. pylori*, a human gastric pathogen, cytochrome c_{553} has been identified as the natural electron donor. The kinetics analysis has shown that the cbb_3 -CcO oxidized cytochrome c_{553} with a small K_m of $0.9 \text{ } \mu\text{M}$ and a V_{max} of about $250 \text{ e}^-/\text{s}$ (Koyanagi *et al.*, 2000). Besides cytochromes c , azurin, a natural electron donor for the copper-containing nitrite reductase, is proposed to be able to donate electrons to cbb_3 -CcO (Pitcher and Watmough 2004).

Although only one proton pathway exists in cbb_3 -CcO, the stoichiometry of proton-pumping in this enzyme is still under debate. In the earlier works, measurements of proton pumping using intact cells of *P. denitrificans* and *R. sphaeroides* showed a stoichiometry of $1 \text{ H}^+/\text{e}^-$ (de Gier *et al.*, 1994; Toledo-Cuevas *et al.*, 1998). In contrast, a reduced pumping stoichiometry of 0.2 to 0.4

H^+/e^- was reported for the purified and reconstituted *cbb₃-CcO* from *B. japonicum* (Arslan *et al.*, 2000), and similar results were obtained for *H. pylori cbb₃-CcO* (Tsukita *et al.*, 1999). In a recent study by Han *et al.* (2011), proton pumping was reexamined in three genetically modified bacterial strains (*H. pylori*, *R. sphaeroides* and *R. capsulatus*), in which the *cbb₃-CcO* is the sole terminal oxidase in the respiratory chain. In all cases, *cbb₃-CcOs* pump protons with a stoichiometry ranging from 0.4 to 0.5 H^+/e^- (Han *et al.*, 2011). However, the correctness of this value was questioned in a later study, which showed that an H^+/e^- ratio of *R. sphaeroides cbb₃-CcO* in both intact cells and proteoliposomes is very close to unity (Rauhamäki *et al.*, 2012).

1.4.4 Regulation and expression of *cbb₃-CcOs*

Many bacteria possess a branched respiratory chain consisting of various terminal oxidases, which differ from each other in terms of oxygen affinity, steady-state concentration and enzymatic activity. The *cbb₃-CcOs* are expressed mainly under microaerobic conditions, and their expression is strongly dependent on peripheral oxygen concentrations and growth conditions. Several transcriptional regulation systems, including ANR (FNR), RegB/RegA (PrrB/PrrA, RoxS/RoxR), FixLJ-K and HvrA⁴, are coordinately involved in the regulation of synthesis of *cbb₃-CcOs* (Swem and Bauer 2002; Cosseau and Batut 2004; Arai 2011).

ANR, a homologue of the oxygen-responsive transcriptional regulator FNR of *E. coli*, regulates the gene expression in response to oxygen depletion (Zimmermann *et al.*, 1991; Green and Paget 2004). ANR (FNR) consists of two domains, an oxygen sensory domain that senses intracellular oxygen concentration by a cysteine-ligated $[4Fe-4S]^{2+}$ cluster, and a DNA-binding domain that recognizes a consensus sequence (FNR-box, TTGAT-N⁴-GTCAA) in the promoter region of the target gene. ANR-mediated regulation of *cbb₃-CcO* has been studied in *Rhodobacter* species, which revealed that ANR functions as an activator of *cbb₃-CcO* expression under low oxygen concentrations (Mouncey and Kaplan 1998; Swem and Bauer 2002). Under this condition, the active form of ANR (FNR), which is a homodimer containing one $[4Fe-4S]^{2+}$ cluster per monomeric unit, activates the transcription of *cbb₃-CcO* genes by binding to the FNR-box. Upon exposure to oxygen, the dimeric form $[4Fe-4S]^{2+}$ cluster is converted to a $[2Fe-2S]^{2+}$ cluster, which

⁴ FNR: fumarate and nitrate reduction regulatory protein from *Escherichia coli*;
ANR: FNR homologs, abbreviation for anaerobic regulation of arginine deaminase and nitrate reduction;
RegB/RegA: two-component regulatory system from *Rhodobacter capsulatus*;
PrrA/PrrB: RegB/RegA homologs in *Rhodobacter sphaeroides*;
RoxS/RoxR: RegB/RegA homologs in *Pseudomonas aeruginosa*;
FixLJ: two-component regulatory system in rhizobial species;
FixK: FNR paralogue, a transcriptional regulator in rhizobial species;
HvrA: a photosynthetic activator in *Rhodobacter capsulatus*.

leads to dimer dissociation and in succession switches off the expression of target genes (Green and Paget 2004). Studies performed in *P. aeruginosa* and *P. putida* indicated that ANR is responsible for the microaerobic activation of one of the two *cbb3*-operons, while ANR has no obvious effect on the other operon that lacks the FNR-box (Comolli and Donohue 2004; Ugidos *et al.*, 2008; Kawakami *et al.*, 2010).

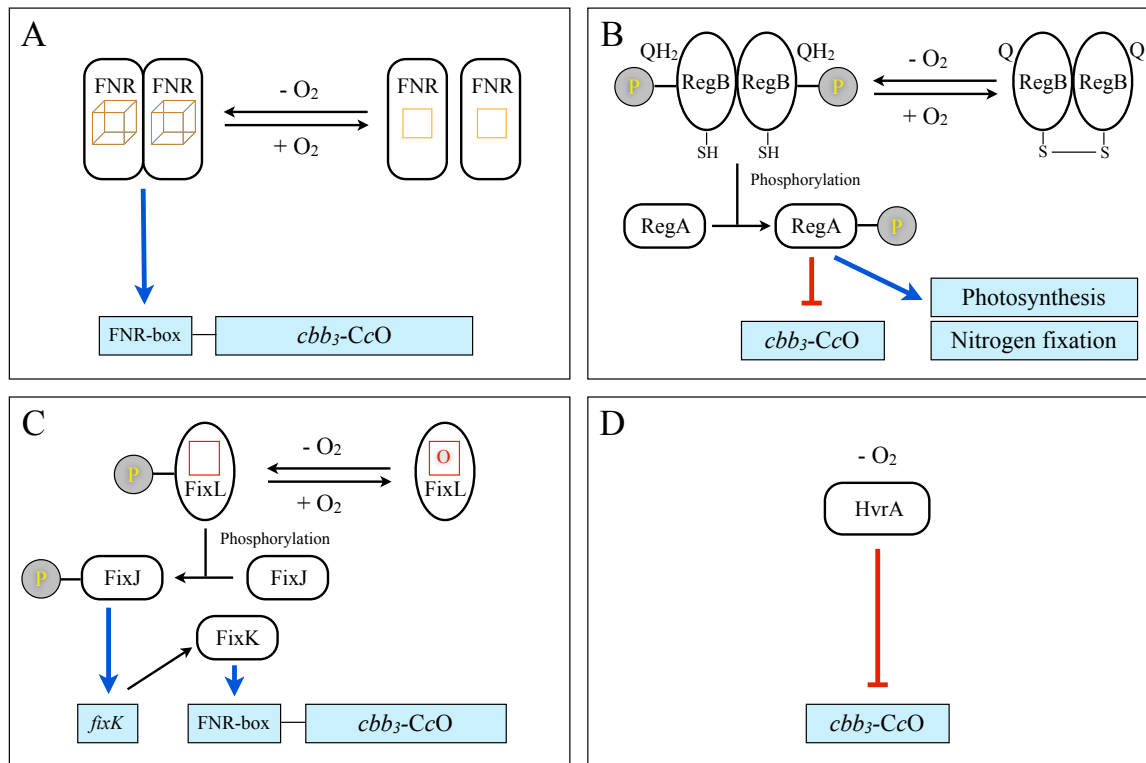


Figure 1-8: Regulation of *cbb3*-gene (*ccoNOQP*) expression. Activation of a target gene (blue box) is represented as blue lines with arrowheads, and inhibition is indicated as red lines with flat heads. (A) ANR (FNR) activates *ccoNOQP* expression under low oxygen concentration. The $[4Fe-4S]^{2+}$ cluster is shown as yellow cube, and $[2Fe-2S]^{2+}$ cluster is shown as yellow square. (B) RegA/RegB two-component regulatory system. The activity of RegB is proposed to be controlled by the redox state of the quinone pool (Q and QH_2). Phosphate groups are shown in yellow. (C) Oxygen-sensing FixLJ-K regulatory system. Under aerobic conditions, a heme-binding region is saturated with molecular oxygen (red). Upon the depletion of oxygen, FixL/FixJ undergoes phosphorylation, and the phosphorylated FixJ activates the expression of FixK, which subsequently activates *ccoNOQP* expression. (D) HvrA functions as a repressor of *ccoNOQP* expression.

The global RegB/RegA (PrrA/PrrB) two-component regulatory system was initially identified in purple photosynthetic bacteria, which has implications for a variety of energy-involving metabolic processes, i.e., photosynthesis, aerobic and anaerobic respiration (Elsen *et al.*, 2004). RegB is a membrane-spanning histidine sensor kinase that is able to detect and respond to the redox status of the ubiquinone pool (Wu and Bauer 2010). RegA is a response regulator containing a helix-turn-helix DNA binding motif. DNase I footprint analysis revealed that RegA regulates the

expression of *cbb₃-CcO* by binding to the promoter region of the *cbb₃-Operon* (Swem *et al.*, 2001). Under anaerobic conditions, RegB protein kinases are phosphorylated and subsequently transfer their phosphate group to RegA. Expression of the *cbb₃-CcO* is repressed by the phosphorylated RegA anaerobically, and activated by the dephosphorylated RegA under aerobic and microaerobic conditions. Based on the studies in *R. sphaeroides*, it has been proposed that electron flow through the *cbb₃-CcO* generates an inhibitory signal resulting in the repression of the PrrB/PrrA- (RegB/RegA homologs) dependent expression of photosynthesis genes under aerobic conditions (O'Gara *et al.*, 1998; Eraso and Kaplan 2000; Kim *et al.*, 2007). In *P. aeruginosa*, the RoxS/RoxR (RegB/RegA homologs) regulon functions as a positive regulator for both isoforms of *cbb₃-CcO* in the exponential and early stationary growth phase, and conversely, represses the expression of *aa₃-CcO* under the same growth conditions (Kawakami *et al.*, 2010). However, the sensing signal of RoxS/RoxR is unknown.

In some rhizobial species, the oxygen-sensing FixLJ-K regulatory system is essential for the regulation of *cbb₃-genes*. FixK is a paralogue of FNR, however, it contains no [4Fe-4S]²⁺ cluster and its activity is controlled on the transcriptional level by the FixL/FixJ two component regulatory system. FixL consists of a heme-binding oxygen sensory domain and a histidine kinase domain (Gilles-Gonzalez and Gonzalez 2005). Under oxygen limitation, the transcription factor FixJ is phosphorylated by the oxygen-inhibitable FixL and activates the transcription of FixK. FixK binds to the FNR-box, thereby activating the synthesis of *cbb₃-CcO* (Batut *et al.*, 1989; Fischer 1996; Rey and Harwood 2010). Besides the rhizobia, the FixLJ-K regulatory system was also found in some non-rhizobial bacteria within the α -proteobacteria (Cosseau and Batut 2004).

In addition to the above mentioned regulation systems, a trans-acting photosynthetic activator, HvrA, also regulates the expression of *cbb₃-CcO*. Under microaerobic and anaerobic conditions, HvrA represses the expression of *cbb₃-CcO* (Swem and Bauer 2002). Furthermore, it has been reported that in *Shewanella oneidensis*, Crp (cAMP receptor protein) is the global regulator controlling expression of the *cbb₃-CcO* (Zhou *et al.*, 2013).

1.4.5 Assembly of *cbb₃-CcOs*

Cbb₃-CcOs are multi-subunit membrane protein complexes that contain various cofactors. Like for other members of HCOs, several processes are required for the assembly of fully functional enzymes, including membrane insertion, maturation of individual subunits, heme biosynthesis, insertion of cofactors, and assembly of subunits (Greiner *et al.*, 2008; Ekici *et al.*, 2011).

In most *cbb₃-CcO* containing bacteria, a *ccoGHIS* (*fixGHIS*) gene cluster is located directly downstream of the *ccoNOQP* operon (Koch *et al.*, 2000). This set of genes was first described in

the nitrogen-fixing bacterium *Sinorhizobium meliloti* (Kahn *et al.*, 1989). Subsequent studies using *B. japonicum* demonstrated that a deletion of the *ccoGHIS* operon leads to the same phenotypes as observed for a *ccoNOQP* deletion mutant: defective symbiotic nitrogen fixation and a decreased CcO activity (Preisig *et al.*, 1996). Although the opposite result has been reported in *A. caulinodans* (Mandon *et al.*, 1993), biogenesis studies of *cbb₃-CcO* from *R. capsulatus* have revealed that gene products of *ccoGHIS* are indeed required for the assembly of *cbb₃-CcO* (Koch *et al.*, 2000; Ekici *et al.*, 2011). Moreover, the expression of *ccoGHIS* is strongly induced under low oxygen concentration, which is similar to the expression of *cbb₃-CcO* (Preisig *et al.*, 1996).

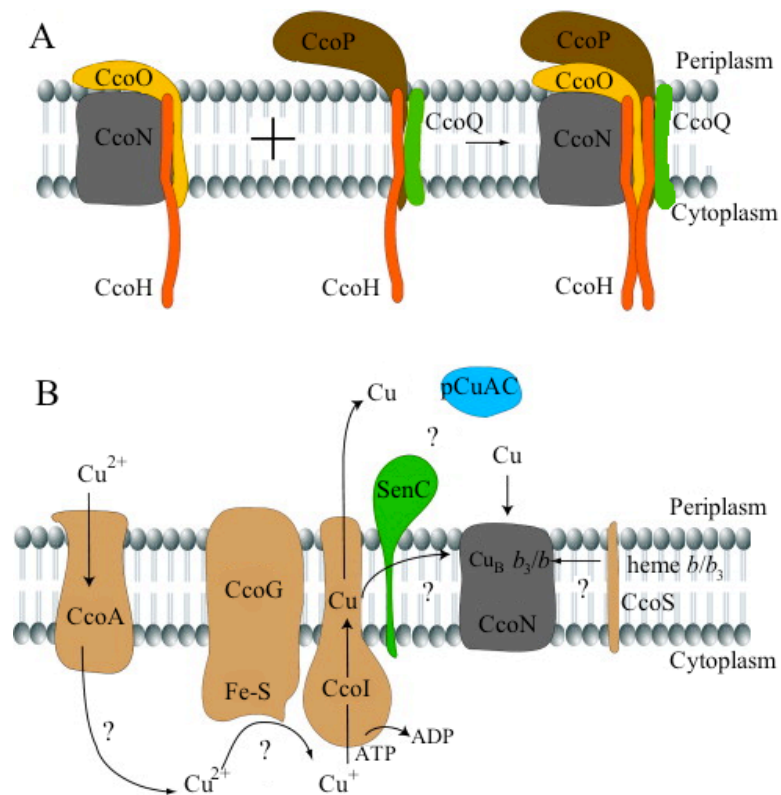


Figure 1-9: Schema of the assembly process for *cbb₃-CcO* in *R. capsulatus*. (A) The single-spanning membrane protein CcoH (red) is involved in the assembly of *cbb₃-CcO* via two assembly intermediates. (B) A model for the maturation of CcoN subunit. The major facilitator superfamily protein CcoA, the ferredoxin-like protein CcoG and the P1-type ATPase CcoI are involved in the copper translocation across the cytoplasmic membrane and copper insertion into the CcoN subunit. Assembly factor CcoS is proposed to mediate the insertion of heme *b* and *b₃*. This figure is reproduced from Ekici *et al.*, 2011.

CcoH, a putative assembly factor, is predicted to consist of a single TMH with the N-terminus facing the cytoplasm (Pawlik *et al.*, 2010). It was found that CcoH is not only present in two assembly intermediate complexes (the larger contains CcoN, CcoO and CcoH; the smaller has CcoP, CcoQ and CcoH), but also in the whole active complex of *cbb₃-CcO* (Figure 1-9 A). Deletion of CcoH resulted in the absence of *cbb₃-CcO* as well as CcoP in membranes, which

indicates that CcoH is essential for the formation and stability of the *cbb*₃-CcO protein complex (Kulajta *et al.*, 2006). It is also hypothesized that a dimerization of the cytoplasmic domain of two CcoHs is responsible for the full assembly of *cbb*₃-CcO (Pawlik *et al.*, 2010).

CcoI is a homologue of the Cu-transporting P-type ATPase CopA (Preisig *et al.*, 1996), and is involved in the copper circulation. It is proposed that the role of CcoI is to deliver Cu to the catalytic center of CcoN, which is the only copper containing subunit in *cbb*₃-CcO. In *R. capsulatus*, CcoI appears to be also required for the assembly of *cbb*₃-CcO, since deletion or mutation of CcoI decreased the steady-state amounts of the *cbb*₃-CcOs (Koch *et al.*, 2000; Kulajta *et al.*, 2006). CcoS is a small membrane protein containing no characteristic sequence motifs. In the absence of CcoS, an inactive form of *cbb*₃-CcO was assembled, which has all the CcoNOP subunits. However, compared to the matured CcoO and CcoP, CcoN was found to have a deficiency of both heme *b* cofactors. This observation therefore suggested that CcoS is required for the heme insertion and maturation of CcoN (Koch *et al.*, 2000). CcoG contains two putative iron-sulfur cluster-binding motifs and five TMHs. Deletion of CcoG has a minimal effect on the assembly of *cbb*₃-CcO (Koch *et al.*, 2000), and it is proposed to perform some unknown functions related to redox sensing and regulation (Neidle and Kaplan 1992; Ekici *et al.*, 2011).

The cytochrome *c* maturation (Ccm) system, containing at least ten membrane-bound proteins (CcmABCDEFGH, CcdA and DsbA/B⁵), is involved in the posttranslational maturation of CcoO and CcoP subunits (Thöny-Meyer 1997; Kranz *et al.*, 2009; Sanders *et al.*, 2010). This process is independent of the maturation of the catalytic subunit CcoN. In addition, several proteins might be also required for the biogenesis of *cbb*₃-CcO, e.g., SenC (Sco1) and CcoA, although their exact functions are not known. SenC, a homolog of the assembly factor Sco1⁶, has been reported to be important for the steady-state stability of *cbb*₃-CcO in *R. capsulatus* (Swem *et al.*, 2005; Lohmeyer *et al.*, 2012), but not in the case of *B. japonicum* (Bühler *et al.*, 2010) and two *Neisseria* species (Seib *et al.*, 2003). CcoA, a major facilitator superfamily-type transporter, appears to control the intercellular copper level and therefore affects the biogenesis of *cbb*₃-CcO (Ekici *et al.*, 2012).

1.5 *Pseudomonas stutzeri*

Pseudomonas stutzeri is a member of the genus of *Pseudomonas (sensu stricto)*, and belongs to the class γ -proteobacteria. *P. stutzeri* cells are phenotypically characterized by Gram-negative non-sporing rods (1 to 3 μm in length and 0.5 μm in width), positive for oxidase and catalase tests, and

⁵ CcdA refers to the cytochrome *c* defective A protein. DsbA/B is disulfide bond formation system.

⁶ Sco1 (synthesis of cytochrome *c* oxidase) is a universal conserved copper chaperone required for the copper insertion into subunit II of *aa*₃-CcOs.

motile by a single polar flagellum. Unlike the species of the fluorescent group of *Pseudomonas*, *P. stutzeri* cannot produce fluorescent pigments. Typically, their genomic DNA has a high G+C content, which ranges from 60 to 66 mol%. DNA–DNA hybridization and 16S rRNA analysis indicated that *P. stutzeri* strains could be assigned into at least 17 genomic groups (genomovars) (Sikorski *et al.*, 2005; Lalucat *et al.*, 2006).

The *P. stutzeri* strains are widely distributed in aquatic and terrestrial habitats. In rare cases, this species has also been isolated as an opportunistic pathogen from humans. Some strains have been studied because of their specific metabolic properties, including nitrogen fixation, nitrification, denitrification and biodegradation of aromatic compounds. They can use a single organic compound as carbon source, e.g., citrate or acetate. The species can grow over a wide range of temperatures (4 to 45 °C). Some deep-sea strains are tolerant to high hydrostatic pressure (up to 100 MPa). All strains are described as facultative anaerobic bacteria that use oxygen as a terminal electron acceptor during aerobic respiration and use nitrate as an alternative electron acceptor during anaerobic respiration (Lalucat *et al.*, 2006).

The first complete genome sequence for *P. stutzeri* (strain A1501) was released in 2008 (Yan *et al.*, 2008). Its genome consists of a single circular chromosome with 4.57 million base pairs (Mb), which is similar in size to the genome of *E. coli* K-12 (4.64 Mb) and smaller than that of *P. aeruginosa* PAO1 (6.26 Mb). To date, six complete genomes of different *P. stutzeri* strains were assembled, while draft genomes were reported for eight other strains (as at April 2013, NCBI Entrez Genome database).

1.5.1 Respiration in *Pseudomonas stutzeri* ZoBell

Pseudomonas stutzeri strain ZoBell (equivalent to ATCC 14405, CCUG 16156) was first isolated from the water column in the Pacific ocean and was originally named *Pseudomonas perfectomarina* (ZoBell and Upham 1944). As mentioned above, this stain performs both aerobic and anaerobic respiration (Figure 1-10).

P. stutzeri ZoBell is a model microorganism for studying the denitrification process that constitutes one important part of the global nitrogen cycle (Zumft 1997). During this process, four metalloproteins are responsible for the four-step sequential reduction of nitrate to molecular nitrogen. Compared to the aerobic respiration process, the nitrogen oxyanions (nitrate and nitrite) and the gaseous nitrogen oxides (nitric oxide and nitrous oxide) are used instead of O₂ as the electron acceptors.

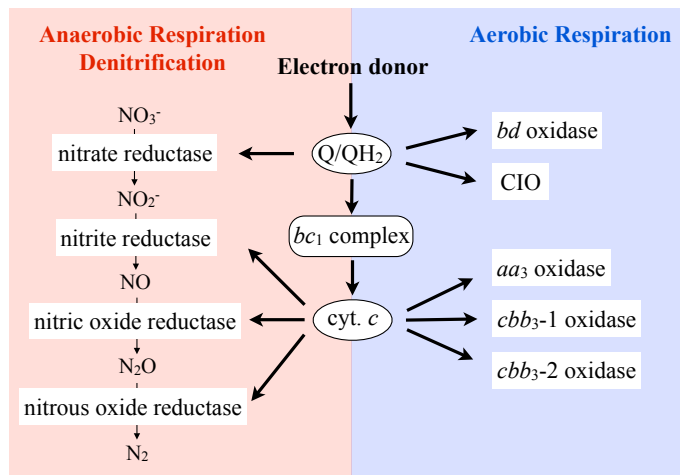


Figure 1-10: Schematic representation of the branched respiratory pathway of *P. stutzeri* ZoBell. This bacterium contains coding regions for five respiratory terminal oxidases. The *bd* oxidase and the cyanide-insensitive oxidase (CIO, *bd*-type) use quinol as a substrate, whereas one *aa*₃-CcO and two *cbb*₃-CcOs use cytochromes *c* as the electron donor. Under anaerobic conditions, denitrification proceeds in four enzymatic reaction steps: nitrate (NO₃⁻) is sequentially reduced to nitrite (NO₂⁻), nitric oxide (NO), nitrous oxide (N₂O) and finally to dinitrogen (N₂).

In *P. stutzeri* ZoBell, the *cbb*₃-CcO is the terminal enzyme in the aerobic respiratory chain. It was purified from the native membrane and was biochemically and structurally studied. However, this bacterium was reported to possess only one *ccoNOQP* operon coding for *cbb*₃-CcO (Pitcher *et al.*, 2002; Cosseau and Batut 2004). More recently, we have reevaluated the sequences and shown the presence of two *cbb*₃-operons in *P. stutzeri* ZoBell (Buschmann *et al.*, 2010). The existence of two isoforms of *cbb*₃-CcO is commonly found in the genus *Pseudomonas*, e.g., in the opportunistic human pathogens *P. aeruginosa* and *P. putida*, but this is rare in other bacteria (Comolli and Donohue 2004; Cosseau and Batut 2004). Previous studies on the differential expression of two *cbb*₃-isoforms from *P. aeruginosa* indicated that they differ from each other in their regulatory properties under different oxygen tensions (Comolli and Donohue 2004; Kawakami *et al.*, 2010; Arai 2011). More specifically, the first isoform (Cbb₃-1, *P. stutzeri* numbering⁷) appeared to be expressed mainly under oxygen-limited conditions, whereas the second isoform (Cbb₃-2) was constitutively expressed from low to high oxygen levels. In addition, the overall expression level of Cbb₃-2 is however three- to six-fold lower than the highest level of Cbb₃-1 found under the microaerobic conditions (Kawakami *et al.*, 2010).

In addition to two *cbb*₃-CcOs, *P. stutzeri* ZoBell has three additional terminal oxidases. The *aa*₃-CcO uses cytochrome *c* as electron donor and the other two, *bd* oxidase and CIO, are quinol

⁷ The numbering system of two *cbb*₃-isoforms in two *Pseudomonas* species is opposite. i.e., the *P. stutzeri* Cbb₃-1 is equivalent to the *P. aeruginosa* Cbb₃-2 and vice versa.

oxidases. This highly branched respiratory chain provides *P. stutzeri* the ability to optimally adapt to various environmental conditions.

1.6 Aim of this work

The aim of this work is to characterize the two isoforms of *cbb*₃-CcO from *P. stutzeri* ZoBell. Previously, only one *cbb*₃-operon was found in *P. stutzeri* Zobell (Pitcher *et al.*, 2002). This work first proved the presence of two *cbb*₃-operons, and confirmed that the genes of both *cbb*₃-operons encode two isoforms of the *cbb*₃-CcO. Although the wild-type Cbb₃-1 has been structural characterized (Buschmann *et al.*, 2010), the isolation of Cbb₃-2 could not be achieved yet due to its high amino acid sequence identity. In order to contribute to a better understanding of the structure and function of *cbb*₃-CcOs, in particular the isoform specificity, and to complement the structural characterization of both *cbb*₃-isoforms, we set out to produce homologously two recombinant *cbb*₃-isoforms.

More specifically, this work aims to: (i) determine the organization and sequences of two operons encoding the *cbb*₃-isoforms in *P. stutzeri* ZoBell; (ii) establish a homologous expression system that consists of *P. stutzeri* *cbb*₃-operon deletion strains and expression vectors carrying the recombinant *cbb*₃-CcOs; (iii) produce, isolate and identify both *cbb*₃-CcOs by chromatography, electrophoresis and mass spectrometry; (iv) biophysically characterize both *cbb*₃-CcOs by UV/Vis spectroscopy, circular dichroism spectroscopy, differential scanning calorimetry and Fourier transform infrared spectroscopy; (v) biochemically and functionally characterize both enzymes by polarographic oxygen measurement; (vi) electrochemically analyze the redox cofactors in both *cbb*₃-CcOs; (vii) identify and characterize the natural electron donors of both *cbb*₃-CcOs; (viii) investigate several highly conserved amino acids near the catalytic site by the mutagenesis approach.

The newly established homologous expression system allows us, for the first time, to characterize and compare the biochemical, biophysical and functional properties of both *cbb*₃-isoforms, and to investigate the differences related to their native substrates, physiological roles and gene expression regulations. Moreover, it opens up the possibility for the ongoing structural investigation of the Cbb₃-2 from *P. stutzeri*.

2 Materials and Methods

In this chapter, only the names of suppliers of all devices, consumptive materials and chemicals are shown. Details of all suppliers and their products are listed alphabetically in Appendix H. For economy of space, primers are listed in Appendix A.

2.1 Materials

2.1.1 Chemicals

If not stated otherwise, all chemicals used in this work were purchased from: Alfa Aesar, Applichem, Carl Roth, Fluka, Gerbu, Merck, Qiagen, Roche, Sigma-Aldrich and VWR.

2.1.2 Bacterial strains

The bacterial strains used in this work are listed in Table 2-1. DNA sequences of the *ccoNO(Q)P* operon from the wild type, Δ Cbb₃-1 strain and Δ Cbb₃-2 strain of *P. stutzeri* ZoBell are shown in Appendix I, J and K, respectively.

Table 2-1: List of bacterial strains.

Strain	Genotype	Reference
<i>E. coli</i> BL21 Star TM (DE3)	F ⁻ <i>ompT hsdS_B(r_B⁻ m_B⁻) gal dcm rne131</i> (DE3)	Invitrogen
<i>E. coli</i> DH5 α	F ⁻ <i>gyrA96</i> (Nal ^r) <i>recA1 relA1 endA1 thi-1 hsdR17</i> (r _K ⁻ m _K ⁺) <i>glnV44 deoR</i> Δ (<i>lacZYA-argF</i>) U169 [Φ 80d Δ (<i>lacZ</i>)M15]	(Hanahan 1983)
<i>E. coli</i> GM2163	F ⁻ <i>dam-13::Tn9</i> (Cam ^r) <i>dcm-6 hsdR2</i> (r _K ⁻ m _K ⁺) <i>leuB6 hisG4 thi-1 araC14 lacY1 galK2 galT22 xylA5 mtl-1 rpsL136</i> (Str ^r) <i>fhuA31 tsx-78 glnV44 mcrA mcrB1</i>	(Palmer and Marinus 1994)
<i>E. coli</i> JM110	<i>rpsL</i> (Str ^r) <i>thr leu thi-1 lacY galK galT ara tonA tsx dam dcm supE44</i> Δ (<i>lac-proAB</i>) [F ⁻ <i>traD36 proAB lacI^qZ</i> Δ M15]	Stratagene
<i>E. coli</i> XL10-Gold [®]	Tet ^r Δ (<i>mcrA</i>) 183 Δ (<i>mcrCB-hsdSMR-mrr</i>)173 <i>endA1 supE44 thi-1 recA1 gyrA96 relA1 lac Hte</i> [F ⁻ <i>proAB lacI^qZ</i> Δ M15 Tn10 (Tet ^r) Amy Cam ^r]	Stratagene
<i>P. stutzeri</i> ZoBell (ATCC14405)	Wild type	(ZoBell and Upham 1944)
<i>P. stutzeri</i> ZoBell Δ Cbb ₃ -1	ATCC14405 Δ <i>ccoNOP-1::Kan^r</i>	this work
<i>P. stutzeri</i> ZoBell Δ Cbb ₃ -2	ATCC14405 Δ <i>ccoNOQP-2::Kan^r</i>	this work

2.1.3 Plasmids

The plasmids used in this work are listed in Table 2-2.

Table 2-2: List of plasmids.

Plasmid	Relevant features	Reference
pACYC177	Amp ^R (Tn3), Kan ^R (Tn903), p15A replication origin	NEB
pACYC184	Cam ^R (Tn9), Tet ^R (pSC101), p15A replication origin	NEB
pBBR1MCS	pBBR1 derivative, multiple cloning site, Cam ^R , T7 promoter, T3 promoter, mobilization gene (mob), pBBR replication origin,	(Kovach <i>et al.</i> , 1994)
pBBR1MCS-2	pBBR1MCS derivative, Kan ^R	(Kovach <i>et al.</i> , 1995)
pBBR1MCS-2- EGFP	pBBR1MCS derivative, Kan ^R , EGFP gene	this work
pBBR1MCS-3	pBBR1MCS derivative, Tet ^R	(Kovach <i>et al.</i> , 1995)
pBBR1MCS-4	pBBR1MCS derivative, Amp ^R	(Kovach <i>et al.</i> , 1995)
pBBR1MCS-5	pBBR1MCS derivative, Gen ^R	(Kovach <i>et al.</i> , 1995)
pBR322	Amp ^R (Tn3), Tet ^R (pSC101), <i>rop</i> gene, pMB1 replication origin	(Sutcliffe 1979)
pBR325	Amp ^R (Tn3), Tet ^R (pSC101), Cam ^R , <i>rop</i> gene, pMB1 replication origin	(Prentki <i>et al.</i> , 1981)
pCM433	Amp ^R , Cam ^R , <i>sacB</i> gene, pBR322 replication origin	(Marx 2008)
pEC86	Tet ^R , Cam ^R , <i>ccmABCDEFGH</i> genes	(Thöny-Meyer <i>et al.</i> , 1995)
pEF-ENTR-LacZ	Kan ^R , T7 promoter, <i>lacZ</i> gene, specific attachment (att) sites, pBR322 replication origin	(Campeau <i>et al.</i> , 2009)
pET-22b(+)	Amp ^R (Tn3), T7 promoter, <i>pelB</i> coding sequence, <i>lacI</i> coding sequence, pBR322 replication origin, fl origin	Novagen
pET-26b(+)	Kan ^R , T7 promoter, <i>pelB</i> coding sequence, <i>lacI</i> coding sequence, pBR322 replication origin, fl origin	Novagen
pET-22-C4	pET-22b(+) derivative, Amp ^R , <i>cycA</i> (cytochrome <i>c</i> ₄) gene	this work
pET-22-C5	pET-22b(+) derivative, Amp ^R , <i>cycB</i> (cytochrome <i>c</i> ₅) gene	this work
pET-22-C551	pET-22b(+) derivative, Amp ^R , <i>nirM</i> (cytochrome <i>c</i> ₅₅₁) gene	this work
pET-22-C552	pET-22b(+) derivative, Amp ^R , <i>nirB</i> (cytochrome <i>c</i> ₅₅₂) gene	this work
pET-26-C551	pET-26b(+) derivative, Kan ^R , <i>nirB</i> (cytochrome <i>c</i> ₅₅₂) gene	this work
pEGFP-N1	Kan ^R , EGFP gene, pUC replication origin, fl origin	Clontech
pJET1.2	Amp ^R , T7 promoter, lethal gene <i>eco47IR</i> , pMB1 replication origin, insertion site for blunt end ligation	Fermentas
pJET-C4	pJET1.2 derivative, Amp ^R , <i>cycA</i> (cytochrome <i>c</i> ₄) gene	this work
pJET-C5	pJET1.2 derivative, Amp ^R , <i>cycB</i> (cytochrome <i>c</i> ₅) gene	this work
pJET-C551+C552	pJET1.2 derivative, Amp ^R , <i>nirM</i> (cytochrome <i>c</i> ₅₅₁) gene, <i>nirB</i> (cytochrome <i>c</i> ₅₅₂) gene	this work
pJET-M6263	pJET1.2 derivative, Amp ^R , amplicon M6263 (<i>ccoNOP-1</i>)	this work
pJET-PCR1	pJET1.2 derivative, Amp ^R , amplicon PCR1	this work
pJET-PCR42	pJET1.2 derivative, Amp ^R , amplicon PCR42	this work

pJET-PCR101	pJET1.2 derivative, Amp ^R , amplicon PCR101 (<i>ccoNOQP-2</i>)	this work
pXH-ΔI-Cm	pXH-B derivative, Kan ^R , homologous flanking arm H1 and H2, Cam ^R as counter-selectable marker	this work
pXH-ΔI-EGFP	pXH-B derivative, Kan ^R , homologous flanking arm H1 and H2, EGFP as counter-selectable marker	this work
pXH-ΔI-SacB	pXH-B derivative, Kan ^R , homologous flanking arm H1 and H2, <i>sacB</i> as counter-selectable marker	this work
pXH-ΔII-Cm	pXH-B derivative, Kan ^R , homologous flanking arm H2 and H3, Cam ^R as counter-selectable marker	this work
pXH-ΔII-EGFP	pXH-B derivative, Kan ^R , homologous flanking arm H2 and H3, EGFP as counter-selectable marker	this work
pXH-ΔII-SacB	pXH-B derivative, Kan ^R , homologous flanking arm H2 and H3, <i>sacB</i> as counter-selectable marker	this work
pXH-ΔI+II-Cm	pXH-B derivative, Kan ^R , homologous flanking arm H1 and H3, Cam ^R as counter-selectable marker	this work
pXH-ΔI+II-EGFP	pXH-B derivative, Kan ^R , homologous flanking arm H1 and H3, EGFP as counter-selectable marker	this work
pXH-ΔI+II-SacB	pXH-B derivative, Kan ^R , homologous flanking arm H1 and H3, <i>sacB</i> as counter-selectable marker	this work
pXH-B	pBBR1MCS-2-EGFP/pACYC184 derivative, Kan ^R , EGFP gene, p15A replication origin	this work
pXH-R	pBBR1MCS-2-EGFP/pBR322 derivative, Kan ^R , EGFP gene, pMB1 replication origin	this work
pXH11	pJET-M6263 derivative, Amp ^R , N-terminal Strep-tag II (<i>ccoN-1</i>)	this work
pXH12	pJET-M6263 derivative, Amp ^R , C-terminal Strep-tag II (<i>ccoN-1</i>)	this work
pXH13	pJET-M6263 derivative, Amp ^R , N-terminal His ₆ -tag (<i>ccoN-1</i>)	this work
pXH14	pJET-M6263 derivative, Amp ^R , C-terminal His ₆ -tag (<i>ccoN-1</i>)	this work
pXH15	pJET-PCR101 derivative, Amp ^R , N-terminal Strep-tag II (<i>ccoN-2</i>)	this work
pXH16	pJET-PCR101 derivative, Amp ^R , C-terminal Strep-tag II (<i>ccoN-2</i>)	this work
pXH17	pJET-PCR101 derivative, Amp ^R , N-terminal His ₆ -tag (<i>ccoN-2</i>)	this work
pXH18	pJET-PCR101 derivative, Amp ^R , C-terminal His ₆ -tag (<i>ccoN-2</i>)	this work
pXH19	pBBR1MCS derivative, Cam ^R , <i>ccoNOP-1</i>	this work
pXH20	pBBR1MCS derivative, Cam ^R , <i>ccoNOQP-2</i>	this work
pXH21	pXH19 derivative, Cam ^R , N-terminal Strep-tag II (<i>ccoN-1</i>)	this work
pXH22	pXH19 derivative, Cam ^R , C-terminal Strep-tag II (<i>ccoN-1</i>)	this work
pXH22-M1	pXH22 derivative, Cam ^R , T215V (<i>ccoN-1</i>)	this work
pXH22-M2	pXH22 derivative, Cam ^R , Y251F (<i>ccoN-1</i>)	this work
pXH22-M5	pXH22 derivative, Cam ^R , Y251A (<i>ccoN-1</i>)	this work
pXH22-M6	pXH22 derivative, Cam ^R , Y251A/I252Y (<i>ccoN-1</i>)	this work
pXH22-M7	pXH22 derivative, Cam ^R , Y317F (<i>ccoN-1</i>)	this work
pXH22-M8	pXH22 derivative, Cam ^R , E323A (<i>ccoN-1</i>)	this work
pXH22-M9	pXH22 derivative, Cam ^R , E323D (<i>ccoN-1</i>)	this work

pXH22-M10	pXH22 derivative, Cam ^R , E323Q (<i>ccoN-1</i>)	this work
pXH22-M11	pXH22 derivative, Cam ^R , N333D (<i>ccoN-1</i>)	this work
pXH22-M12	pXH22 derivative, Cam ^R , N333L (<i>ccoN-1</i>)	this work
pXH22-M13	pXH22 derivative, Cam ^R , H337I (<i>ccoN-1</i>)	this work
pXH22-M14	pXH22 derivative, Cam ^R , H337V (<i>ccoN-1</i>)	this work
pXH22-M16	pXH22 derivative, Cam ^R , Y251A/G211Y (<i>ccoN-1</i>)	this work
pXH22-TEV	pXH22 derivative, Cam ^R , <i>ccoN-1</i> +TEV+Strep-tagII	this work
pXH22-TEV-EGFP	pXH22 derivative, Cam ^R , <i>ccoN-1</i> +TEV+EGFP+Strep-tagII	this work
pXH23	pXH19 derivative, Cam ^R , N-terminal His ₆ -tag (<i>ccoN-1</i>)	this work
pXH24	pXH19 derivative, Cam ^R , C-terminal His ₆ -tag (<i>ccoN-1</i>)	this work
pXH25	pXH20 derivative, Cam ^R , N-terminal Strep-tag II (<i>ccoN-2</i>)	this work
pXH26	pXH20 derivative, Cam ^R , C-terminal Strep-tag II (<i>ccoN-2</i>)	this work
pXH26-TEV	pXH26 derivative, Cam ^R , <i>ccoN-2</i> +TEV+Strep-tagII	this work
pXH26-TEV-EGFP	pXH26 derivative, Cam ^R , <i>ccoN-2</i> +TEV+EGFP+Strep-tagII	this work
pXH27	pXH20 derivative, Cam ^R , N-terminal His ₆ -tag (<i>ccoN-2</i>)	this work
pXH28	pXH20 derivative, Cam ^R , C-terminal His ₆ -tag (<i>ccoN-2</i>)	this work
pXH29	pXH19 derivative, Cam ^R , Lac promoter + <i>ccoNOP-1</i>	this work
pXH36	pXH26 derivative, Cam ^R , Lac promoter + <i>ccoNOQP-2</i>	this work
pXH36-TEV	pXH36 derivative, Cam ^R , <i>ccoN-2</i> +TEV+Strep-tagII	this work
pXH39	pXH26 derivative, Cam ^R , Cbb ₃ -1 promoter + <i>ccoNOQP-2</i>	this work
pXH39-TEV	pXH39 derivative, Cam ^R , <i>ccoN-2</i> +TEV+Strep-tagII	this work
pXH39-TEV-EGFP	pXH39 derivative, Cam ^R , <i>ccoN-2</i> +TEV+EGFP+Strep-tagII	this work

The plasmids pXH22 and pXH39 were used for the expression of recombinant Cbb₃-1 and Cbb₃-2, respectively. Their plasmid maps are shown in Figure 2-1 and Figure 2-2. The location of relevant features is shown below (Table 2-3 and Table 2-4).

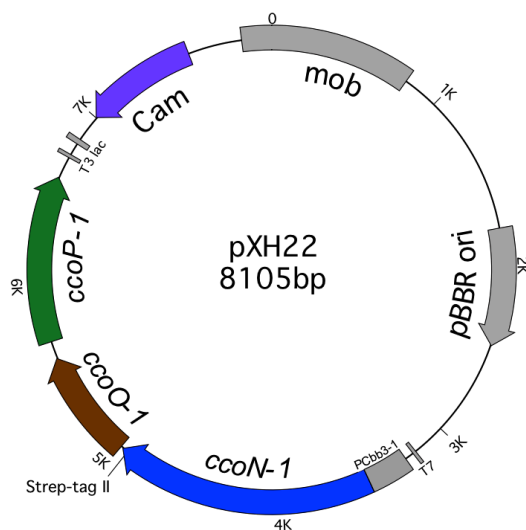


Table 2-3: Location of pXH22 features.

Feature	Locations
mobilization gene (mob)	7938-8105, 1-799
pBBR origin	1793-2455
T7 promoter	3188-3206
Cbb ₃ -1 promoter region	3257-3493
<i>ccoN-1</i>	3495-4949
Strep-tag II	4917-4946
<i>ccoO-1</i>	4963-5574
<i>ccoP-1</i>	5673-6608
T3 promoter	6732-6751
<i>lac</i> promoter	6821-6850
Cam resistance gene	7002-7632

Figure 2-1: Plasmid map of pXH22.

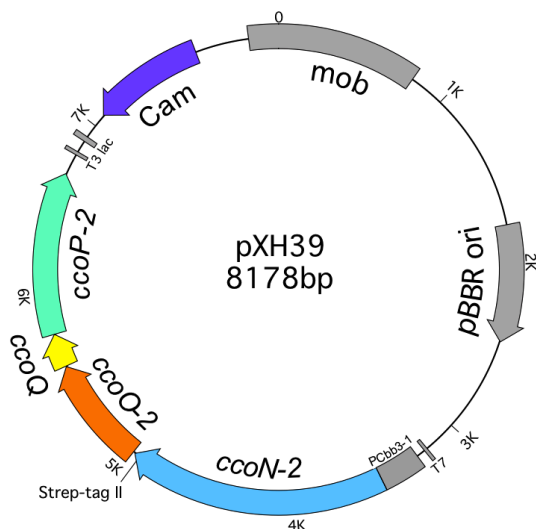


Figure 2-2: Plasmid map of pXH39.

Table 2-4: Location of pXH39 features.

Features	Location
mobilization gene (mob)	8011-8178, 1-799
pBBR origin	1793-2455
T7 promoter	3188-3206
Cbb ₃ -1 promoter region	3257-3494
<i>ccoN-2</i>	3495-4952
Strep-tag II	4920-4949
<i>ccoO-2</i>	4964-5575
<i>ccoQ</i>	5579-5767
<i>ccoP-2</i>	5768-6685
T3 promoter	6805-6824
<i>lac</i> promoter	6894-6923
Cam resistance gene	7075-7705

2.1.4 Microbial media and supplements

All microbiological media (see Table 2-5) were prepared in deionized water and sterilized by autoclaving at 121°C for 20 min. Agar plates were prepared by adding 1.5% (w/v) agar to media before autoclaving. Media supplements (see Table 2-6) were filtered through 0.2 µm membrane filters. Agar plates were supplemented with antibiotics, which were added to the cooled medium (≈ 50°C) after autoclaving. Stock solutions of antibiotics were stored at -20°C.

Table 2-5: List of microbial media.

Medium	Composition
Asparagine medium ^a	0.2% (w/v) L-asparagine, 0.7% (w/v) Na ₃ C ₆ H ₅ O ₇ · 2H ₂ O, 0.2% (w/v) KH ₂ PO ₄ , 0.2% (w/v) MgSO ₄ · 7H ₂ O, 0.01% (w/v) CaCl ₂ · 2H ₂ O, 1% (w/v) NaCl, 1× trace element mix (see below). Adjust pH to 8.0 with NaOH.
Trace element mix (1000×) for asparagine medium	3.2% (w/v) FeCl ₃ · 6H ₂ O, 0.017% (w/v) CuCl ₂ · 2H ₂ O, 0.16% (w/v) NH ₄ NO ₃ , 2.2% (w/v) KBr, 2.0% (w/v) MnCl ₂ · 2H ₂ O, 2.5% (w/v) ZnCl ₂
Lysogeny broth (LB) medium	0.5% (w/v) yeast extract, 1% (w/v) tryptone, 1% (w/v) NaCl. Adjust pH to 7.0 with NaOH.
NZY ⁺ B medium	1% (w/v) NZ amine (casein hydrolysate), 0.5% (w/v) yeast extract, 0.5% (w/v) NaCl, 12.5 mM MgCl ₂ , 12.5 mM MgSO ₄ , 20 mM glucose. Adjust pH to 7.5 with NaOH.
SOC medium	0.5% (w/v) yeast extract, 2% (w/v) tryptone, 10 mM NaCl, 2.5 mM KCl, 10 mM MgCl ₂ , 10 mM MgSO ₄ , 20 mM glucose. Adjust pH to 7.0 with NaOH.
2× YTG medium	1% (w/v) yeast extract, 1.6% (w/v) tryptone, 0.5% (w/v) NaCl, 15% (v/v) glycerol. Adjust pH to 7.0 with NaOH.

^a According to Urbani *et al.* (2001) and further modified by Sabine Buschmann (MPI of Biophysics, Frankfurt am Main) concerning the supplementation of trace elements.

Table 2-6: List of medium supplements.

Medium supplement	Composition
Ampicillin (Amp), 1000×	10% (w/v) Amp in 50% (v/v) H ₂ O + 50% (v/v) glycerol
Carbenicillin (Car), 1000×	5% (w/v) Car in 50% (v/v) H ₂ O + 50% (v/v) EtOH
Chloramphenicol (Cam), 1000×	3.4% (w/v) Cam in EtOH
Gentamicin (Gen), 1000×	1% (w/v) Gen in 50% (v/v) H ₂ O + 50% (v/v) glycerol
Kanamycin (Kan), 1000×	5% (w/v) Kan in 50% (v/v) H ₂ O + 50% (v/v) glycerol
Spectinomycin (Spc), 1000×	10% (w/v) Spc in 50% (v/v) H ₂ O + 50% (v/v) glycerol
Streptomycin (Str), 1000×	2.5% (w/v) Str in 50% (v/v) H ₂ O + 50% (v/v) glycerol
Tetracycline (Tet), 1000×	1.25% (w/v) Tet in H ₂ O
IPTG	1M IPTG in H ₂ O
X-Gal (500×	4% (w/v) X-Gal in DMF

2.1.5 Buffers and solutions

All buffers and solutions used in this work were prepared with ddH₂O. The compositions of buffers and solutions are shown within the text of the corresponding sections.

2.1.6 Enzymes, proteins, markers and kits

All restriction and DNA modifying enzymes with corresponding buffers were purchased from Fermentas and New England Biolabs. Other enzymes, proteins, markers and kits used in this work are listed in Table 2-7.

Table 2-7: List of enzymes, proteins, markers and kits.

Name	Supplier	Application
Albumin Standard (bovine serum)	Pierce	Protein concentration assay
Albumin fraction V (bovine serum, biotin-free)	Carl Roth	Western blot
Avidin (egg white)	Gerbu	Avidin-biotin interaction
BenchMark TM Fluorescent Protein Standard	Invitrogen	Protein standard
Catalase (<i>Micrococcus lysodeikticus</i>)	Fluka	Catalase activity assay
CloneJET TM PCR Cloning Kit	Fermentas	Molecular cloning
Crimson TM Taq DNA Polymerase	NEB	PCR
Cytochrome <i>c</i> (equine heart)	Biomol	Protein activity assay
Cytochrome <i>c</i> (<i>Saccharomyces cerevisiae</i>)	Sigma-Aldrich	Protein activity assay
Deoxyribonuclease I	Roche	Protein purification
DNA Clean & Concentrator TM -25 Kit	Zymo Research	DNA purification
Fast-Link TM DNA Ligation Kit	Epicentre	Molecular cloning
Fluorescent Molecular Weight Marker	Sigma-Aldrich	Protein standard
GeneRuler TM 1 kb Plus DNA Ladder	Fermentas	DNA standard
GeneRuler TM 100 bp Plus DNA Ladder	Fermentas	DNA standard
Gentra [®] Puregene [®] Yeast/Bact. Kit	Qiagen	Genomic DNA extraction

Glucose oxidase (Type X-S, <i>Aspergillus niger</i>)	Sigma-Aldrich	Protein activity assay
G-spin™ Genomic DNA Extraction Kit (for bacteria)	iNtRON	Genomic DNA extraction
In-Fusion® HD Cloning Kit	Clontech	Molecular cloning
Lambda DNA-Mono Cut Mix	NEB	DNA standard
Lysozyme (egg white)	Fluka	Protein purification
NativeMark™ Protein Standard	Invitrogen	Protein standard
PageRuler™ Prestained Protein Ladder	Fermentas	Protein standard
PageRuler™ Prestained Protein Ladder Plus	Fermentas	Protein standard
PeriPreps™ Periplasting Kit	Epicentre	Protein purification
Phire® Hot Start II DNA Polymerase	Finnzymes	PCR
Phusion® High-Fidelity DNA Polymerase	Finnzymes	PCR
ProteoExtract® Digestion kit	Calbiochem	PMF
QIAGEN® Plasmid <i>Plus</i> Midi Kit	Qiagen	DNA extraction
QIAprep® Spin Miniprep Kit	Qiagen	DNA extraction
QIAquick® Gel Extraction Kit	Qiagen	DNA purification
QIAquick® PCR Purification Kit	Qiagen	DNA purification
QuickExtract™ DNA Extraction Solution 1.0	Epicentre	DNA extraction
QuikChange® Lightning Site-Directed Mutagenesis Kit	Stratagene	Cloning and mutagenesis
Ribonuclease A	Roche	DNA extraction
SeeBlue® Plus2 Prestained Standard	Invitrogen	Protein standard
Supercoiled DNA Ladder	NEB	DNA standard
SilverQuest™ Staining Kit	Invitrogen	Protein staining
Zymoclean™ Gel DNA Recovery Kit	Zymo Research	DNA purification

2.1.7 Databases, servers and software

The databases and servers used in this work are listed in Table 2-8.

Table 2-8: List of databases and servers.

Database and server	URL
EMBL	http://www.embl.org/
ExPASy: SIB Bioinformatics Resource Portal	http://www.expasy.org/
HCO: Heme Copper Oxygen reductase classification tool	http://www.evocell.org/hco
Mascot	http://www.matrixscience.com/
Membrane Protein Data Bank MPDB	http://www.mpdb.tcd.ie/
MultAlin	http://multalin.toulouse.inra.fr/
NCBI: National Center for Biotechnology Information	http://www.ncbi.nlm.nih.gov/
PDB: Protein Data Bank	http://www.rcsb.org/
PROMISE	http://bioinf.leeds.ac.uk/promise/
Proteopedia	http://www.proteopedia.org/
Pseudomonas Genome Database	http://www.pseudomonas.com/
ScanProsite	http://prosite.expasy.org/scanprosite/
SignalP Server	http://www.cbs.dtu.dk/services/SignalP/

Signal Peptide Database	http://www.signalpeptide.de/
SOSUI WWW Server	http://bp.nuap.nagoya-u.ac.jp/sosui/
TMHMM Server	http://www.cbs.dtu.dk/services/TMHMM/
UniProt: Universal Protein Resource	http://www.uniprot.org/
Web of Knowledge	http://www.webofknowledge.com/

The software used in this work is listed in Table 2-9.

Table 2-9: List of software.

Software	Version	Application	Company or reference
BioTools	3.1 (build 2.22)	MS data analysis	Bruker Daltonics
Chromas Lite	2.01	Chromatogram editor	Technelysium
Clone Manager	Professional 9	Cloning simulation	Sci-Ed Software
ClustalX	2.1	Multiple sequence alignment	(Thompson <i>et al.</i> , 1997)
Compass/Hystar	1.4	MS data analysis	Bruker Daltonics
Endnote	X5	Reference management	Thomson Reuters
iWork	09 version 4.1	Apple office software	Apple
JalView	2.8	Multiple sequence alignment	(Waterhouse <i>et al.</i> , 2009)
MacVector	11.0.4	Cloning simulation	MacVector
Microsoft Office	2010	Microsoft office software	Microsoft
Origin	8.6.0	Data processing and analysis	OriginLab
Photoshop	CS5 extended 12.0	Image editor	Adobe
PyMOL	1.3	3D molecular visualizer	Schrödinger, LLC
Unicorn	5.11	Äkta control system	GE Healthcare

2.2 Methods

2.2.1 Molecular biological methods

All general molecular biological techniques were performed as described elsewhere (Sambrook and Russell 2001), unless otherwise stated. General cloning was performed using *E. coli* strain DH5 α . The *E. coli dam/dcm*-deficient strains GM2163 and JM110 were used to prepare non-methylated plasmid DNA. The growth of bacteria was monitored by measuring the optical density (OD) of the bacterial culture in an UltrospecTM 2100 pro UV/Vis spectrophotometer (Amersham).

2.2.1.1 Isolation of plasmid DNA

LB media containing appropriate selection antibiotics were inoculated with a single bacterial colony and incubated at 32°C (*P. stutzeri* ZoBell) or at 37°C (*E. coli*) with shaking at 220 rpm overnight. 5 ml and 25 to 50 ml bacterial cultures were used for isolation of high-copy-number or low-copy-number plasmids, respectively. Plasmid DNA was isolated using the Qiagen plasmid mini/midi kit according to the manufacturer's protocols, which are based on a modified alkaline lysis procedure and anion exchange chromatography. The plasmid DNA was stored in ddH₂O at -20°C for long-term storage.

2.2.1.2 Isolation of genomic DNA from *Pseudomonas stutzeri*

For general cloning purposes, the G-spin genomic DNA extraction kit (iNtRON) was used to isolate genomic DNA from 2 ml *P. stutzeri* cultures (OD₅₅₀ = 0.8 to 1.0) according to the manufacturer's protocol for gram-negative bacteria. The typical yield was 5 to 10 μ g/ml culture.

For genome sequencing, high molecular weight genomic DNA was extracted from 0.6 ml *P. stutzeri* cultures (OD₅₅₀ = 1.0) using the Puregene yeast/bact kit (Qiagen). The average yield was 50 μ g/ml culture. The length of extracted genomic DNA was roughly estimated to be between 50 and 100 kb on a 0.5% agarose gel as compared to the Lambda DNA. The genomic DNA was stored in TE buffer (10 mM Tris/HCl, pH 8.0, 1 mM EDTA) at 4°C for long-term storage.

2.2.1.3 Electrophoresis of nucleic acids

Agarose gel electrophoresis was used for the separation of DNA fragments by size. For most analyses, 1% agarose (NEEO ultra quality, Carl Roth) in TBE buffer (Table 2-10) was used for the separation of 0.5 to 10 kb DNA fragments. TAE buffer (Table 2-10) was used to separate genomic and supercoiled DNA. The agarose was boiled in 1 \times TAE/TBE buffer using a microwave until it was completely dissolved. The boiled agarose was casted into a self-made horizontal gel tray and

the gel combs were inserted. Once the gel was polymerized, the gel tray was placed into the gel chamber that was filled with 1× TAE/TBE buffer. DNA samples were mixed 5:1 (v:v) with 6× DNA gel-loading solution (Table 2-10) before loading into the slots of the agarose gel. An appropriate DNA marker was used to determine the size of the DNA in each experiment. Electrophoresis was carried out at 120 V (6 V/cm) for 60 to 90 min at RT until the dyes had migrated an appropriate distance (PowerPac™ Basic power supply, Bio-Rad). The gel was stained by soaking in ethidium bromide aqueous solution (0.0002% [w/v]) after electrophoresis for 10 to 15 min at RT. The DNA band patterns were visualized and photographed using a Bio-Rad gel documentation system with a 302 nm UV transilluminator.

Table 2-10: List of buffers and solution for DNA electrophoresis.

Buffer and solution	Composition
DNA gel-loading solution (6×)	0.25% (w/v) bromophenol blue, 0.25% (w/v) xylene cyanol FF, 15% (w/v) ficoll (type 400)
TAE buffer (50×)	2 M Tris, 1 M HAc, 50 mM EDTA, approx. pH 8.4
TBE buffer (5×)	445 mM Tris, 445 mM boric acid, 10 mM EDTA, approx. pH 8.3

2.2.1.4 Purification of DNA fragments from agarose gels

The DNA fragments were extracted and purified using the Zymoclean gel DNA recovery kit (Zymo Research) according to the manufacturer's protocols. After agarose gel electrophoresis separation, the band with the desired DNA fragment was visualized under UV light (312 nm, Biometra TII transilluminator) and excised from the gel with a clean scalpel. The gel was dissolved in a chaotropic agent, containing guanidine thiocyanate, at 50°C for 10 min. The sample was added to a spin column and washed with 80% ethanol. The DNA fragments were eluted with 8 to 12 µl ddH₂O.

2.2.1.5 Estimation of nucleic acid concentration and purity

The concentration of DNA was spectrophotometrically determined by measuring the absorbance at 260 nm in a NanoDrop® ND-1000 spectrophotometer. One A₂₆₀ unit of double stranded DNA is equal to 50 µg/ml. Two ratios of absorbance, A₂₆₀/A₂₈₀ and A₂₆₀/A₂₃₀ were used to estimate the purity of nucleic acid samples. In general, pure DNA has an A₂₆₀/A₂₈₀ ratio between 1.8 and 2.0 and an A₂₆₀/A₂₃₀ ratio slightly higher than the respective A₂₆₀/A₂₈₀ values between 2.0 and 2.2.

2.2.1.6 Plasmid screening and sizing using single colony lysates

Plasmid DNA was prepared from single bacterial colonies for screening potential recombinant clones. One single *P. stutzeri* colony (0.5 to 1.5 mm diameter) was picked from an appropriate

agar plate and resuspended in 20 μl of Rusconi Mix (25 mM Tris/HCl, pH 7.5, 0.5 mg/ml lysozyme, 0.1 mg/ml RNase, 0.2 mg/ml bromophenol blue, 10% [v/v] glycerol, 25 mM EDTA)⁸. The mixture was incubated for 30 min at RT. The total DNA was extracted by adding 10 μl of phenol/chloroform (1:1) mixture followed by vortexing. The cell debris was removed by centrifugation for 5 min at $16,000 \times g$ (Centrifuge 5415D, Eppendorf) and the supernatant was separated for 120 min at 120 V on a 1% TAE-agarose gel. A supercoiled DNA ladder (NEB) was used to estimate the size of the supercoiled plasmid DNA. This method was used for screening of both low (< 5 kb) and high (> 6 kb) molecular weight plasmids because the *P. stutzeri* genomic DNA was observed as a heavy band between 5 and 6 kb.

2.2.1.7 Polymerase chain reaction

The polymerase chain reaction (PCR) was used in this work to amplify DNA fragments for cloning and screening of constructs. Phusion DNA polymerase (Finnzymes) was used for routine PCR amplifications of variant amplicons (0.5 to 7 kb). Colony PCR was used to screen clones with targeted allelic exchange during the *ccoNO(Q)P* gene disruption experiments. The QuickExtract DNA extraction solution (Epicentre) was used to extract PCR-ready genomic DNA from a single *P. stutzeri* colony. To introduce a point mutation or a small insertion (up to 40 bp) into *ccoN-1* and *ccoN-2* genes, the mutagenesis PCR was carried out using the QuikChange lightning site-directed mutagenesis kit (Stratagene) according to the protocol supplied by the manufacturer.

Table 2-11: PCR master mix.

Component	Amount
nuclease-free H ₂ O	560 μl
5 \times Phusion GC/HF reaction buffer	200 μl
dNTPs mix (2.5 mM for each dNTP)	80 μl
DMSO	30 μl
Phusion DNA polymerase (2U/ μl)	10 μl

For a reproducible and effective PCR amplification, PCR master mix (20 \times 44 μl) was prepared as described in Table 2-11, which is stable at -20°C for at least three months. GC buffer was used for amplification with GC-rich templates, e.g., *P. stutzeri* genomic DNA.

Table 2-12: Reaction mixture for a typical PCR amplification.

Component	Amount	Final concentration
PCR master mix	44 μl	1 \times reaction buffer, 200 μM of each dNTP, 0.02 U/ μl Phusion DNA polymerase, 3% (v/v) DMSO
Primer A (10 μM)	2.5 μl	0.5 μM
Primer B (10 μM)	2.5 μl	0.5 μM
DNA template	1 μl	various concentrations

A typical reaction mixture using the PCR master mix is shown in Table 2-12. In a 50 μl reaction volume, 2-5 ng plasmid DNA or 50-200 ng genomic DNA were used.

⁸ This method is based on several standard procedures: lysozyme digestion, RNase treatment and phenol/chloroform extraction.

Analytical and preparative PCR was carried out in a volume of 10 and 50 μl , respectively. All reactions were set up on ice to avoid nonspecific amplification. PCR was performed using a Biometra T Gradient thermocycler. The typical PCR cycling program is outlined in Table 2-13. Gradient PCR was used in this study to determine the optimum annealing temperature between 63 and 73°C. The PCR products were verified by gel electrophoresis and purified using a gel extraction kit or PCR purification kit for downstream subcloning and sequencing.

Table 2-13: PCR cycling programs.

Routine PCR program and mutagenesis PCR program are shown in blue and orange, respectively.

Cycle step		Temperature	Duration	Number of cycles
1	Initial denaturation	98°C, 95°C	30 s, 2 min	1, 1
2	Denaturation	98°C, 95°C	10 s, 20 s	30-35, 18-20
	Annealing	63-73°C, 60°C	30 s, 10 s	
	Extension	72°C, 68°C	20-35 s/kb, 30 s/kb	
3	Final extension	72°C, 68°C	10 min, 5 min	1, 1
4	Refrigeration	4°C, 4°C	-	-

2.2.1.8 Restriction digestion

The analytical restriction digestion typically contains 50 to 200 ng of plasmid DNA and 5 units of restriction enzyme in a final volume of 10 μl . For a scaled up preparative restriction digestion, 0.2 to 2 μg of plasmid DNA were digested in a final volume of 50 μl . The digestion reaction was performed in the buffer recommended by the manufacturer and incubated for 15 min (FastDigest[®] restriction) or 60 min (conventional restriction) at 37°C (Thermomixer[®] compact, Eppendorf). Subsequently, the DNA fragments were analyzed by gel electrophoresis (see 2.2.1.3). In this study, the restriction enzyme BstBI was often used to analyze pXH1 1-39 constructs and their derivatives.

2.2.1.9 Ligation

The ligation of DNA inserts into plasmid vectors was done using the conventional T4 DNA ligase and the reaction was incubated at 16°C overnight (Thermomixer comfort, Eppendorf). The Fast-Link DNA ligation (Epicentre) was performed for 5 to 15 min at RT. Normally a molar ratio of 3:1 and 5:1 (insert:vector) was used for cohesive-end ligations and blunt-end ligations, respectively. Conversion of double stranded DNA (μg to pmol) was calculated as one basepair equals 660 g/mol. Calf intestinal alkaline phosphatase (CIAP) was used to dephosphorylate the linearized vector DNA to prevent self-ligation. T4 polynucleotide kinase was used to phosphorylate the 5' hydroxyl group of the blunt-end amplicons prior to ligation at 37°C for 20 min.

2.2.1.10 Ligation independent cloning

Ligation independent cloning⁹ was performed for directional cloning without restriction digestion and ligation (Aslanidis and de Jong 1990; Haun *et al.*, 1992; Li *et al.*, 2011). The primers for amplification of target inserts were designed to have lengths between 28 and 35 bases with the addition of 15 bases overlapping the 3' end, which are gene-specific and homologous to the vector ends. The insert was amplified and the vector was linearized by PCR using Phusion DNA polymerase (see 2.2.1.7). The amplified insert and vector were analyzed by gel electrophoresis and afterwards purified from agarose gel (see 2.2.1.3 and 2.2.1.4). The ligation independent cloning reaction was carried out as described elsewhere (Li *et al.*, 2011) or using the In-Fusion HD cloning kit following the supplier's instructions (Clontech), followed by transformation into chemically competent cells (see 2.2.1.12).

2.2.1.11 DNA sequencing

Sequencing of the constructs and PCR products was performed by SeqLab or Eurofin MWG Operon. The obtained sequences were edited using Chromas Lite. Multiple sequence alignment from a group of related sequences was created with MultAlin (Corpet 1988).

Genome sequencing of *P. stutzeri* ZoBell was performed on the Roche 454 Life Sciences Genome Sequencer FLX+ platform (Max Planck Genome Centre Cologne, unpublished data).

2.2.1.12 Preparation of chemically competent cells and transformation

The chemically competent cells for bacterial transformation were prepared according to the rubidium chloride method as described elsewhere (Hanahan 1983). A 5 ml of LB medium was inoculated with a single colony from a rich plate and incubated at 37°C and 220 rpm overnight. 2.5 ml of the overnight culture were subcultured 1:100 (v/v) in 250 ml SOC medium in a 1 liter baffled flask. The culture was incubated at 37°C with shaking at 180 rpm until an OD₆₀₀ of 0.4 to 0.6 was reached¹⁰. The cells were then chilled on ice and centrifuged at 4,400 × g at 4 °C for 15 min (Sigma 4K15 centrifuge, 6 × 40 ml in 50 ml tubes). The supernatant was discarded and the cell pellets were resuspended in 96 ml (6 × 16 ml) RF1 buffer (100 mM KCl/HAc, pH 5.8, 50 mM MnCl₂, 30 mM potassium acetate, 10 mM CaCl₂, 15% [v/v] glycerol) and incubated on ice for 20 min. The cells were then centrifuged again at 1,600 × g at 4 °C for 5 min (Sigma 4K15

⁹ In this work, this cloning strategy is used for two reasons. First, the *ccoNOP-1* operon and *ccoNOQP-2* operon contain the most commonly used restriction sites. Second, this method allows to insert PCR products into a specific location of the vector directly.

¹⁰ The *E. coli* culture was often incubated at 18 to 26 °C overnight prior to the preparation. Incubation at low temperature has been shown to increase the transformation efficiency of *E. coli* cells (Inoue *et al.*, 1990)

centrifuge). The supernatant was again discarded and the cell pellets were resuspended in 9.6 ml (6×1.6 ml) RF2 buffer (10 mM MOPS/NaOH, pH 6.8, 10 mM RbCl, 75 mM CaCl₂, 15% [v/v] glycerol) and incubated on ice for 15 min. The resulting chemically competent cells were distributed into pre-chilled microfuge tubes in 100 μ l aliquots, flash frozen in liquid nitrogen and stored at -80 °C.

Transformation of plasmid DNA into chemically competent cells was performed using the heat shock method. 10 to 50 ng of transforming DNA or 0.1 to 0.2 volumes of the ligation reaction was added to 100 μ l of competent cells. The DNA/cells mixture was incubated on ice for 5 min. To induce heat shock the cells were treated at 42°C for 90 sec (Thermomixer compact, Eppendorf). After the heat shock, the cells were incubated on ice for 10 min followed by the addition of 900 μ l SOC medium. The culture was transferred into a 13 ml culture tube and finally incubated at 37°C and 220 rpm for 60 min to allow the bacteria to recover and to express the antibiotic resistant gene prior to plating.

2.2.1.13 Preparation of electrocompetent cells and electroporation

In this study, electroporation was used to introduce plasmid DNA into *P. stutzeri* cells. The electrocompetent cells were freshly prepared using the modified protocol according to (Choi *et al.*, 2006). A 5 ml of LB medium was inoculated with the glycerol stock of the *P. stutzeri* strain and incubated at 37 °C and 220 rpm until early stationary phase ($OD_{550} = 1.5$ to 2.0). 1 ml of this overnight culture was transferred to a 1.5 ml microfuge tube and the cells were harvested by centrifugation at $16,000 \times g$ at RT for 2 min (Centrifuge 5415D, Eppendorf). The cell pellet was washed twice with 1 ml of 300 mM sucrose at RT followed by centrifugation as described above. The cell pellet was finally resuspended in 100 μ l of 300 mM sucrose. For electroporation, 100 to 500 ng of plasmid DNA were added to 100 μ l electrocompetent cells and mixed in a 1 mm electroporation cuvette (PEQLAB or Bio-Rad). A high voltage electroporation was performed using a Bio-Rad Gene Pulser[®] at 25 μ F, 200 Ω and 2.5 kV. After applying a pulse, 900 μ l of SOC medium was immediately added to the DNA/cells mixture. The culture was transferred to a 13 ml culture tube and incubated at 37°C at 220 rpm for 60 min. Cells were plated on LB agar plates with appropriate antibiotic and incubated at 32°C. The colonies were visible after 2 to 3 days.

2.2.1.14 Preparation of bacterial glycerol stock

The glycerol stock was used to store both *E. coli* and *P. stutzeri* strains at -80°C. 5 ml of LB medium were inoculated with a single colony and incubated at 37 °C and 220 rpm until late exponential phase. Afterwards 500 μ l of 2 \times YTG medium were added to 500 μ l of the overnight culture in a 2 ml cryovial. Glycerol stocks were flash frozen in liquid nitrogen and stored at -80°C.

2.2.2 Biochemical methods

2.2.2.1 Cultivation of *P. stutzeri* ZoBell

For large-scale expression and purification of wt. *cbb₃-CcO* from *P. stutzeri* cells, the culture was grown using a previously published protocol for microaerobic growth (Urbani *et al.*, 2001), which was adapted by Sabine Buschmann (MPI of Biophysics, Frankfurt am Main) concerning the content of trace elements in the asparagine medium (Table 2-5).

Cultivation of *P. stutzeri* for large-scale expression and purification of rec. *cbb₃-CcO* was performed as described below:

1. 50 µl of *P. stutzeri* cells from a glycerol stock were plated on LB agar plate containing 100 µg/ml kanamycin (Kan) and 170 µg/ml chloramphenicol (Cam) and incubated at 32°C overnight (Incubator Biotherm 37, Julabo)¹¹.
2. A bacterial lawn was inoculated in 50 ml of asparagine medium in a 100 ml baffled Erlenmeyer flask (100 µg/ml Kan and 170 µg/ml Cam). This preculture was incubated at 180 rpm and 32°C for 4 to 6 hours (LabShaker, Adolf Kühner).
3. 2 × 25 ml of the preculture was subcultured in 2 × 100 ml of asparagine medium in a 300 ml baffled Erlenmeyer flask (100 µg/ml Kan and 170 µg/ml Cam). The subculture was incubated at 180 rpm and 32°C overnight (Shaker CH-4103, Infors-HT).
4. The main culture consists of 6 × 1 liter of asparagine medium per 5 liter baffled Erlenmeyer flask (50 µg/ml Kan and 68 µg/ml Cam). The main culture was inoculated with 6 × 40 ml of subculture and incubated at 160 rpm and 32°C for 24 hours (Shaker CH-4103, Infors-HT).

The cells were harvested by centrifugation at 10,540 × *g* at 4°C for 30 min (Centrifuge Avanti J-26XP, Rotor JLA-8.1000, Beckman Coulter). A typical cell yield of *P. stutzeri* was 6 to 10 g of wet cells per liter of main culture. The cells were either directly used for membrane preparation or flash frozen in liquid nitrogen for storage at -80°C.

2.2.2.2 Preparation of *P. stutzeri* cell membrane

The preparation of *P. stutzeri* cell membranes was performed at 4°C by using the following procedures¹²:

1. *P. stutzeri* cells were resuspended in ice-cold resuspension buffer I (20 mM Tris/HCl, pH 7.5, 500 mM NaCl, 2 mM MgCl₂, DNaseI and approx. 1 mM Pefabloc) using an

¹¹ We often found that a low yield of protein was obtained, when the glycerol stock was used directly for inoculation of the preculture.

¹² This preparation was partially described by Urbani *et al.* (2001) and modified by Sabine Buschmann.

Ultra-Turrax[®] (T25 basic, IKA). A ratio of 5 to 7 ml buffer I per gram of wet cells was used.

2. Cells were broken by one pass through a French pressure cell at a pressure of 19,000 psi using a pre-chilled cell (40K cell, Thermo Fisher Scientific).
3. After cell disruption, 5 mM EDTA were added to the cell suspension prior to centrifugation.
4. The solution was stirred on ice for 5 min and afterwards centrifuged at $214,000 \times g$ at 4°C (Ultracentrifuge Optima L-90K, Rotor 45 Ti, Beckman Coulter) for 2.5 hours.
5. The supernatant was discarded and the pellets were resuspended in ice-cold resuspension buffer II (20 mM Tris/HCl, pH 7.5, 50 mM NaCl, 0.5 mM EDTA). A ratio of 5 ml buffer II per gram of cells was used. The resulting solution was centrifuged again as described above.

The pellets containing crude membranes were collected and flash-frozen in liquid nitrogen for storage at -80°C prior to solubilization. A typical yield was 0.4 to 0.5 g of crude membranes per gram of wet cells.

2.2.2.3 Solubilization of membrane proteins from *P. stutzeri*

Solubilization was carried out as described elsewhere (Urbani *et al.*, 2001) with slight modifications. The crude membranes were resuspended in solubilization buffer (20 mM Tris/HCl, pH 7.5, 50 mM NaCl, 0.5 mM EDTA, 1 to 2 mM Pefabloc, 12% [v/v] glycerol) at a protein concentration of 3 mg/ml. The total protein concentration was determined using the bicinchoninic acid assay or Bradford protein assay (see 2.2.2.12). For purification of Strep-tagged rec. *cbb₃-CcO*, 0.20 to 0.24 mg/ml avidin was added to prevent nonspecific binding of free biotin and biotinylated proteins to Strep-Tactin[®] resins (see 2.2.2.5). The membrane proteins were solubilized by moderate stirring of the resuspended membranes with 2.5 g n-dodecyl- β -D-maltoside (DDM, GLYCON Biochemicals) per gram of protein at 4°C for 5 to 10 min. Subsequently, the protein solution was centrifuged at $214,000 \times g$ at 4°C for 60 min (Ultracentrifuge Optima L-90K, Rotor 45 Ti, Beckman Coulter). For preparation of rec. *cbb₃-CcO*, the obtained supernatant containing solubilized membrane proteins was filtered through a $0.45 \mu\text{m}$ polyethersulfone (PES) membrane prior to further purification.

2.2.2.4 Purification of wild type *cbb₃-CcO* from *P. stutzeri*

The purification of the 1st isoform of wt. *cbb₃-CcO* from *P. stutzeri* was performed by Sabine Buschmann (MPI of Biophysics, Frankfurt am Main) according to the protocol previously published (Buschmann *et al.*, 2010). Briefly, four chromatographic steps were applied for protein purification: A Q Sepharose High Performance anion exchange column with a linearly increasing NaCl gradient followed by chromatofocusing on PBE94 and immobilized-metal affinity

chromatography (IMAC) on Chelating Sepharose Fast Flow (GE Healthcare). The final column (Q Sepharose High Performance), which was pre-equilibrated with 20 mM Tris/HCl, pH 7.5, 0.02% (w/v) DDM, was eluted with a single step of 150 mM NaCl in equilibration buffer. The resulting eluate was optionally applied to a PD10 desalting column to remove NaCl. The purified 1st isoform of wt. *cbb₃-CcO* in 20 mM Tris/HCl, pH 7.5, 0.02% (w/v) DDM and alternatively 150 mM NaCl was eventually concentrated to a protein concentration of about 15 mg/ml, flash frozen in liquid nitrogen and stored at -80°C.

2.2.2.5 Purification of Strep-tagged recombinant *cbb₃-CcO* from *P. stutzeri*

The purification of Strep-tagged rec. *cbb₃-CcO* from *P. stutzeri* (with or without EGFP fusion) was performed after solubilization at 4°C using the following steps:

1. Affinity chromatography¹³: The solubilizate was loaded onto a 30 ml Strep-Tactin Superflow[®] high capacity column (IBA) which was pre-equilibrated with ST-Q-A buffer (20 mM Tris/HCl, pH 7.5, 100 mM NaCl, 0.5 mM EDTA, 10% [v/v] glycerol, 0.02% [w/v] DDM), at a flow rate of 0.2 to 0.5 ml/min. The unusually low flow rate was necessary to allow sufficient binding of rec. *cbb₃-CcO* to the column. The unbound proteins were washed off the column with ST-Q-A buffer until the absorbance at 280 nm returned to baseline, at a flow rate of 1 to 1.5 ml/min. The bound proteins were eluted with ST-E buffer (ST-Q-A buffer + 5 mM desthiobiotin) at a flow rate of 2 ml/min.
2. Ion exchange chromatography: The eluate from Strep-Tactin column was applied directly onto a 10 ml Q Sepharose High Performance anion exchange column (GE Healthcare) which was pre-equilibrated with ST-Q-A buffer. After washing with 10 column volumes (CV) of ST-Q-A buffer the *cbb₃-CcOs* bound to the matrix were eluted with QS-E buffer (ST-Q-A + 300 mM NaCl). The *cbb₃-CcO* was concentrated using Amicon concentrators (Ultra-4 & Ultra-15, 100K MWCO, Millipore).
3. Size exclusion chromatography: The purified *cbb₃-CcO* was loaded onto a Superdex 200 10/300 GL column connected to an ÄKTA Purifier chromatography system (GE Healthcare). The gel filtration chromatography was performed with ST-Q-A buffer at a flow rate of 0.5 ml/min. Absorbance at 280 nm and 411 nm was monitored and the chromatography fractions containing *cbb₃-CcO* were collected.

¹³ D-Desthiobiotin was purchased from IBA. A single path monitor UV-1 (Pharmacia Biotech) combined with a data chart recorder (BD41, Kipp & Zonen) was used for monitoring protein in column effluents. The Strep-Tactin Superflow high capacity column was regenerated with ST-R buffer (100 mM Tris/HAc, pH 8.0, 1 mM EDTA, 4 mM HABA). HABA can be efficiently removed by washing with 2 CV of ST-S buffer (20 mM Tris/HCl) at pH 7.5 followed by washing with 2 CV of ST-S buffer at pH 10.5.

The purified rec. *cbb*₃-CcO was concentrated to a protein concentration of 100 to 200 μ M and flash frozen in liquid nitrogen for storage at -80°C. A typical protein yield was 2 to 4 mg purified rec. *cbb*₃-CcO per liter of main culture.

In this study, both Strep-tagged isoforms of rec. *cbb*₃-CcO were also purified to a relatively high homogeneous level for the crystallization, and the purification was performed in sequence with Strep-tag affinity chromatography, chromatofocusing, IMAC and ion exchange chromatography as described above (see 2.2.2.4 and 2.2.2.5).

2.2.2.6 Purification of His-tagged recombinant *cbb*₃-CcO from *P. stutzeri*

The purification of His-tagged rec. *cbb*₃-CcO was performed using IMAC on nickel nitrilotriacetic acid (Ni-NTA) resins (Qiagen) in a batch procedure. 3 ml of Ni-NTA agarose resin was pre-equilibrated with 5 CV of Ni-NTA-A buffer (20 mM Tris/HCl, pH 7.5, 300 mM NaCl, 0.02% [w/v] DDM). 10 ml of solubilizate in Ni-NTA-B buffer (Ni-NTA-A buffer + 10 mM imidazole) was added to the resin in a final volume of 20 ml. The protein-resin mixture was gently mixed on a rotator (SB3, Stuart) at 4°C for 2 hours prior to loading into a 5 ml column. The resin was washed with 5 CV of Ni-NTA-B buffer and eluted by gravity flow with a step-gradient of Ni-NTA-B buffer with increasing concentrations of imidazole (20 mM, 50 mM, 100 mM, 150 mM, 250 mM and 350 mM). Elution fractions were collected and analyzed by SDS-PAGE and heme staining (see 2.2.2.13 and 2.2.2.16).

2.2.2.7 Cultivation of *E. coli*

For the heterologous expression and purification of *P. stutzeri* cytochrome *c* (*c*₄, *c*₅ and *c*₅₅₁) from *E. coli* BL21(DE3), cultivation of *E. coli* was performed using the following steps¹⁴:

1. 50 ml LB medium (100 ml unbaffled Erlenmeyer flask), supplemented with 100 μ g/ml Amp and 68 μ g/ml Cam, was inoculated with 100 μ l of *E. coli* cells from a glycerol stock. This preculture was incubated at 160 rpm and 30°C overnight (Lab-Shaker, Adolf Kühner).
2. 3 \times 10 ml of the overnight culture were added into 3 \times 50 ml LB medium with 100 μ g/ml Amp and 68 μ g/ml Cam (100 ml unbaffled Erlenmeyer flask) and incubated at 32°C with shaking at 180 rpm until an OD₆₀₀ of 1.0 to 1.4 was attained (6 to 8 hours in Shaker CH-4103, Infos-HT).
3. 6 \times 2.5 liter of LB medium (5 liter unbaffled Erlenmeyer flask), supplemented with 50 μ g/ml Amp and 34 μ g/ml Cam, were inoculated with 6 \times 20 ml of the subculture and incubated at 32°C with shaking at 160 rpm overnight (16 to 18 hours in Shaker CH-4103, Infos-HT).

¹⁴ IPTG induction was not used in this expression system. For more details, see 3.6.3.

The cells were harvested by centrifugation at $8000 \times g$ at 4°C for 15 min (Centrifuge Avanti J-26XP, Rotor JLA-8,1000, Beckman Coulter). A typical cell yield was 3.5 to 5.0 g of wet cells per liter of main culture. Cells were not frozen to prevent lysis.

2.2.2.8 Small-scale preparation of periplasmic protein from *E. coli*

The periplasmic and spheroplastic proteins were isolated from 2×10^9 *E. coli* cells (1 OD₆₀₀ unit $\approx 10^9$ cells/ml) at different growth phases using the PeriPreps Periplasting kit (Epicentre) according to the manufacture's protocol. The isolation is based on a combination of lysozyme digestion and osmotic shock procedures. The obtained fractions were analyzed by SDS-PAGE followed by heme staining (see 2.2.2.13 and 2.2.2.16).

2.2.2.9 Large-scale preparation of periplasmic protein from *E. coli*

A large-scale preparation of periplasmic protein was performed as described elsewhere (Witholt *et al.*, 1976; Oubrie *et al.*, 2002) with slight modifications. The freshly harvested cells were resuspended in Peri-A buffer (200 mM Tris/HCl, pH 8.0) in a ratio of 10 ml of buffer per gram of wet cells. The suspension was diluted 2-fold with Peri-B buffer (200 mM Tris/HCl, pH 8.0, 1 M Sucrose, 1 mM EDTA, 1 mM Pefabloc) and briefly incubated with 120 $\mu\text{g/ml}$ lysozyme before the osmotic shock. The suspension was diluted 2-fold with ddH₂O, followed by gentle stirring on ice for 30 min. The addition of MgCl₂ for spheroplast stabilization was omitted in favour of stronger protein binding during the first chromatographic step of the protein purification procedure (see 2.2.2.10). Periplasmic fractions were separated from the spheroplasts by centrifugation at $16,000 \times g$ at 4°C for 30 min (Ultracentrifuge Optima L-90K, Rotor 45 Ti, Beckman Coulter).

2.2.2.10 Purification of recombinant *P. stutzeri* cytochrome *c* in *E. coli*

The purification of heterologously expressed *P. stutzeri* cytochrome *c* (*c*₄, *c*₅ and *c*₅₅₁) in *E. coli* was established and performed by Sabine Buschmann (MPI of Biophysics, Frankfurt am Main). Complete purification was carried out at 4°C using the following steps:

1. Ion exchange chromatography: The red periplasmic fraction was diluted 2-fold with ddH₂O to reduce the conductivity of the solution and loaded onto a 80 ml pre-equilibrated Q Sepharose High Performance anion exchange column (GE Healthcare) at a flow rate of 8 ml/min. The column was washed with 2.5 CV equilibration buffer (20 mM Tris/HCl, pH 8.0, 0.5 mM EDTA) and eluted in 6 CV of a linear gradient from 0 to 200 mM NaCl in equilibration buffer. The red coloured fractions containing the desired cytochrome *c* were pooled and concentrated approx. 35-fold using Amicon concentrators (Ultra-15, 10 K MWCO, Millipore).

2. Chromatofocusing: The concentrated protein solution was diluted (1:6) with CF-start buffer (25 mM Tris/HCl, pH 7.5) and loaded onto a 125 ml PBE 94 chromatofocusing column (GE Healthcare) which was pre-equilibrated with degassed CF-start buffer. The proteins were eluted with a pH 7 to 4 gradient with CF-elution buffer (1:9 diluted Polybuffer 74/HCl, pH 4.0, degassed).
3. Size exclusion chromatography: The protein solution was loaded onto a Superdex 75 10/30 GL column, which was pre-equilibrated with 20 mM Tris/HCl, pH 7.5, 150 mM NaCl. The gel filtration chromatography was performed at a flow rate of 0.5 ml/min and absorbance at 280 nm and 415 nm were monitored.

The fractions of the final size exclusion chromatography containing the pure cytochrome *c* of interest were collected and concentrated prior to flash freezing in liquid nitrogen and storage at -80°C.

2.2.2.11 Preparation of reduced cytochrome *c*

The reduced form of cytochrome *c* was prepared by addition of a small amount of sodium dithionite and the excess of sodium dithionite was removed by using two successive PD-10 desalting columns (GE Healthcare), which were pre-equilibrated with 20 mM Tris/HCl, pH 7.5, 150 mM NaCl. The reduction of cytochrome *c* was confirmed by measuring the absorption changes of α , β and Soret band using UV/Vis spectroscopy (see 2.2.3.1). An oxygen electrode was used to ensure the complete removal of sodium dithionite after each preparation (see 2.2.3.2).

2.2.2.12 Determination of protein concentration

Protein concentration was roughly determined by measuring the absorbance at 280 nm in a NanoDrop ND-1000 spectrophotometer (one A_{280} unit = 1 mg/ml). To determine the concentration of total protein during the solubilization and purification precisely, the bicinchoninic acid (BCA) protein assay (Smith *et al.*, 1985) and the Bradford protein assay (Bradford 1976) were used.

The BCA protein assay is based on the colorimetric detection of cuprous ions (Cu^+) from cupric ions (Cu^{2+}) in alkaline solutions of proteins using BCA. The BCA reagent was obtained from Pierce. Bovine serum albumin (BSA) was used to create a calibration curve (0 to 1.0 mg/ml). The reaction was performed in 96-well microplate (Nunc) for 30 min at 37 °C. The absorbance at 562 nm was recorded using a microplate reader (Trista LB 941 Multimode, Berthold) and the protein concentration was calculated by comparison to the standard curve using the software Origin 8.6 (OriginLab).

The Bradford protein assay is based on the binding of the Coomassie dye to protein residues (Arg, Trp, Tyr, His and Phe). Bradford reagent was purchased from Bio-Rad. Cytochrome *c* (equine

heart) was used as a protein standard. The assay was performed using polystyrene cuvettes (Sarstedt) and the absorbance at 595 nm was measured in a spectrophotometer (Spectronic BioMate 3, Thermo).

Protein concentration of purified *cbb*₃-CcO and cytochrome *c* was spectroscopically determined by using the specific extinction coefficients (see 2.2.3.1).

2.2.2.13 SDS-PAGE

Sodium dodecyl sulfate polyacrylamide gel electrophoresis (SDS-PAGE) was used to separate the proteins and protein subunits by size under denaturing conditions. In this work, 12.5% and 15% Tris-glycine gels (Laemmli 1970) were used for the separation of protein subunits of *cbb*₃-CcO. The Tris-glycine gels were cast in the 1.0 mm thick gel cassettes (Invitrogen) as described in Table 2-14. The gels were stored at 4°C. The electrophoresis was carried out with 1× Tris-glycine running buffer at 40 mA/gel at 4°C for 90 min (PowerPac HC power supply, Bio-Rad).

Table 2-14: Components of 12.5% and 15% Tris-glycine gels for SDS-PAGE analysis.

The recipes given below are used for casting 4 mini Tris-glycine gels (8 cm × 8 cm × 1 mm). The acrylamide/bis mixture was obtained from Carl Roth (Rotiphorese[®] Gel 30; acrylamide/bisacrylamide 37.5:1). 10% APS was freshly prepared prior to use.

Chemical component	5% stacking gel	12.5% resolving gel	15% resolving gel
30% (w/v) acrylamide/bis solution	2 ml	12.5 ml	15 ml
4 × upper Tris buffer	3 ml	-	-
4 × lower Tris buffer	-	7.5 ml	5 ml
TEMED	5 µl	15 µl	15 µl
10% (w/v) APS	100 µl	300 µl	300 µl
ddH ₂ O	6.9 ml	9.7 ml	9.7 ml
Total volume	12 ml	30 ml	30 ml

The NuPAGE[®] precast gel system was used according to the manufacturer's instructions (Invitrogen). 4-12% Bis-Tris gels with 1× MES/MOPS running buffer were generally used for the analysis of proteins mixtures. 12% Bis-Tris gels with 1× MES running buffer were used to visualize cytochrome *c* in the low-molecular-weight range during the expression and purification. An appropriate prestained protein ladder was used to estimate the size of protein bands. Gel electrophoresis was performed at 200 V at 4°C for 35 to 50 min.

Gels were stained with Coomassie blue staining solution at RT overnight and destained with Coomassie blue destaining solution until the protein bands were clearly visible. Gels were dried on Whatman 3MM Chr paper at 80°C under vacuum for 90 min (Membrane vacuum pump MP40 & Mididry D62, Biometra).

Table 2-15: List of buffers and solutions for SDS-PAGE.

Buffer and solution	Composition
Coomassie blue staining solution	0.04% (w/v) Coomassie brilliant blue G-250/R-250 in 40% (v/v) MeOH + 50% (v/v) ddH ₂ O + 10% (v/v) HAc
Coomassie blue destaining solution	30% (v/v) EtOH + 60% (v/v) ddH ₂ O + 10% (v/v) HAc
SDS PAGE lower Tris buffer (4×)	3 M Tris/HCl, pH 8.8, 0.4% (w/v) SDS
SDS PAGE MES running buffer (1×)	50 mM MES, 50 mM Tris, 0.1% (w/v) SDS, 1 mM EDTA, approx. pH 7.3
SDS PAGE MOPS running buffer (1×)	50 mM MOPS, 50 mM Tris, 0.1% (w/v) SDS, 1 mM EDTA, approx. pH 7.7
SDS PAGE protein loading solution (5×)	0.25 mM Tris/HCl, pH 8.0, 25% (v/v) glycerol, 12.5% (v/v) β-ME, 7.5% (w/v) SDS, 0.05% (w/v) bromophenol blue
SDS PAGE Tris-glycine running buffer (5×)	250 mM Tris, 950 mM glycine, 0.5 (w/v) SDS
SDS PAGE upper Tris buffer (4×)	0.5 M Tris/HCl, pH 6.8, 0.4% (w/v) SDS

2.2.2.14 BN-PAGE

Blue native polyacrylamide gel electrophoresis (BN-PAGE) was used to separate protein complexes under native conditions (Schägger and von Jagow 1991). BN-PAGE was performed with precast NativePAGE™ 4-16% Bis-Tris gels in an XCell SureLock™ Mini-Cell chamber according to the manufacturer's instructions (Invitrogen). The lower and upper chamber was filled with 600 ml of 1× BN-PAGE running buffer and 200 ml of 1× dark blue BN-PAGE cathode buffer, respectively. The protein samples were mixed with BN-PAGE sample buffer and with 0.5% (w/v, final conc.) Coomassie G-250 before loaded onto the gel. A NativeMark protein standard (Invitrogen) was used to determine the molecular weight of separated proteins and protein complexes. The electrophoresis was performed at 150 V for 60 min and followed by 250 V for 30 min at 4°C (Pharmacia LKB ECPS 3000/150 power supply).

Table 2-16: List of buffers for BN-PAGE.

Buffer and solution	Composition
BN-PAGE cathode buffer (20×)	0.4% (w/v) Coomassie G-250 in H ₂ O
BN-PAGE running buffer (20×)	1 M BisTris, 1 M Tricine, without pH adjustment
BN-PAGE sample buffer (1×)	50 mM BisTris, 6N HCl, 50 mM NaCl, 10% (w/v) glycerol, 0.001% (w/v) Ponceau S, approx. pH 7.2

2.2.2.15 Silver staining

Silver staining was used for sensitive detection (minimum detection limits in the range of 0.3 to 10 ng) of proteins separated by SDS-PAGE, which is based on the binding of silver ions to certain protein residues (Asp, Glu, His, Lys, Cys and Met) and the reduction of silver ions to metallic silver (Switzer *et al.*, 1979; Rabilloud 1990). Silver staining was performed with a SilverQuest Silver staining kit following the supplier's basic staining protocol (Invitrogen).

2.2.2.16 Heme staining

Heme staining was used to detect the heme-associated peroxidase activity of proteins (cytochrome *c*) or protein subunits (CcoO and CcoP of *cbb₃-CcO*), which contain the covalently attached heme *c* (Thomas *et al.*, 1976; Goodhew *et al.*, 1986). This method is based on the peroxidase-catalyzed oxidation of 3,3',5,5'-tetramethylbenzidine (TMBZ) in the presence of hydrogen peroxide (H₂O₂), to yield green-blue colored products (Josephy *et al.*, 1982). After SDS-PAGE, the gels were briefly soaked in heme staining solution III and afterwards incubated in 3 volumes of freshly prepared heme staining solution I and 7 volumes of heme staining solution II with gentle shaking in the dark at RT (Orbital-Rocking Shaker 3011, GFL) for 1 hour. The gels were then washed 2 times with heme staining solution III and stained by the addition of 0.2% (v/v, \approx 60 mM) H₂O₂. After shaking in the dark until the bands were developed (2 to 20 min), the gels were washed with ddH₂O and scanned.

Table 2-17: List of solutions for heme staining.

Buffer and solution	Composition
Heme staining solution I	6.3 mM TMBZ in MeOH
Heme staining solution II	0.25 M sodium acetate/HAc, pH 5.0
Heme staining solution III	40% (v/v) MeOH + 60% (v/v) heme staining solution II

2.2.2.17 Western blot

Western blot was used to detect His-tagged or Strep-tagged rec. *cbb₃-CcO*. Prior to blotting, the polyvinylidene difluoride (PVDF) membrane (Immobilon-P, Millipore) was pre-wetted for 30 sec in methanol and then soaked briefly in ddH₂O. The SDS-PAGE gels, Whatman filter papers and the pre-activated membrane were soaked and equilibrated in transfer buffer for 10 min. The blotting setup was assembled carefully to avoid air bubbles between gel and PVDF membrane. The proteins were transferred from SDS-PAGE gels onto a PVDF membrane using Novex[®] Semi-Dry Blotter (Invitrogen) and the blotting was performed at 20 V for 1 hour at 4°C. A prestained protein ladder was used to check the efficiency of transfer. The gel was post-stained

with Coomassie blue staining solution overnight, while the membrane was stained with Ponceau S solution for 5 min. The membrane was blocked with blocking buffer at 4°C overnight¹⁵. The membrane was washed three times for 5 min each with 1× TBST buffer and afterwards incubated with alkaline phosphatase conjugated antibody at RT for 2 hours¹⁶. Subsequently, the membrane was washed three times for 5 min each with 1× TBST buffer and three times for 5 min each with AP buffer. The colour was developed in staining buffer containing BCIP and NBT and stopped by washing with ddH₂O. The membrane was allowed to air dry and then scanned. In this work, the i-Blot[®] Blotting system (Invitrogen) and the SNAP i.d.[®] system (Millipore) were also used for fast transfer and detection according to the manufacturer's instructions.

Table 2-18: List of buffers and solution for Western blot.

Buffer and solution	Composition
Western blot AP buffer	100 mM Tris/HCl, pH 9.5, 100 mM NaCl, 5 mM MgCl ₂
Western blot blocking buffer	1× TBST buffer + 2% (w/v) BSA
Western blot Ponceau S solution	0.1% (w/v) Ponceau S + 5% (v/v) HAc
Western blot staining buffer	AP buffer + 250 µg/ml BCIP in DMF + 500 µg/ml NBT in DMF
Western blot TBST buffer (10×)	100 mM Tris/HCl, pH 8.0, 1.5 M NaCl, 0.5% (v/v) Tween-20
Western blot transfer buffer	25 mM Tris/HCl, pH 8.3, 150 mM glycine, 10% (v/v) MeOH

¹⁵ A biotin-free BSA was used in the blocking buffer for the detection of Strep-tagged *cbb*₃-CcO.

¹⁶ Alkaline phosphatase conjugated secondary antibody was diluted (1:2000) in 1× TBST buffer with addition of 1% (w/v) BSA. Monoclonal anti-polyHistidine alkaline phosphatase antibody was obtained from Sigma-Aldrich. Anti-Streptavidin alkaline phosphatase conjugate was purchased from Amersham.

2.2.3 Biophysical methods

2.2.3.1 Ultraviolet/visible spectroscopy

Ultraviolet/visible (UV/Vis) spectroscopy was used to determine the concentration and redox state of heme-containing proteins, e.g., CcO and cytochrome *c*. The measurement was performed using a Lambda 35 UV/Vis spectrometer (Perkin Elmer) and 10 mm quartz micro-cuvettes (104.002-B, Hellman). The concentrated heme-containing protein solutions were diluted with an appropriate buffer¹⁷. The absorption of the Soret band was checked to be in the range of 0.5 to 1.2 in all experiments (≈ 0.8 to $2.0 \mu\text{M}$ *cbb*₃-CcO). Absorption spectra were measured between 380 and 650 nm with a scan rate of 120 nm/min (data interval: 0.2 nm; slit width: 1 nm). The specific extinction coefficients, which were used for determination of protein concentrations according to the Beer-Lambert law, are listed in Table 2-19.

Table 2-19: List of used extinction coefficients.

Protein	Extinction coefficient	Reference
<i>cbb</i> ₃ -CcO (<i>P. stutzeri</i>)	$\epsilon_{411} = 5.85 \times 10^5 \text{ M}^{-1}\text{cm}^{-1}$ (oxidized)	(Pitcher <i>et al.</i> , 2003)
Cytochrome <i>c</i> ₄ (<i>P. stutzeri</i>)	$\epsilon_{550} = 44.4 \times 10^3 \text{ M}^{-1}\text{cm}^{-1}$ (reduced)	(Pettigrew and Brown 1988)
Cytochrome <i>c</i> ₅ (<i>P. stutzeri</i>)	$\epsilon_{555} = 19.3 \times 10^3 \text{ M}^{-1}\text{cm}^{-1}$ (reduced)	(Ogawa <i>et al.</i> , 2007)
Cytochrome <i>c</i> ₅₅₁ (<i>P. stutzeri</i>)	$\epsilon_{551} = 27.8 \times 10^3 \text{ M}^{-1}\text{cm}^{-1}$ (reduced)	(Miller <i>et al.</i> , 2000)
Cytochrome <i>c</i> (equine heart)	$\Delta\epsilon_{550} = 19.6 \times 10^3 \text{ M}^{-1}\text{cm}^{-1}$ (reduced minus oxidized)	(Yonetani and Ray 1965)
Cytochrome <i>c</i> (<i>S. cerevisiae</i>)	$\Delta\epsilon_{550} = 21.2 \times 10^3 \text{ M}^{-1}\text{cm}^{-1}$ (reduced minus oxidized)	(Yonetani and Ray 1965)

For measuring the spectroscopic changes in different redox states, air-oxidized (as purified) *cbb*₃-CcO was further oxidized with 10-fold molar excess of potassium hexacyanoferrate(III) and afterwards fully reduced by adding a small amount of sodium dithionite (crystalline powder). The cyanide-induced changes were obtained by addition of 2 mM ($> 1,000$ -fold molar excess) potassium cyanide to the reduced *cbb*₃-CcO and spectra were recorded after different incubation times. Hydrogen peroxide (5, 50 and 500 molar equivalents) was added to the oxidized *cbb*₃-CcO to test the formation of reaction intermediates. The concentration of hydrogen peroxide in solution was determined spectrophotometrically from absorption at 240 nm using a disposable UV/Vis cuvette (UV-Cuvette micro, BRAND) and an extinction coefficient of $\epsilon_{240} = 39.4 \text{ M}^{-1}\text{cm}^{-1}$ (Nelson and Kiesow 1972; Aebi 1984). The obtained spectra were analyzed using the software Origin 8.6.

¹⁷ For *cbb*₃-CcO: 20 mM Tris/HCl, pH 7.5, 100 mM NaCl, 50 μM EDTA, 0.02% (w/v) DDM. For cytochrome *c*: 20 mM Tris/HCl, pH 7.5, 150 mM NaCl.

2.2.3.2 Polarographic oxygen measurement

The oxygen reductase activity of *cbb₃-CcO* was determined polarographically using a Clark-type oxygen electrode (OX-MR, Unisense), based on the diffusion of oxygen through a silicone membrane to an oxygen-sensing platinum cathode, which is polarized against an Ag/AgCl anode (Revsbech 1989). The electrode was polarized at -0.8 V for at least 24 hours prior to use. The electrode was connected to a picoammeter (PA2000 Multimeter, Unisense) to enable the recording of current signals in the pA range. The analog signals were converted into digital signals using an A/D-converter (ADC-216, Unisense) and then recorded with the software (Sensor Trace Basic 2.1) supplied by the manufacturer.

A two-point calibration of the oxygen sensor was performed every day before starting the measurements. An oxygen-free aqueous solution containing 0.1 M NaOH and 0.1 M sodium ascorbate was used to measure the 0% oxygen calibration point, while air-saturated buffer (by stirring for at least 20 min) was used to determine the oxygen saturation. The oxygen concentration in air-saturated buffer was calculated as a function of temperature and salinity (Weiss 1970; Garcia and Gordon 1992). Oxygen consumption was measured in 2 ml glass vials with stirring in a water bath at RT. The reaction vial was filled with standard *cbb₃*-measuring buffer (50 mM Tris/HCl, pH 7.5, 100 mM NaCl, 50 μ M EDTA, 0.02% [w/v] DDM¹⁸) followed by addition of 3 mM sodium ascorbate and 1 mM *N,N,N',N'*-tetramethyl-*p*-phenylenediamine dihydrochloride (TMPD) to a final volume of 600 μ l. The reaction was then initiated by adding 5 pmol of the *cbb₃-CcO*. The reaction was inhibited by the addition of 1 mM potassium cyanide.

In this work, the dependence of oxygen reduction activity on pH and ionic strength was measured by varying the pH from 5.7 to 8.7 and the concentration of NaCl from 0 to 500 mM, respectively. The measurements were also performed with different concentrations of TMPD (0.5 to 4.0 mM) and with different molar ratios of ascorbate to TMPD. Cytochrome *c* was used to investigate the natural electron donor of the *cbb₃-CcO*. The concentrations of cytochrome *c* were varied from 20 to 100 μ M in a reaction volume of 400 μ l.

To compare the catalase activity between wt. *cbb₃-CcO* and rec. *cbb₃-CcO*, oxygen production was determined using the oxygen electrode. The measurements were performed as described elsewhere (Hilbers *et al.*, 2013). Briefly, hydrogen peroxide was added to the standard *cbb₃*-measuring buffer to a final concentration of 600 μ M and the reaction was initiated by adding *cbb₃-CcO* to a final

¹⁸ After addition of ascorbate and TMPD, the pH of the buffer changes approx. 0.1 to 0.5 units depending on the buffer composition and concentration of ascorbate/TMPD. Tris, HEPES and phosphate buffer were tested on their ability to maintain the pH during the measurement, and for effects on the enzymatic activity assay (data not shown). Tris buffer was chosen for all the experiments. The pH values, which are given to describe the activity, are the measured pH of the reaction (\pm 0.05).

concentration of 500 nM.

The steady-state activity of *cbb*₃-CcO was determined from the slope within 10 sec after the reaction initiation. Data processing and analyses were performed with the software Origin 8.6.

2.2.3.3 Circular dichroism spectroscopy

Circular dichroism (CD) spectroscopy was used to compare the secondary structure of wt. *cbb*₃-CcO and rec. *cbb*₃-CcO. CD measurements were performed on a spectropolarimeter (J-810, Jasco) equipped with a Peltier thermoelectric type temperature control system (PTC-423S, Jasco). Far-UV CD spectra were recorded from 190 to 260 nm with a scanning speed of 20 nm/min at RT (data pitch: 0.5 nm; response: 1 sec; band width: 1 nm). The *cbb*₃-CcO proteins were diluted in 200 µl potassium phosphate (KPi) buffer (20 mM KPi, pH7.5, 20 mM NaCl, 0.02% [w/v] DDM) to a final concentration of 0.3 µM. For all experiments the high tension voltage was controlled to be less than 600 V. Each spectrum was averaged over 10 continuous scans (accumulation: 10). The spectrum of the buffer was subtracted from the spectrum of the proteins. The spectra obtained were normalized to the concentration of *cbb*₃-CcO and smoothed with a Savitzky-Golay algorithm (Savitzky and Golay 1964). Afterwards, the resulting ellipticity data (millidegrees) were converted to mean molar ellipticity per residue ($[\Theta]$, deg \times cm² \times dmol⁻¹).

2.2.3.4 Differential scanning calorimetry

Differential scanning calorimetry (DSC) was used to characterize the thermophysical properties of *cbb*₃-CcO, which was performed on a VP-DSC Capillary Cell Micro-Calorimeter (Microcal) with an external nitrogen pressure at approx. 380 kPa (\approx 55 psi). The cell volume was 0.137 ml. Prior to use, all sample/reference solutions were degassed and then loaded into the 96-well plate (MicroLiter Analytical Supplies) at 4°C. Protein samples were added shortly (5 to 10 min) before each scan. The protein sample (3.5 mg/ml *cbb*₃-CcO in 20 mM Tris/HCl, pH7.5, 100 mM NaCl, 0.02% [w/v] DDM) and the corresponding buffer were loaded into sample and reference cells via an autosampler (Microcal). Scans were carried out using the following parameter settings: 10 to 120°C, 90°C/hour, 10 sec filtering period and low feedback mode. Data were normalized and analyzed with the software supplied by the manufacturer. Thermophysical parameters (e.g., T_m and ΔH) were further validated using a Gaussian function in Origin 8.6 software.

2.2.3.5 Mass spectrometry

Peptide mass fingerprinting (PMF) was used to identify the SDS-PAGE- and BN-PAGE-separated membrane proteins and the periplasmic proteins in solution. PMF was performed in the mass spectrometry (MS) facility of the department of molecular membrane biology (Dr. Julian Langer,

ESFRI-INSTRUCT Core Centre, MPI of Biophysics, Frankfurt am Main).

Before digestion, disulfide bonds in proteins were reduced and free cysteines were alkylated. The chemically modified proteins were digested with trypsin, chymotrypsin or a combination of both enzymes using customized digestion protocols (Buschmann *et al.*, 2010). For in-solution digests, proteins were denatured using up to 4M urea when applicable. The proteolytic digests were separated by reverse-phase high performance liquid chromatography (HPLC) using two C18 columns in series (trapping column: particle size 3 μ m or 5 μ m, L = 20mm; analytical column: particle size 3 μ m or 5 μ m, L = up to 15cm; NanoSeparations) on a nano-HPLC system (EASY-nLC, Proxeon). Peptides were eluted in gradients of buffer A (water with 0.1% [v/v] formic acid, HPLC grade) and buffer B (acetonitrile with 0.1% [v/v] formic acid, HPLC grade). Typically, gradients were ramped from 5% to 65% of buffer B in up to 120 min at a flow rate of 300 nl/min. Peptides eluting from the column were ionized online using a Bruker Apollo electrospray ionization (ESI)-source with a nanoSprayer emitter or a chip-based nano-ESI source (TriVersa NanoMate, Advion BioSciences) and analysed in a quadrupole time-of-flight (Q-TOF) mass spectrometer (maXis, Bruker Daltonics). Mass spectra were acquired over the mass range of 50 to 2200 m/z, and sequence information was acquired by computer-controlled, data-dependent automated switching to MS/MS mode using collision energies based on mass and charge state of the candidate ions. When applicable, the obtained peptides from nano-HPLC were simultaneously loaded onto a 384 AnchorChip matrix-assisted laser desorption/ionization (MALDI) target (Bruker Daltonics) and subsequently analysed using MALDI-TOF/TOF mass spectrometry (Autoflex III Smartbeam, Bruker Daltonics).

The data sets were processed using a standard proteomics script with the software Compass/Hystar (Bruker Daltonics) and exported as mascot generic format files. Spectra were internally recalibrated on autoproteolytic trypsin fragments when applicable. Proteins were identified by matching the derived mass lists against the NCBI non-redundant protein database or a custom *Pseudomonas* database (FASTA files were updated on a monthly basis) on a local Mascot server (version 2.3). In general, a mass tolerance of ± 0.05 Da for parent ion and fragment spectra, two missed cleavages, oxidation of methionine and fixed modification of carbamidomethyl cysteine were selected as matching parameters in the search program. Data and results from re-sequencing the open reading frames were analyzed and validated using the Bruker BioTools 3.1 software.

2.2.3.6 Crystallization screening

Initial crystallization screening of EGFP-fused 2nd isoform of rec. *cbb*₃-CcO was performed on the Rigaku CrystalMation system in the crystallization unit of the department of molecular membrane biology (ESFRI-INSTRUCT Core Centre, MPI of Biophysics, Frankfurt am Main (Thielmann *et*

al., 2012)). After gel filtration, the purified homogeneous protein was concentrated to a final concentration of 12 mg/ml. For screening, 100 nl protein solution was added to 100 nl reservoir solution using the Phoenix drop setter (Rigaku). The drops were equilibrated against 50 μ l reservoir solution by sitting-drop vapour diffusion at 18°C. Sparse matrix screens, which were used to test initial conditions for protein crystallization, are listed in Table 2-20. Crystallization trials were incubated over a period of three months and imaged on an automated and regular basis. Evaluation of the crystallization outcome was performed using the software CrystalTrak web (Rigaku) and by manual inspection on a Leica M165C microscope.

Table 2-20: List of crystallization screens.

Screen	Reference	Number of conditions
MbClass Suite	Qiagen	96
MemGold	Molecular Dimensions	96
MemStart + MemPlus	Molecular Dimensions	96
MemSys	Molecular Dimensions	96
MPI pHScreen	MPI of Biophysics, Frankfurt am Main	96
MPI Custom pH 7.0 A	MPI of Biophysics, Frankfurt am Main	96
MPI Custom pH 7.0 B	MPI of Biophysics, Frankfurt am Main	96
MPI Custom pH 7.0 C	MPI of Biophysics, Frankfurt am Main	96
MPI Custom pH 7.0 D	MPI of Biophysics, Frankfurt am Main	96
JBScreen Pentaerythritol HTS	Jena Bioscience	96
PGA Screen	Molecular Dimensions	96

2.2.3.7 Cyclic voltammetry

Cyclic voltammetry was used to investigate the electrochemical properties of immobilized *cbb*₃-CcO on gold nanoparticles. The measurements were performed by Thomas Meyer and Dr. Frédéric Melin at the University of Strasbourg in France in the group of Prof. Petra Hellwig. The gold colloid was prepared and stabilized with sodium citrate and subsequently deposited on a polished polycrystalline gold disc electrode as described elsewhere (Meyer *et al.*, 2011). The electrode was then modified with a mixture of thiols (1 mM hexanethiol and 1 mM 6-mercapto-1-hexanol in EtOH) overnight. The protein was deposited on the electrode at 4°C overnight. Measurements were carried out in 50 mM KPi buffer pH 7.0 with and without oxygen. The oxygen-free buffer was prepared by flushing with argon. The cyclic voltammograms were obtained using a VersaSTAT 4 potentiostat (Princeton Applied Research) with a conventional three-electrode cell. An Ag/AgCl electrode was used as a reference electrode and a platinum wire as a counter electrode. Cyclic voltammetry was performed from +0.3 V to -0.65 V (vs. Ag/AgCl, 3M KCl) at a scan rate of 0.02 V/s for 2 cycles at RT.

2.2.3.8 Fourier transform infrared spectroscopy

The measurements were performed in the group of Prof. Petra Hellwig (University of Strasbourg, France). The electrochemically induced Fourier-transformed infrared (FTIR) difference spectra of *cbb*₃-CcO were recorded using the optically transparent thin layer electrochemical cell (Moss *et al.*, 1990; Hellwig *et al.*, 1998). A gold grid electrode was chemically modified with an equal mixture of 2 mM cysteamine and 2 mM 3-mercaptopropionic acid. To accelerate electron transfer, mediators were added to the protein solution to a final concentration of 40 μM. The FTIR difference spectra as a function of applied potential were recorded at 12°C in the spectral range 1800-1200 cm⁻¹ using a FTIR spectrophotometer (Vertex 70, Bruker). After equilibration with an initial potential for 7 min, the full potential step from -0.4 V to +0.4 V (vs. Ag/AgCl, 3M KCl) was applied. For each single-beam spectrum, 256 interferograms at 4 cm⁻¹ resolution were coadded and Fourier-transformed using triangular apodization. Scans were carried out in 20 mM Tris/HCl, pH7.5, 100 mM NaCl, 0.02% (w/v) DDM.

2.2.3.9 Potentiometric titration

Potentiometric titration was performed in the group of Prof. Petra Hellwig (University of Strasbourg, France). A mixture of 17 mediators with a final concentration of 25 μM was added to the protein sample. The titration was performed using an electrochemical thin layer cell mounted with CaF₂ windows. A gold grid functionalized with a 1:1 solution of mercaptopropionic acid and cysteamine was used as working electrode. An aqueous Ag/AgCl 3M KCl was used as reference electrode and a platinum contact as counter electrode. The experiments were performed at 12°C. The spectra were recorded using a Cary 300 spectrometer coupled to a potentiostat. For the oxidative titration, the spectrum at -300 mV was taken as reference whereas for the reductive, the spectrum at +300 mV was taken as reference. A spectra was recorded every 25 mV with an equilibration time of at least 20 minutes. The potential was changed when the spectra did not evolve anymore.

3 Results

This work describes the characterization of the two isoforms of *cbb₃-CcO* from *P. stutzeri* ZoBell. A homologous expression system was developed for obtaining both genetically engineered Cbb₃-1 and Cbb₃-2. Both purified recombinant *cbb₃*-isoforms were compared to the wild-type *cbb₃-CcO*, and studied by biochemical and biophysical techniques.

3.1 Identification of the two *cbb₃*-operons

To identify the organization of *cbb₃*-operons from *P. stutzeri* ZoBell, three genomic DNA-derived PCR products were amplified and sequenced (Figure 3-1). Primers were designed based on the highly conserved regions identified by comparison of the published genome sequences from several related *Pseudomonas* species. The following primer pairs were used: 1_Fw/3_Rev for PCR-1, 5_Fw/4_Rev for PCR-101 and 7_Fw/6_Rev for PCR- M6263. Sequence data were submitted to GenBank under the accession number HM130676.

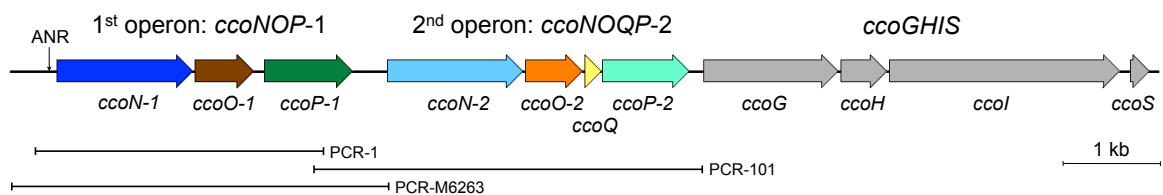


Figure 3-1: Schematic representation of the organization of two *cbb₃*-operons and the *ccoGHIS* gene cluster on the *P. stutzeri* ZoBell chromosome. Genes are denoted by arrowheads according to their encoded products. The *ccoGHIS* gene cluster (in grey) is located downstream of *ccoNOQP-2*. The ANR box is found in the upstream region of *ccoN-1*. PCR products used for the sequencing are underlined. Length standard (1 kb) is shown on the right.

P. stutzeri ZoBell possesses two *cbb₃*-operons (*ccoNOP-1* and *ccoNOQP-2*) and one *ccoGHIS* gene cluster. The numbering order of the two *cbb₃*-operons is based on the genome annotation of *P. stutzeri* strain A1501 (Yan *et al.*, 2008). Each of the two *cbb₃*-operons, separated by a 352-bp segment, encodes the subunits of two isoforms of *cbb₃-CcO*, namely, Cbb₃-1 and Cbb₃-2. Both *cbb₃*-operons contain the genes coding for CcoN, CcoO and CcoP of *cbb₃-CcO*, whereas the gene *ccoQ* is only present in *ccoNOQP-2*. A consensus ANR-box (TTGAT-N⁴-gTCAA), the binding site for the FNR-type transcriptional regulator (ANR), is located directly upstream of the transcription start site of the gene *ccoN-1*. The *ccoGHIS* cluster is located 137 bp downstream of the stop codon of the *ccoP-2* gene, and their gene products are required for the maturation and assembly of a functional *cbb₃-CcO* (Ekici *et al.*, 2011).

3.2 Microbiological characterization of *P. stutzeri* ZoBell

Although *P. stutzeri* ZoBell has been extensively used for the studies of denitrification processes (Zumft 1997), basic microbiological information needed for this work was limited. Therefore, *P. stutzeri* ZoBell cells were examined for their doubling time, relationship between the number of cells and optical density, and their antibiotic resistance profiles.

3.2.1 Growth of *P. stutzeri* ZoBell

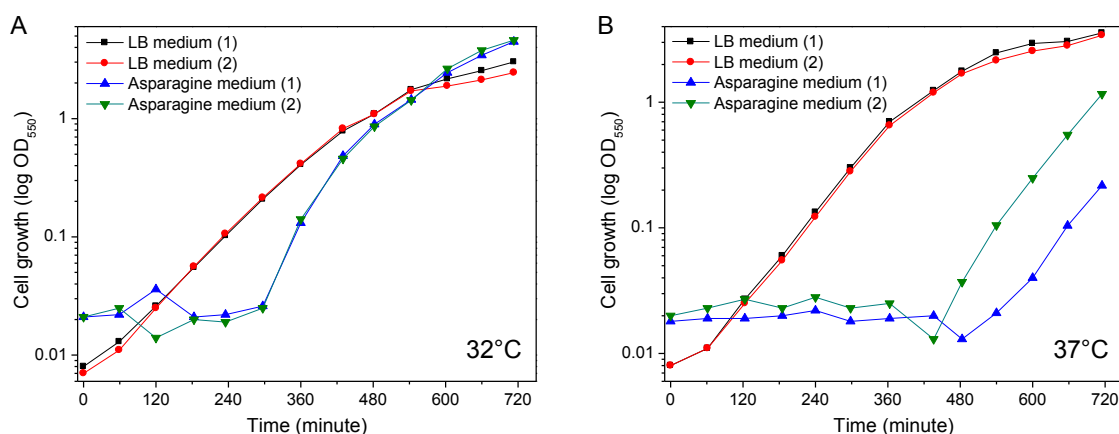


Figure 3-2: Growth of wild-type *P. stutzeri* ZoBell in LB and asparagine medium. The culture was inoculated with a glycerol stock, which was stored at -80°C prior to use. Cells were grown with shaking in 100 ml of culture medium in a 300 ml unbaffled Erlenmeyer flask at 32°C (A) and 37°C (B). Samples were collected every 60 min for 12 hours, and the optical density was measured at 550 nm. Cell growth in each condition was measured in two independent experiments (1 and 2).

To study the growth behavior of wild-type *P. stutzeri* ZoBell, growth experiments were performed at two different temperatures (32°C and 37°C) using LB and asparagine medium. Figure 3-2 shows the logarithmic plot of optical density at 550 nm against time. In LB medium, the exponential growth phase of *P. stutzeri* cells was observed to occur between 2 and 6 hours after the start of incubation, and the cells entered the early stationary phase at an OD_{550} of about 0.8. Compared to LB medium, *P. stutzeri* cells needed 5 hours (32°C) or 7 hours (37°C) to adapt to asparagine medium before dividing. After adaptation, a fast growth phase was observed. Doubling times¹⁹ were calculated from an average slope of the linear relationship between $\log \text{OD}_{550}$ and time of two experiments. The *P. stutzeri* cells grew in LB medium at 32°C or 37°C with a doubling time of 50 and 59 min, respectively. In contrast, doubling time in asparagine medium, which is usually used for cultivation of denitrifying bacteria, was 34 to 36 min.

¹⁹ The doubling time, however, varies with culture conditions, e.g., culture volume and shaking speed. Therefore, the values shown here can only play a reference role to monitor the growth of *P. stutzeri*.

3.2.2 Relationship between cell number and optical density

The relationship between cell number and optical density is linear and shown in Table 3-1. Cell numbers were counted using a Neubauer chamber and a phase contrast microscope. From the OD₅₅₀ reading, an average number of $1.12 \pm 0.36 \times 10^9$ *P. stutzeri* cells per OD₅₅₀ unit was calculated. The number of viable cells was further determined by dilution plating of a cell culture on LB agar plates. The number of colony-forming units (CFU)/ml was determined to be $0.55 \pm 0.28 \times 10^9$ at an OD₅₅₀ of 1.0.

Table 3-1: Correlation between cell number and optical density.

OD ₅₅₀	Cells / ml (\pm SD) ^a	Cells / one unit of OD ₅₅₀
0.050	$2.88 \pm 0.47 \times 10^7$	0.57×10^9
0.109	$1.34 \pm 0.21 \times 10^8$	1.23×10^9
0.243	$1.86 \pm 0.10 \times 10^8$	0.77×10^9
0.301	$4.06 \pm 1.11 \times 10^8$	1.35×10^9
0.435	$6.06 \pm 1.30 \times 10^8$	1.39×10^9
0.567	$7.94 \pm 1.85 \times 10^8$	1.40×10^9

^a Cell numbers were averaged by a count of four random squares of Neubauer chamber. Each square contained 20-50 cells.

3.2.3 Antibiotic resistance analysis

Antibiotic resistance profiles were generated by measuring the ability of *P. stutzeri* ZoBell cells to grow in the LB medium in the presence of each of several antibiotics at different concentrations (5 to 100 μ g/ml). The growth was monitored by measuring the optical density of overnight cultures at 550 nm. The results were summarized in Table 3-2. It was shown that *P. stutzeri* ZoBell cells are naturally resistant to ampicillin and spectinomycin. However, they are sensitive to several other antibiotics, including chloramphenicol, gentamicin, kanamycin, streptomycin and tetracycline. These antibiotics could potentially be used as selection markers for later molecular genetic studies.

Table 3-2: Antibiotic sensitivities of wild-type *P. stutzeri* ZoBell^a.

Antibiotic	Final concentration (μ g/ml)					Overall results
	5	10	25	50	100	
Ampicillin	R	R	R	R	R	R
Chloramphenicol	R/S	n.d.	R/S	S	S	S
Gentamicin	S	S	S	S	S	S
Kanamycin	R/S	S	S	S	S	S
Spectinomycin	R	R	R	R	R	R
Streptomycin	R/S	n.d.	S	S	S	S
Tetracycline	S	S	S	S	S	S

^a R, resistant; S, sensitive; n.d., not determined.

3.3 Construction of *ccoNO(Q)P* knock-out strains

Using the method of homologous recombination, two deletion strains lacking either the *ccoNOP-1* or the *ccoNOQP-2* operon were constructed. This method requires a non-replicative plasmid, which has to be transformed into *P. stutzeri* competent cells with a relatively high efficiency.

3.3.1 Transformation of *P. stutzeri* ZoBell

P. stutzeri chemically competent cells were prepared using the standard rubidium chloride method (Hanahan 1983), and the transformation efficiency was determined to be 310 CFU/ μ g DNA. Transformation efficiency was increased to 510 CFU/ μ g DNA by using magnesium chloride instead of rubidium chloride. Ultrasound-mediated DNA delivery was performed using a previously published method²⁰ (Song *et al.*, 2007). Although this method was reported to be efficient for delivery of plasmids into *P. putida*, the efficiency examined in this work was low (370 CFU/ μ g DNA). Because the transformation efficiencies mentioned above were extremely low, both methods were not further optimized nor used.

For high transformation efficiency, electrocompetent cells were prepared using different protocols and resuspension buffers²¹ (Smith and Iglewski 1989; Diver *et al.*, 1990), and the related data are summarized in Table 3-3. At a fixed electrical field strength of 8 kV/cm, the best results with *P. stutzeri* cells was obtained using LB medium, which yielded a transformation efficiency of 3×10^3 CFU/ μ g DNA. In contrast, a lower efficiency of 370 CFU/ μ g DNA was observed when the cells were grown in the asparagine minimal medium and subsequently treated with 300 mM sucrose. In addition, a supplement of magnesium ions (1 mM) into resuspension buffer could improve the yield of asparagine-grown cells, while it showed no effect on LB-grown cells (Table 3-3).

Table 3-3: Transformation efficiency of electrocompetent cells.

Growth medium	Resuspension buffer	Transformation efficiency (CFU/ μ g DNA)
LB medium	300 mM sucrose	3100
LB medium	SMEB buffer ^a	2960
Asparagine medium	300 mM sucrose	370
Asparagine medium	SMEB buffer ^a	1210
Asparagine medium	10% (v/v) glycerol	10

^a SMEB, sucrose-magnesium electroporation buffer (1 mM Hepes, pH 7.0, 300 mM sucrose, 1 mM MgCl₂), according to Diver *et al.*, 1990.

²⁰ The parameters used in this experiment were as follows: an ultrasound frequency of 35 kHz, ultrasound exposure time of 10 s, 50 mM CaCl₂, plasmid concentration of 0.8 ng/ μ l, 2×10^9 cells/ml, 22°C.

²¹ *P. stutzeri* cells were grown in LB or asparagine medium at 37°C to OD₅₅₀ = 0.8 to 1.0. The cells were chilled on ice and centrifuged at 4°C. The pellet was gently resuspended three times in ice-cold resuspension buffer. The cells were electroporated with 100 ng of pBBR1MCS-2 at 25 μ F, 200 Ω and 0.8 kV.

To examine the effect of the electric field strength on transformation efficiency, applied field strength was varied between 6 and 18 kV/cm with an increment of 2 kV/cm (data not shown). Using LB medium and 300 mM sucrose, the highest efficiency (3×10^5 CFU/ μ g DNA) was reached at 18 kV/cm. It was also found that *P. stutzeri* cells could be electroporated after being frozen at -80 °C for three days; however, its efficiency was dramatically decreased (about 50 fold) (data not shown).

Although the optimized transformation efficiency (about 10^5 CFU/ μ g DNA) is high enough for routine molecular cloning procedures, a higher efficiency is still required for the construction of specific gene deletions in *P. stutzeri* because of the relatively low frequency of double recombination events. By applying a rapid electroporation method (for details, see Material and methods), which was developed for *P. aeruginosa* (Choi *et al.*, 2006), an efficiency ranging from 10^5 to 10^8 CFU/ μ g DNA was achieved.

3.3.2 Maintenance of plasmids in *P. stutzeri* ZoBell

For general cloning and expression of *cbb₃*-CcOs, a shuttle plasmid that replicates in both *E. coli* and *P. stutzeri* is required. A broad-host-range cloning vector pBBR1MCS has been found to replicate in *P. fluorescens* and *P. putida* (Kovach *et al.*, 1995). Four derivatives of pBBR1MCS were tested for their ability to replicate and confer antibiotic resistance in *P. stutzeri* (Table 3-4). Chloramphenicol- and kanamycin-resistant transformants were isolated following electroporation with pBBR1MCS and pBBR1MCS-2, respectively, which indicates that pBBR-based plasmids are capable of replication in *P. stutzeri*. Subsequent plasmid isolation and agarose gel electrophoresis also confirmed the stable maintenance of both plasmids. However, no transformants were obtained with pBBR1MCS-3 and pBBR1MCS-5, which might have been caused by the lack of expression of the antibiotic-resistance genes present in the plasmids in *P. stutzeri* cells.

Table 3-4: Maintenance of a variety of plasmids in *P. stutzeri* ZoBell.

Plasmid	Size (bp)	Replicon	Antibiotic resistance	Maintenance in <i>P. stutzeri</i>
pBBR1MCS	4707	pBBR	Cam ^R	yes
pBBR1MCS-2	5144	pBBR	Kan ^R	yes
pBBR1MCS-3	5228	pBBR	Tet ^R	no
pBBR1MCS-5	4768	pBBR	Gen ^R	no
pACYC184	4245	p15A	Cam ^R , Tet ^R	no
pBR325	5996	pMB1	Cam ^R , Tet ^R , Amp ^R	no

In addition to the pBBR-based plasmids, two *E. coli* plasmids, including pACYC184 and pBR325, were also evaluated (Table 3-4). The plasmid pACYC184 harbours the p15A replicon, while

pBR325 carries the pMB1 replicon (a close relative of ColE1). When these two plasmids were separately electroporated into *P. stutzeri*, no transformants were obtained, indicating that both replicons do not function in *P. stutzeri* cells. Thus, the plasmids containing the p15A or pMB1 replicon may serve as suicide vectors in *P. stutzeri* and could therefore be used for the targeted disruption of genes on its chromosome.

3.3.3 Construction of suicide plasmids and gene deletion

In order to disrupt the genes coding for *cbb₃-CcO*, suicide plasmids were constructed, which contain a p15A replicon, a kanamycin resistance gene flanked by two large fragments (~ 500 bp) homologous to the DNA sequences bordering the target site and a second selectable marker for the identification of double-crossover gene replacement events.

The construction of EGFP-based suicide plasmids was accomplished in the following steps (Figure 3-3): (i) a 751-bp BamHI-XbaI fragment from pEGFP-N1 was ligated into pBBR1MCS-2 digested by the same enzymes, resulting in pBBR1MCS-2-EGFP. This plasmid was electroporated into *P. stutzeri* ZoBell and the green fluorescent cells confirmed the expression of EGFP (Figure 3-3). Since EGFP is expressed from the *lac* promoter without any induction, it could be potentially used as a reporter protein to distinguish the single-crossover recombination from the desired double-crossover events; (ii) a 2.6-kb fragment containing the pBBR1 replicon and mobilization (*mob*) gene was replaced by the p15A replicon of pACYC184, yielding the plasmid pXH-B. This plasmid was electroporated into *P. stutzeri* to test its ability to replicate in the cells. As expected, no transformants were obtained; (iii) three plasmids were designed to delete *ccoNOP-1* and *ccoNOQP-2* operons separately or together by flanking a kanamycin resistance cassette of pXH-B with the corresponding homologous regions (H1, H2 and H3) of the desired deletion. For pXH-ΔI-EGFP, the kanamycin resistance cassette was flanked by the H1-fragment (-532 to +1 bp upstream of the translation start of *ccoN-1*) and the H2-fragment (-57 to +448 bp of the stop codon of *ccoP-1*) as 5' and 3' homologous regions. Correspondingly, the same cassette was flanked at 5' by the H2-fragment and at 3' by the H3-fragment (-365 to +100 bp of the stop codon of *ccoP-2*), yielding the vector pXH-ΔII-EGFP. Furthermore, the same procedures were used to generate pXH-ΔI+II-EGFP, which contains H1- and H3-fragments at 5' and 3' sites, respectively.

In addition to EGFP, the *sacB* gene²² from *Bacillus subtilis* was also used as a counter-selectable marker. Three *sacB*-based negative selection plasmids were constructed and used for the selection of deletion strains (data not shown).

²² The *sacB* gene encodes the enzyme levansucrase. It catalyzes the conversion of sucrose into levan, which is toxic for most bacteria.

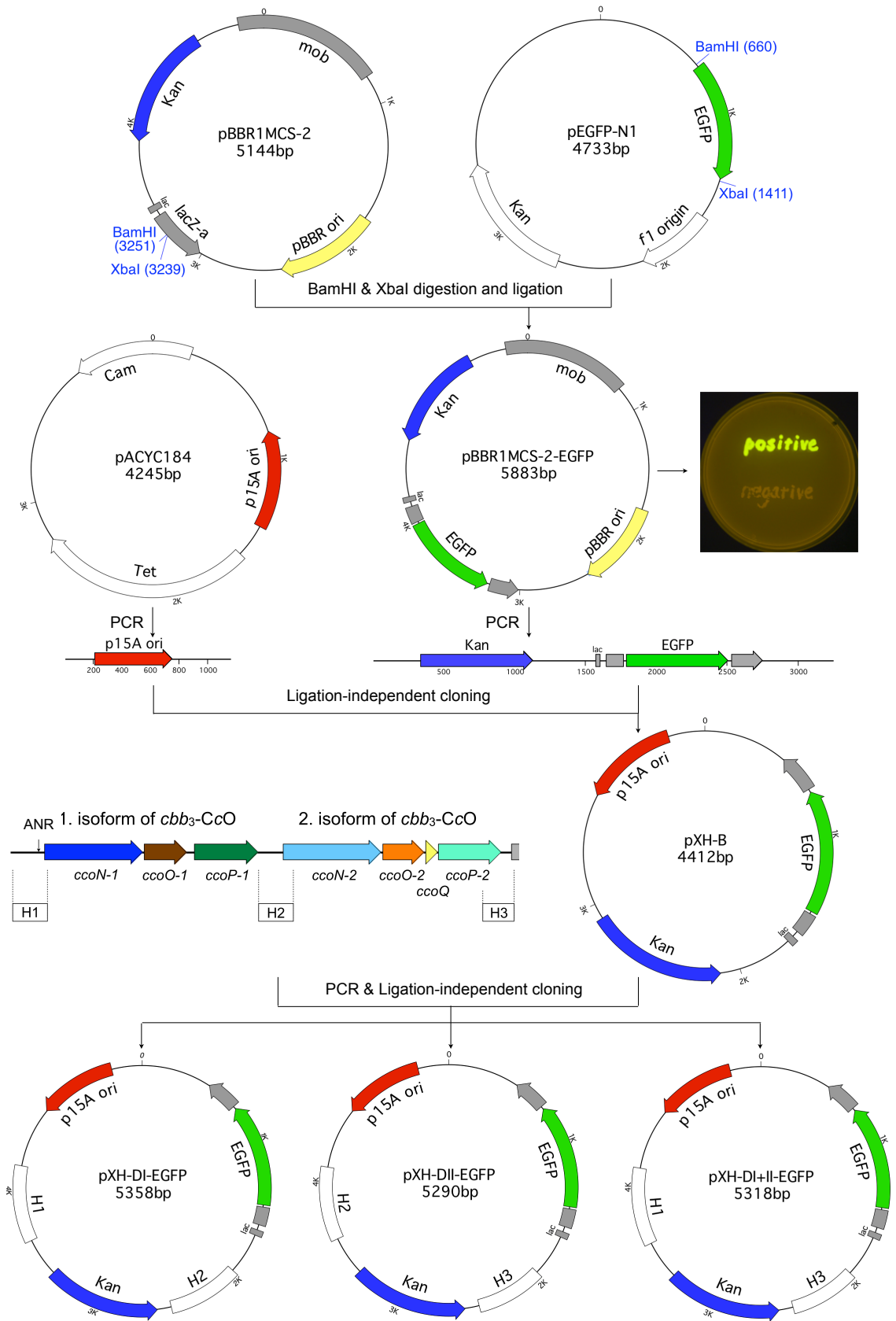


Figure 3-3: Schematic representation of the construction of the suicide plasmids. Three suicide plasmids were designed to create the deletion strains of *P. stutzeri* *cbb₃-CcO*s. For details, see text.

All suicide vectors were electroporated individually into *P. stutzeri* ZoBell cells. In the case of EGFP-based suicide plasmids, the double crossover event was selected for by an EGFP-negative and kanamycin-resistant phenotype. Although different strategies with different plasmids were used, only two deletion strains $\Delta\text{Cbb}_3\text{-1}$ and $\Delta\text{Cbb}_3\text{-2}$ were obtained by using the plasmid pXH- ΔI -EGFP and pXH- ΔII -EGFP, respectively (Figure 3-4). No mutant strain containing a double deletion of both *cbb*₃-operons was detected.

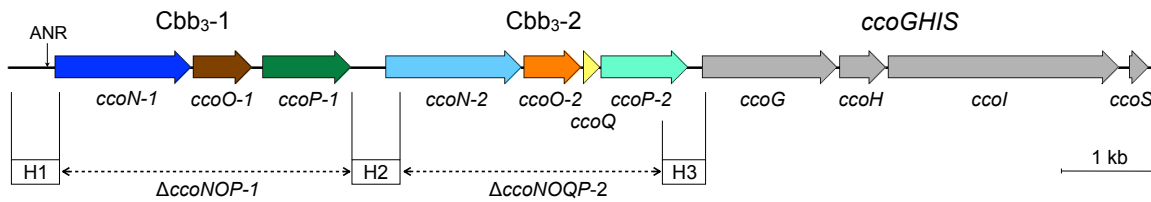


Figure 3-4: Genetic maps of two *cbb*₃-CcO deletion strains. Three homologous regions (H1, H2 and H3) are shown in boxes. The regions deleted and replaced with a kanamycin gene in deletion strains $\Delta\text{Cbb}_3\text{-1}$ and $\Delta\text{Cbb}_3\text{-2}$ are indicated as dashed lines. Length standard (1 kb) is shown on the right.

In addition to circular plasmids, the linear double-stranded DNA fragment containing the kanamycin resistance cassette and two flanking regions were generated either by PCR (for non-methylated DNA) or by restriction digestion (for methylated DNA). They were transformed into *P. stutzeri* cells to test the linear DNA-mediated genomic deletion. However, no transformants were observed in all cases, even when the recovery time following electroporation was extended to 5 h. The failure of using linear DNA to obtain deletion mutants might be caused by the low transformation efficiency and the rapid degradation of linear DNA fragments.

3.3.4 Verification of deletion strains

PCR analysis was performed to verify the deletion of one of two *cbb*₃-operons in the two deletion strains ($\Delta\text{Cbb}_3\text{-1}$ and $\Delta\text{Cbb}_3\text{-2}$) by using their genomic DNA as a template (Figure 3-5). The primer pairs used (Table 3-5) were selected to give a maximal coverage of the putatively deleted regions.

PCR analysis confirmed the substitution of the desired *ccoNO(Q)P* operons with the kanamycin resistance cassette in both deletion strains, because the relative positions of all amplicons accorded well with the expected sizes. As an example, analysis of the wild-type *P. stutzeri* strain harboring both *cbb*₃-operons yielded a DNA fragment of 2210 bp using primers 9_Fw and 8_Rev (Figure 3-5 A, lane 5). As expected, this fragment was not detected in the genome when the operon *ccoNOP-1* was deleted in strain $\Delta\text{Cbb}_3\text{-1}$ (Figure 3-5 B, lane 5).

Table 3-5: Primer pairs used to verify the deletion of *cbb₃-CcOs* loci. The lane numbers are corresponding to the numbers of Figure 3-4 (see below). The expected PCR product sizes for each amplicon length are indicated in base pairs.

Lane	1	2	3	4	5	6	7 ^a	8 ^b	9	10	11	12
Primer pair	8_Fw 8_Rev	9_Fw 9_Rev	10_Fw 10_Rev	11_Fw 11_Rev	9_Fw 8_Rev	11_Fw 10_Rev	Km_N Km_C	lacZ_N lacZ_C	2_Fw 7_Rev	4_Fw 5_Rev	2_Fw 5_Rev	2_Fw 4_Rev
WT	1223	1034	1320	1363	2210	2356	-	-	3526	3680	6431	6770
Δ<i>Cbb₃-1</i>	-	-	1320	1363	-	2356	919	-	1666	-	4571	4910
Δ<i>Cbb₃-2</i>	1223	1034	-	-	2210	-	919	-	3526	2146	4897	5236

^a Primers Km_N and Km_C are specific for the kanamycin resistance cassette. ^b Primers lacZ_N and lacZ_C are specific for the second selectable marker, e.g., EGFP-gene.

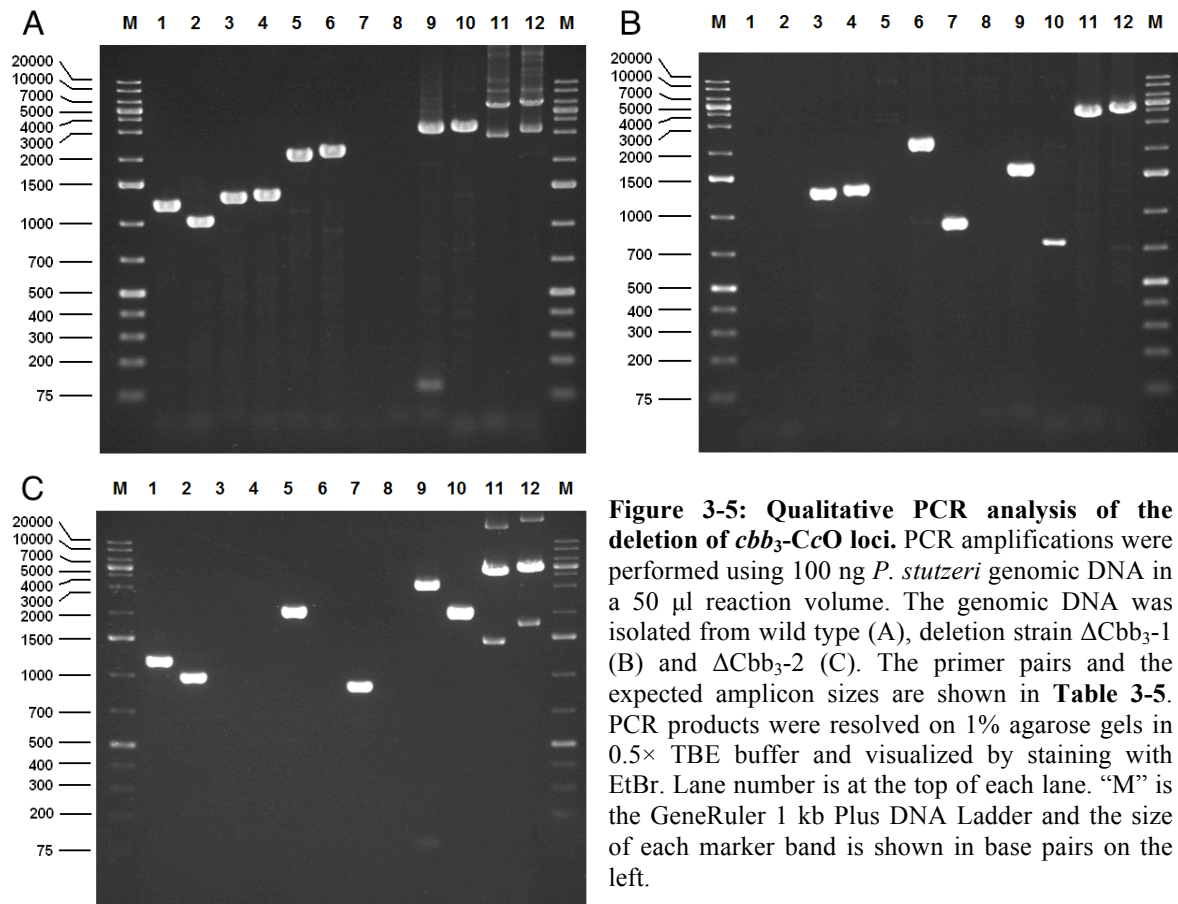


Figure 3-5: Qualitative PCR analysis of the deletion of *cbb₃-CcO* loci. PCR amplifications were performed using 100 ng *P. stutzeri* genomic DNA in a 50 μ l reaction volume. The genomic DNA was isolated from wild type (A), deletion strain Δ *Cbb₃-1* (B) and Δ *Cbb₃-2* (C). The primer pairs and the expected amplicon sizes are shown in **Table 3-5**. PCR products were resolved on 1% agarose gels in 0.5 \times TBE buffer and visualized by staining with EtBr. Lane number is at the top of each lane. “M” is the GeneRuler 1 kb Plus DNA Ladder and the size of each marker band is shown in base pairs on the left.

In addition to the PCR-based verification of a gene disruption, the results of the direct sequencing of the target region showed that no unexpected mutations had taken place in Δ *Cbb₃-1* and Δ *Cbb₃-2* strains (the sequence data are shown in Appendix J and K).

3.4 Construction and purification of the tagged *cbb₃-CcOs*

To express and purify both isoforms of *cbb₃-CcO* from *P. stutzeri*, two *cbb₃*-operons were individually cloned into a low-copy-number vector pBBR1MCS and two different affinity tags were separately introduced into the recombinant proteins. Both *cbb₃-CcOs* were purified to apparent homogeneity in two chromatographic steps.

3.4.1 Construction of the expression vectors

To construct the expression vectors for both isoforms of *cbb₃-CcO*, two DNA fragments containing *ccoNOP-1* (3,932 bp) and *ccoNOQP-2* (4,033 bp) with corresponding promoter regions were first amplified from *P. stutzeri* ZoBell genomic DNA (Figure 3-1) and cloned separately into the plasmid pJET1.2, resulting in two vectors pJET-M6263 and pJET-PCR101, respectively. Both vectors were used for subcloning since they have a relatively small size and high copy number.

To efficiently purify both *cbb₃-CcOs*, it was decided to test two small affinity tags (the His₆-tag and Strep-tag II), and to compare their effect on the protein expression and purification. The two affinity tags were fused to the N- and C-terminus of the *ccoN-1* (in pJET-M6263) and *ccoN-2* (pJET-PCR101) using the site-directed mutagenesis method. To construct the expression vector for Cbb₃-1, the 3.4-kb fragment containing Strep- or His₆-tagged *ccoNOP-1* was amplified, digested with BamHI and HindIII endonucleases, and subcloned into the same site of pBBR1MCS, resulting in pXH21-24 (Figure 3-6). Because the *ccoNOQP-2* operon contained all the restriction sites needed for subcloning, the 3.6-kb fragment containing tagged *ccoNOQP-2* was cloned into pBBR1MCS using a ligation independent cloning strategy, yielding pXH25-28 (Figure 3-6). All constructed expression vectors were electroporated into the corresponding *P. stutzeri* *cbb₃*-deletion strains, and the resulting recombinant strains were cultivated for the expression of target proteins. It should be noted that all vectors (pXH21-28) were designed for the expression of recombinant Cbb₃-1 or Cbb₃-2 under the control of their native promoters.

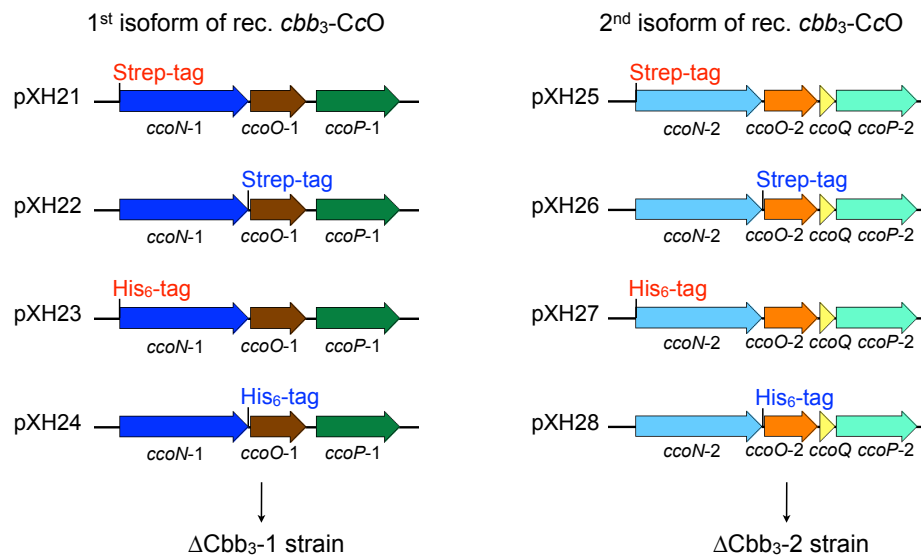


Figure 3-6: A schematic summary of the constructed expression vectors for both *cbb3*-CcOs. Only the *cbb3*-operon with corresponding promoter region is shown. Constructs pXH21-24 were designed for the expression of the Cbb₃-1, and vectors pXH25-28 were used for the expression of the Cbb₃-2. The N- and C-terminal affinity tags are shown in red and blue, respectively.

3.4.2 Expression screening of Strep- and His₆-tagged *cbb3*-CcOs

To monitor the expression of the recombinant *cbb3*-CcOs, the *P. stutzeri* deletion strains containing the respective complementation plasmids were cultured in asparagine medium for the small-scale expression trials. Membranes were prepared and solubilized as described in the Materials and Methods section. For purification of Strep-tagged recombinant Cbb₃-1 and Cbb₃-2, each solubilizate was loaded onto a Strep-Tactin affinity column. After washing, the bound proteins were eluted using 10 mM desthiobiotin. The obtained eluate was collected and analyzed by SDS-PAGE, followed by heme staining and Coomassie staining. As shown in the lane 1 of Figure 3-7 A, no obvious bands corresponding to subunits of Cbb₃-1 were detected from the recombinant strain, which harbors an expression vector (pXH21) with Strep-tag II on the N-terminus of *ccoN*-1. The same results were observed for the Cbb₃-2 with an N-terminal Strep-tag II (Figure 3-7 B, lane 3). In both cases, the recombinant *cbb3*-CcOs were neither found in the flow-through nor in the wash fractions of the Strep-Tactin column (data not shown). Therefore, it is suggested that the absence of the desired proteins in the eluate is not due to the deficiency of the specific binding, but possibly to the lack of *cbb3*-CcO at least in the membrane.

When the Strep-tag II is fused to the C-terminus of the *ccoN* gene, the CcoNOP subunits of both isoforms of *cbb₃-CcO* can be found in the affinity eluate (lane 2 of Figure 3-7 A and lane 4 of Figure 3-7 B). In addition, the heme-staining assay indicated the incorporation of hemes *c* into CcoO and CcoP subunits of both enzymes. Furthermore, protein bands on both gels (Figure 3-7, lane 2 and 4, Coomassie staining) were sliced out and identified by peptide mass fingerprinting (data not shown). The identity of three major bands as CcoNOP of each isoform of *cbb₃-CcO* was confirmed. Besides the subunits of *cbb₃-CcO*, several ribosomal proteins as general contaminants were also identified, which could be observed as weak bands between CcoO and CcoP.

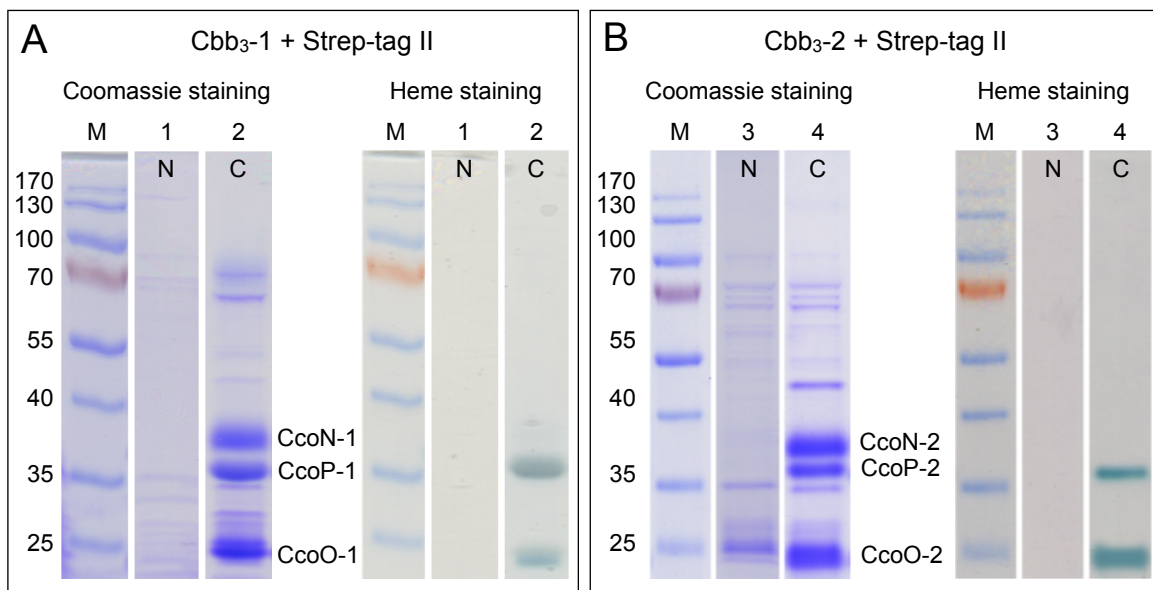


Figure 3-7: SDS-PAGE gels of the small-scale expression and purification of Strep-tagged *cbb₃-CcOs*. The solubilized membranes of four recombinant strains were loaded onto a Strep-Tactin affinity column. The eluate was collected and analyzed on a 12.5% Tris-glycine gel. (A) The Strep-tag II was fused to the N-terminus (lane 1) or the C-terminus (lane 2) of the subunit CcoN of Cbb₃-1. (B) The Strep-tag II was fused to the N-terminus (lane 3) or the C-terminus (lane 4) of the subunit CcoN of Cbb₃-2. Coomassie staining (left of each panel) and heme staining (right of each panel) were used to visualize the protein bands. The standard molecular weights (kDa) of the marker proteins (M, PageRuler Prestained protein ladder) are indicated on the left. Bands of interest (subunit N, P and O) are indicated in the middle.

To check the effect of a His₆-tag on the expression level of the desired recombinant *cbb₃-CcOs*, the solubilizate was loaded onto a Ni-NTA affinity column and the bound proteins were eluted with a multiple-step gradient of imidazole. In contrast to the Strep-tag II, expression and purification of Cbb₃-2 with either a N-terminal (Figure 3-8, lane 1) or a C-terminal His₆-tag (Figure 3-8, lane 2) were achieved. It was found that the bound His₆-tagged *cbb₃-CcOs* could be eluted with 50 to 100 mM imidazole. However, a large amount of impurities still remained after the Ni-NTA column (Figure 3-8). An additional purification step was performed using Superdex 200 column, but little improvement in purity was obtained (data not shown).

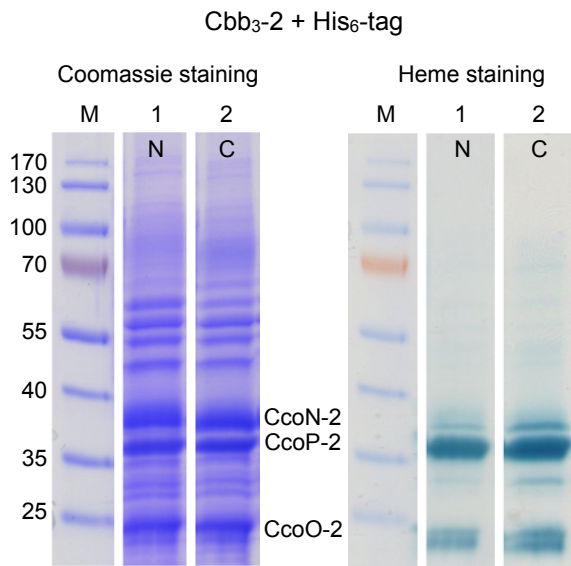


Figure 3-8: SDS-PAGE gels of the small-scale expression and purification of His₆-tagged Cbb₃-2. The solubilized membranes of two recombinant strains were loaded onto a Ni-NTA affinity column. The eluate (100 mM imidazole fraction) was collected and analyzed on the 12.5% Tris-glycine gel. The His₆-tag was fused to the N-terminus (lane 1) or the C-terminus (lane 2) of the Cbb₃-2. Coomassie staining (left of each panel) and heme staining (right of each panel) were used to visualize the protein bands. The standard molecular weights (kDa) of the marker proteins (M, PageRuler Prestained protein ladder) are indicated on the left. Bands of interest (subunit N, P and O) are indicated in the middle.

A summary of the test of expression vectors is given in Table 3-6. Because the recombinant *cbb₃-CcOs* can be more efficiently purified using Strep-tag II, two expression vectors (pXH22 and pXH26, shown in blue in Table 3-6) were selected for the further optimization of the purification of both isoforms of *cbb₃-CcO*.

Table 3-6: Summary of eight expression vectors^a. Two expression vectors, pXH22 and pXH26 (blue), are used for the routine expression of Cbb₃-1 and Cbb₃-2.

Vector	Isoform	Terminus	Affinity tag	Expression
pXH21	Cbb ₃ -1	N-terminus	Strep-tag II	no
pXH22		C-terminus	Strep-tag II	yes
pXH23		N-terminus	His ₆ -tag	n.d.
pXH24		C-terminus	His ₆ -tag	n.d.
pXH25	Cbb ₃ -2	N-terminus	Strep-tag II	no
pXH26		C-terminus	Strep-tag II	yes
pXH27		N-terminus	His ₆ -tag	yes
pXH28		C-terminus	His ₆ -tag	yes

^a n.d., not determined.

3.4.3 Large-scale purification of Strep-tagged *cbb₃-CcOs*

As mentioned in the previous section, affinity purification (Strep-tag II and Strep-Tactin column) allows the specific isolation of both recombinant Cbb₃-1 and Cbb₃-2, although small amounts of impurities and aggregates were present. To remove traces of impurities, protein samples were further purified by ion exchange chromatography using a Q Sepharose column. After intensive washing, the specifically bound protein (reddish in color) was eluted in the presence of 300 mM

NaCl (Figure 3-10 B). Afterwards, the concentration of NaCl in the buffer was reduced to 100 mM during the concentration steps. As an example²³ shown in Figure 3-9, homogenous Cbb₃-1 was obtained after two purification steps, although some aggregates were still visible in the high molecular weight region of the gel (lane 2). Both recombinant Cbb₃-1 and Cbb₃-2 purified by two-step chromatography were used for further biochemical and biophysical analysis.

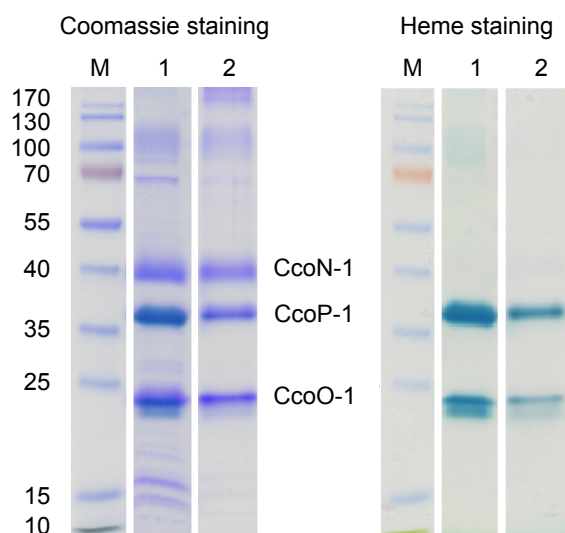


Figure 3-9: SDS-PAGE gels of the two-step purification of recombinant Cbb₃-1. After each purification step, the protein samples were collected and analyzed on the 15% Tris-glycine gel. The pooled samples obtained after affinity chromatography and ion exchange chromatography are shown in lane 1 and 2, respectively. Coomassie staining (left) and heme staining (right) were used to visualize the protein bands. The standard molecular weights (kDa) of the marker proteins (M, PageRuler Prestained protein ladder) are indicated on the left. Bands of interest (subunit N, P and O) are indicated in the middle.

The homogeneity of *cbb*₃-CcOs could be further improved using an additional size-exclusion chromatography step. However, this was only necessary when the enzymatic activity of recombinant *cbb*₃-CcOs was compared to the true wild-type Cbb₃-1, because the latter was purified by four chromatographic steps (see 2.2.2.4)²⁴. As an example, the chromatograms obtained from the three-step purification of recombinant Cbb₃-1 is presented in Figure 3-10. The absorbance was monitored at 280 and 411 nm, in which absorbance at 411 nm is specifically related to the oxidized *cbb*₃-CcOs. During size exclusion chromatography (Figure 3-10 C), the recombinant Cbb₃-1 was eluted as a single peak centered at approx. 12.2 ml. As shown in Table 3-7, Strep-Tactin affinity chromatography led to a 15.2-fold enrichment of purification, and a final 22.7-fold enrichment was achieved after three purification steps.

²³ Both *cbb*₃-isoforms exhibited similar properties during the purification process. Therefore, only the recombinant Cbb₃-1 is shown as an example for the demonstration in this section.

²⁴ The wild-type Cbb₃-1 is purified for the crystallization experiments and, therefore, more homogeneous.

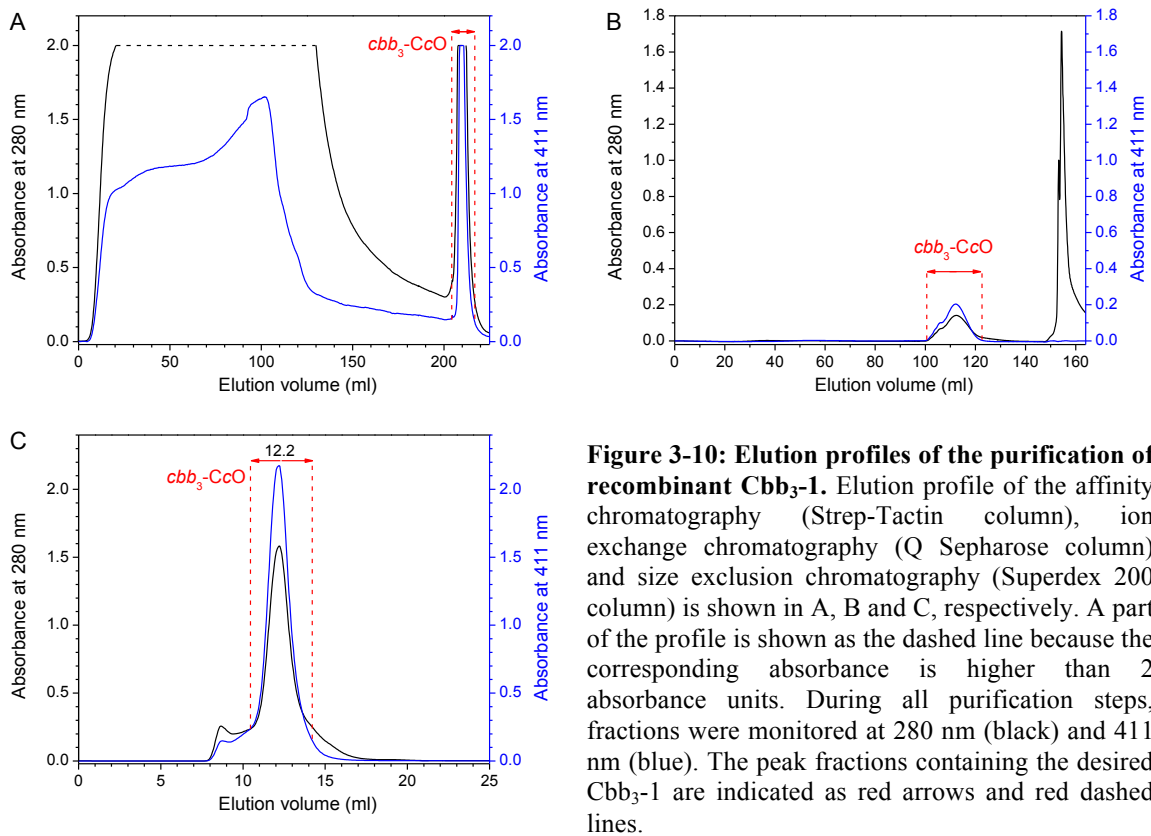


Figure 3-10: Elution profiles of the purification of recombinant Cbb₃-1. Elution profile of the affinity chromatography (Strep-Tactin column), ion exchange chromatography (Q Sepharose column) and size exclusion chromatography (Superdex 200 column) is shown in A, B and C, respectively. A part of the profile is shown as the dashed line because the corresponding absorbance is higher than 2 absorbance units. During all purification steps, fractions were monitored at 280 nm (black) and 411 nm (blue). The peak fractions containing the desired Cbb₃-1 are indicated as red arrows and red dashed lines.

Table 3-7: Purification of Strep-tagged Cbb₃-1.

Purification step	Volume (ml)	Total protein concentration (mg/ml) ^a	Total protein (mg)	Total activity (U) ^b	Specific activity (U/mg)	Yield (%)	Purification fold
Crude cell extract	250.0	13.66	3,415.0	4,052	1.2	-	-
Crude membrane	107.5	10.09	1,084.7	3,484	3.2	100	1.0
Solubilization	380.0	2.33	885.4	2,913	3.3	82	1.0
Strep-Tactin	50.0	0.17	8.5	412	48.5	0.78	15.2
Q Sepharose	23.0	0.33	7.6	433	57.1	0.70	17.8
Superdex 200	9.6	0.78	7.5	544	72.6	0.69	22.7

^a Protein concentration determined by BCA assay using BSA as a standard protein. ^b Enzyme activity was measured using an oxygen electrode. One U is defined as the amount of Cbb₃-1 required to reduce 1 μmol of O₂ in 1 min at 25°C.

3.4.4 Control of the expression of two *cbb₃*-isoforms

In the vectors pXH22 and pXH26, expression of *cbb₃*-CcOs is under the control of their native promoter. Figure 3-11 shows the nucleotide sequences of the two native promoters of the *ccoNOP-1* and the *ccoNOQP-2* operon. The potential ribosomal binding site (Shine-Dalgarno

sequence, SD) is located directly upstream (6-7 bases) of the start codon of *ccoN-1* and *ccoN-2*. Both promoters contain the putative binding motif for RNA polymerase σ^{70} subunit. Despite the similarities, a putative ANR binding site (TTGAT-N⁴-gTCAA), which is required for the activation of transcription under low oxygen tension, is only present in the promoter region of the *ccoN-1* gene.

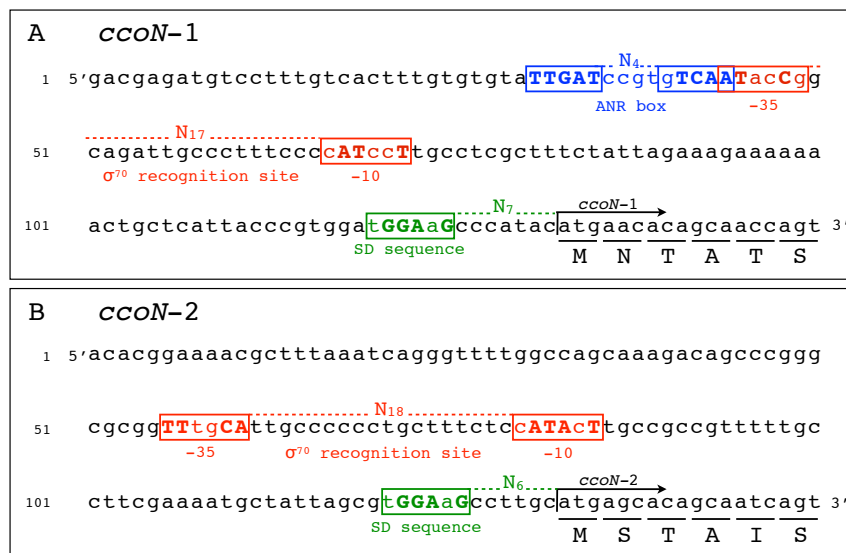


Figure 3-11: Structure of the promoter region of the gene *ccoN*. The nucleotide sequences (5'-3') with the predicted promoter regions of *ccoN-1* (A) and *ccoN-2* genes (B) are shown. An ANR-box (TTGAT-N⁴-gTCAA) is located upstream from transcription start site of the *ccoN-1* gene and is shown in blue. The putative RpoD (σ^{70}) recognition site is shown in red, both -35 and -10 promoter regions are indicated. In panel A, the -35 and -10 regions are proposed based on the previously identified data from *P. putida* (Ugidos *et al.*, 2008). The putative Shine-Dalgarno sequence is shown in green. Conserved nucleotides (as compared to the consensus sequence) are shown in bold and capitalized. The start site of translation is indicated by arrows. The first six amino acids are underlined.

Under the control of the native promoter, the yield of Cbb₃-1 was determined to be 2 to 4 mg per liter of culture medium after two purification steps, as measured using the specific extinction coefficient for *cbb₃-CcO*. In contrast, a relatively low yield was observed for the Cbb₃-2, which is approx. 0.5 mg per liter of culture medium (Table 3-8). To increase the expression level of Cbb₃-2, the native promoter region of Cbb₃-2 was first replaced by the exogenous *lac* promoter, yielding pXH36. By using this vector, the protein yield could be increased by twofold without any induction treatment. The yield of Cbb₃-2 was further improved by the replacement of the Cbb₃-2 promoter with the endogenous promoter of Cbb₃-1. The yield was increased 4- to 6-fold to 2 to 3 mg purified protein per liter of culture medium, which is comparable to the yield of Cbb₃-1 (Table 3-8). Therefore, instead of pXH26, the expression vector pXH39 was used for the expression of recombinant Cbb₃-2 throughout the present work.

Table 3-8: A summary of typical protein yields of *cbb₃*-CcOs.

Recombinant isoform	Promoter	Feature of promoter	Plasmid	Yield
Cbb ₃ -1	<i>cbb₃</i> -1	native	pXH22	2-4 mg/liter
Cbb ₃ -2	<i>cbb₃</i> -2	native	pXH26	< 0.5 mg/liter
Cbb ₃ -2	<i>lac</i>	exogenous (from <i>E. coli</i>)	pXH36	> 1 mg/liter
Cbb ₃ -2	<i>cbb₃</i> -1	endogenous	pXH39	2-3 mg/liter

3.4.5 SDS-PAGE analysis of Cbb₃-1 and Cbb₃-2

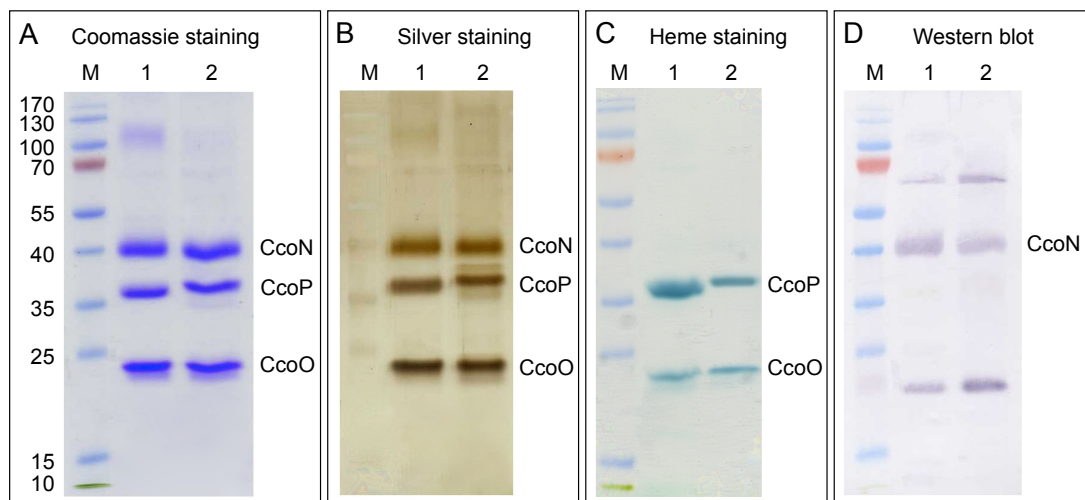


Figure 3-12: SDS-PAGE gels of both purified recombinant Cbb₃-1 and Cbb₃-2. The Cbb₃-1 (lane 1) and Cbb₃-2 (lane 2) were separated on a 15% Tris-glycine gel. After electrophoresis, the gels were stained with Coomassie brilliant blue (A) and silver (B). Heme staining (C) was performed to detect the subunit CcoO and CcoP, which contain covalently bound heme *c*. Western blot (D) was used to detect the Strep-tagged CcoN subunit. The standard molecular weights (kDa) of the marker proteins (M, PageRuler Prestained protein ladder) are indicated on the left in panel A. Bands of interest (subunit N, P and O) are indicated.

Both purified recombinant Cbb₃-1 and Cbb₃-2 were analyzed by SDS-PAGE (Figure 3-12). After staining with Coomassie blue or silver, three distinct bands with apparent molecular weights of 42, 36 and 24 kDa were visible, which correspond to subunits CcoN, CcoP and CcoO of the *cbb₃*-CcO as mentioned above (Figure 3-12 A and B). When heme staining was performed, two major stained bands corresponding to subunits CcoP and CcoO were observed (Figure 3-12 C). Due to the strong hydrophobic properties of CcoN and the binding of detergent, CcoN of both isoforms migrated significantly faster than expected from their molecular masses (52.79 kDa for CcoN-1 and 53.17 kDa for CcoN-2). Although the predicted masses of CcoP-1 (34.89 kDa) and CcoP-2 (35.01 kDa) are very similar, a difference in the migration distance has been observed. In contrast to subunit CcoP, the sizes of CcoO-1 (23.43 kDa) and CcoO-2 (23.46 kDa) were too close to show

any difference. The subunit CcoQ was not detectable using the current electrophoresis protocol due to its low molecular weight (6.91 kDa) and poor staining properties. Since subunit CcoN of both recombinant *cbb*₃-CcOs carried a Strep-Tag II, they could be detected by Western blot using anti-Strep-tag antibody. However, two nonspecific bands are also observed (Figure 3-12 D).

3.4.6 Determination of the oligomeric state of Cbb₃-1 and Cbb₃-2

To evaluate the oligomeric state and molecular weight of purified recombinant Cbb₃-1 and Cbb₃-2 in their native state, protein samples were separated on BN-PAGE (Figure 3-13). Considering the mass contribution of bound heme ligands, the molecular weight of Cbb₃-1 and Cbb₃-2, based on the amino acid sequence of the monomeric form, was calculated to be 112.3 and 119.8 kDa, respectively. On the BN-PAGE, both isoforms were resolved as a single sharp band with an apparent molecular weight of 165 kDa. Although this value is slightly higher than expected for its calculated molecular weight, it still suggests that Cbb₃-1 and Cbb₃-2 are both present in a monomeric state because the migration behavior of membrane proteins is strongly affected by the binding of lipids and detergents to the hydrophobic surface. Furthermore, the BN-PAGE gels demonstrated that both purified isoforms are highly monodisperse and homogeneous.

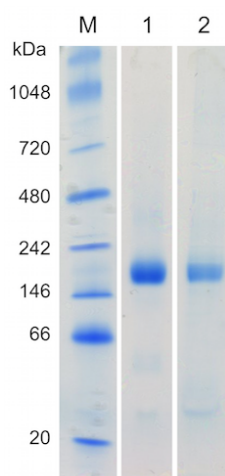


Figure 3-13: BN-PAGE gels of purified recombinant *cbb*₃-isoforms. Cbb₃-1 (lane 1) and Cbb₃-2 (Lane 2) were solubilized and purified with DDM, and analyzed on 4-16% (v/v) NativePAGE Bis-Tris gels. The molecular weights (kDa) of the marker proteins (lane M) are indicated on the left.

3.4.7 Subunit composition of both *cbb*₃-isoforms

To determine the subunit composition, protein bands in BN-PAGE were cut out and subsequently analyzed by MS based PMF. The overall sequences coverage for each of the three subunits of Cbb₃-1 were 36.1% (CcoN-1), 74.5% (CcoO-1) and 66.6% (CcoP-1), and a similar sequence coverage for Cbb₃-2 was observed, which was 31.9% (CcoN-2), 69.6% (CcoN-2) and 82.6% (CcoP-2). The low sequence coverage of subunit CcoN was due to its hydrophobic character. In

addition, the PMF analysis provided the following results: (i) Unique peptides from subunits CcoNOP of Cbb₃-1 and Cbb₃-2 were found only in the corresponding isoforms. No chimeric proteins or fragments were detected (Figure 3-14 A-C). (ii) The CcoQ subunit was observed only in Cbb₃-2 with a sequence coverage of 35.5% (Figure 3-14 D). (iii) The assembly protein CcoH was observed in both rec. *cbb*₃-Cco complexes (Figure 3-15). (iv) Ribosomal proteins and a histone-like DNA binding protein were also detected as general contaminants.

A		N Subunit											
1 st isoform of <i>cbb</i> ₃ -Cco (Cbb ₃ -1)													
1	MNTA	TS-TAY	SYK	VVRQFAI	MTVVWGI	VGM	GLGVF	IAAQL	AWP	FLNFDLP	WTSFGRLRPL	HTNAVIFAFG	GCALFATSYY
81	SVQRTCQ	TTL	FAPK	LAAFTF	GWQL	LVILLA	AI	SLPLGFTS	SKEYAELEWP	IDILITLVVW	AYAVVFFGTL	AKRKVKHIYV	
161	GNWFFGAFIL	TVAlLh	VvNN	LEIPV	TAMKS	YS	LYAGATDA	MVQW	WYGHNA	VGFFLT	AGFL	GIMYYFV	PKQ AERP
241	SIVHF	WALIT	VYI	WAGPHHL	HY	TALPD	WAQ	SLGM	VMSLIL	LAPSWG	GMIN	GMMT	LSGAWH
321	STFEGP	MMAI	KTN	NALSHYT	DWT	TIGHV	HAG	ALGW	VAMVSI	GALY	HLV	PKV	FGREQMHS
401	WVNGI	AQGLM	WR	AIN	DDGTL	TYS	FVE	SLEA	SHP	GFV	VRMI	GGA	I
481	POFEK												
2 nd isoform of <i>cbb</i> ₃ -Cco (Cbb ₃ -2)													
1	MSTA	IS	ETAY	NYK	VVRQFAI	MTVVWGI	I	GM	GLGVF	IAAQL	VWP	SLN	LDLP
81	VVQRTCQ	ARL	FSD	GLAAFTF	GWQ	AVI	VLA	VI	TLP	MGYTS	SKEYAELEWP	IDILITLVVW	SYIAV
161	GNWFFGAFIL	VTAM	LHIVNN	LEIPV	SLF	FKS	YSIY	AGATDA	MVQW	WYGHNA	VGFFLT	TGFL	GIMYYFV
241	SIVHF	WALIT	LYI	WAGPHHL	HY	TALPD	WAQ	SLGM	VMSIIL	LAPSWG	GMIN	GMMT	LSGAWH
321	STFEGP	MMAI	KTN	NALSHYT	DWT	TIGHV	HAG	ALGW	VAMIT	ISMY	HLI	PKV	FGREQMHS
401	WVNGI	TQGLM	WR	AIN	EDGTL	TYS	FVE	ALEA	SHP	GFV	VR	AV	GGA
481	POFEK												
B		O Subunit											
1 st isoform of <i>cbb</i> ₃ -Cco (Cbb ₃ -1)													
1	MK	SHE	KLEKN	V	GLLTLFMIL	AVSIGGLTQI	VPL	FFQD	SvN	EPVEG	MKPYT	ALQLEGRDLY	IREGCVGCHS
81	ERYGHYSVAG	ESVYDHPFLW	GSKRTGPD	LA	RVGGRYSDDW	HRAHLYNPRN	VVPESKMP	SY	PWLVENTLDG	KDTAKKMSAL			
161	RMLGVPYTEE	DIAGARD	SvN	GK	TEMDAMVA	YLQVLGTALT	NKR						
2 nd isoform of <i>cbb</i> ₃ -Cco (Cbb ₃ -2)													
1	MK	NHE	I	LEKN	I	GLLTLFMIL	AVSIGGLTQI	VPL	FFQD	AvN	EPVEG	MKPYT	ALQLEGRDLY
81	ERYGHYSVAG	ESVYDHPFLW	GSKRTGPD	LA	RVGGRYSDDW	HRAHLYNPRN	VVPESKMP	SY	PWLVENTLDG	KDTAKKMSAL			
161	RMLGVPYTEE	DIAGARD	AvR	GK	TEMDAMVA	YLQVLGTALT	NKR						

(Figure continued on next page)

C		P Subunit	
1 st isoform of <i>cbb₃</i> -Cco (Cbb ₃ -1)			
1	M	S	T
81	N	W	K
161	A	D	D
241	G	E	G
2 nd isoform of <i>cbb₃</i> -Cco (Cbb ₃ -2)			
1	M	S	T
81	N	W	K
161	T	D	D
241	A	K	G

Figure 3-14: Peptide mass fingerprinting analysis of two *cbb₃*-isoforms (Cbb₃-1 and Cbb₃-2). Amino acid sequences of the four subunits, CcoN, CcoO, CcoP and CcoQ, are shown in A-D, respectively. The first amino acid on each line is numbered on the left. The unique residues associated with both *cbb₃*-isoforms are shown as enlarged characters. The sequence coverage obtained using simultaneous nLC-ESI- and nLC-MALDI-MS/MS is indicated in red (ESI only), blue (MALDI only) and purple (detected in both ESI and MALDI-MS). Eight amino acids of Strep-tag II are indicated by black underlining. The CcoQ subunit was detected only in Cbb₃-2.

D		Q Subunit	
2 nd isoform of <i>cbb₃</i> -Cco (Cbb ₃ -2)			
1	M	M	E

Figure 3-15: The sequence coverage obtained by peptide mass fingerprinting analysis for the assembly protein CcoH. CcoH was found in both recombinant Cbb₃-1 and Cbb₃-2. The first amino acid on each line is numbered on the left. Peptides detected by ESI-MS peptide mass fingerprinting are shown in red.

CcoH	
1	M
81	R
161	A

3.5 Characterization of Cbb₃-1 and Cbb₃-2

3.5.1 UV/Vis spectra of *cbb₃*-CcO

For comparison, the room temperature electronic absorption spectra of fully oxidized, fully reduced and reduced-minus-oxidized difference spectra of wild-type Cbb₃-1 are shown in Figure 3-16. As expected, all spectra are identical to those obtained from the recombinant Cbb₃-1. Therefore, a detailed description is given below using the recombinant Cbb₃-1 as an example.

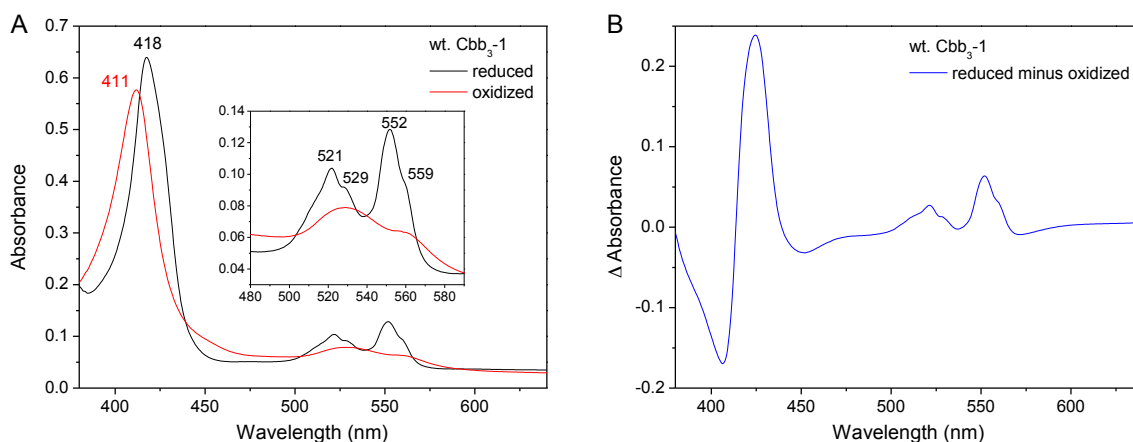


Figure 3-16: UV/Vis spectra of wild-type Cbb₃-1. The absorption spectra were recorded from 380 to 640 nm at 25°C. The insert shows an enlarged view of the α and β bands from 480 to 590 nm. (A) The wild-type Cbb₃-1 was fully oxidized (red) by adding potassium hexacyanoferrate (III) and was subsequently reduced (black) by addition of sodium dithionite. (B) The reduced-minus-oxidized difference spectrum of wild-type Cbb₃-1.

For a better comparison between both recombinant Cbb₃-1 and Cbb₃-2, their oxidized, reduced and reduced-minus-oxidized spectra are shown together in Figure 3-17. In the oxidized state, the absorption spectra of both *cbb₃*-isoforms are characterized by an intense Soret maximum at 411 nm. In addition, two broad features centered at 529 and 559 nm, which are mostly contributed by heme *b* and *b₃*, are also observed (Figure 3-17 A). After reduction with dithionite, the Soret band was shifted to 418 nm with increased intensity (Figure 3-17 B). Two absorption maxima appeared at 521 and 552 nm, which are attributed to the ferrous forms of hemes *c*. Moreover, the intensity of the 552-nm peak is higher than that of the 521-nm peak. In addition to hemes *c*, the reduction of both hemes *b* is accompanied by changes in two regions at 529 and 559 nm. However, the maximum at 529 nm is only slightly increased. In contrast, an obvious increasing trend was observed at 559 nm. Two slight differences between Cbb₃-1 and Cbb₃-2 were found in the alpha band of the reduced spectra. Cbb₃-2 has a maximum at 551.2 nm with a more intense shoulder at 559 nm, whereas the same maximum is red-shifted to 551.8 nm with a less intense shoulder in

Cbb₃-1. In the reduced-minus-oxidized difference spectra, one distinction occurs in the region of 420 to 440 nm (Figure 3-17 C), which indicates that the environment of heme *b* of the two *cbb*₃-isoforms reacts slightly differently upon the reduction. Furthermore, the reduced-minus-oxidized difference spectra of both *cbb*₃-isoforms have a small peak centered at 695 nm (Figure 3-17 D). This spectral feature is characteristic of heme *c* with methionine as an axial ligand (García-Horsman *et al.*, 1994).

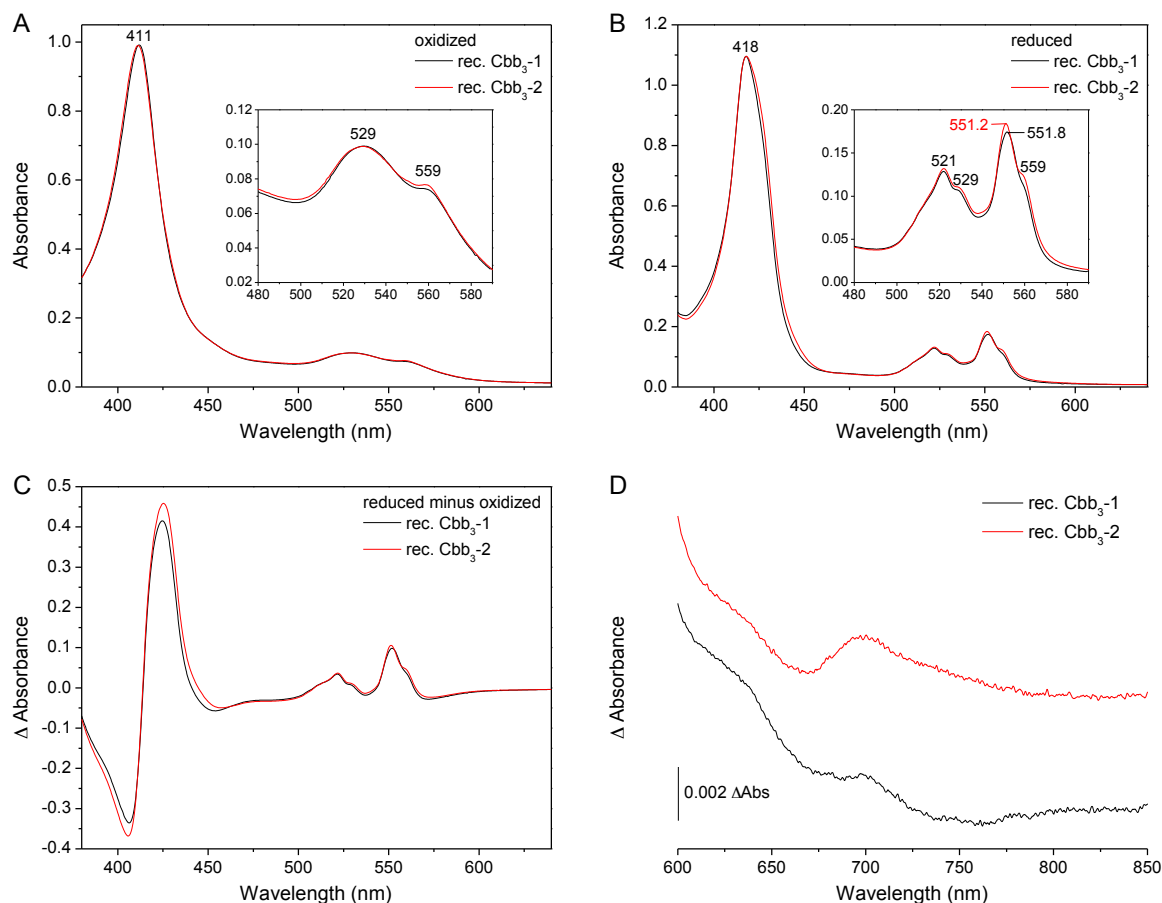


Figure 3-17: UV/Vis spectra of both recombinant *cbb*₃-isoforms. The absorption spectra of 2 μ M Cbb₃-1 (black line) and Cbb₃-2 (red line) were recorded from 380 to 640 nm (panel A to C) at 25°C. The insert in panel A and B shows an enlarged view of the α and β bands. (A) The *cbb*₃-CcOs are fully oxidized by adding potassium hexacyanoferrate (III). (B) The *cbb*₃-CcOs are fully reduced by adding sodium dithionite. (C) The reduced-minus-oxidized difference spectra of *cbb*₃-CcOs. (D) The reduced-minus-oxidized difference spectra in the near-infrared region.

3.5.2 Circular dichroism spectra of *cbb*₃-CcO

To compare the secondary structure of the two recombinant Cbb₃-1 and Cbb₃-2, as well as the wild-type Cbb₃-1, the far-UV CD spectra between 190 and 260 nm were recorded at 25 °C. As shown in Figure 3-18, spectra of three proteins are indistinguishable. The CD spectra are

characterized by two troughs at 222 and 209 nm with mean residue molar ellipticity of about $-19,000 \text{ deg cm}^2 \text{ dmol}^{-1}$, and by a maximum centered at 193 nm with an amplitude of $39,000 \text{ deg cm}^2 \text{ dmol}^{-1}$. These structural features indicate a predominantly alpha-helical secondary structure as expected from the X-ray structure of wild-type Cbb₃-1. In addition, identical spectra revealed that both recombinant Cbb₃-1 and Cbb₃-2 have essentially the same secondary structure as the wild-type Cbb₃-1, which confirms a correct folding of the recombinant *cbb*₃-CcOs.

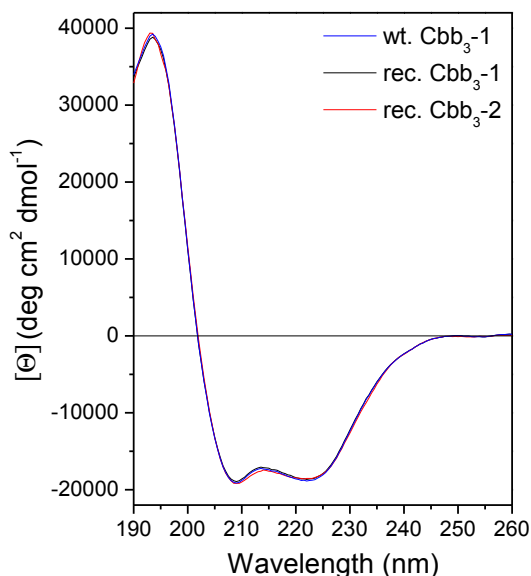


Figure 3-18: Far-UV circular dichroism spectra of *cbb*₃-CcOs. Far-UV (190 to 260 nm) CD spectra were recorded for wild-type Cbb₃-1 (blue), recombinant Cbb₃-1 (black) and recombinant Cbb₃-2 (red) at a concentration of $0.3 \mu\text{M}$ in 20 mM potassium phosphate buffer (pH 7.5) at 25°C . The recorded spectra were normalized and converted to mean residue ellipticity ($[\Theta]$).

3.5.3 Thermal stability of *cbb*₃-CcO

To determine the thermal stability of both recombinant *cbb*₃-isoforms and the wild-type Cbb₃-1, the differential scanning calorimetry analyses were performed in the range between 10 and 120°C (Figure 3-19). As a rescan of the same protein sample displayed no endothermic signal, this thermal denaturation was found to be irreversible (Figure 3-19 B). The calculated thermodynamic parameters are shown in Table 3-9.

With wild-type Cbb₃-1, two well-separated steps of temperature dependent denaturation were observed. Two midpoint temperatures (T_m) at 54.0 and 74.6°C are associated with the enthalpy change (ΔH) of 760 and $1,512 \text{ kJ mol}^{-1}$, respectively. The ratio of the enthalpy of the high-temperature to the low-temperature phase transition ($\Delta H_H / \Delta H_L$) is calculated to be 2. Compared to the wild-type Cbb₃-1, recombinant Cbb₃-1 has two similar peaks centered at 51.2 and 75.0°C , whereas the latter has an enlarged shoulder at about 88°C . Although the intensities of both peaks are significantly decreased, ΔH values only change slightly to 705 and $1,311 \text{ kJ mol}^{-1}$ for

low and high temperature transition, respectively, due to the broadening of the peaks (Table 3-9). The calculated $\Delta H_H / \Delta H_L$ ratio is 1.9, which is consistent with the observation from wild-type Cbb₃-1. In the case of recombinant Cbb₃-2, two transition peaks are apparently less intense and less separated. The T_m of both peaks shifted to 41.4 and 65.1°C, which indicates that recombinant Cbb₃-2 denatures 10°C earlier in comparison to the recombinant Cbb₃-1. Moreover, ΔH_L and ΔH_H are correspondingly decreased to 402 and 1,154 kJ mol⁻¹, respectively, which confirmed that recombinant Cbb₃-2 is less stable. The $\Delta H_H / \Delta H_L$ ratio of 2.9, as calculated for Cbb₃-2, is different to the observed ratio of Cbb₃-1.

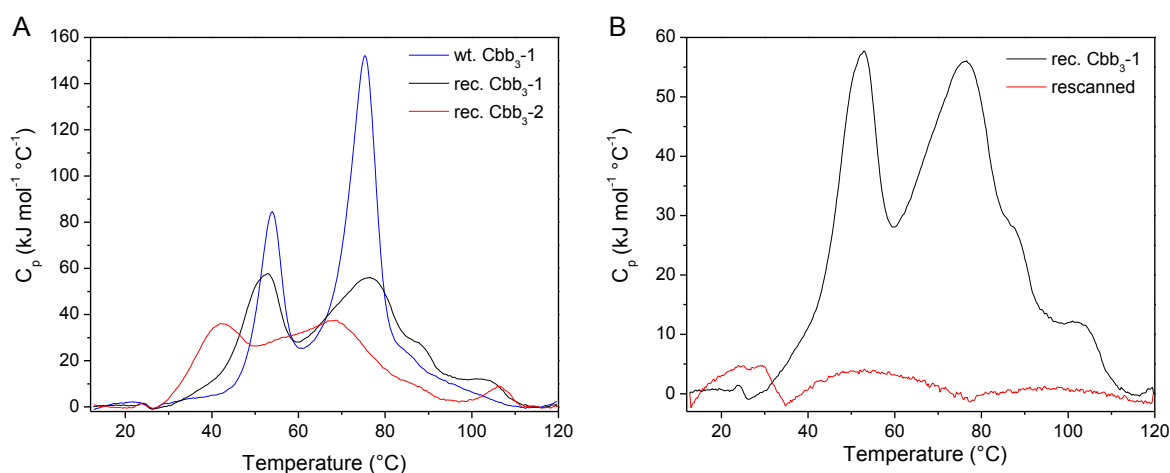


Figure 3-19: Differential scanning calorimetry curves of *cbb₃*-CcOs. (A) DSC curves of wild-type Cbb₃-1 (blue), recombinant Cbb₃-1 (black) and recombinant Cbb₃-2 (red) were measured at a concentration of 3.5 mg/ml. (B) A rescanned DSC curve of recombinant Cbb₃-1 (red). Measurements were performed at a heating rate of 90°C per hour. The dependence of heat capacity ($[C_p]$) on temperature was further analyzed to obtain thermophysical properties.

Table 3-9: Thermodynamic parameters for the thermal denaturation of *cbb₃*-CcOs.

Protein	The 1 st transition peak			The 2 nd transition peak		
	T_m (°C)	ΔH (kJ/mol)	FWHM ^a (°C)	T_m (°C)	ΔH (kJ/mol)	FWHM (°C)
wt. Cbb ₃ -1	54.0	759.6	10.0	74.6	1512.1	10.8
rec. Cbb ₃ -1	51.2	705.2	12.9	75.0	1311.0	22.5
rec. Cbb ₃ -2	41.4	402.1	13.0	65.1	1154.2	13.0

^a FWHM: full width at half maximum.

3.5.4 Fourier transform infrared spectra of *cbb*₃-CcO

Figure 3-20 shows the oxidized-minus-reduced FTIR difference spectra of the recombinant Cbb₃-1 and Cbb₃-2 for the potential step from the reduced (-400 mV) to the oxidized (400 mV) state. Both difference spectra are quite similar to each other and show the same band shapes. However, clear differences between the two isoforms can be observed in the amide I region (1,690 to 1,610 cm⁻¹) and the $\nu(\text{C}=\text{O})$ spectral region (above 1,710 cm⁻¹). Two signals at 1687 (Cbb₃-1) and 1,690 cm⁻¹ (Cbb₃-2) can be assigned to the protonated heme propionates, while the $\nu(\text{C}=\text{O})$ mode of protonated aspartic or glutamic acid side chains can be observed at 1,712, 1,741 (Cbb₃-1) and 1,744 cm⁻¹ (Cbb₃-2). Although differences exist, further site-directed mutagenesis experiments are required for the precise assignment of the obtained signals to any heme vibrational modes or individual amino acid.

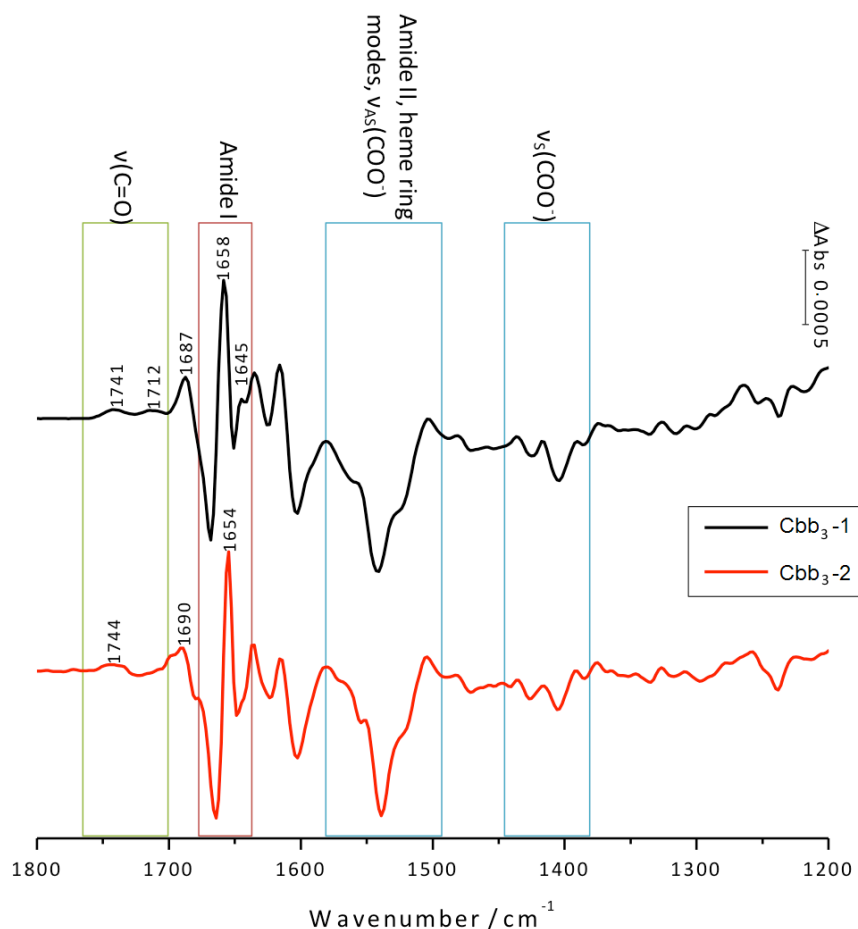


Figure 3-20: Oxidized-minus-reduced FTIR difference spectra of two recombinant *cbb*₃-isoforms from *P. stutzeri*. Spectra of recombinant Cbb₃-1 (black) and recombinant Cbb₃-2 (red) were measured from -400 to 400 mV (vs. Ag/AgCl, 3 M NaCl) in 20 mM Tris/HCl, pH 7.5, 100 mM NaCl and 0.02% (w/v) DDM.

3.5.5 Electrochemical measurement of *cbb₃-CcO*

The UV/Vis redox titrations were undertaken to determine the midpoint redox potentials of heme cofactors of both *cbb₃*-isoforms. The redox titrations were performed by stepwise setting the potentials in the range of -300 and +300 mV. Figure 3-21 and 3-22 show the titration curves and the corresponding spectral changes of heme cofactors of *Cbb₃-1* and *Cbb₃-2*, respectively. And the potentials obtained for each redox titration are summarized in Table 3-10.

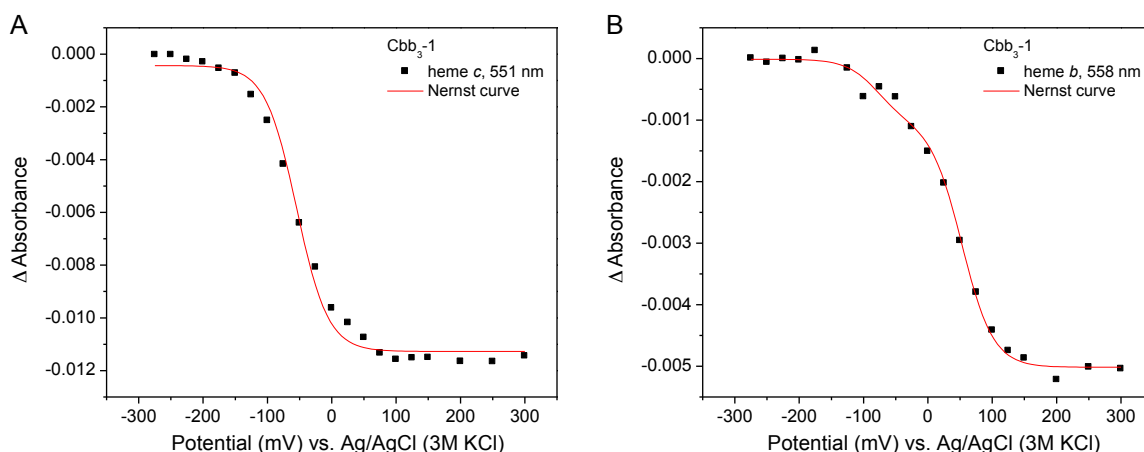


Figure 3-21: Potentiometric titration of recombinant *Cbb₃-1*. Potential dependence of the α band of heme *c* at 551 nm and of heme *b* at 558 nm is shown in panel A and B, respectively. Black squares represent the oxidative redox titration. The data were fitted to a Nernst equation ($n=1$ for heme *c* and $n=2$ for heme *b*) and the calculated Nernst fittings are shown as the solid curves. All potentials (mV) are shown against the reference electrode (Ag/AgCl, 3 M NaCl).

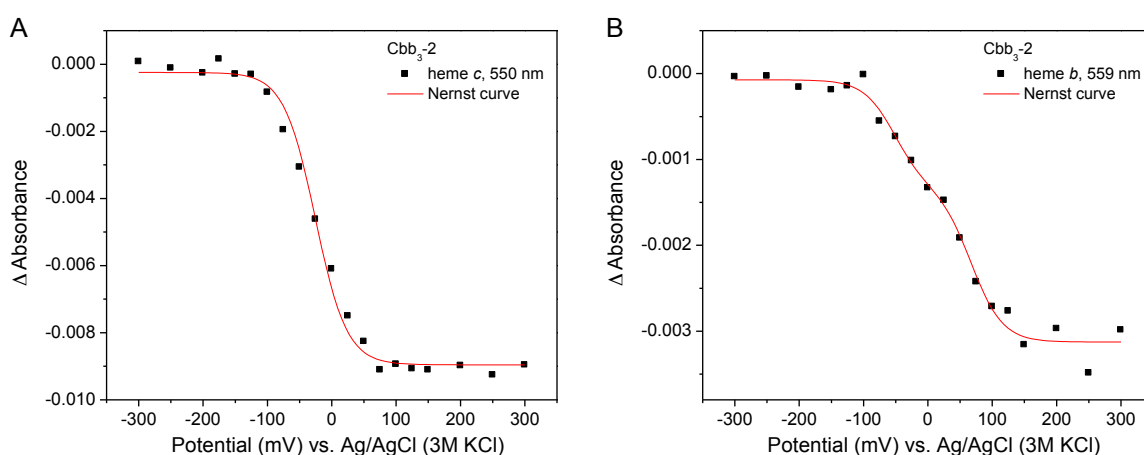


Figure 3-22: Potentiometric titration of recombinant *Cbb₃-2*. Potential dependence of the α band of heme *c* at 550 nm and of heme *b* at 559 nm is shown in panel A and B, respectively. Black squares represent the oxidative redox titration. The data were fitted to a Nernst equation ($n=1$ for heme *c* and $n=2$ for heme *b*) and the calculated Nernst fittings are shown as the solid curves. All potentials (mV) are shown against the reference electrode (Ag/AgCl, 3 M NaCl).

The midpoint redox potentials of three hemes *c* are too close to be distinguished, therefore, only one value can be determined for each *cbb*₃-isoform from the theoretical Nernst curve (155 mV for Cbb₃-1 and 185 mV for Cbb₃-2). For hemes *b* of Cbb₃-1, two midpoint redox potentials were obtained. The low-spin heme *b* has a higher midpoint redox potential (263 mV) than the high-spin heme *b*₃ (132 mV). In the case of Cbb₃-2, the midpoint redox potentials of both hemes *b* are only slightly higher than the values obtained for Cbb₃-1 (Table 3-10).

Table 3-10: Summary of midpoint redox potentials of heme cofactors of *cbb*₃-CcOs. The midpoint redox potentials are shown in mV (vs. standard hydrogen electrode) at pH 7.5.

	Midpoint potential of heme (vs. SHE)		
	hemes <i>c</i>	heme <i>b</i>	heme <i>b</i> ₃
recombinant Cbb ₃ -1	155 mV	263 mV	132 mV
recombinant Cbb ₃ -2	185 mV	278 mV	158 mV

3.5.6 Determination of the oxygen reductase activity

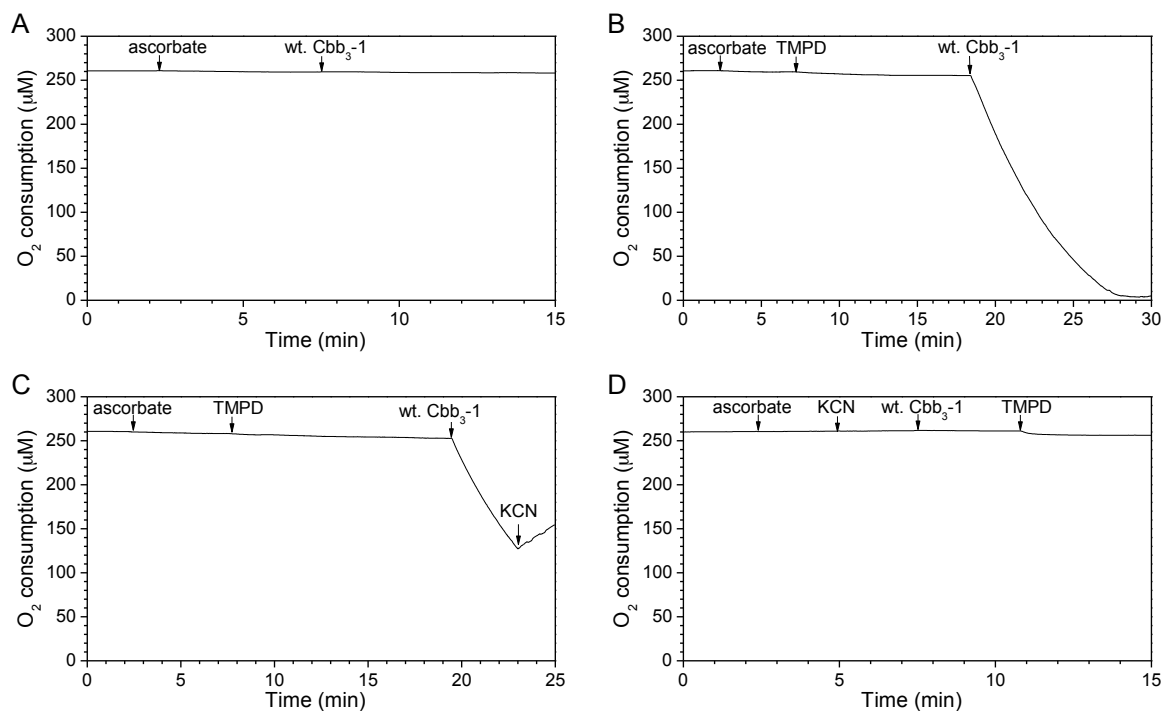


Figure 3-23: Measurements of oxygen reductase activity of wild-type Cbb₃-1. The addition of 3 mM ascorbate, 1 mM TMPD, 8.3 nM *cbb*₃-CcO and 1 mM KCN is indicated by arrows. (A) No oxygen consumption was observed in the absence of TMPD. (B) The reaction was initiated by adding *cbb*₃-CcO to a reaction mixture containing ascorbate and TMPD. (C) Inhibition of the *cbb*₃-CcO by KCN during the turnover. (D) No oxygen consumption was present when KCN was added before the reaction initiation.

The oxygen reductase activity of *cbb*₃-CcO was measured using a Clark-type oxygen electrode. A combination of ascorbate and TMPD was used as the artificial respiratory substrate to deliver the electrons required for the oxygen reduction reaction. As shown in Figure 3-23, oxygen consumption does not occur in the absence of TMPD, and can be completely inhibited by addition of 1 mM KCN.

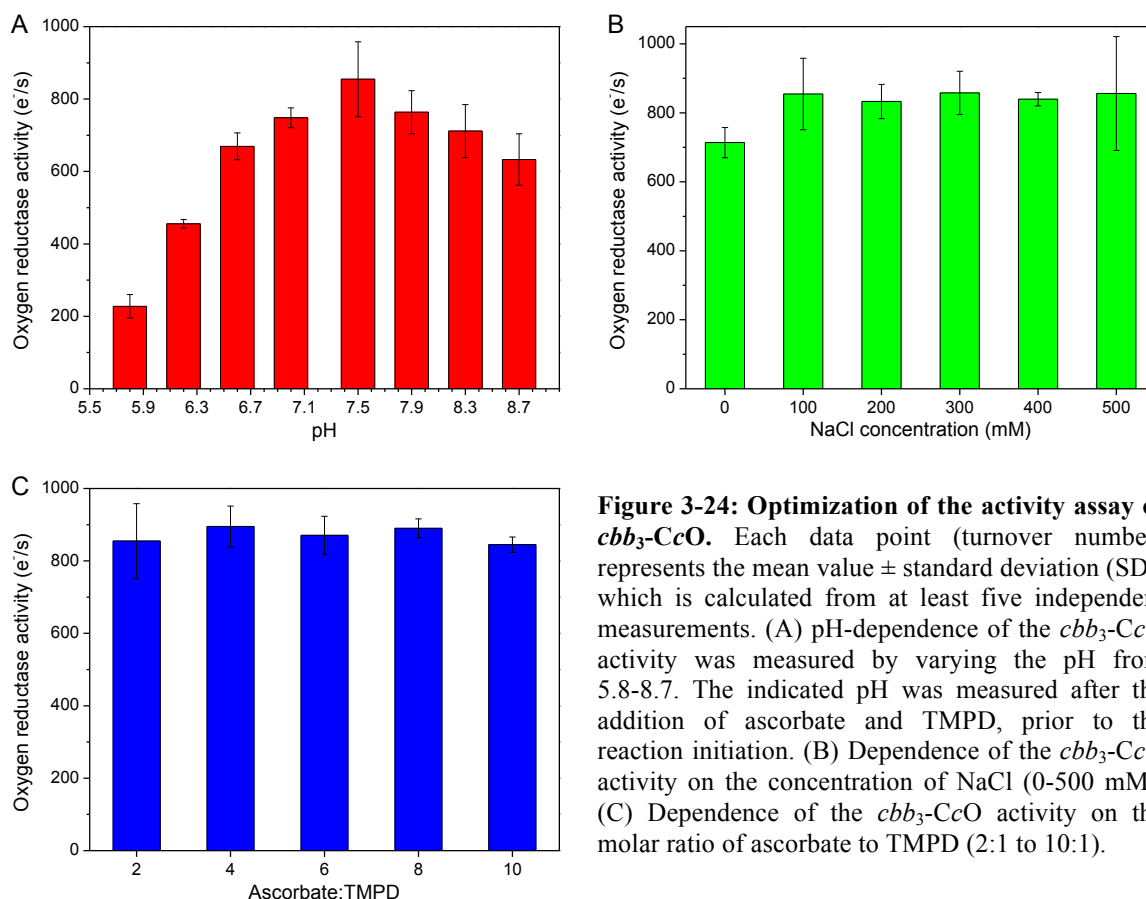
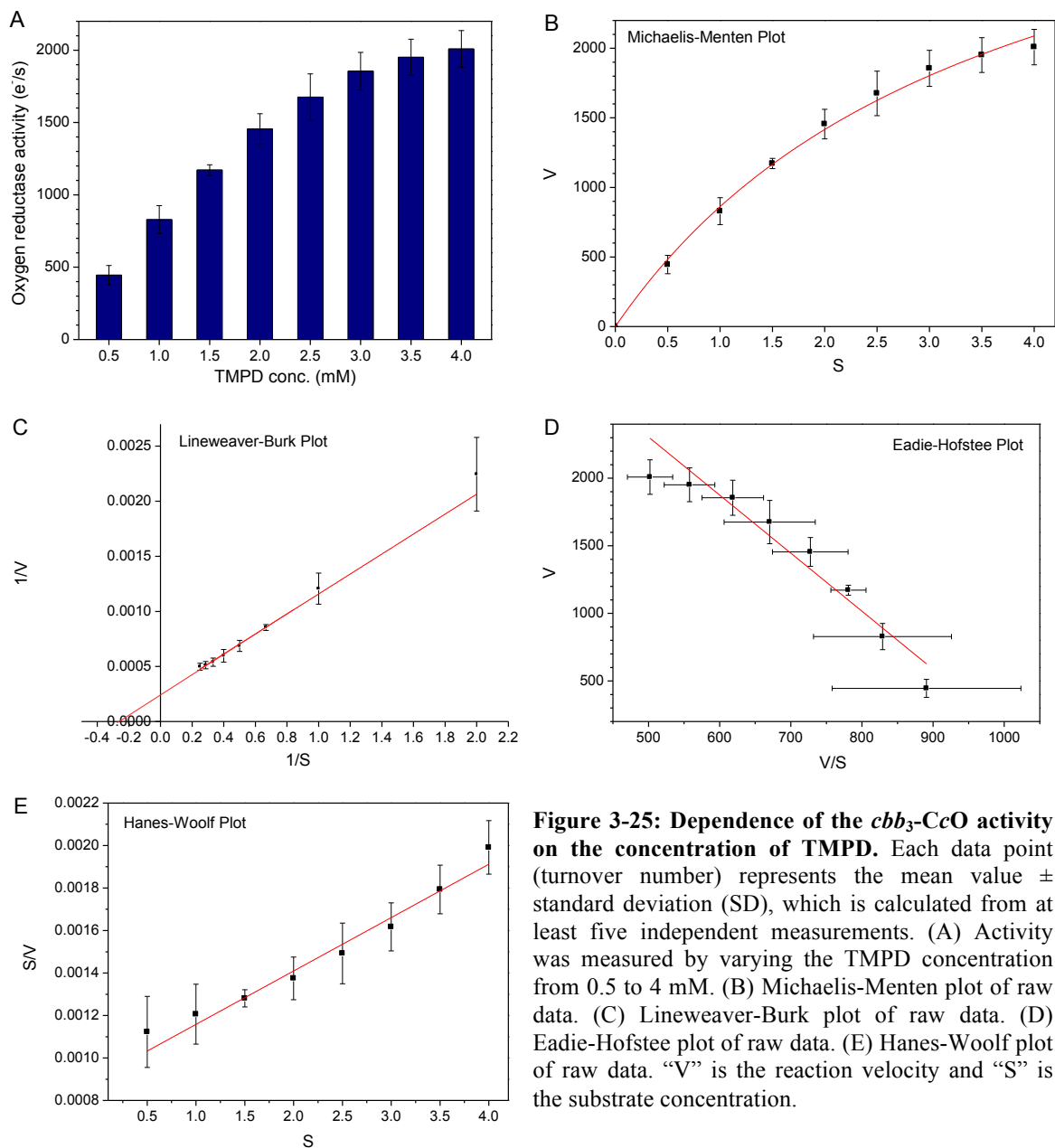


Figure 3-24: Optimization of the activity assay of *cbb*₃-CcO. Each data point (turnover number) represents the mean value \pm standard deviation (SD), which is calculated from at least five independent measurements. (A) pH-dependence of the *cbb*₃-CcO activity was measured by varying the pH from 5.8-8.7. The indicated pH was measured after the addition of ascorbate and TMPD, prior to the reaction initiation. (B) Dependence of the *cbb*₃-CcO activity on the concentration of NaCl (0-500 mM). (C) Dependence of the *cbb*₃-CcO activity on the molar ratio of ascorbate to TMPD (2:1 to 10:1).

To accurately measure the enzymatic activity of *cbb*₃-CcO, the reaction conditions were first optimized by varying the pH, salt concentration and the ascorbate/TMPD ratio. Upon addition of various concentrations of ascorbate and TMPD, it was found that the pH value of the reaction system dropped approx. 0.1 to 0.5 units depending on the buffer composition. Therefore, three different buffers (Tris, HEPES and phosphate) were tested for their effects on the enzymatic activity assay. Tris buffer was chosen, and the pH was checked to verify that it was within ± 0.05 units of the desired value during all the experiments. As shown in Figure 3-24 A, the optimal pH for the activity of *cbb*₃-CcO is approximately 7.5. By varying the concentration of NaCl in the range of 0 to 500 mM, the interaction between TMPD and *cbb*₃-CcO appears independent of ionic strength (Figure 3-24 B). Moreover, a molar ratio of 2:1 to 10:1 for ascorbate to TMPD shows no strong

effect on the TMPD-mediated oxygen reductase activity of *ccb₃-CcO* (Figure 3-24 C).



Under the optimized conditions (50 mM Tris/HCl, pH 7.5, 100 mM NaCl, 50 μ M EDTA, 0.02% [w/v] DDM and ascorbate:TMPD = 3:1), a non-linear dependence of enzyme activity of wild-type Cbb₃-1 as a function of the concentration of TMPD was observed (Figure 3-25 A). At a high concentration of TMPD (4 mM), the highest steady-state turnover rate of wild-type Cbb₃-1 was measured to be 2,000 e⁻/s. Although a saturation plateau was not reached, the rates of oxygen reduction catalyzed by *ccb₃-CcO* still followed Michaelis-Menten kinetics (Figure 3-25 B). In order to determine the kinetic parameters (V_{\max} and K_m) of this reaction, the measured activity data

were transformed into a linear curve by using different plotting methods, including Lineweaver-Burk, Eadie-Hofstee and Hanes-Woolf analysis. As shown in Figure 3-25 C, a Lineweaver-Burk plot of reciprocal of the initial rates against reciprocal of TMPD concentration was linear with a R-squared value of 0.991, and V_{\max} and K_m values were estimated to be 3,978 e^-/s and 3.6 mM, respectively. In addition, similar results were obtained from Eadie-Hofstee and Hanes-Woolf plots of transformed data. In both cases, the resulting values for V_{\max} and K_m are about 4,000 e^-/s and 3.6 mM, respectively.

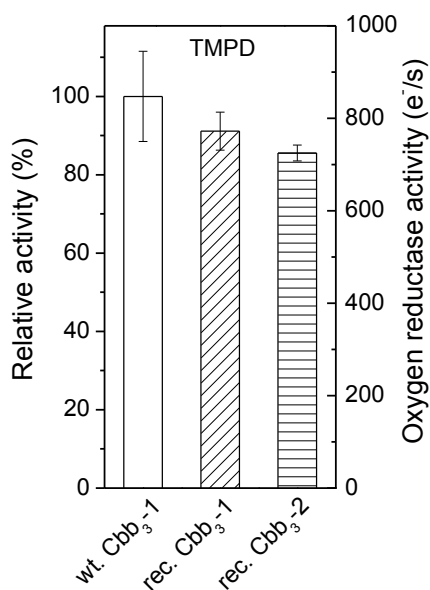


Figure 3-26: Comparison of the oxygen reductase activity between wild-type *Cbb3-1*, recombinant *Cbb3-1* and *Cbb3-2*. Each bar represents the mean value \pm SD, which are calculated from at least five independent measurements. The relative activity was calculated by assuming that the activity observed from wild-type *Cbb3-1* was 100%. Oxygen reductase activity was measured in the presence of 3 mM ascorbate, 1 mM TMPD and 8.3 nM *cbb3-CcO* at pH 7.5.

In order to compare the oxygen reductase activity of both recombinant *cbb3*-isoforms with the wild-type *Cbb3-1*, 3 mM ascorbate and 1 mM TMPD were used. As shown in Figure 3-26, the activities of recombinant *Cbb3-1* and *Cbb3-2* were determined to be between 700 and 800 e^-/s , which is only slightly lower than that of wild-type *Cbb3-1*. This indicates that there is no significant difference either between the wild-type and the recombinant proteins or between the two *cbb3*-isoforms.

3.5.7 Determination of the catalase activity

Besides the reduction of oxygen, a side reaction, in which hydrogen peroxide (H_2O_2) can be decomposed into H_2O and O_2 , was also observed for both *cbb3*-isoforms. This so-called ‘‘catalase activity’’ was originally found in A-type HCOs, e.g., *aa3-CcO* from bovine heart (Orii and Okunuki 1963), and was measured as described for *aa3-CcO* from *P. denitrificans* (Hilbers *et al.*, 2013) using 600 μM H_2O_2 and 500 nM *cbb3-CcOs*. Catalase activity measurements of the *cbb3-CcO* show no significant difference either between the wild-type and the recombinant *Cbb3-1*

or between the recombinant Cbb₃-1 and Cbb₃-2 (Figure 3-27). Moreover, the catalase activity of *cbb*₃-CcO was measured to be in the range of 1.6-2.4 O₂/min/oxidase (Figure 3-27), which is comparable to the reported values for wild-type *aa*₃-CcO from *P. denitrificans* (Hilbers *et al.*, 2013).

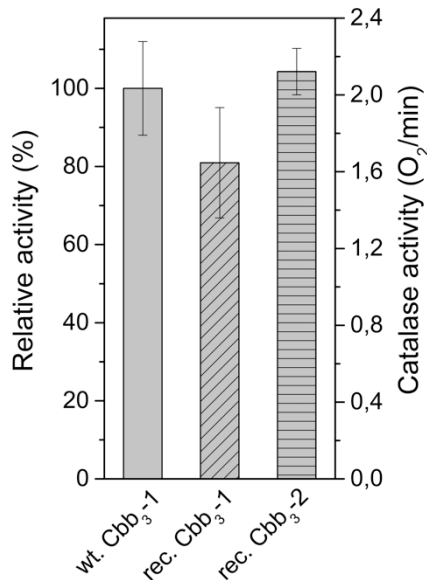


Figure 3-27: Comparison of the catalase activity between wild-type Cbb₃-1, recombinant Cbb₃-1 and Cbb₃-2. Each bar represents the mean value \pm SD, which are calculated from at least five independent measurements. The relative activity was calculated by assuming that the activity observed from wild-type Cbb₃-1 was 100%. Catalase activity was measured in the presence of 600 μ M hydrogen peroxide and 500 nM *cbb*₃-CcO.

3.5.8 The redox active tyrosine residue

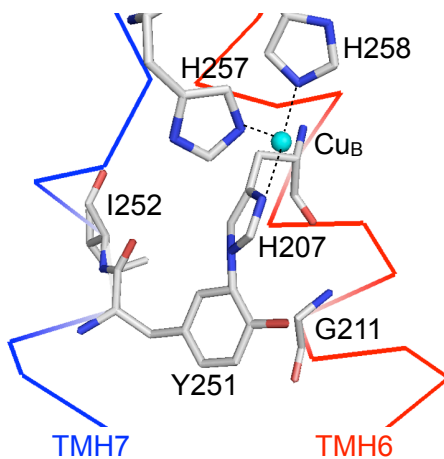


Figure 3-28: The His-Tyr cross-link in *cbb*₃-CcO and the location of the selected residues for site-directed mutagenesis studies. The Y251 is covalently bound to a Cu_B ligand (H207). The copper ion is shown as a cyan sphere. The transmembrane helices (TMH) 6 and 7 are shown in ribbon representation and coloured red and blue, respectively. The residues I252 and G211 are separately replaced by tyrosine (for details, see text). Atomic coordinates were taken from PDB entry 3MK7. The figure was prepared using the PyMol software.

In the active site of all CcOs, one of the three histidine ligands of Cu_B is covalently linked to a tyrosine residue. In A- and B-type CcOs, this critical tyrosine is located four amino acids away from the histidine ligand and both residues (His and Tyr) reside in the same helix (TMH6). By

comparison, in the *cbb₃-CcOs*, this redox active tyrosine (Tyr251) is located in a different helix (TMH7). In addition, sequence alignments show that the *P. stutzeri cbb₃-CcO* has a glycine (Gly211) at the equivalent position in the subunit CcoN (Figure 3-28).

To investigate the role of the cross-linked tyrosine in *cbb₃-CcO*, four variants of the Cbb₃-1 were created by site-directed mutagenesis, namely, Y251F, Y251A, Y251A/I252Y and Y251A/G211Y. The variants Y251F and Y251A were created to prevent the enzymatic formation of the tyrosine radical, whereas the double variants Y251A/I252Y and Y251A/G211Y were designed to test the possibility that the His-Tyr cross-link could be restored if the tyrosine residue was present in an alternative location.

The four Tyr251 variants were purified to apparent homogeneity, and subsequently analyzed by SDS-PAGE followed by heme staining. All four variants contained wild-type amounts of the CcoN, CcoO and CcoP subunits, and the results of heme staining confirmed the correct incorporation of the heme *c* (data not shown). In addition, all variants exhibited the same UV/vis spectra as the wild-type *cbb₃-CcO* (Figure 3-29), which indicated that the substitution of this tyrosine residue did not alter the environments of heme *b* and heme *b₃*.

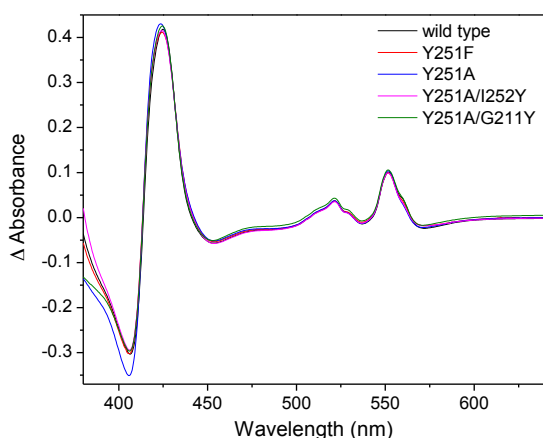


Figure 3-29: The reduced-minus-oxidized difference spectra of wild-type Cbb₃-1 and four variants.

Table 3-11: Comparison of activities of wild type and variants.

Enzyme	Relative activity
Wild type	100%
Y251F	0%
Y251A	0%
Y251A/I252Y	0%
Y251A/G211Y	0%

The oxygen reductase activities of the wild-type *cbb₃-CcO* and four variants were measured polarographically in the presence of ascorbate and TMPD and the results are summarized in Table 3-11. The results showed that two variants of the *cbb₃-CcO* were totally inactive when the tyrosine was substituted by a phenylalanine (Y251F) or an alanine (Y251A) residue. Moreover, both double variants Y251A/I252Y and Y251A/G211Y also lost the enzymatic activity completely.

3.5.9 Variants of Glu323

In the *cbb₃-CcO* of *P. stutzeri*, one glutamate residue (E323) is hydrogen-bonded to the histidine ligand (H345) of the high spin heme (Figure 3-30). This glutamate residue is highly conserved in the bacterial *cbb₃-CcOs*, but not present in other oxidases (Hemp *et al.*, 2007).

In order to investigate the role of E323, three variants of the Cbb₃-1 were created by site-directed mutagenesis, namely, E323A, E323Q and E323D. All variants were purified from the detergent-solubilized membrane of *P. stutzeri*. The oxygen reductase activities of the variants were measured polarographically and compared with the wild-type *cbb₃-CcO* (Table 3-12). It was found that the enzymatic activity was completely abolished when this glutamate residue was replaced by an alanine (E323A) or a glutamine (E323Q) residue, whereas the variant E323D had about 40% of the wild-type oxidase activity (Table 3-12).

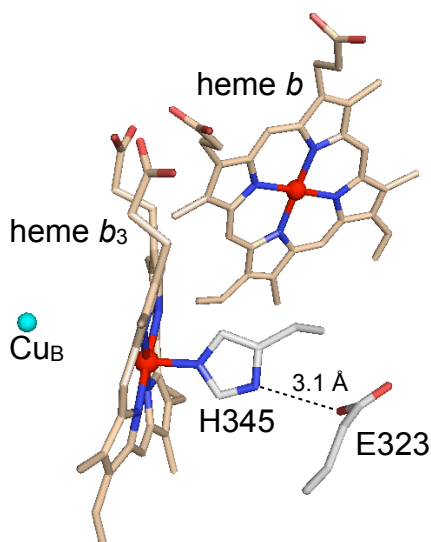


Table 3-12: Variants of Glu323.

Enzyme	Relative activity
Wild type	100%
E323A	0%
E323Q	0%
E323D	40%

Figure 3-30: The active site of *cbb₃-CcO* of *P. stutzeri*. E323 is hydrogen-bonded to His345. Heme *b* and *b₃* are represented as sticks. The copper ion is shown as a cyan sphere. Atomic coordinates were taken from PDB entry 3MK7. The figure was prepared using the PyMol software.

3.6 Identification and characterization of the natural electron donor of *cbb₃-CcO*

Following well established procedures (Reincke *et al.*, 1999; Londer 2011), untagged recombinant cytochromes *c* from *P. stutzeri* ZoBell were heterologously expressed in *E. coli* to investigate the physiological electron donors of *cbb₃-CcO*.

3.6.1 Prediction of *c*-type cytochromes of *P. stutzeri*

Cytochromes *c* are characterized by the covalent attachment of heme *c* to an apocytochrome via a CXXCH motif (Ambler 1991). By analyzing this motif in the recently published draft genome sequence of *P. stutzeri* ZoBell (Peña *et al.*, 2012), a total of 63 matches were found in 45 proteins²⁵. Among them, 16 proteins were predicted to be cytochromes *c* based on homology analyses (see Appendix B). Four cytochromes *c* (Table 3-13) are considered as reasonable candidates for heterologous expression in *E. coli* because their existence was previously reported and verified by biochemical experiments (Liu *et al.*, 1983; Pettigrew and Brown 1988). Besides the well-known electron donor (cytochrome *c₅₅₁*) for cytochrome *cd₁* nitrite reductase, the cytochromes *c₄* and *c₅₅₂* are believed to be involved in electron transfer to oxygen and nitrite, respectively (Pettigrew and Brown 1988; Jüngst *et al.*, 1991). However, like cytochrome *c₅*, their virtual ability to transfer electrons to *cbb₃-CcO* in *P. stutzeri* has not been experimentally validated.

Table 3-13: Selected cytochromes *c* of *P. stutzeri*^a.

Protein	Gene	UniProt ID	Location	No. of hemes	MW-1 (Da)	MW-2 (Da)	CL	Function
Cyt. <i>c₄</i>	<i>cycA</i>	H7EVH9	IM, PP	2	21,718	20,886	IC	oxygen reduction?
Cyt. <i>c₅</i>	<i>cycB</i>	H7EWL8	IM, PP	1	13,900	11,963	IE	unknown
Cyt. <i>c₅₅₁</i>	<i>nirM</i>	H7EQG5	PP	1	10,797	9,179	ID	e ⁻ donor for NIR
Cyt. <i>c₅₅₂</i>	<i>nirB</i>	H7EQG6	PP	2	30,426	29,413	-	nitrite reduction?

^a CL: Ambler's classification; IM: inner membrane; MW-1: molecular weight of gene product; MW-2: molecular weight of mature holocytochrome; NIR: cytochrome *cd₁* nitrite reductase; PP: periplasm.

3.6.2 Construction of expression vectors for cytochromes *c*

Three DNA fragments containing the *cycA* gene encoding cytochrome *c₄* (1498 bp), the *cycB* gene encoding cytochrome *c₅* (1163 bp) and *nirMB* encoding cytochromes *c₅₅₁* and *c₅₅₂* (2874 bp) were amplified by PCR using genomic DNA from *P. stutzeri* ZoBell as a template. The following

²⁵ Protein motif analyzing was performed using a web-based scanning tool (ScanProsite) against the protein database UniProt (taxonomy:32042).

primer pairs were used: C4-Fw/C4-Rev for *cycA*, C5-Fw/C5-Rev for *cycB* and C551-C552-Fw/C551-C552-Rev for *nirMB*. These fragments were cloned into the vector pJET1.2 and their sequence was verified. All four cytochromes *c* are predicted to have a signal peptide preceding the N-terminus of the mature protein (Table 3-14). Using the primer pairs C4-IF-N/C4-IF-C and C551-IF-N/C551-IF-C, two DNA fragments encoding the mature cytochromes *c*₄ and *c*₅₅₁ were cloned via ligation-independent cloning into the pET-22b(+) vector, resulting in pET-22-C4 and pET-22-C551. Correspondingly, two DNA fragments encoding the mature cytochromes *c*₅ and *c*₅₅₂ were amplified using the primer pairs C5-NcoI/C5-BamHI and C552-NcoI/C552-BamHI and subsequently inserted into the NcoI/BamHI site of pET-22b(+) to generate pET-22-C5 and pET-22-C552. Afterwards, the resulting expression vectors were sequenced and the fusion of the genes encoding the mature cytochromes *c* to the *pelB* leader sequence was confirmed.

Table 3-14: The predicted signal peptides of 4 selected cytochromes^a.

Protein	N-terminal signal peptide sequence	Length (amino acids)
Cytochrome <i>c</i> ₄	M-N-K-V-L-V-S-L-L-L-T-L-G-I-T-G-M-A-H-A	20
Cytochrome <i>c</i> ₅	M-N-L-I-K-K-I-L-V-A-Q-T-A-V-V-A-L-W-A-M-S-A-Q-A	24
Cytochrome <i>c</i> ₅₅₁	M-K-K-I-L-I-P-M-L-A-L-G-G-A-L-A-M-Q-P-A-L-A	22
Cytochrome <i>c</i> ₅₅₂	M-K-K-T-L-M-A-S-A-V-G-A-V-I-A-F-G-T-H-G-A-M-A	23

^a Signal peptide prediction was performed using the SignalP 4.1 server. The predicted signal peptides of cytochromes *c*₅₅₁ and *c*₅₅₂ are in agreement with previously published data (Jüngst *et al.*, 1991).

3.6.3 Cell growth and small-scale expression of cytochromes *c*

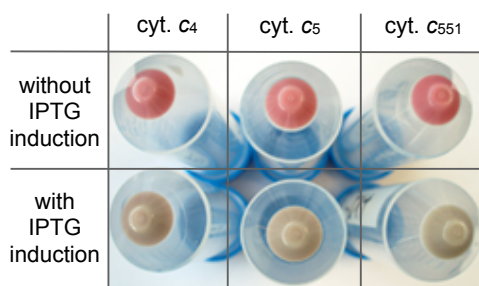


Figure 3-31: Comparison of uninduced and IPTG-induced cells containing the expression vector with the gene encoding cytochrome *c*. Cells were pelleted from 50 ml of overnight culture by centrifugation at $5,000 \times g$ for 20 min.

Four recombinant expression vectors were introduced individually into the *E. coli* BL21 Star (DE3) strain which was previously transformed with pEC86 containing the *E. coli* cytochrome *c* maturation genes *ccmABCDEFGH* (Arslan *et al.*, 1998)²⁶. For small-scale expression and analysis, the cells were grown aerobically in 50 ml of LB medium at 32°C containing 50 µg/ml Amp and 34 µg/ml Cam. In addition to uninduced cells, 0.5 mM IPTG was added to the bacterial culture

²⁶ The plasmid pEC86 was kindly provided by Prof. Linda Thöny-Meyer (Empa Materials Science and Technology, St. Gallen, Switzerland), which allows the aerobic expression of cytochrome *c* in *E. coli*.

when an OD_{600} of 0.5 to 0.8 was reached. By monitoring the cell density, an inhibition of cell growth was observed as the result of treatment with IPTG, and which is believed to be caused by the toxicity of overproduced apocytochrome in *E. coli*. On the other hand, high-yield expression of cytochromes c_4 , c_5 , and c_{551} was achieved without IPTG induction. The red color of pelleted cells indicated the incorporation of heme c into the apocytochrome c (Figure 3-31).

To determine the expression pattern and the location of the recombinant cytochromes c in the cellular fractions of *E. coli*, the periplasmic and spheroplasmic fractions were prepared from cells treated with lysozyme (see 2.2.2.8). The periplasmic and spheroplasmic proteins were analyzed by SDS-PAGE followed by heme staining and Coomassie staining (Figure 3-32). As shown in Figure 3-32 A (left part of each gel), no specific band was detected in control cells containing an empty vector. This result confirms that the *E. coli* does not express its endogenous cytochromes c under normal aerobic conditions.

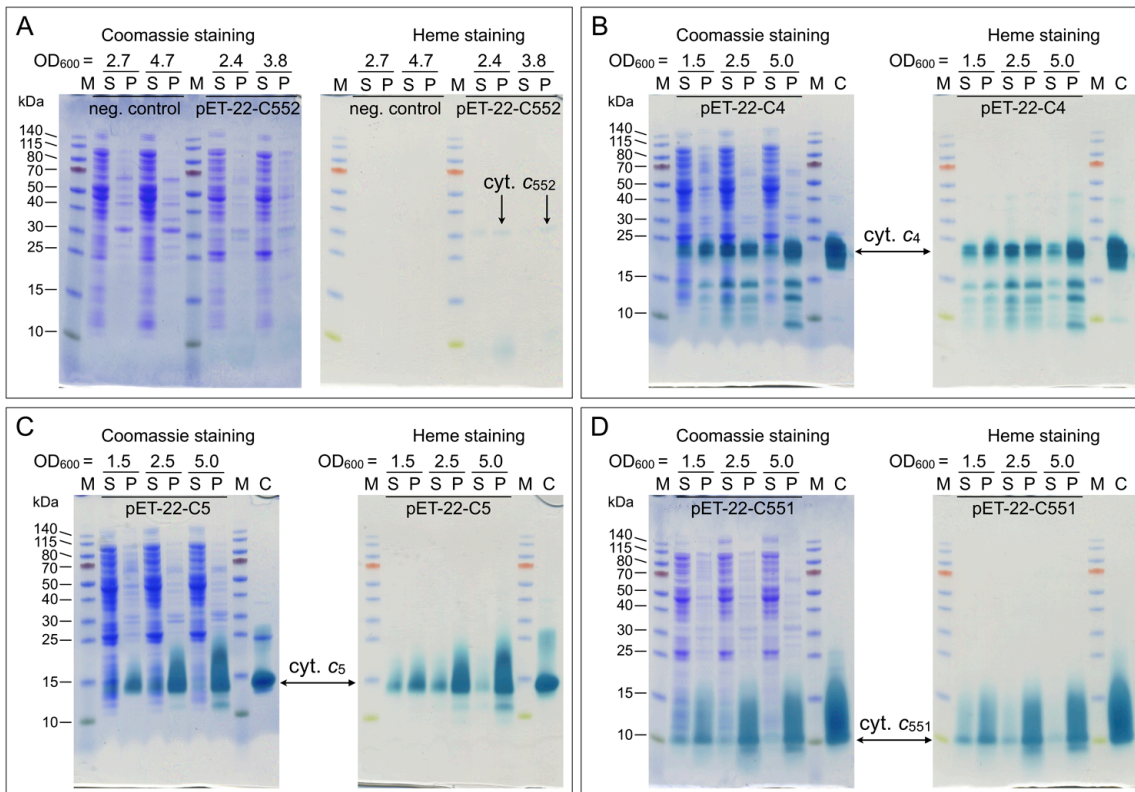


Figure 3-32: SDS-PAGE gels of small-scale expression of recombinant cytochromes c . The cells (approx. 2×10^9 cells) were collected at different cell densities (OD_{600} of 1.5 to 5.0). Total spheroplasmic “S” and periplasmic “P” proteins of *E. coli* cells expressing cytochromes c from *P. stutzeri* ZoBell were separated on 12% Bis-Tris SDS-PAGE gels. Proteins that contain covalently bound heme c were detected by heme staining (on the left of each panel). Afterwards the total proteins were visualized by Coomassie staining, which are shown on the right of each panel. “M” is the PageRuler Prestained Protein Ladder and the molecular weights of marker proteins are shown in kDa. Samples from *E. coli* cells containing empty pET-22(b)+ vector served as negative control (A). The expression of cytochromes c_{552} , c_4 , c_5 and c_{551} are shown in panel A-D, respectively. “C” indicates the native cytochromes, which are purified from wild-type *P. stutzeri* ZoBell cells.

In contrast to the negative control, expression of the four recombinant cytochromes *c* was observed, although the expression level of cytochrome *c*₅₅₂ (Figure 3-32 A, right part of each gel) was relatively lower in comparison to the other three cases. In the case of cytochromes *c*₄, *c*₅, and *c*₅₅₁ (Figure 3-32 B-D), the results of SDS-PAGE analysis showed that: (i) the heterologously expressed cytochromes *c* are mostly found in the periplasm of *E. coli*. The heme signals, which were detected in the spheroplasmic fractions, are believed to be predominantly caused by cross-contamination of periplasmic fractions with the spheroplasmic proteins; (ii) the highest level of expression was observed at high cell density (OD₆₀₀ = 5); (iii) the recombinant cytochromes *c* showed a profile similar to that of wild-type proteins.

To increase the yield of cytochrome *c*₅₅₂, different culture conditions were tested, including cultivation temperature, IPTG concentration and induction time. However, only a little improvement was observed (data not shown). Therefore, only three cytochromes *c* (*c*₄, *c*₅, and *c*₅₅₁) were selected for the further large-scale expression and purification.

3.6.4 Purification of recombinant cytochromes *c*

The recombinant cytochromes *c* were purified from the periplasm of *E. coli* cells by a three-step procedure, consisting of ion exchange chromatography, chromatofocusing and size exclusion chromatography.

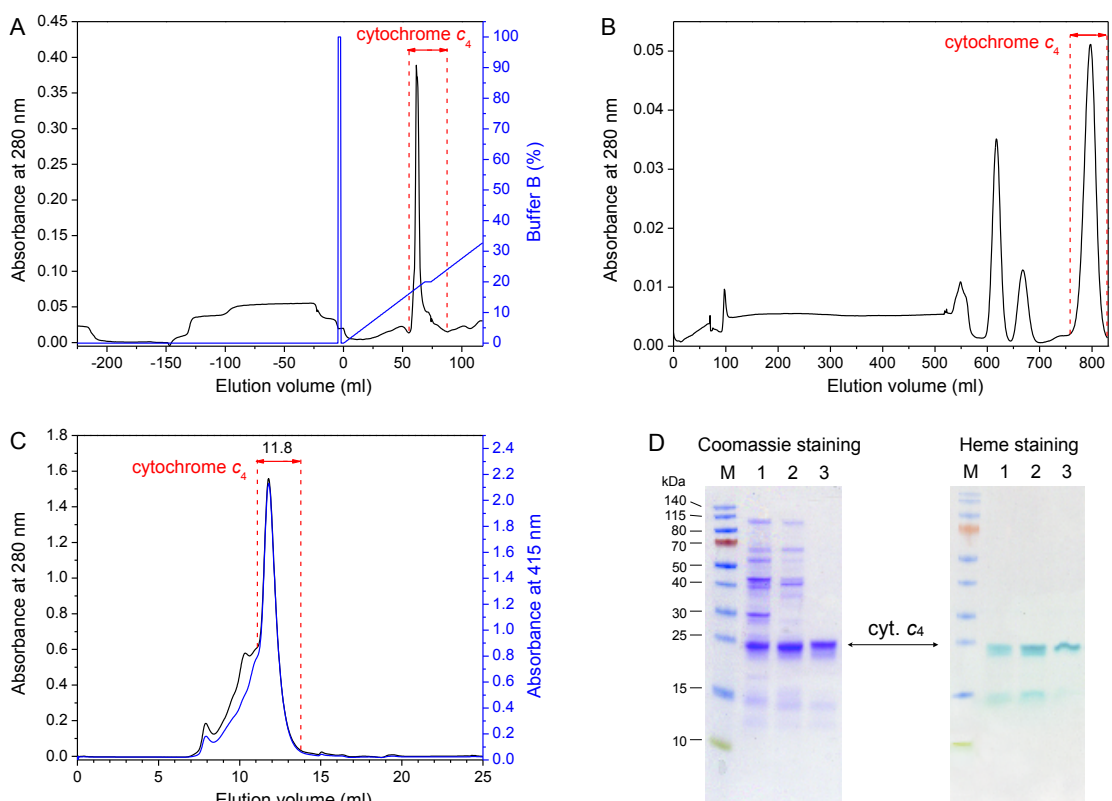


Figure 3-33: Purification of recombinant cytochrome c_4 . Elution profile of the ion exchange chromatography (Q Sepharose column), chromatofocusing (PBE 94 column) and size exclusion chromatography (Superdex 75 column) is shown in A, B and C, respectively. During all purification steps, fractions were monitored at 280 nm (black). The peak fractions containing the desired cytochrome c_4 are indicated as red arrows and red dashed lines. The blue line in panel A indicates the gradient used for elution, and the percentage represents the concentration of NaCl in the elution buffer (100% = 1M NaCl). During size exclusion chromatography (panel C), fractions were also monitored at 415 nm (blue) for heme c detection. Panel D shows the SDS-PAGE (12% Bis-Tris) analysis of eluted fractions collected from three chromatographic steps. “M” is the PageRuler Prestained Protein Ladder and the molecular weights of marker proteins are shown in kDa.

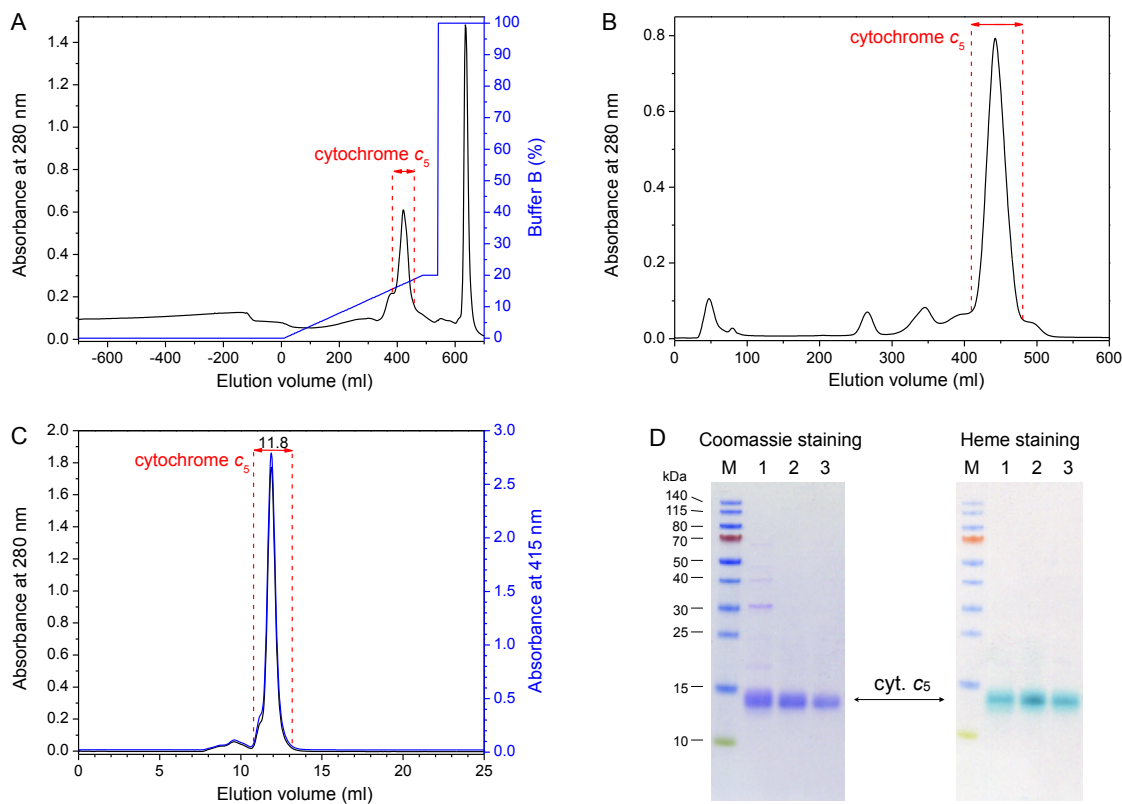


Figure 3-34: Purification of recombinant cytochrome c_5 . Elution profile of the ion exchange chromatography (Q Sepharose column), chromatofocusing (PBE 94 column) and size exclusion chromatography (Superdex 75 column) is shown in A, B and C, respectively. During all purification steps, fractions were monitored at 280 nm (black). The peak fractions containing the desired cytochrome c_5 are indicated as red arrows and red dashed lines. The blue line in panel A indicates the gradient used for elution, and the percentage represents the concentration of NaCl in the elution buffer (100% = 1M NaCl). During size exclusion chromatography (panel C), fractions were also monitored at 415 nm (blue) for heme c detection. Panel D shows the SDS-PAGE (12% Bis-Tris) analysis of eluted fractions collected from three chromatographic steps. “M” is the PageRuler Prestained Protein Ladder and the molecular weights of marker proteins are shown in kDa.

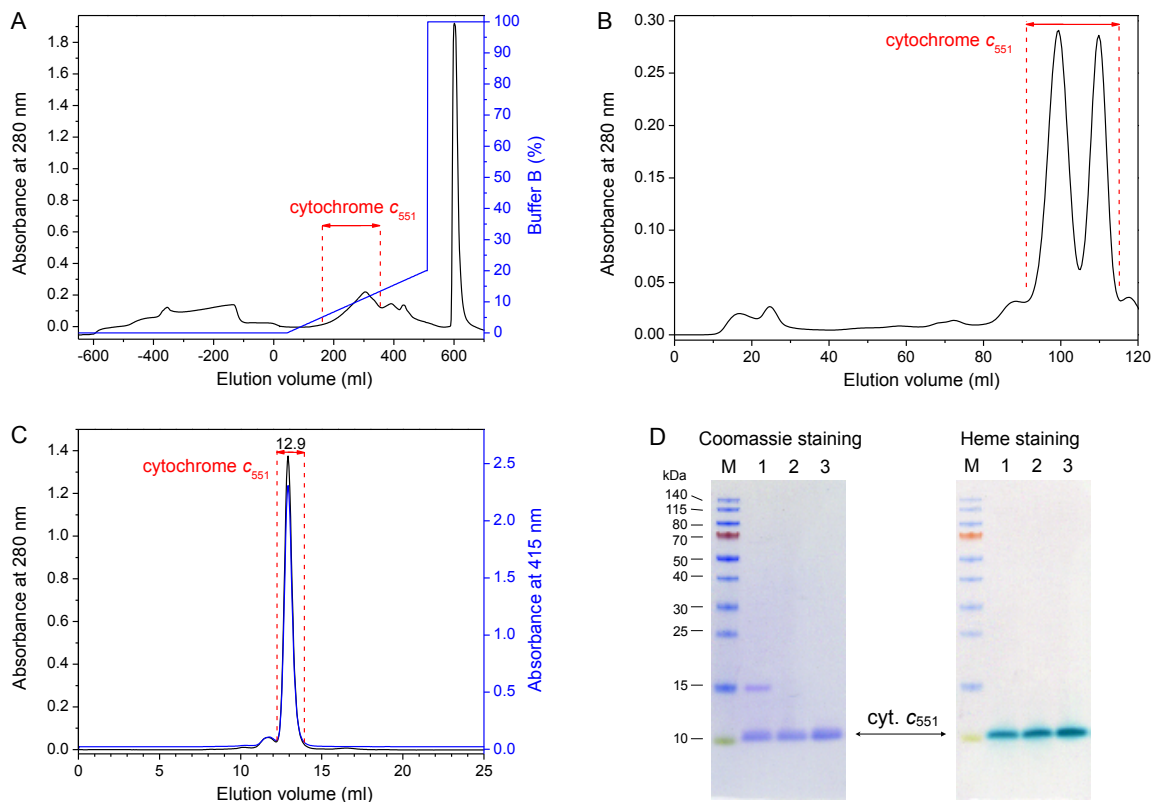


Figure 3-35: Purification of recombinant cytochrome c_{551} . Elution profile of the ion exchange chromatography (Q Sepharose column), chromatofocusing (PBE 94 column) and size exclusion chromatography (Superdex 75 column) is shown in A, B and C, respectively. During all purification steps, fractions were monitored at 280 nm (black). The peak fractions containing the desired cytochrome c_{551} are indicated as red arrows and red dashed lines. The blue line in panel A indicates the gradient used for elution, and the percentage represents the concentration of NaCl in the elution buffer (100% = 1M NaCl). During size exclusion chromatography (panel C), fractions were also monitored at 415 nm (blue) for heme c detection. Panel D shows the SDS-PAGE (12% Bis-Tris) analysis of eluted fractions collected from three chromatographic steps. “M” is the PageRuler Prestained Protein Ladder and the molecular weights of marker proteins are shown in kDa.

Figure 3-33 to 34 show the typical purification profiles of cytochromes c_4 , c_5 , and c_{551} , respectively. During the first chromatographic step (panel A in Figure 3-33 to 34), three cytochromes c were eluted at relatively low concentrations of NaCl (160 to 240 mM for c_4 , 160 to 190 mM for c_5 and 50 to 130 mM for c_{551}). Subsequently, chromatographic fractions were subjected to chromatofocusing separation. At this purification step, cytochrome c_{551} was resolved as two peaks (Figure 3-35 B), representing the oxidized and reduced forms of the protein, as determined spectrophotometrically. In contrast, both cytochrome c_4 and c_5 were eluted as a single peak. After a final size exclusion chromatography step, all three recombinant cytochromes c were purified to apparent homogeneity, as indicated by single bands on SDS-PAGE gels stained for protein and heme. In addition, the apparent size of the protein band corresponds well to the calculated molecular mass of the three mature cytochromes c .

Table 3-15 shows the typical yields of recombinant cytochromes c , which were determined spectrophotometrically using specific extinction coefficients (see 2.2.3.1). The cytochrome c_5 has the highest yield of 10 mg per liter of culture medium, while the yield of purified cytochrome c_4 and c_{551} was around 2 and 4 mg per liter of culture medium, respectively. Despite the difference between the three proteins, their yields are sufficient for the further biochemical analysis.

Table 3-15: Summary of typical protein yields of recombinant cytochromes c .

	Cytochrome c_4	Cytochrome c_5	Cytochrome c_{551}
Yield	2 mg/liter	10 mg/liter	4 mg/liter

3.6.5 UV/Vis spectra of recombinant cytochromes c

Figure 3-36, 3-36 and 3-37 show the oxidized, reduced and reduced-minus-oxidized spectra of purified recombinant cytochrome c_4 , c_5 and c_{551} , respectively. The spectra of the three recombinant cytochromes c are identical to the spectra obtained from the wild-type proteins (data not shown). Furthermore, the spectral features of cytochrome c_4 and c_{551} are consistent with previously published data (Liu *et al.*, 1983; Pettigrew and Brown 1988).

In the oxidized form, the Soret maximum was observed at 410 nm for cytochrome c_4 , 414 nm for cytochrome c_5 and 409 nm for cytochrome c_{551} . Upon complete reduction of the protein with dithionite, this Soret peak was red-shifted to 415, 419 and 417 nm for cytochrome c_4 , c_5 and c_{551} , respectively (Figure 3-36 to 3-38).

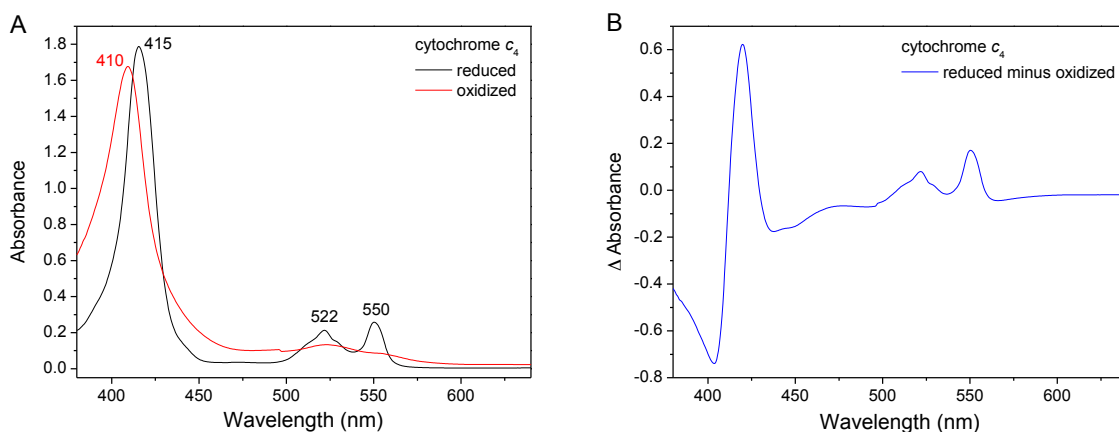


Figure 3-36: UV/Vis spectra of recombinant cytochrome c_4 . The absorption spectra were recorded from 380 to 640 nm at 25°C. (A) The recombinant cytochrome c_4 was fully oxidized (red) by adding potassium hexacyanoferrate (III) and was subsequently reduced (black) by addition of sodium dithionite. (B) The reduced-minus-oxidized difference spectrum of recombinant cytochrome c_4 .

The reduced absorption spectrum of cytochrome c_4 has two additional maxima at 550 and 522 nm, corresponding to the α and β bands, respectively (Figure 3-36). The ratio of the peak maximum (α/β) is calculated to be 1.2. In the case of reduced cytochrome c_5 , the maxima of α and β band are at 555 and 525 nm and the α/β ratio is 1.4 (Figure 3-37). In addition, the peaks at 551 and 522 nm are characteristic of the reduced cytochrome c_{551} , and a high ratio ($\alpha/\beta = 2.0$) was observed (Figure 3-38).

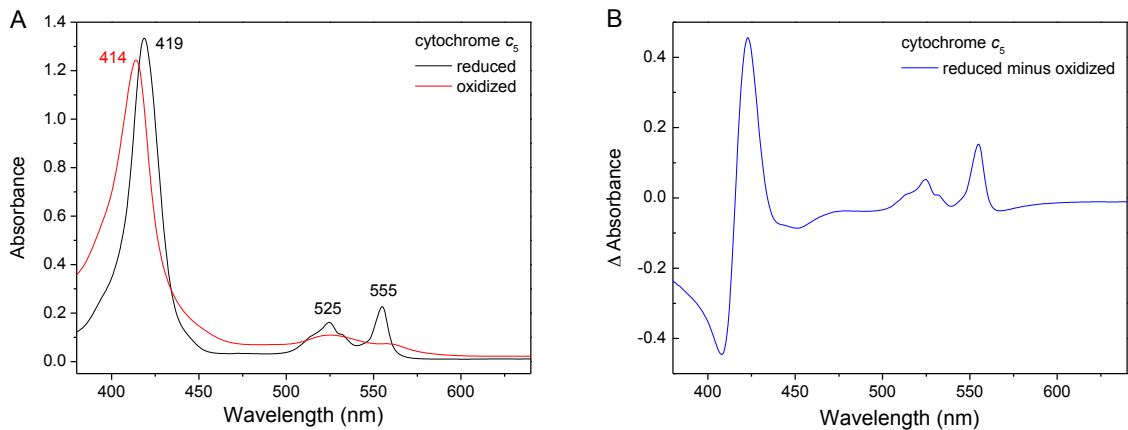


Figure 3-37: UV/Vis spectra of recombinant cytochrome c_5 . The absorption spectra were recorded from 380 to 640 nm at 25°C. (A) The recombinant cytochrome c_5 was fully oxidized (red) by adding potassium hexacyanoferrate (III) and was subsequently reduced (black) by addition of sodium dithionite. (B) The reduced-minus-oxidized difference spectrum of recombinant cytochrome c_5 .

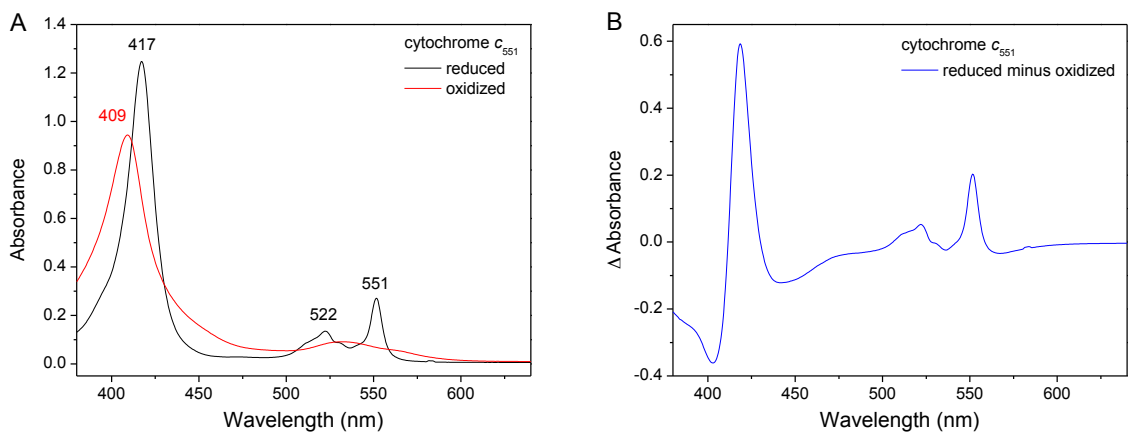


Figure 3-38: UV/Vis spectra of recombinant cytochrome c_{551} . The absorption spectra were recorded from 380 to 640 nm at 25°C. (A) The recombinant cytochrome c_{551} was fully oxidized (red) by adding potassium hexacyanoferrate (III) and was subsequently reduced (black) by addition of sodium dithionite. (B) The reduced-minus-oxidized difference spectrum of recombinant cytochrome c_{551} .

3.6.6 Electrochemical measurement of recombinant cytochromes *c*

The cyclic voltammetry measurements were performed to determine the midpoint redox potentials of heme cofactors for the three recombinant cytochromes *c*. In all three cases, well-defined anodic and cathodic peaks are observed (Figure 3-39). The midpoint potentials were calculated as the average of the oxidation (E_{pa}) and reduction (E_{pc}) peaks, and 208 mV was added to the experimental data to convert these values into the potentials vs. SHE (Table 3-16). For the diheme cytochrome c_4 , two distinctly different redox potentials were determined to be 208 and 308 mV. And the midpoint potentials measured for cytochrome c_5 and c_{551} are 273 and 248 mV, respectively.

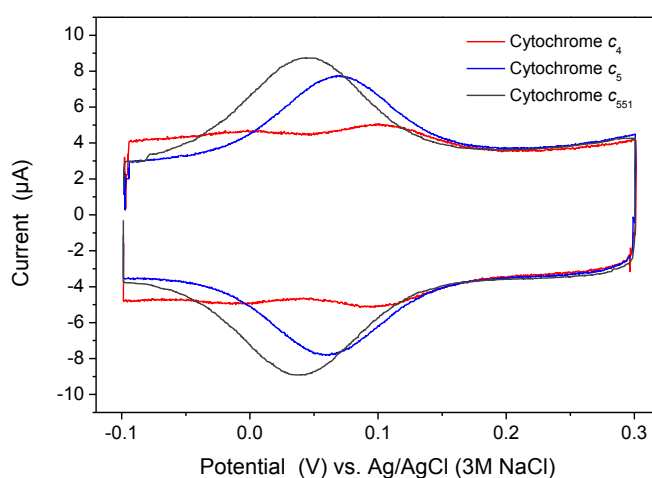


Figure 3-39: Cyclic voltammetry of three recombinant cytochromes *c*. Cyclic voltammograms of cytochrome c_4 , c_5 and c_{551} are shown as red, blue and black curves. Protein samples were immobilized on gold nanoparticles modified with a mixture of thiols. The solution contained 50 mM KPi (pH 7.5). The experimental potential was measured against Ag/AgCl reference electrode (3M NaCl).

The UV/Vis redox titration curves of the three recombinant cytochromes *c* are presented in Figure 3-40. The redox titrations were performed by stepwise setting of the potentials in the range of -400 and +300 mV for cytochrome c_4 and between -200 and +300 for cytochrome c_5 and c_{551} . In order to calculate the midpoint potential of each heme *c*, the measured data was fitted to a calculated Nernst curve ($n=2$ for cytochrome c_4 and $n=1$ for cytochrome c_5 and c_{551}). The calculated potentials are given in Table 3-16. In the case of cytochrome c_4 , two redox midpoint potentials were also determined, which are identical to the results obtained from the cyclic voltammetry measurements. On the other hand, for cytochrome c_5 and c_{551} , the potentials observed by UV/Vis redox titration are slightly shifted when compared to the corresponding values from the cyclic voltammetry measurements (Table 3-16).

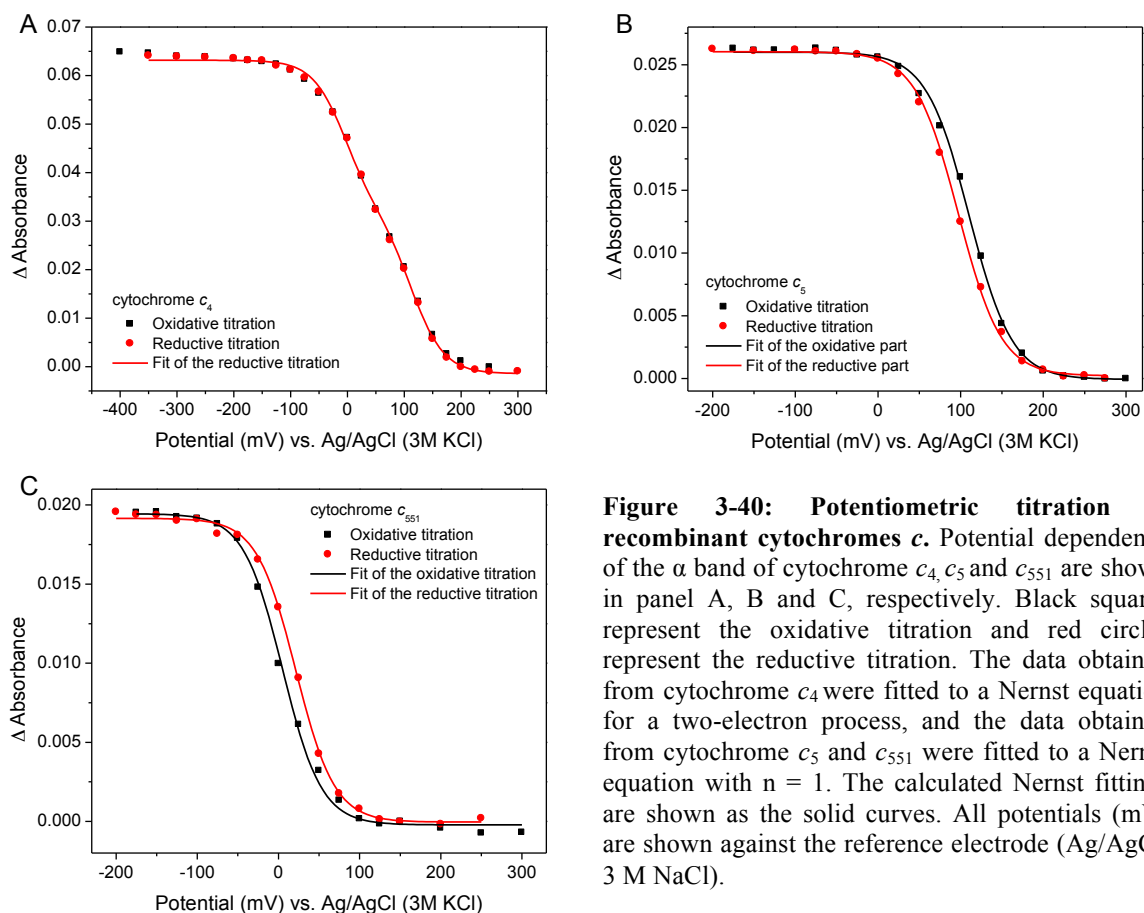


Figure 3-40: Potentiometric titration of recombinant cytochromes c . Potential dependence of the α band of cytochrome c_4 , c_5 and c_{551} are shown in panel A, B and C, respectively. Black squares represent the oxidative titration and red circles represent the reductive titration. The data obtained from cytochrome c_4 were fitted to a Nernst equation for a two-electron process, and the data obtained from cytochrome c_5 and c_{551} were fitted to a Nernst equation with $n = 1$. The calculated Nernst fittings are shown as the solid curves. All potentials (mV) are shown against the reference electrode (Ag/AgCl, 3 M NaCl).

Table 3-16: Summary of midpoint redox potentials of heme c . The midpoint redox potentials determined by two methods are shown in mV (vs. standard hydrogen electrode) at pH 7.5.

	Midpoint potential of heme (vs. SHE)	
	Cyclic voltammetry	Potentiometric titration (UV/Vis)
Cytochrome c_4	208 mV and 308 mV	208 mV and 308 mV
Cytochrome c_5	273 mV	308 mV
Cytochrome c_{551}	248 mV	223 mV

3.6.7 Determination of the natural electron donor of cbb_3 -CcOs

Three different recombinant cytochromes c were used to test their ability to serve as the physiological electron donor for cbb_3 -CcOs. The oxygen reductase activity of cbb_3 -CcO was measured with an oxygen electrode in the absence of TMPD, since TMPD can be exploited to directly donate electrons to the oxidase. As shown in Figure 3-41, apparent oxygen consumption could be observed when the reduced cytochrome c was used as the sole substrate. The observed oxidase activity can be further inhibited upon addition of KCN.

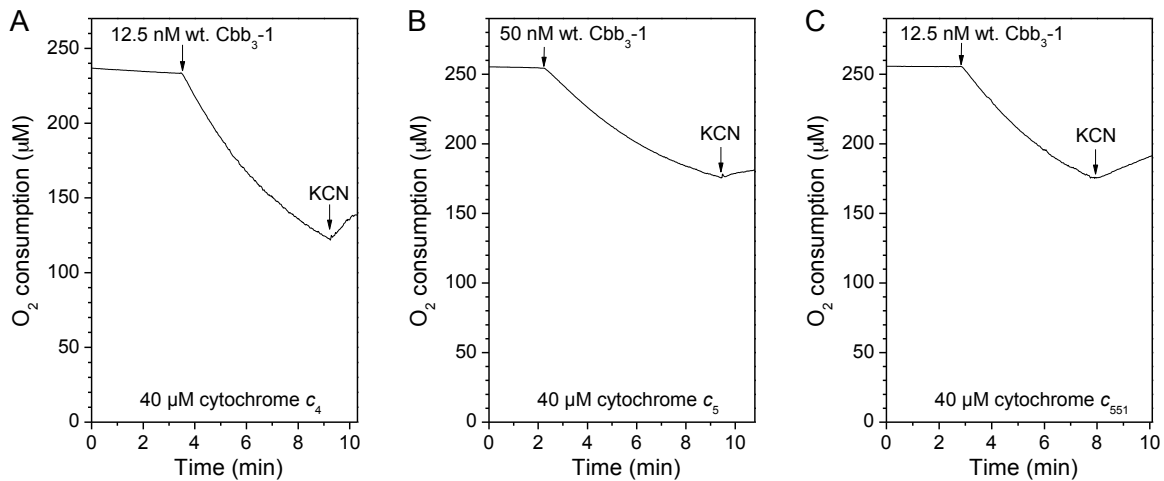


Figure 3-41: Inhibition of the oxidase activity by KCN. The reaction was initiated by adding wild-type *Cbb₃-1* to a reaction system containing 40 μM cytochrome *c₄* (A), cytochrome *c₅* (B) and cytochrome *c₅₅₁* (C). The oxygen reductase activity of *cbb₃-CcO* was inhibited by adding 1 mM KCN. The oxygen consumption was measured using an oxygen electrode at RT.

Using cytochrome *c* as the substrate, the optimum ionic strength for the activity assay of *cbb₃-CcO* was determined by adding 0 to 500 mM NaCl to the reaction mixture (Figure 3-42). The resulting bell-shaped curves indicate that interactions between the three cytochromes *c* and *cbb₃-CcO* are sensitive to ionic strength. In all cases, the lowest activity was observed in the absence of NaCl, as well as at 500 mM NaCl. Furthermore, it was found that cytochrome *c₅* and *c₅₅₁* are less dependent on ionic strength than cytochrome *c₄*. Additionally, the optimal conditions concerning the ionic strength were determined and used for the later studies. For the activity assay using cytochrome *c₅* or *c₅₅₁* as the electron donor, 150 mM NaCl was added. And 250 mM NaCl was used for the measurements with cytochrome *c₄*.

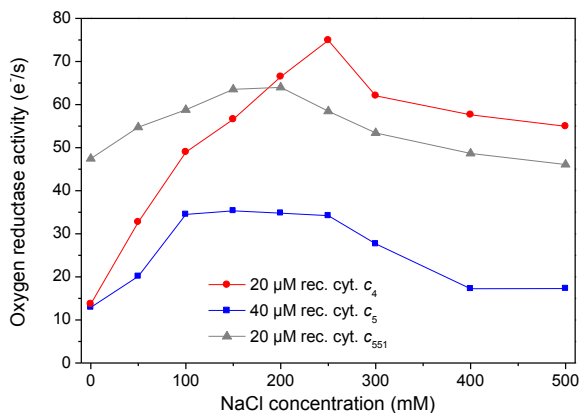


Figure 3-42: Dependence of the cytochrome *c*-mediated oxygen reductase activity of *cbb₃-CcO* on the ionic strength. The measurements were performed in the presence of 20 μM cytochrome *c₄* (red curve), 40 μM cytochrome *c₅* (blue curve) and 20 μM cytochrome *c₅₅₁* (grey curve). The salt concentration was varied from 0 mM to 500 mM. The reaction was initiated by adding 5 pmol of the wild-type *Cbb₃-1*.

Figure 3-43 shows the comparison of the results using wild-type or recombinant cytochrome c_{551} as a substrate for cbb_3 -CcO. There are apparently no significant differences between both proteins. This indicates that the recombinant cytochromes c produced in *E. coli* exhibit the same properties as the native protein. Although the wild-type cytochrome c_4 and c_5 could be also isolated from *P. stutzeri*, their amounts were not adequate for this assay.

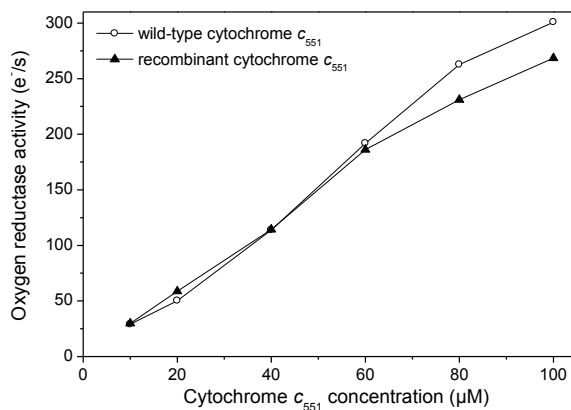


Figure 3-43: A comparison between the wild-type and the recombinant cytochrome c_{551} . The oxygen reductase activity of cbb_3 -CcO was measured in the presence of different concentrations of wild-type (white circles) or recombinant (black triangles) cytochrome c_{551} . The reaction was initiated by adding 5 pmol of the wild-type Cbb₃-1.

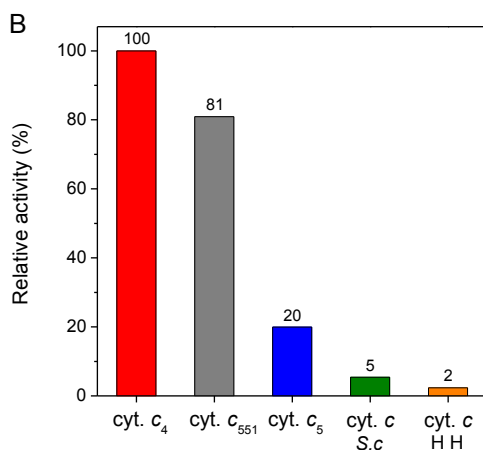
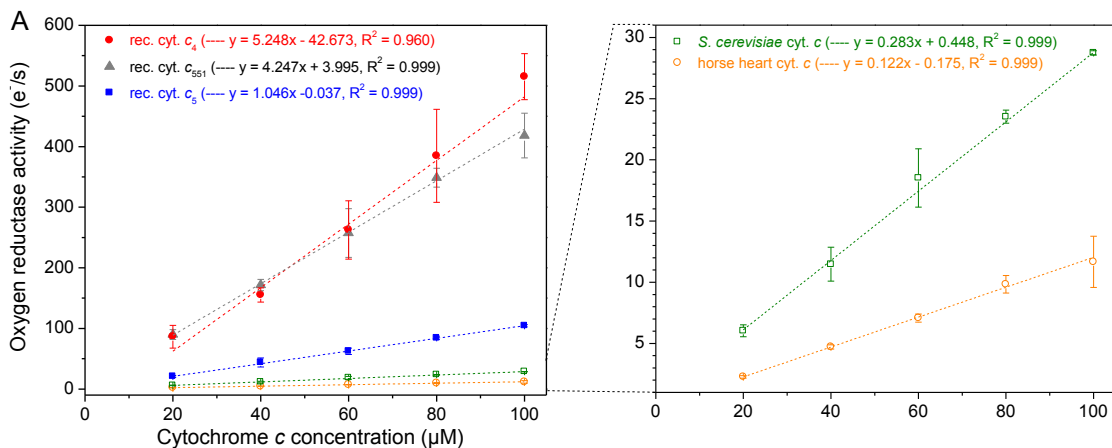


Figure 3-44: Oxygen reductase activity of wild-type Cbb₃-1. Dependence on the concentration of recombinant cytochrome c_4 (red), cytochrome c_5 (blue), cytochrome c_{551} (grey), cytochrome c from *S. cerevisiae* (green) and from horse heart (orange). The reaction system contained 50 mM Tris/HCl, pH 7.5, 50 μM EDTA, 0.02% (w/v) DDM, 5 mM sodium ascorbate and the indicated amount of cytochrome c . The reaction was initiated by adding 5 pmol of the wild-type Cbb₃-1. Each data point represents the mean value \pm SD, which is calculated from at least three independent measurements. The data were fitted with a linear regression (dotted lines). (B) A comparison between five different cytochromes c . The relative activity was calculated by assuming that the activity observed for cytochrome c_4 was 100%.

Figure 3-44 compares the oxygen reductase activity of wild-type *Cbb₃-1* measured with five different cytochromes *c*. All data show a linear dependence on the concentration of cytochromes *c* and exhibit no saturation at a concentration of substrate up to 100 μM . At this highest concentration tested, the turnover measured with cytochrome *c*₄ was 515 e^-/s , which is higher than that obtained for cytochrome *c*₅₅₁ (418 e^-/s) and for cytochrome *c*₅ (104 e^-/s) (Figure 3-44 A). In contrast, the activities determined using eukaryotic cytochrome *c* as a substrate are quite low, 29 e^-/s for cytochrome *c* from yeast and 12 e^-/s for cytochrome *c* from horse heart (Figure 3-44 A). Due to the lack of saturation in the activity measurements, the relative activity was calculated from the slope of linear regression and by assuming that the rate of cytochrome *c*₄ was 100%. As shown in Figure 3-44 B, cytochrome *c*₅₅₁ and *c*₅ can support the oxidase activity at a rate of 81% and 20%, respectively, when compared to cytochrome *c*₄. In addition, the cytochromes *c* from yeast (5%) and from horse heart (2%) are virtually ineffective as substrates for *cbb₃-CcO*.

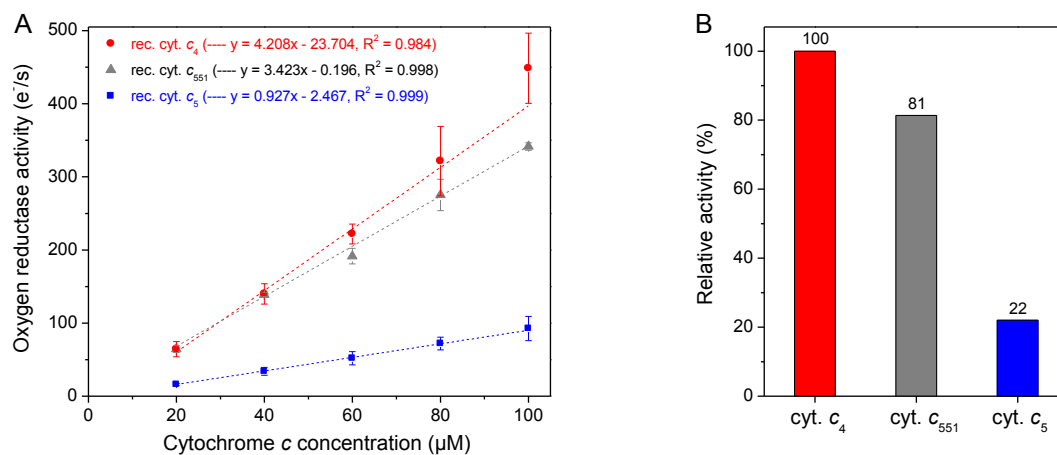


Figure 3-45: Oxygen reductase activity of recombinant *Cbb₃-1*. (A) Dependence on the concentration of recombinant cytochrome *c*₄ (red), cytochrome *c*₅ (blue) and cytochrome *c*₅₅₁ (grey). The reaction system contained 50 mM Tris/HCl, pH 7.5, 50 μM EDTA, 0.02% (w/v) DDM, 5 mM sodium ascorbate and the indicated amount of cytochrome *c*. The reaction was initiated by adding 5 pmol of the recombinant *Cbb₃-1*. Each data point represents the mean value \pm SD, which is calculated from at least three independent measurements. The data were fitted with a linear regression (dotted lines). (B) A comparison between three different cytochromes *c*. The relative activity was calculated by assuming that the activity observed for cytochrome *c*₄ was 100%.

Cytochrome *c*₄, *c*₅ and *c*₅₅₁ were also used for the activity measurements of recombinant *Cbb₃-1* (Figure 3-45) and *Cbb₃-2* (Figure 3-46). Similar to the observations from wild-type *Cbb₃-1* (Figure 3-44), the enzymatic activities show a linear dependence on the amount of cytochromes *c*. In the case of recombinant *Cbb₃-1* (Figure 3-45 A), the highest rate of oxygen reduction was determined to be 448 e^-/s for cytochrome *c*₄, 341 e^-/s for cytochrome *c*₅₅₁ and 92 e^-/s for cytochrome *c*₅. As shown in Figure 3-45 B, the relative activities obtained for cytochrome *c*₄, *c*₅₅₁ and *c*₅ are 100%,

81% and 22%, respectively. For recombinant Cbb₃-2, the highest rate of oxygen reduction was determined to be 158 e⁻/s for cytochrome *c*₄, 157 e⁻/s for cytochrome *c*₅₅₁ and 29 e⁻/s for cytochrome *c*₅ (Figure 3-46 A). Although the overall activity is low, the results from the comparison between the three cytochromes *c* are similar to the observations from Cbb₃-1. Specifically, the relative activities calculated for cytochrome *c*₄, *c*₅₅₁ and *c*₅ are 100%, 92% and 16%, respectively (Figure 3-46 B).

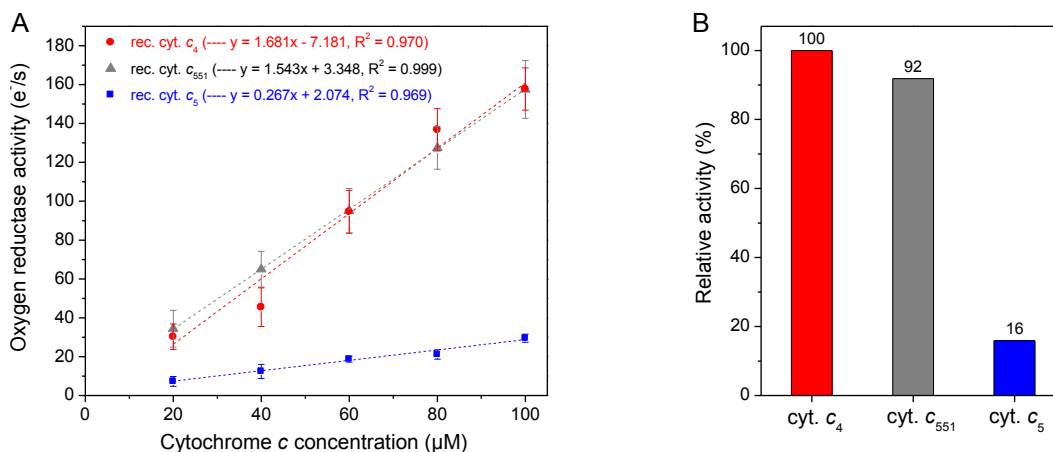


Figure 3-46: Oxygen reductase activity of recombinant Cbb₃-2. (A) Dependence on the concentration of recombinant cytochrome *c*₄ (red), cytochrome *c*₅ (blue) and cytochrome *c*₅₅₁ (grey). The reaction system contained 50 mM Tris/HCl, pH 7.5, 50 µM EDTA, 0.02% (w/v) DDM, 5 mM sodium ascorbate and the indicated amount of cytochrome *c*. The reaction was initiated by adding 5 pmol of the recombinant Cbb₃-2. Each data point represents the mean value ± SD, which is calculated from at least three independent measurements. The data were fitted with a linear regression (dotted lines). (B) A comparison between three different cytochromes *c*. The relative activity was calculated by assuming that the activity observed for cytochrome *c*₄ was 100%.

As may be concluded from the data above (Figure 3-44, 3-45 and 3-46), a clear distinction can be made between the different cytochromes *c* with respect to their ability to function as electron donors for *cbb*₃-CcOs. It is shown that reduced cytochrome *c*₄ and *c*₅₅₁ from *P. stutzeri* are very likely the endogenous substrates for the *cbb*₃-CcOs, whereas cytochrome *c*₅ is not a good substrate. In addition, both eukaryotic cytochromes *c* (from yeast and horse heart) are poor substrates.

Besides the comparison between different cytochromes *c*, a comparison between the wild-type Cbb₃-1 and the two recombinant *cbb*₃-isoforms is also provided in Figure 3-47. For such comparison, the relative activities were calculated by assuming that the activity obtained from wild-type Cbb₃-1 was 100%. The data show that the oxygen reductase activities of the recombinant Cbb₃-1 are slightly less (80 to 90%) than those observed for the wild-type Cbb₃-1. This is also consistent with the observation that the oxidase activity is similar for both wild-type and recombinant Cbb₃-1, when TMPD was used as the artificial substrate (see 3.5.6, Figure 3-26).

In contrast, although the activity of the recombinant Cbb₃-2 is also comparable to that of wild-type Cbb₃-1 when using TMPD as an electron donor (Figure 3-26), an obvious difference between Cbb₃-2 and Cbb₃-1 was observed using the recombinant cytochromes *c* as the substrate. As shown in the Figure 3-47, the three different cytochromes *c* can only support the activity of recombinant Cbb₃-2 to a level of 26 to 36%, when compared to the wild-type Cbb₃-1. This finding indicates that both *cbb*₃-isoforms have different substrate specificity.

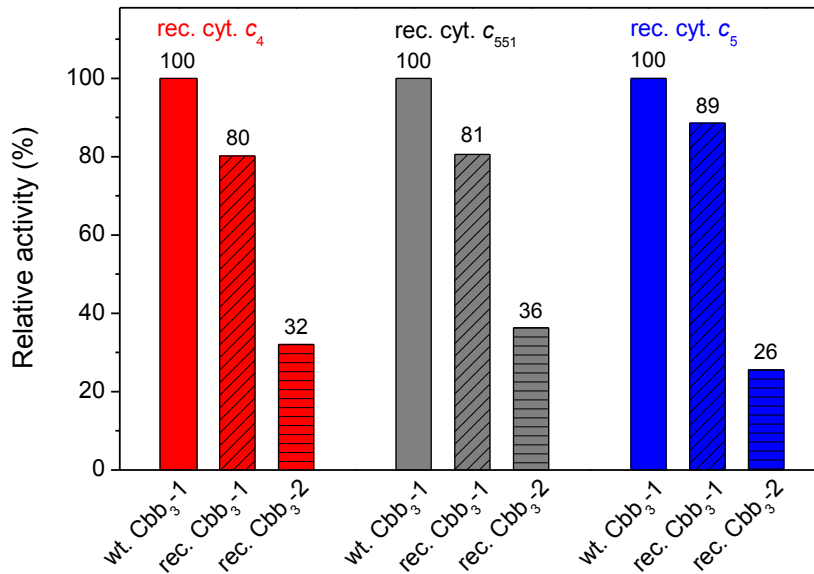


Figure 3-47: Comparison of the oxidase activity between wild-type Cbb₃-1 and recombinant Cbb₃-1 and Cbb₃-2. Enzymatic activities of *cbb*₃-CcOs were measured in the presence of cytochrome *c*₄ (red column), cytochrome *c*₅ (blue column) and cytochrome *c*₅₅₁ (grey column). The relative activity was calculated by assuming that the activity observed for the wild-type Cbb₃-1 was 100%.

4 Discussion

4.1 The presence of the two *cbb*₃-CcOs in *P. stutzeri*

P. stutzeri is a facultative anaerobic bacterium²⁷, capable of respiring aerobically using *cbb*₃-CcO as the terminal enzyme of the electron transport chain. The presence of a *cbb*₃-CcO in *P. stutzeri* ZoBell was initially suggested by Vollack *et al.* (1998 and 1999) based on the analysis of the *ccoN* gene both at DNA and mRNA level. Later, Pitcher *et al.* (2002) sequenced the operon encoding the *cbb*₃-CcO by using degenerate primers and reported that this bacterium possesses only one *ccoNOQP* operon.

In 2010, during the process of structure determination of the *P. stutzeri cbb*₃-CcO, the presence of only one *cbb*₃-CcO was questioned on the basis of the following observations: (i) the original deduced amino acid sequences of *cbb*₃-CcO (kindly provided by R. S. Pitcher) did not match the electron density map; (ii) these sequences were also not in accordance with the results of mass spectroscopic identification of the dissolved crystals (Buschmann *et al.*, 2010). In addition, the published genome sequence of another *P. stutzeri* strain (A1501) revealed the presence of two *cbb*₃-operons encoding the subunits of two different *cbb*₃-CcOs (Yan *et al.*, 2008).

The first goal of this study was to determine the authentic nucleotide sequences of the *cbb*₃-operon from *P. stutzeri* ZoBell. For this purpose, a series of primers was designed, based on highly conserved regions identified by comparison of the published genome sequences from *P. stutzeri* strain A1501 and several related *Pseudomonas* species. Our sequence data show that the two *cbb*₃-operons are tandemly arranged in a 7-kb segment of the genome (see Figure 3-1) and the gene organization in the two *cbb*₃-operons is identical to that in *P. stutzeri* strain A1501²⁸. This was also later confirmed by the draft genome sequence of *P. stutzeri* ZoBell (Peña *et al.*, 2012 and our unpublished data)²⁹. A comparison of DNA sequences showed that the previously reported sequence was a PCR artifact that fused the 5' region of the *ccoN*-1 gene of the first *cbb*₃-operon (around 200 bp) to the second *cbb*₃-operon. This could explain why only one *cbb*₃-CcO was found previously.

²⁷ *P. stutzeri* has a branched electron transport chain that utilizes several terminal respiratory pathways.

²⁸ For *cbb*₃-CcOs, the average nucleotide identity between these two *P. stutzeri* strains (ZoBell and A1501) is 90%, and the average amino acid identity is 98%.

²⁹ At the beginning of this work, no genome sequence data were available for *P. stutzeri* ZoBell. Later on, we sequenced the genome of this strain at the Max-Planck Genome Centre Cologne. The obtained sequence contained 10 scaffolds that cover 4.6 Mb of the genome. However, during our assembly process, the draft genome sequence was published by Peña *et al.* (2012).

4.2 The presence of multiple *cbb*₃-CcOs in proteobacteria

The *cbb*₃-CcOs are widely distributed within the bacterial phyla, but particularly abundant in proteobacteria³⁰ (Cosseau and Batut 2004; Ducluzeau *et al.*, 2008). Unlike *P. stutzeri* ZoBell, many proteobacteria (including representatives from all subgroups of the proteobacteria) possess only one *cbb*₃-operon on the chromosome. Within this single operon, the structural genes are generally arranged in the same order: *ccoN-ccoO-ccoQ-ccoP* (Figure 4-1).

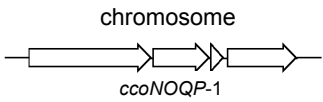
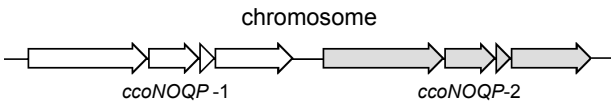
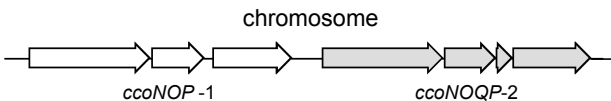
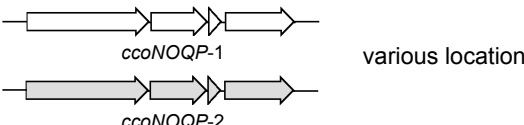
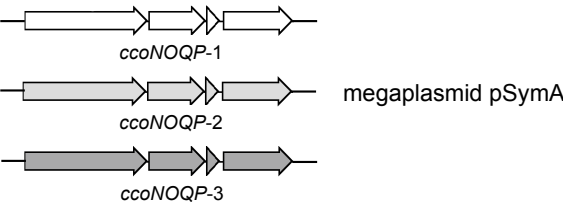
	Gene organization and location of the <i>cbb</i> ₃ -Operon	Bacterium
1		<i>Bradyrhizobium japonicum</i> (α) <i>Paracoccus denitrificans</i> (α) <i>Rhodobacter capsulatus</i> (α) <i>Rhodobacter sphaeroides</i> (α) <i>Neisseria meningitidis</i> (β) <i>Pseudomonas syringae</i> (γ) <i>Vibrio cholerae</i> (γ) <i>Campylobacter jejuni</i> (ε) <i>Helicobacter pylori</i> (ε)
2		<i>Pseudomonas aeruginosa</i> (γ) <i>Pseudomonas fluorescens</i> (γ) <i>Pseudomonas putida</i> (γ) <i>Pseudomonas mendocina</i> (γ)
		<i>Pseudomonas stutzeri</i> (γ)
		<i>Rhizobium leguminosarum</i> (α) <i>Rhizobium etli</i> (α)
3		<i>Sinorhizobium meliloti</i> (α)

Figure 4-1: Organization of the *ccoNOQP* genes in proteobacteria. The canonical *cbb*₃-operon contains four genes ordered as *ccoNOQP* (denoted by arrowheads). Different operons are shown using different colors. The subclass of proteobacteria is shown in parentheses behind each bacterium. The genome database (NCBI) was used to identify the organization and location of *cbb*₃-operons.

³⁰ The phylum proteobacteria is divided into five major classes (α-, β-, γ-, δ- and ε-proteobacteria).

Tandem repeats of the *cbb*₃-operon are frequently found in the genomes of pseudomonads, such as *P. aeruginosa* (Stover *et al.*, 2000), *P. putida* (Nelson *et al.*, 2002) and *P. fluorescens* (Silby *et al.*, 2009). In all these species, two *cbb*₃-operons are located close to each other on the chromosome and each *cbb*₃-operon is comprised of a complete set of the *ccoNOQP* genes. Although the organization of the two *cbb*₃-operons is similar, a significant difference could be observed between *P. stutzeri* and other *Pseudomonas* species. In *P. stutzeri*, the *ccoQ* gene is missing in the first *cbb*₃-operon (Figure 4-1), whereas it is present in both *cbb*₃-operons in other *Pseudomonas* species.

Besides pseudomonads, two *cbb*₃-operons have also been identified in several rhizobial species. However, in the case of rhizobia, two copies of the *ccoNOQP* are normally located on separate genetic elements. For instance, in *Rhizobium leguminosarum* and *Rhizobium etli*, one *cbb*₃-operon is located on the symbiotic plasmid, whereas the other resides either on the chromosome or on a second megaplasmid (Schlüter *et al.*, 1997; Girard *et al.*, 2000; Granados-Baeza *et al.*, 2007; Talbi *et al.*, 2012). In addition, in the endosymbiotic diazotroph *Sinorhizobium meliloti*, three copies of *cbb*₃-operons are located far apart from each other on the symbiotic plasmid pSymA (Torres *et al.*, 2013).

Due to its high affinity for oxygen, many bacteria employ the *cbb*₃-CcO as the sole terminal oxidase to adapt to microaerophilic conditions (Preisig *et al.*, 1996; Jackson *et al.*, 2007). Accordingly, it has been suggested that *cbb*₃-CcO is produced only under low oxygen tensions (Pitcher and Watmough 2004). However, this might be true only for certain bacteria, which have a single *cbb*₃-CcO. Previous studies on the two *cbb*₃-isoforms from *P. aeruginosa* indicated that two isoforms are differentially expressed in response to environmental oxygen levels (Comolli and Donohue 2004; Kawakami *et al.*, 2010). Thus, it is likely that the presence of multiple *cbb*₃-CcOs contributes to the respiratory flexibility of these bacteria.

4.3 Construction of a homologous expression system to produce both *cbb*₃-isoforms from *P. stutzeri*

4.3.1 Homologous vs. heterologous protein expression

The *cbb*₃-CcOs are multi-subunit membrane protein complexes that contain several cofactors, including metal ions. In addition to the structural genes (*ccoNOQP*) for *cbb*₃-CcO, the *P. stutzeri* genome contains a number of open reading frames encoding proteins that are essential for the cofactor biosynthesis and for the proper assembly of a fully functional *cbb*₃-CcO. Therefore, the selection of an appropriate expression system is crucial to achieve successful production of the

recombinant *cbb*₃-CcO.

For heterologous expression, the *E. coli*-based system is commonly employed for the over-production of membrane proteins, but it is not suitable for the production of *cbb*₃-CcO because *E. coli* does not possess either the *cbb*₃-CcO or the genes responsible for the biosynthesis of *cbb*₃-CcO. The *P. denitrificans* strain AO1, which carries a deletion in the gene coding for the subunit CcoN of *cbb*₃-CcO and lacks the expression of *aa*₃-CcO (Pfitzner *et al.*, 1998), has been used for the heterologous production of *R. sphaeroides cbb*₃-CcO (Rauhamäki *et al.*, 2012). However, the presence of the original *ccoOQP* genes of *P. denitrificans cbb*₃-CcO in its genome may be problematic for the production of the exogenous *cbb*₃-CcO. In *P. aeruginosa*, a close relative of *P. stutzeri*, two *cbb*₃-operons have been separately or jointly deleted from the genome (Comolli and Donohue 2004). Nevertheless, the *cbb*₃-operon-deletion strain of *P. aeruginosa* was not considered as a host to produce the *P. stutzeri cbb*₃-CcO, because *P. aeruginosa* is a human pathogenic microorganism (biosafety level 2).

For homologous expression, the advantages are rooted in the availability of the gene cluster assuring proper assembly of the *cbb*₃-CcO. Consequentially, for the retention of the functional and structural properties of the enzyme, the production of both *cbb*₃-isoforms in a homologous system would be preferable. Moreover, well-established procedures have been developed for obtaining the *cbb*₃-CcO in high yield from *P. stutzeri* membranes (Urbani *et al.*, 2001; Buschmann *et al.*, 2010). In contrast, new deletion strains have to be constructed.

4.3.2 Construction of the *cbb*₃-knockout strains

For functional studies, especially for the mutagenesis studies, it is necessary to produce the recombinant *cbb*₃-CcO in a host strain that contains a deletion of the entire *cbb*₃-operon. Therefore, two *P. stutzeri* deletion strains, each lacking one of the two *cbb*₃-operons, were first constructed.

Two approaches are commonly used for the disruption of a target gene of interest: the insertional inactivation and the gene replacement/deletion (Beliaev 2005; Narayanan and Chen 2011). The first approach, involving the insertion of foreign sequences (e.g., transposon or plasmid) into the target gene, was not used in this study because a single insertion may not be sufficient to inactivate all structural genes in one *cbb*₃-operon substantially. The second approach, based on the gene replacement/deletion by homologous recombination, is capable of replacing or deleting a desired region in the genome, and has been used for the construction of *cbb*₃-operon-deletion mutants in *R. sphaeroides* (Oh and Kaplan 2002) and *P. aeruginosa* (Comolli and Donohue 2004). Therefore, the gene replacement strategy was chosen for the construction of *cbb*₃-operon-deletion strains of *P. stutzeri* in this work.

Traditionally, gene replacement involves transformation of a suicide plasmid containing a mutated allele followed by integration of this vector into the host genome via homologous recombination and subsequent selection for double-crossover events (Beliaev 2005; Ortiz-Martín *et al.*, 2006). In this work, we constructed a suicide plasmid for the genetic manipulation of *P. stutzeri* (see Figure 3-3). This plasmid contains several important elements, including the origin of replication, two selection marker genes and the homologous flanking regions. The features of these elements are discussed as follows:

- (i) Our results showed that the p15A- and pMB1-derived plasmids do not replicate in *P. stutzeri*, which is consistent with the previous observation that most *E. coli* replicons do not function in pseudomonads (Choi *et al.*, 2008). The narrow-host-range p15A replicon was used in this work to construct the suicide plasmid (pXH-B). Since this plasmid cannot autonomously replicate in *P. stutzeri*, under the selective pressure of antibiotics plasmid integration (single crossover event) or allelic exchange (double crossover event) have to occur in order to ensure that the *P. stutzeri* cells become resistant to the lethal effects (Figure 4-2). Moreover, genetic manipulation of this plasmid containing the *E. coli* p15A replicon can be easily achieved using *E. coli* cells.
- (ii) The suicide plasmid must contain a selectable marker, e.g., an antibiotic resistance gene, to identify transformants. Our sensitivity tests showed that *P. stutzeri* cells are sensitive to many antibiotics (see Table 3-2). However, among these antibiotics, only chloramphenicol and kanamycin resistance genes from the pBBR1MCS-based plasmids were able to confer resistance in *P. stutzeri* (see Table 3-4). Rather than chloramphenicol, the kanamycin resistance gene was chosen as the selectable marker because *P. stutzeri* cells showed high sensitivity to this antibiotic.
- (iii) The recombination efficiency can be affected by the length of homologous sequences, and the minimal length required for efficient recombination varies greatly among different organisms. In *E. coli*, recombination can be efficiently achieved with 20 to 90 bp of sequence homology (Watt *et al.*, 1985; Shen and Huang 1986), while relatively long homologous flanking fragments (from several hundreds to a few thousand bp) are generally used in other bacteria (Nelson *et al.*, 2003; Ortiz-Martín *et al.*, 2006; Bao *et al.*, 2012; Kung *et al.*, 2013). In *P. stutzeri*, the minimum length of homology required for efficient recombination has not been assessed. Therefore, we used flanking regions of about 500 bp in length, because this is usually sufficient to produce recombination.
- (iv) Since single crossover recombinations occur more often than double crossovers, a way of screening for allelic exchange is needed. The commonly used approach is to incorporate a counter-selection marker (e.g., the *sacB* gene from *B. subtilis*, conferring

sucrose sensitivity) into the suicide plasmid (Davison 2002; Philippe *et al.*, 2004; Beliaev 2005; Choi *et al.*, 2008). However, using a counter-selection marker is technically demanding and time-consuming because a three-step procedure has to be performed to yield the mutant strain. First, integration of the suicide plasmid into the chromosome by a single crossover event is selected by antibiotic pressure. Second, spontaneous excision of the integrated plasmids (a second single crossover event) can be selected with counter-selection markers. During this step, the recombination event can take place at two different locations, which leads to either a wild-type or mutant phenotype. Therefore, in the final step, the presence of the desired deletion in the resulting strains must be checked by PCR or Southern blot.

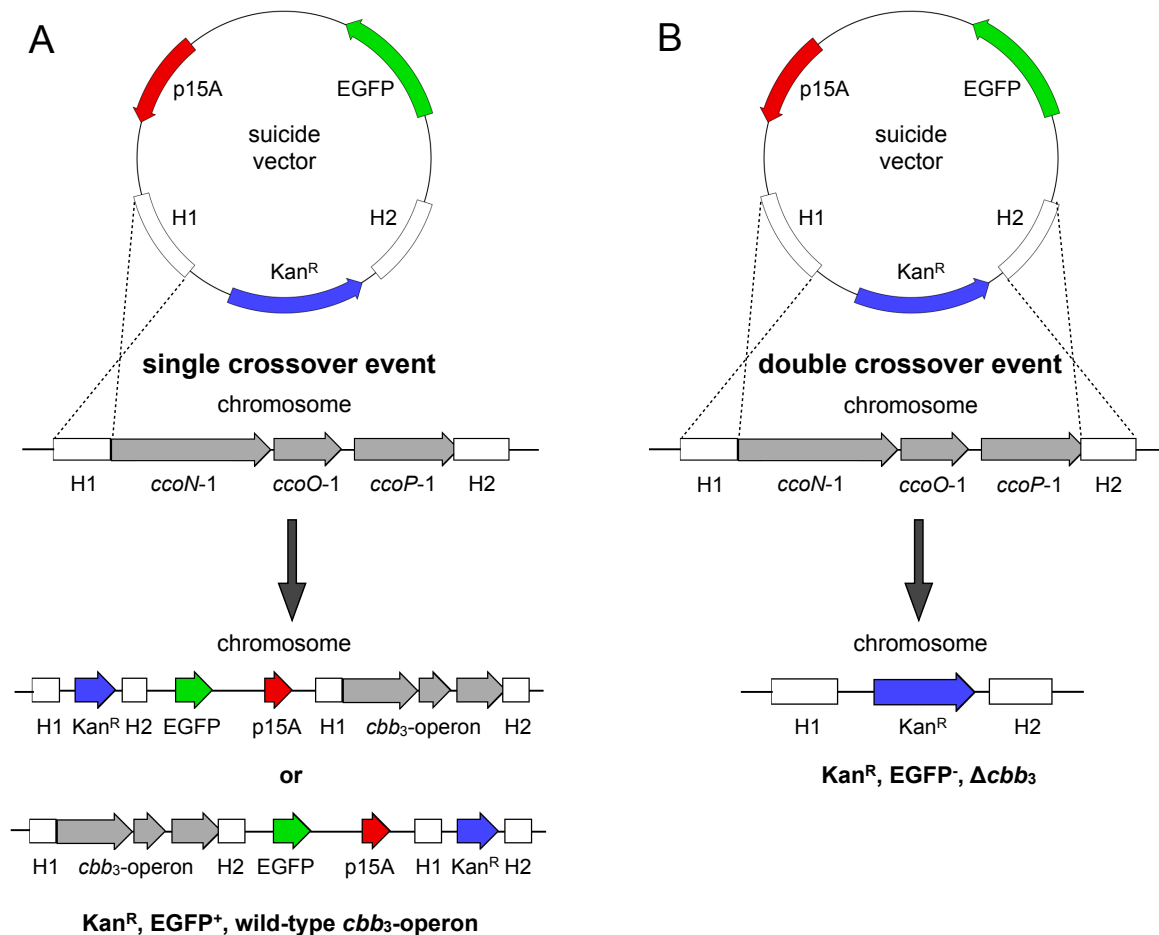


Figure 4-2: Selection of allelic exchange mutant using one-step selection strategy based on the EGFP-based suicide plasmid. (A) When a single crossover recombination occurs, the suicide plasmid is integrated into the chromosome. The resulting merodiploid strains are resistant to kanamycin and positive for EGFP. (B) A double crossover event results in the deletion of *cbb3*-operon. The resulting deletion strains are resistant to kanamycin and negative for EGFP.

Instead of a counter-selection marker, we used the EGFP protein as a second selection marker to distinguish the desired double crossover event from the single crossover recombination event. When a single crossover event occurs, entire plasmid integration is observed and the resulting recombinant strain is resistant to kanamycin and shows EGFP expression under the control of a constitutive promoter (*lac* promoter) (Figure 4-2 A). Alternatively, double crossover recombination results in the exclusive replacement of the *cbb*₃-operon with the kanamycin resistance cassette and in an EGFP-negative phenotype (Figure 4-2 B). Using an UV illuminator, positive *cbb*₃-deletion strains can be easily selected from negative strains on the kanamycin plate by the direct visualization of EGFP fluorescence. As a result, using of an EGFP-based suicide plasmid greatly simplifies the screening procedures.

Using our constructed suicide plasmids, two single deletion strains, Δ Cbb₃-1 and Δ Cbb₃-2, were successfully created. However, our attempts to isolate a double-deletion strain (Δ Cbb₃-1+2), based on the above-mentioned strategy, were unsuccessful. This is unlikely to be due to the lethal effects induced by the simultaneous lack of both *cbb*₃-isoforms, because *P. stutzeri* also contains other terminal oxidases (see Figure 1-10) for aerobic respiration. Furthermore, construction of a mutant strain carrying a targeted deletion of both *cbb*₃-operons has been achieved in *P. aeruginosa* (Comolli and Donohue 2004). Therefore, future experiments (e.g., optimization of the composition of the suicide plasmid; increasing the transformation efficiency) are required to obtain a double-deletion strain.

4.3.3 Purification of the wild-type *cbb*₃-CcOs

Previously, a purification method has been developed to obtain large amounts of stable *cbb*₃-CcOs from the native membranes of *P. stutzeri* ZoBell (Urbani *et al.*, 2001). The purification procedure involved the solubilization of membrane proteins with the mild detergent DDM followed by three chromatographic separations. Such a preparation has been used by different research groups to isolate and characterize the *P. stutzeri* *cbb*₃-CcO (Forte *et al.*, 2001; Urbani *et al.*, 2001; Pitcher *et al.*, 2002). However, it should be noted that this method is not applicable to specifically separate the two *cbb*₃-isoforms.

Due to the high homology between Cbb₃-1 and Cbb₃-2, both isoforms are usually found as a mixture in the same chromatographic fractions during the purification process. The difficulty in the separation of both isoforms has been partially resolved by the utilization of an improved purification procedure, which involved four conventional chromatographic steps (Buschmann *et al.*, 2010). By applying the new protocol, the wild-type Cbb₃-1 was successfully purified to homogeneity and its structure was determined by X-ray crystallography (Buschmann *et al.*, 2010).

However, isolation of the Cbb₃-2 from the protein mixture could not be achieved using the same purification strategy.

Since two *cbb*₃-operon-deletion strains are available, we have tried to isolate the individual wild-type *cbb*₃-isoform directly from the corresponding deletion strains, namely, isolation of Cbb₃-1 from the *P. stutzeri* ΔCbb₃-2 strain and of Cbb₃-2 from the ΔCbb₃-1 strain. However, we found that this strategy was not applicable for *P. stutzeri* because the expression of both isoforms seems to be interdependent. Based on the heme staining analysis on the solubilized membrane proteins (Sabine Buschmann, data not shown), it was observed, that the expression of Cbb₃-2 was nearly not detectable when ΔCbb₃-1 cells were grown under microaerobic and aerobic growth conditions. Furthermore, if the operon *ccoNOQP*-2 was deleted from the genome (ΔCbb₃-2 strain), the amount of Cbb₃-1 was also drastically decreased. These observations are, however, not in line with published data obtained on the two *P. aeruginosa* *cbb*₃-isoforms with a similar methodology, where the expression of a respective *cbb*₃-isoform was not influenced by the presence or absence of the second one (Comolli and Donohue 2004). Because of a lack of experimental evidence, we cannot propose a straightforward explanation for these diverging results. In addition, compared with the wild type, the growth rate of the two *P. stutzeri* deletion strains was only moderately changed under the same growth conditions. Therefore, it can be assumed that *P. stutzeri* cells could use other oxidases as substitute for the missing *cbb*₃-CcOs.

4.3.4 Design of expression vectors for recombinant *cbb*₃-CcOs

In order to simplify the separation and purification of the two recombinant *cbb*₃-isoforms, we decided to use the affinity purification strategy. Two affinity tags (His₆-tag and Strep-tag II) were selected because they are small and, therefore, often do not need to be removed prior to downstream applications (Terpe 2003). Furthermore, a polyhistidine-tag has been successfully used for purification of the *cbb*₃-CcO from *R. sphaeroides* (Oh and Kaplan 2002; Lee *et al.*, 2011) and *V. cholerae* (Hemp *et al.*, 2005; Chang *et al.*, 2010).

The *cbb*₃-CcO consists of three major subunits (CcoNOP) and both N- and C-terminal ends of each subunit could potentially serve as the attachment site for the affinity tag. The position of affinity tags was first evaluated using the reported structure of Cbb₃-1 (Figure 4-3) because their placement can interfere with the expression, folding and complex formation of the protein. Both N- and C-termini of the CcoN subunit were chosen as the candidates on the basis of two following considerations. First, they are exposed on the cytoplasmic face of the enzyme and may thus allow a sufficient exposure of the peptide tags to affinity matrices. Second, they are located relatively distant from any function-related component such as subunit interfaces, redox cofactors and proton/electron transfer pathways.

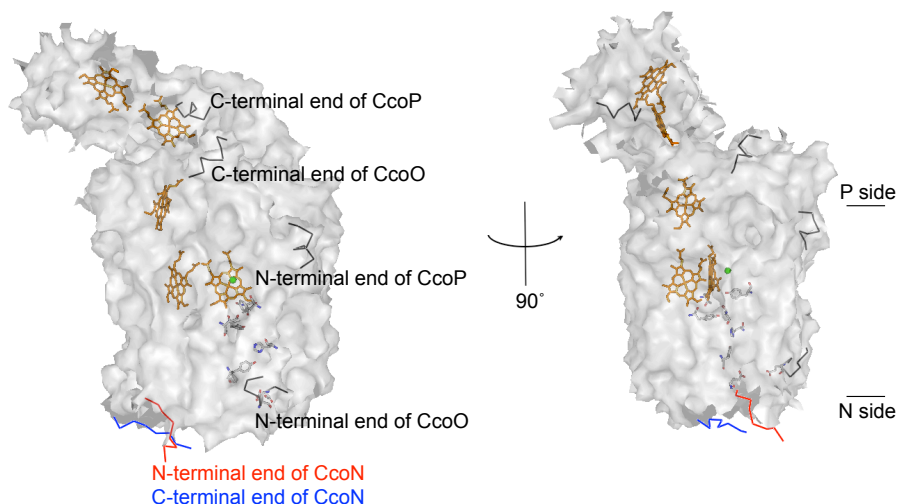


Figure 4-3: Location of the both N- and C-termini of the three subunits CcoNOP. Two orthogonal views, the “front” (left) and the “side” (right), of the molecular surface of Cbb₃-1 are shown. The N- and C-termini of the CcoN subunit are colored red and blue, respectively. Hemes are represented as yellow sticks. Amino acids, which are involved in proton translocation, are shown as sticks. The structural image was generated using PDB entry 3MK7 and the PyMOL software.

To optimize the protein expression, a series of vectors were constructed and tested (Table 3-6). When a His₆-tag was attached to either the N- or the C-terminal end of the CcoN subunit, solubilized *cbb*₃-CcOs could be purified by Ni-NTA chromatography, confirming that the His₆-tag is functional. Furthermore, there was no significant difference on expression level of *cbb*₃-CcO between N- and C-terminally tagged proteins (Figure 3-8). By comparison, apparent expression of *cbb*₃-CcO could be only observed with a C-terminal Strep-tag II (Figure 3-7). Because we could not detect the N-terminally Strep-tagged *cbb*₃-CcOs in the membrane, we speculated that the presence of a Strep-tag II in this position might interfere with mRNA stabilization or with membrane insertion.

Rather than His₆-tag, we used the constructs with a C-terminal Strep-tag II for a large-scale expression of both *cbb*₃-isoforms because the recombinant Strep-tagged *cbb*₃-CcOs could be more efficiently purified (see Section 3.4.2). Additionally, it is preferable for the purification of metalloproteins, since the use of a Strep-tag is independent from metal ions (Skerra and Schmidt 2000). Finally, the C-terminal Strep-tag II ensures that only full-length CcoN is purified.

4.3.5 Isolation of the individual recombinant *cbb*₃-isoforms

To isolate the two *cbb*₃-isoforms separately, expression vectors containing the genes coding for the recombinant *cbb*₃-CcO were reintroduced into the respective *P. stutzeri* deletion strains. Specifically, the expression vector pXH22, harboring the operon *ccoNOP*-1, was transformed into

the deletion strain Δ Cbb₃-1 to produce the recombinant Strep-tagged Cbb₃-1. Likewise, the expression vectors pXH26 or pXH39 containing the operon *ccoNOQP-2* were introduced into the deletion strain Δ Cbb₃-2 to obtain the recombinant Cbb₃-2.

Despite the fact, that now both *cbb₃*-operons are present again in the same strain, purification of the recombinant *cbb₃*-CcO can be easily achieved by affinity chromatography on Strep-Tactin columns. However, due to the current genetic situation, the presence of a chimeric protein complex of *cbb₃*-CcO between Cbb₃-1 and Cbb₃-2 must be considered and investigated thoroughly. Therefore, both purified *cbb₃*-isoforms were analyzed by electrophoresis followed by peptide mass fingerprinting. Because the sequence identity between the two *cbb₃*-isoforms is very high (87% for subunit CcoN, 97% for subunit CcoO and 63% for subunit CcoP), two approaches were used to increase the sequence coverage and number of peptide identification. First, samples were digested with a combination of trypsin and chymotrypsin. Second, proteolytic digests were analyzed by a coupling of nLC-ESI- and nLC-MALDI-MS/MS. With a sequence coverage ranging from 32% to 80%, the isoform-specific peptides of interest could be only detected in the corresponding *cbb₃*-isoforms (see Section 3.4.7). Thus, the presence of a chimeric form of *cbb₃*-CcO can be excluded in our enzyme preparation.

Using the newly established expression system and purification procedure, a homogeneous preparation of the two *cbb₃*-isoforms was obtained. In addition, as both recombinant *cbb₃*-isoforms are expressed from a plasmid, targeted functional studies become possible.

4.4 Characterization of the two *cbb₃*-isoforms

4.4.1 Regulation of the expression of both *cbb₃*-isoforms

Based on the DNA sequence analysis, we found that the promoters of the two *cbb₃*-operons contain different regulatory elements (Figure 3-11). Both promoters (P1 and P2³¹) contain the putative sigma factor RpoD (σ^{70}) recognition site, while only the P1 promoter possesses a consensus binding site (ANR box) for the transcription activator ANR (a homologue of *E. coli* FNR), which is centered at position -95.5 relative to the start codon of *ccoN-1*. This ANR box overlaps with the -35 region of the P1 promoter by one base pair. Such overlapping is a typical feature of the ANR/FNR-dependent promoters, and allows the activation of transcription of a target gene by direct interaction with the RNA polymerase (Wing *et al.*, 2000; Körner *et al.*, 2003). In the genomes of *P. aeruginosa* and *P. putida*, which contain two *cbb₃*-operons, also only one of

³¹ P1 and P2 represent the promoter region of the operon *ccoNOP-1* and *ccoNOQP-2*, respectively.

the two operons is preceded by an ANR binding site in its promoter region (Comolli and Donohue 2004; Ugidos *et al.*, 2008). Moreover, we found that the organization of the ANR binding site and -35 promoter elements in *P. stutzeri* is similar to those published previously for *P. putida* (Ugidos *et al.*, 2008).

For the *cbb₃*-CcOs, ANR has been reported to function as a positive regulator of gene expression in response to oxygen deficiency (Mouncey and Kaplan 1998; Swem and Bauer 2002; Comolli and Donohue 2004; Ugidos *et al.*, 2008; Kawakami *et al.*, 2010). In *P. aeruginosa*, the expression pattern and regulation of the two *cbb₃*-isoforms under different growth conditions have been investigated in detail (Comolli and Donohue 2004; Kawakami *et al.*, 2010). It has been shown that the expression of *P. aeruginosa* Cbb₃-2 (corresponding to *P. stutzeri* Cbb₃-1) from its ANR-dependent promoter is highly dependent on the oxygen concentration in the environment and is dramatically upregulated under low oxygen conditions or in the stationary phase. The induction of *P. aeruginosa* Cbb₃-2 in the latter case was also suggested to be the result of an excessive oxygen consumption due to the high cell density (Arai 2011). In contrast, the genes coding for *P. aeruginosa* Cbb₃-1 (corresponding to Cbb₃-2 of *P. stutzeri*) are constitutively expressed under regulation of an ANR-independent *cbb₃*-promoter, and its expression is not directly correlated to the different levels of oxygen or certain growth phases (Comolli and Donohue 2004; Kawakami *et al.*, 2010). Similar observations have been also reported for the *cbb₃*-CcO from *P. putida*, in which ANR is required for efficient expression of Cbb₃-1 under conditions of oxygen limitation (Ugidos *et al.*, 2008).

In this work, although the oxygen level was not controlled during the cultivation of both recombinant strains, we found that the oxygen concentration in the culture was normally below 5 μ M (\approx 3 mm Hg) after the cells had entered the exponential growth phase. Under this microaerobic condition, the yield of pure Cbb₃-1 was 6- to 8-fold higher than that of Cbb₃-2 if the proteins were expressed under control of their native promoters in the respective *P. stutzeri* deletion strains (see Table 3-8). This observation is well consistent with the previously reported finding that the ANR-dependent *cbb₃*-promoter in *P. aeruginosa* showed an 8-fold-higher activity than the ANR-independent one under low oxygen conditions (Kawakami *et al.*, 2010). To increase the yield of recombinant Cbb₃-2, we changed the promoter region of the operon *ccoNOQP-2*. Our results show that the yield of recombinant Cbb₃-2 can be increased to the same level as Cbb₃-1 when its native ANR-independent promoter P2 is replaced by the ANR-dependent promoter P1. Additionally, a slightly increased expression of Cbb₃-2 from the *lac* promoter could be observed, which is in agreement with the concept that the *lac* promoter has a constitutive activity in most pseudomonads (Choi *et al.*, 2008).

Confirming the literature (Comolli and Donohue 2004; Kawakami *et al.*, 2010), our data indicate

that the expression of Cbb₃-1 (*P. stutzeri* nomenclature) is regulated by the environmental oxygen concentration and that this isoform plays a primary role under oxygen-limited conditions. Supposedly, the different expression patterns of the two *cbb₃*-isoforms could reflect their different affinities for oxygen which awaits further investigation.

4.4.2 The role of the CcoQ subunit

As already mentioned above (see Section 4.2), a distinct feature of the two *cbb₃*-operons in *P. stutzeri* is that the *ccoQ* gene is only present in the second operon (*ccoNOQP-2*). Nevertheless, it is still possible that CcoQ can associate with both *cbb₃*-isoforms. Because CcoQ has a low molecular weight (6.91 kDa) and poor staining properties, identification of this subunit by SDS-PAGE and subsequent peptide mass fingerprinting is more difficult. To determine the presence and distribution of CcoQ, in-gel digestion of the native *cbb₃*-complex following BN-PAGE was performed and the resulting peptides were analyzed by a combination of ESI- and MALDI-based LC-MS. Our results clearly revealed that CcoQ is only associated with Cbb₃-2, which is in line with the observations that the *ccoQ* gene is only found in the *ccoNOQP-2* operon and that this gene product does not associate with the Cbb₃-1 complex as has already been documented by its X-ray structure (Buschmann *et al.*, 2010).

The physiological role of CcoQ in *cbb₃*-CcOs is still under debate. In *B. japonicum* and *R. sphaeroides*, it was shown that deletion of CcoQ had no effect on assembly or catalytic activity of *cbb₃*-CcO (Zufferey *et al.*, 1996; Oh and Kaplan 1999). In contrast, the activity of *R. capsulatus* *cbb₃*-CcO was significantly reduced in the absence of CcoQ (Peters *et al.*, 2008). In addition, it has been demonstrated that CcoQ is required to protect the *R. sphaeroides* *cbb₃*-CcO from degradation under aerobic conditions (Oh and Kaplan 2002). The absence of CcoQ in the *P. stutzeri* Cbb₃-1 may be a consequence of the fact that this isoform is mainly expressed at very low oxygen tensions, i.e., CcoQ is not required to protect the core complex from the oxygen-induced instability and degradation.

4.4.3 Identification of an unknown transmembrane helix in the crystal structure of Cbb₃-1

Unexpectedly, an extra transmembrane helix of unknown identity is present as seen in the crystal structure of wild-type Cbb₃-1 (Buschmann *et al.*, 2010). It consists of 29 amino acids and is located in close contact to helices IX and XI of the CcoN subunit. It was initially presumed that this α -helix was the CcoQ subunit of the *cbb₃*-CcO. However, this possibility was subsequently excluded because our data clearly demonstrated that the *P. stutzeri* Cbb₃-1 does not contain a subunit corresponding to CcoQ (see Section 4.4.2). Furthermore, the amino acid sequence of

CcoQ was observed not to be capable to match the electron density map.

In an attempt to identify this helix, dissolved crystals of Cbb₃-1 were investigated by mass spectrometry (Sabine Buschmann and Julian D. Langer). Among all amino acid sequences derived from the mass spectra, several putative peptides (8 to 14 amino acids long) were detected, which could be potentially assigned to the uncharacterized α -helix. The putative peptides were searched within the NCBI protein database as well as our custom *Pseudomonas* database³². Unfortunately, no matches to known protein sequences were found, although we cannot rule out the possibility that the sequences obtained from our MS analysis were incorrect.

In *R. capsulatus*, the putative assembly factor CcoH can interact directly with the assembly intermediates of the *R. capsulatus* cbb₃-CcO (Kulajta *et al.*, 2006; Pawlik *et al.*, 2010). It has been also suggested that this protein may function as a *bona fide* subunit of cbb₃-CcO (Pawlik *et al.*, 2010; Ekici *et al.*, 2011). In this work, we found that CcoH can be detected in both purified cbb₃-isoforms by MS analysis (see Section 3.4.7). The *P. stutzeri* CcoH is predicted to contain one transmembrane spanning α -helix between residues 15 and 37. Therefore, it is possible that the uncharacterized α -helix observed in the crystal structure may originate from CcoH. However, due to the relatively low resolution (3.2 Å) of the Cbb₃-1 structure, attempts to fit the residues of CcoH into the electron density map were unsuccessful. So far, the identity of this α -helix remains unclear, and further investigation of its exact nature is necessary.

4.4.4 Both cbb₃-isoforms share high levels of similarity

As mentioned before, the earlier spectroscopic and functional studies of *P. stutzeri* cbb₃-CcO (Forte *et al.*, 2001; Pitcher *et al.*, 2002) were performed with a mixture of both cbb₃-isoforms. Since the two cbb₃-isoforms can be separately purified for the first time (this work), it is now possible to accurately investigate the enzymatic characteristics of the individual cbb₃-CcOs. The basic biochemical and biophysical properties of the recombinant Cbb₃-1 and Cbb₃-2 were compared to each other and also to the true wild-type Cbb₃-1.

SDS-PAGE analyses of the two purified recombinant cbb₃-isoforms showed the presence of three major protein bands corresponding to the subunit CcoN, CcoO and CcoP (see Section 3.4.5). The electrophoretic pattern is identical to that of the wild-type Cbb₃-1 and similar to the previously reported results for cbb₃-CcOs from other organisms (García-Horsman *et al.*, 1994; Gray *et al.*, 1994). In the case of subunit CcoP, a small but significant difference of migration could be observed between the two cbb₃-isoforms. This result is consistent with that reported for the two

³² Besides the protein sequences for known pseudomonads, this database also contains all possible open reading frame sequences that are derived from the genome of the *P. stutzeri* ZoBell.

P. aeruginosa cbb₃-isoforms (Comolli and Donohue 2004).

Both purified *cbb₃*-isoforms appeared as a single band with an apparent size of 165 kDa on BN-PAGE (see Section 3.4.6). This indicates that the recombinant protein was successfully purified to homogeneity. Since the electrophoretic mobility of integral membrane proteins on BN-PAGE is strongly affected by the binding of detergents, lipids and Coomassie dyes (Heuberger *et al.*, 2002), we concluded that the two *cbb₃*-isoforms are monomeric, which supported the previous suggestion based on the analytical ultracentrifugation experiments (Urbani *et al.*, 2001). In *R. capsulatus* membranes, the presence of a monomeric *cbb₃*-CcO complex has been also suggested (Kulajta *et al.*, 2006). Moreover, in all three-dimensional structures solved so far, the bacterial CcOs are present in the monomeric state (Iwata *et al.*, 1995; Soulimane *et al.*, 2000; Buschmann *et al.*, 2010).

To compare the heme content of each *cbb₃*-isoform, heme staining was carried out and UV/Vis spectra were recorded using the purified *cbb₃*-CcOs. The heme-staining assays revealed that hemes *c* are covalently bound in the subunit CcoO and CcoP of both recombinant *cbb₃*-isoforms. The oxidized, reduced and reduced-minus-oxidized difference spectra of both recombinant Cbb₃-1 and Cbb₃-2 are well consistent with the results observed with the wild-type Cbb₃-1, which indicates a proper assembly of heme and metal centers (see Section 3.5.1). Furthermore, the spectral features of the *P. stutzeri cbb₃*-CcOs are very similar to those of the previously characterized *cbb₃*-CcOs from other bacteria (García-Horsman *et al.*, 1994; Gray *et al.*, 1994; Pereira *et al.*, 2000; Hemp *et al.*, 2005).

Far-UV circular dichroism spectroscopy was also employed to compare the secondary structural content of the two *cbb₃*-isoforms. However, no differences were observed either between Cbb₃-1 and Cbb₃-2 or between wild-type and recombinant *cbb₃*-CcOs (see Section 3.5.2).

4.4.5 The thermal stability of both *cbb₃*-isoforms

DSC analyses were performed to investigate the thermal stability of both *cbb₃*-isoforms. We showed that the thermal denaturation of the *cbb₃*-CcOs is an irreversible process, which is consistent with the results obtained from the yeast and *P. denitrificans aa₃*-CcOs (Morin *et al.*, 1990; Haltia *et al.*, 1994). Due to the irreversible nature of the thermal denaturation process, the calorimetric data cannot be directly analyzed in terms of equilibrium thermodynamics (Manetto *et al.*, 2005). Therefore, the calorimetric enthalpy change (ΔH) of thermal transition may not represent the true enthalpy change of unfolding. Nevertheless, the calorimetric enthalpy change can still be used to compare the thermal stability of the two *cbb₃*-isoforms.

Our DSC results show that Cbb₃-1 is more stable than Cbb₃-2. The total calorimetric enthalpy

changes of the recombinant Cbb₃-1 and Cbb₃-2 are 2,016 and 1,556 KJ mol⁻¹, respectively. Both values are similar to the reported value of 1,560 KJ mol⁻¹ for the *aa*₃-CcO from *P. denitrificans* (Haltia *et al.*, 1994). The DSC scan of *aa*₃-CcO showed two transition peaks. The low-temperature transition centered at 48°C was assigned to the denaturation of subunit III of *aa*₃-CcO, while subunit I and II denatures as a single cooperative unit at 68°C (Haltia *et al.*, 1994). In the case of *cbb*₃-CcO, two transition peaks can be identified, although they are not as well separated as observed for Cbb₃-2. Based on the observation that two assembly intermediates are present in *cbb*₃-CcO (Kulajta *et al.*, 2006; Ekici *et al.*, 2011), we hypothesize that the low-temperature peak corresponds to the thermal denaturation of subunit CcoP, whereas the second peak is caused by denaturation of subunits CcoN and CcoO. In addition, besides the presence of CcoQ in Cbb₃-2, small structural differences may lead to the difference in thermal stability between Cbb₃-1 and Cbb₃-2.

When the total calorimetric enthalpy changes of both *cbb*₃-isoforms were normalized on a weight basis, two different values are obtained (4.3 and 3.1 cal/g for the recombinant Cbb₃-1 and Cbb₃-2, respectively). Both values are slightly higher than those (2.4 to 2.9 cal/g) reported for the *aa*₃-CcOs (Morin *et al.*, 1990; Haltia *et al.*, 1994), but significantly lower than the enthalpy change associated with unfolding of a typical water-soluble protein (Haltia *et al.*, 1994; Grinberg *et al.*, 2001). These results may indicate that the thermal denaturation of *cbb*₃-CcOs does not lead to a complete unfolding of the molecule, which has been suggested to be a common feature of membrane protein unfolding (Haltia *et al.*, 1994; Haltia and Freire 1995; Grinberg *et al.*, 2001).

4.4.6 Oxygen reductase activity of the two *cbb*₃-isoforms using an artificial electron donor

The physiological function of the bacterial *cbb*₃-CcOs is to catalyze the reduction of O₂ to water. Since the combination of TMPD and ascorbate is widely used in respiratory assays for CcOs, we also applied such an artificial electron-donating system to determine the enzymatic activity of both *cbb*₃-isoforms. As a substrate, TMPD can directly donate electrons to *cbb*₃-CcO, while ascorbate maintains TMPD in the reduced state. Under conditions optimized for pH, ionic strength and the molar ratio of ascorbate to TMPD, we showed that the purified recombinant Cbb₃-1 and Cbb₃-2 catalyze the reduction of oxygen at a rate comparable to the wild-type Cbb₃-1 (Figure 3-26). This suggests that the recombinant proteins produced in our newly established expression system are fully active.

We found that the oxygen reductase activity of *cbb*₃-CcO increased with increasing concentrations of TMPD up to a maximum at 4 mM (Figure 3-25 A). At 0.5 mM TMPD, the enzymatic activity of 450 e⁻ s⁻¹ is comparable with the activities of 200 to 600 e⁻ s⁻¹ measured for the purified

cbb₃-CcO from *R. sphaeroides* under similar conditions³³ (Sharma *et al.*, 2006; Huang *et al.*, 2008; Lee *et al.*, 2011). Moreover, our values of 700 to 800 e⁻ s⁻¹ determined at 1 mM TMPD are in good agreement with the values previously reported for the *P. stutzeri cbb₃-CcO* using the same TMPD concentration (Forte *et al.*, 2001; Urbani *et al.*, 2001). However, we found that the oxygen reductase activity of *cbb₃-CcO* is not saturated by 1 mM TMPD. With an increased TMPD concentration of 4 mM, a rate of about 2,000 e⁻ s⁻¹ was determined. Although the activity displayed Michaelis-Menten kinetics for the substrate TMPD, a saturation plateau was still not attained due to two technical difficulties in using a concentration of TMPD above 4 mM. First, it was difficult to maintain the pH of the reaction buffer at 7.5 (the optimal pH for *cbb₃-CcO*) because the addition of large amounts of TMPD and ascorbate led to a dramatic decrease in pH. Second, at high concentrations of TMPD, a relatively high level of TMPD autoxidation caused a significant decrease of the oxygen concentration, which resulted in a very long equilibrium time before the reaction could be initiated.

According to our analysis, two kinetic parameters could be calculated (a K_m of 3.6 mM and a V_{max} of about 4,000 e⁻ s⁻¹). Both values, obtained in the absence of well-defined saturation, are unusually high and may not represent true kinetic constants. Nevertheless, we can safely conclude that the *P. stutzeri cbb₃-CcOs* can catalyze the reduction of oxygen at a rate of at least 2,000 e⁻ s⁻¹ *in vitro*, and that the K_m for TMPD must be higher than 1 mM. These kinetic features do not seem to apply to other *cbb₃-CcOs* because kinetic studies on the *H. pylori cbb₃-CcO* showed a very high affinity for TMPD ($K_m = 108 \mu\text{M}$), but a relatively low V_{max} (247 e⁻ s⁻¹) (Tsukita *et al.*, 1999). It has to be noted that in the case of *H. pylori cbb₃-CcO*, the catalytic activity was measured by monitoring the pH shift with sodium ascorbate as the ultimate electron donor (Nagata *et al.*, 1996; Tsukita *et al.*, 1999). This excludes a direct comparison between our results and those from the *H. pylori cbb₃-CcO*. In the *caa₃-CcO*, a member of the A2 subclass of the A-type HCOs (Pereira *et al.*, 2001), subunit II contains a single *c*-type heme, which can directly receive the electrons from TMPD. Interestingly, it has been shown that for the *caa₃-CcO* of *Bacillus subtilis*, a high level of TMPD (at least 5 mM) is also required to reach the maximal activity of *caa₃-CcO* (Assempour *et al.*, 1998).

The oxygen reductase activities of *aa₃-CcOs* are normally in the range of 400 to 600 e⁻ s⁻¹ (Dürr *et al.*, 2008), which is about four-fold lower than the highest activity (2,000 e⁻ s⁻¹) observed for *cbb₃-CcO* in this work. In the case of *aa₃-CcO*, TMPD functions only as a redox mediator between

³³ It should be noted that the oxygen reductase activity of *R. sphaeroides cbb₃-CcO* was measured in the presence of both TMPD (0.5-0.6 mM) and horse heart cytochrome *c* (34 μM or 100 μM). Due to the lack of experimental evidence, it is unclear if either TMPD or horse heart cytochrome *c* are direct electron donors to *R. sphaeroides cbb₃-CcO*.

the mobile cytochrome *c* and the Cu_A-containing subunit II of *aa*₃-CcO. The formation and dissociation of a complex between cytochrome *c* and *aa*₃-CcO are required for the electron transfer to occur (Maneg *et al.*, 2004; Richter and Ludwig 2009). This may represent a rate-limiting step in the overall reaction sequence and result in a less efficient electron transfer compared to *cbb*₃-CcO. By contrast, the presence of three *c*-type cytochromes in the subunit CcoO and CcoP of the *cbb*₃-CcOs may provide multiple electron entry sites and support simultaneous interaction between TMPD and *cbb*₃-CcOs. As confirmed by the *cbb*₃-CcO structure (Buschmann *et al.*, 2010), the edge-to-edge distances from heme *c* of CcoO to heme *b* and from heme *b* to heme *b*₃ are clearly shorter than the distances observed for the corresponding redox centers in *aa*₃-CcO. As previously suggested (Verkhovskiy *et al.*, 1996; Buschmann *et al.*, 2010), the shorter distance may accelerate the rate of electron transfer and therefore increase the rate of oxygen reduction. All of these features led us to propose that electron transfer in the *cbb*₃-CcOs is more efficient than that in *aa*₃-CcOs under these *in vitro* assay conditions.

Comparison of the oxygen reductase activity of the two isoforms Cbb₃-1 and Cbb₃-2, however, revealed only marginal differences. It may be due to the fact that an artificial electron donor was used, which has a high efficiency for both *cbb*₃-isoforms. A different picture may evolve if a specific endogenous electron donor for the isoforms is available for activity assays (see discussion in Section 4.5).

4.4.7 Catalase activity of the two *cbb*₃-isoforms

The catalase activity is a side reaction of CcOs, in which H₂O₂ is dismutated to water and oxygen. In earlier works, this reaction has been studied biochemically with respect to its mechanism (Bolshakov *et al.*, 2010) and to its biological significance (Sedlák *et al.*, 2010). Recently, Hilbers *et al.* (2013) reported that the recombinant wild-type *aa*₃-CcO from *P. denitrificans* exhibited a 20-fold increase in turnover number of the catalase activity compared to the native wild-type *aa*₃-CcO, whereas no difference in oxygen reductase activity was observed. It was suggested that this unexpected difference in catalase activity might be attributed to the potential overproduction of one plasmid-encoded subunit of the recombinant *aa*₃-CcO. Such overproduction may reduce the extent of cofactor incorporation into the protein complex and may cause small structural changes (Hilbers *et al.*, 2013).

In order to investigate if such a difference in catalase activity exists between the recombinant and native *cbb*₃-CcO, as well as between both *cbb*₃-isoforms, measurements were performed according to Hilbers *et al.* (2013). It was shown that the *P. stutzeri* *cbb*₃-CcOs could catalyze the dismutation of hydrogen peroxide at a rate comparable to the *P. denitrificans* *aa*₃-CcO (see Section 3.5.7). Furthermore, no significant difference was observed between the recombinant *cbb*₃-isoforms and

the native enzyme. This observation does not match the result for the *P. denitrificans aa₃-CcOs*, which might be due to the advantage that an expression plasmid carrying the entire *cbb₃*-operon was used for the expression of both recombinant *cbb₃*-isoforms.

4.4.8 Electrochemical properties of the redox cofactors

The *cbb₃-CcO* contains five heme cofactors, four of them are hexa-coordinated low spin hemes (three hemes *c* and one heme *b*), whereas one is a penta-coordinated high spin heme (heme *b₃*). The determination of midpoint redox potentials of individual heme centers is a prerequisite for the understanding of the electron transfer processes in *cbb₃-CcOs*. Previously, the electrochemical properties of *cbb₃-CcOs* from several organisms have been investigated (Table 4-1). However, the results are partly contradictory in the different publications. In this work, we have determined the midpoint redox potentials of the heme cofactors in the two *cbb₃*-isoforms from *P. stutzeri* using redox titrations in the UV/Vis spectral range. We were particularly interested in the reduction potential of the hemes *c* from CcoP, as well as that of the heme *b₃* in the active site.

Table 4-1: Summary of the midpoint redox potentials of five heme cofactors in *cbb₃-CcOs*.

Midpoint redox potentials (E_m) are shown in mV (vs. standard hydrogen electrode) at different pH values.

Redox cofactor	E_m (mV)					
	<i>R. marinus</i> ^a	<i>P. stutzeri</i> ^b	<i>B. japonicum</i>		<i>R. sphaeroides</i> ^e	<i>P. stutzeri</i> ^f
	pH 7.0	pH 7.0	pH 7.7 ^c	pH 8.0 ^d	pH 7.0	pH 7.5
Heme <i>c</i> (low)	-50	+185	+220	+180	+234	+155, +185
Heme <i>c</i> (middle)		+245	+300	+180	+320	
Heme <i>c</i> (high)	+195	+245	+390	+400	+351	
Heme <i>b</i>	+120	+310	+375		+418	+263, +278
Heme <i>b₃</i>	-50	+225	+290		-59	+132, +158

^a Values are taken from Pereira *et al.* (2000). The value of “-50 mV” was assigned to both heme *c* and *b₃*.

^b Values are taken from Pitcher and Watmough (2004).

^c Values are taken from Verissimo *et al.* (2007).

^d Values are taken from Todorovic *et al.* (2008).

^e Values are taken from Rauhamaki *et al.* (2009).

^f This work; In each cell, the first value was obtained with Cbb₃-1 and the second was obtained with Cbb₃-2.

Contrary to the results in the previous studies, we found that the redox potentials of the three *c*-type hemes in the *P. stutzeri cbb₃-CcOs* are too close to be differentiated. The redox potentials that we determined for the *c*-type hemes in Cbb₃-1 and Cbb₃-2 are +155 mV and +185 mV, respectively (Table 4-1). Both values are comparable to those previously reported for the lowest potential *c*-type heme (+180 to +234 mV) in the *cbb₃-CcO* and fall within the range expected for a His/Met-coordinated *c*-type heme (Moore and Pettigrew 1990). This result is in disagreement with previous studies (Pitcher and Watmough 2004; Todorovic *et al.*, 2008), which suggest that the

CcoP subunit of *cbb*₃-CcO possesses two different *c*-type hemes, one of which is a bis-His coordinated heme *c* and the other exhibits His/Met axial coordination. Furthermore, the redox potential of this bis-His ligated heme *c* from CcoP has been determined to be +185 mV for the *P. stutzeri* *cbb*₃-CcO (Pitcher and Watmough 2004) and +400 mV for the *B. japonicum* *cbb*₃-CcO (Todorovic *et al.*, 2008). Nevertheless, our result is supported by the following observations: (i) in the crystal structure of *P. stutzeri* Cbb₃-1, the irons of both *c*-type hemes in CcoP are axially ligated to His and Met (Buschmann *et al.*, 2010); (ii) multiple sequence alignment of CcoP shows that there is no third conserved histidine residue near the ligand binding site of the heme group (see Appendix F); (iii) due to a reduced ability to stabilize ferrous iron, hemes with bis-His ligation are generally expected to have low reduction potentials that range from 0 to -400 mV (Moore and Pettigrew 1990; Dolla *et al.*, 1994).

Potentiometric titrations indicated that the low-spin heme *b* has the highest redox potential among the five hemes (+263 mV for Cbb₃-1 and +278 mV for Cbb₃-2), whereas the high-spin heme *b*₃ has a low potential (+132 mV for Cbb₃-1 and +158 mV for Cbb₃-2). The observed spacing of redox potentials between heme *b* and *b*₃ was found to be approximately 120 mV in both *cbb*₃-isoforms. These electrochemical characteristics are consistent with previous observations obtained with *P. stutzeri* *cbb*₃-CcO (Pitcher and Watmough 2004) and with *B. japonicum* *cbb*₃-CcO (Veríssimo *et al.*, 2007), although our values are slightly lower than reported previously. In contrast to our results, a very low potential of approximately -50 mV has been determined for the heme *b*₃ in both *R. marinus* and *R. sphaeroides* *cbb*₃-CcOs (Pereira *et al.*, 2000; Rauhamaki *et al.*, 2009). The conflicting results might be due to the different species studied. However, the redox potential difference between two hemes *b* is close to 500 mV in the case of the *R. sphaeroides* enzyme (Rauhamaki *et al.*, 2009), which is considered to be a thermodynamic barrier for the reduction of heme *b*₃.

4.5 The physiological electron donor for the *cbb*₃-CcO

4.5.1 The presence of *c*-type cytochromes in *P. stutzeri*

Understanding the physiological significance and difference of both *cbb*₃-isoforms requires the identification of their endogenous electron donor(s). Like many other bacteria, pseudomonads have multiple cytochromes *c* in the electron transport system. Based on the search for the heme *c* binding motif and homology analyses of the deduced amino acid sequences, a total of 16 proteins in *P. stutzeri* are predicted to represent the *c*-type cytochromes, which are targeted to the cell envelope (see Section 3.6.1). Of these, several *c*-type cytochromes, including cytochrome *c*₄, *c*₅,

c_{551} and c_{552} , have already been detected and isolated from aerobically grown cells (Liu *et al.*, 1981; Liu *et al.*, 1983; Pettigrew and Brown 1988; Hunter *et al.*, 1989). Although they have been studied extensively for their biochemical properties, there is no indication which of these c -type cytochromes is the natural electron donor for the *P. stutzeri* cbb_3 -CcOs. Thus, they were investigated in this study for their ability to donate electrons to the both cbb_3 -isoforms.

4.5.2 Production of the *P. stutzeri* cytochromes c in *E. coli*

We could purify three endogenous cytochromes c (c_4 , c_5 and c_{551}) from the periplasm of wild-type *P. stutzeri* cells (Sabine Buschmann); however, relatively low yields rendered detailed biochemical studies difficult.

Due to its well-studied genetic properties and the absence of endogenous cytochromes c under aerobic growth conditions, the *E. coli* expression system has been widely used for the production of recombinant c -type cytochromes (Miller *et al.*, 2003; Londer 2011). In this work, four cytochromes c (c_4 , c_5 , c_{551} and c_{552}) from *P. stutzeri* were cloned and expressed heterologously in *E. coli* under aerobic growth conditions. However, only cytochrome c_4 , c_5 and c_{551} were successfully expressed at reasonable levels (see Section 3.6.3).

Three untagged cytochromes c (c_4 , c_5 and c_{551}) were successfully purified to homogeneity (see Section 3.6.4). The results of SDS-PAGE followed by heme staining indicated the proper incorporation of the c -type heme. MALDI-MS analysis showed that all recombinant cytochromes c had the expected molecular weight of the mature holocytochrome (data not shown). Three purified recombinant proteins have spectroscopic properties identical to those observed for the native one and also similar to those reported in the literatures (Liu *et al.*, 1983; Pettigrew and Brown 1988). In addition, electrochemical measurements were performed to determine the redox potential of heme cofactors (see Section 3.6.6). For all three cytochromes c , the results obtained with two different methods (voltammetry and potentiometric titration) confirm each other and are similar to previous reports (Carter *et al.*, 1985; Leitch *et al.*, 1985; Pettigrew and Brown 1988; Scott and Mauk 1996).

During the purification of the recombinant cytochromes c , we have observed that the cytochrome c_4 is present in both soluble and membrane-attached forms in *E. coli*. This observation is well consistent with the report that cytochrome c_4 from several bacterial species, including *P. stutzeri*, was predominantly membrane-bound (around 80%) (Pettigrew and Brown 1988; Hunter *et al.*, 1989). Nevertheless, only the soluble cytochrome c_4 was isolated and used for downstream analyses in this work because it has been reported that both free and membrane-attached forms of cytochrome c_4 are indistinguishable concerning their spectroscopic and electrochemical properties

(Pettigrew and Brown 1988).

4.5.3 The natural electron donor for the *P. stutzeri* *cbb*₃-CcOs

Although *cbb*₃-CcOs have been isolated and characterized from several different species of proteobacteria, little is known about their natural electron donor(s). In this study, we investigated the abilities of three cytochromes *c* (*c*₄, *c*₅ and *c*₅₅₁) to donate their electrons to the *P. stutzeri* *cbb*₃-CcOs (see Section 3.6.7). The cytochrome *c*-dependent oxidase activity was measured polarographically in the presence of ascorbate and reduced cytochrome *c*. All measurements were carried out in the absence of TMPD because it can transfer electrons directly to *cbb*₃-CcOs at a high rate (see 4.4.6). Since the electrostatic interaction between cytochrome *c* and CcO is an ionic strength-dependent process (Witt *et al.*, 1998; Drosou *et al.*, 2002), the dependence of activity of *cbb*₃-CcOs on ionic strength was studied by varying the concentration of NaCl from 0 to 500 mM. For all three cytochromes *c* tested, nearly bell-shaped ionic strength dependence was observed and the maximum turnover number was obtained at higher ionic strength conditions (150 to 250 mM). For both *cbb*₃-isoforms from *P. stutzeri*, the highest rate of oxygen reduction (e.g., 515 e⁻/s for the wild-type Cbb₃-1) was obtained when 100 μM reduced cytochrome *c*₄ was used. The oxygen reductase activities measured with cytochrome *c*₅₅₁ are comparable (80 to 90%) to those found with cytochrome *c*₄, while the ones observed with cytochrome *c*₅ are reduced by about 80%. These results indicate that all three cytochromes *c* can undoubtedly donate electrons to the *cbb*₃-CcOs from *P. stutzeri*. However, only cytochrome *c*₄ and *c*₅₅₁ can serve as efficient substrates. In an attempt to explain this discrepancy, we investigated the electrochemical properties of the three cytochromes *c*. The relatively high reaction rate observed with cytochrome *c*₄ and *c*₅₅₁ can probably be attributed to the fact that both cytochromes harbour one low-potential heme *c* (i.e., 208 mV in *c*₄ and 223 to 248 mV in *c*₅₅₁). In contrast, cytochrome *c*₅ exhibits a high redox potential of 273 to 308 mV, which may hinder the electron transfer to the *cbb*₃-CcO.

Our results obtained with cytochrome *c*₄ confirm an earlier study by Chang *et al.* (2010), in which the cytochrome *c*₄ from *V. cholera*, supporting oxygen reductase activity at a rate of 300 e⁻/s, was identified as a natural electron donor to the *V. cholera* *cbb*₃-CcO. Furthermore, our data are consistent with the proposal that cytochrome *c*₄ provide alternative electron flows to the *cbb*₃-CcO, as in the case of *Azotobacter vinelandii* (Bertsova and Bogachev 2002) and *Neisseria gonorrhoeae* (Li *et al.*, 2010).

Cytochrome *c*₅₅₁ is most often found in *Pseudomonas* species as well as in *Azotobacter*. This cytochrome is known to function as the physiological electron donor for the cytochrome *cd*₁ nitrite reductase (Jüngst *et al.*, 1991; Zumft 1997; Hasegawa *et al.*, 2001). Interestingly, our analysis

demonstrates that cytochrome c_{551} is also an efficient substrate for both cbb_3 -isoforms from *P. stutzeri*, indicating its dual role in promoting both oxygen respiration and anaerobic nitrate respiration (i.e., denitrification). Such degeneracy is a common feature of many bacteria (e.g., cytochrome c_{550} is the electron donor both to the aa_3 -CcO and to the nitrite reductase in *P. denitrificans* [Otten *et al.*, 2001]) and may provide high efficiency and adaptability in response to environmental changes.

In all the experiments performed in this work, saturation kinetics were not obtained within the concentration range examined (20 to 100 μ M cytochromes c). The lack of saturation is unusual and makes it impossible to determine the true kinetic parameters (K_m and V_{max}). Similar to our observations, the nearly linear dependence of enzymatic activity of *V. cholera* cbb_3 -CcO on the concentration of cytochrome c_4 (up to 100 μ M) has been reported (Chang *et al.*, 2010). The authors proposed that the apparent lack of saturation was due to the presence of significant amounts of oxidized cytochrome c_4 during the assay, which suppressed the interaction between reduced cytochrome c_4 and the cbb_3 -CcO and significantly changed the kinetic behavior of the reaction (Chang *et al.*, 2010). So far, we could only assume that this unexpected kinetic behavior is an *in vitro* artifact rather than a natural phenomenon. Further studies are required to improve our understanding of the kinetic interaction between cbb_3 -CcOs and their physiological redox partners. Besides the three endogenous cytochromes c , assays were also performed using two eukaryotic cytochromes c (from horse heart and from *S. cerevisiae*). Our data clearly show that reaction rates obtained with both eukaryotic cytochromes c were 20- to 50-fold lower as compared with the cytochrome c_4 , indicating that neither the horse heart cytochrome c nor the yeast cytochrome c is effective as electron donor for *P. stutzeri* cbb_3 -CcOs. This is consistent with a published report that horse heart cytochrome c is a poor substrate for *V. cholera* cbb_3 -CcO (Chang *et al.*, 2010). Otherwise, horse heart cytochrome c has been widely used for measuring the oxygen reductase activity of *R. sphaeroides* cbb_3 -CcO (García-Horsman *et al.*, 1994; Sharma *et al.*, 2006; Huang *et al.*, 2008; Lee *et al.*, 2011). However, in these cases, the results may be misleading because significant amounts of TMPD were also present in the reaction mixture.

4.5.4 Substrate specificity of both cbb_3 -isoforms

When oxidase activity was measured using endogenous cytochrome c as substrate, substantial differences between the two cbb_3 -isoforms were found. Catalytic activities measured for the Cbb₃-2 were reduced by about 70% when compared with Cbb₃-1 (see Figure 3-47). This is apparently not consistent with our observation that, using TMPD as an artificial electron donor, both cbb_3 -isoforms catalyzed the reduction of oxygen at a comparable level (see Figure 3-26).

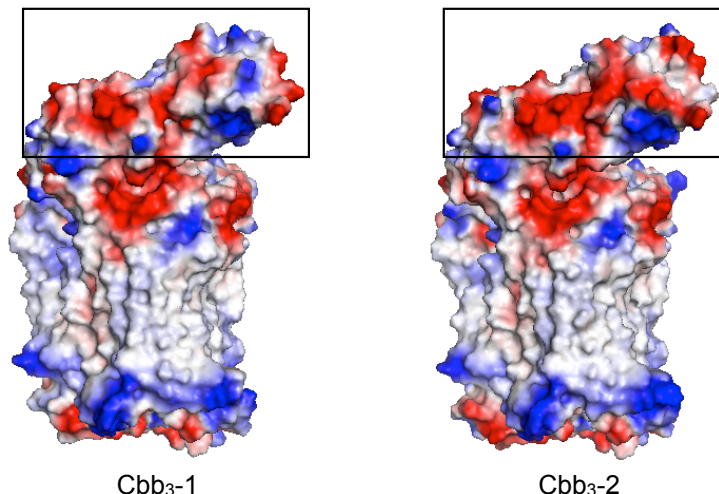


Figure 4-4: Comparison of the electrostatic surface potentials of both *cbb*₃-isoforms. The electrostatic surface potentials were calculated on the crystal structure of Cbb₃-1 (3MK7) and on a model of Cbb₃-2. Red and blue colors indicate negatively charged and positively charged regions, respectively. Black boxes highlight the charge differences in the CcoP subunit of both *cbb*₃-isoforms.

Inferring from the amino acid sequences and a surface charge calculation based on the X-ray structure of Cbb₃-1 as well as a model of Cbb₃-2, we found that the most pronounced structural changes and surface charge differences may occur in the solvent exposed domains of subunits CcoP-1 and CcoP-2 (Figure 4-4). In this area, Cbb₃-2 possesses more negatively charged residues when compared to the Cbb₃-1. Because this area may constitute the putative cytochrome *c* binding site with the respective electron entry area, even small changes may influence the electron transfer rate between the cytochrome *c* and the *cbb*₃-CcO. This could provide a partial explanation for the differences in rates of oxygen reduction between the two *cbb*₃-CcOs. Future studies, including docking experiments and mutagenesis studies, are warranted to shed light on this issue.

In summary of this section, we conclude that cytochrome *c*₄ and *c*₅₅₁ are both efficient substrates to the two *cbb*₃-isoforms in *P. stutzeri* and both *cbb*₃-isoforms have different substrate specificity. Our results do not exclude the possibility that this bacterium contains other electron donors for *cbb*₃-CcO. As previously suggested, a membrane-anchored tetraheme cytochrome *c* (NirT) as well as a monoheme cytochrome *c* (NirC) may also have putative electron donor function (Zumft 1997). Hopefully, a more detailed picture of electron transfer network will emerge from future investigations, which will help to improve our understanding of the physiology of aerobic and anaerobic energy metabolism in *P. stutzeri*.

5 References

1. P. Ädelroth, M. Ek, D. Mitchell, R. Gennis, P. Brzezinski, Glutamate 286 in cytochrome *aa*₃ from *Rhodobacter sphaeroides* is involved in proton uptake during the reaction of the fully-reduced enzyme with dioxygen. *Biochemistry* **36**, 13824 (1997).
2. H. Aebi, Catalase *in vitro*. *Methods Enzymol* **105**, 121 (1984).
3. T. Althoff, D. J. Mills, J. L. Popot, W. Kühlbrandt, Arrangement of electron transport chain components in bovine mitochondrial supercomplex I₁III₂IV₁. *EMBO J* **30**, 4652 (2011).
4. R. P. Ambler, Sequence variability in bacterial cytochromes *c*. *Biochim Biophys Acta* **1058**, 42 (1991).
5. T. M. Antalis, G. Palmer, Kinetic characterization of the interaction between cytochrome oxidase and cytochrome *c*. *The Journal of biological chemistry* **257**, 6194 (1982).
6. H. Arai, Regulation and function of versatile aerobic and anaerobic respiratory metabolism in *Pseudomonas aeruginosa*. *Frontiers in microbiology* **2**, 103 (2011).
7. E. Arslan, H. Schulz, R. Zufferey, P. Künzler, L. Thöny-Meyer, Overproduction of the *Bradyrhizobium japonicum* *c*-type cytochrome subunits of the *cbb*₃ oxidase in *Escherichia coli*. *Biochem Biophys Res Commun* **251**, 744 (1998).
8. E. Arslan, A. Kannt, L. Thöny-Meyer, H. Hennecke, The symbiotically essential *cbb*₃-type oxidase of *Bradyrhizobium japonicum* is a proton pump. *FEBS Lett* **470**, 7 (2000).
9. C. Aslanidis, P. J. de Jong, Ligation-independent cloning of PCR products (LIC-PCR). *Nucleic Acids Res* **18**, 6069 (1990).
10. M. Assempour, D. Lim, B. C. Hill, Electron transfer kinetics during the reduction and turnover of the cytochrome *caa*₃ complex from *Bacillus subtilis*. *Biochemistry* **37**, 9991 (1998).
11. Z. Bao, S. Cartinhour, B. Swingle, Substrate and target sequence length influence RecTE(Psy) recombineering efficiency in *Pseudomonas syringae*. *PLoS ONE* **7**, e50617 (2012).
12. R. Baradaran, J. M. Berrisford, G. S. Minhas, L. A. Sazanov, Crystal structure of the entire respiratory complex I. *Nature* **494**, 443 (2013).
13. J. Batut, M. L. Daveran-Mingot, M. David, J. Jacobs, A. M. Garnerone, D. Kahn, *fixK*, a gene homologous with *fnr* and *crp* from *Escherichia coli*, regulates nitrogen fixation genes both positively and negatively in *Rhizobium meliloti*. *EMBO J* **8**, 1279 (1989).
14. I. Belevich, D. A. Bloch, N. Belevich, M. Wikström, M. I. Verkhovskiy, Exploring the proton pump mechanism of cytochrome *c* oxidase in real time. *Proc Natl Acad Sci U S A* **104**, 2685 (2007).
15. A. S. Beliaev, in *Microbial Functional Genomics*. (John Wiley & Sons, Inc., 2005), pp. 207-240.
16. Y. V. Bertsova, A. V. Bogachev, Operation of the *cbb*₃-type terminal oxidase in *Azotobacter vinelandii*. *Biochemistry Mosc* **67**, 622 (2002).
17. D. Bickar, J. Bonaventura, C. Bonaventura, Cytochrome *c* oxidase binding of hydrogen peroxide. *Biochemistry* **21**, 2661 (1982).

18. D. Bloch, I. Belevich, A. Jasaitis, C. Ribacka, A. Puustinen, M. I. Verkhovsky, M. Wikström, The catalytic cycle of cytochrome *c* oxidase is not the sum of its two halves. *P Natl Acad Sci USA* **101**, 529 (2004).
19. I. A. Bolshakov, T. V. Vygodina, R. Gennis, A. A. Karyakin, A. A. Konstantinov, Catalase activity of cytochrome *c* oxidase assayed with hydrogen peroxide-sensitive electrode microsensor. *Biochemistry. Biokhimiia* **75**, 1352 (2010).
20. V. B. Borisov, R. B. Gennis, J. Hemp, M. I. Verkhovsky, The cytochrome *bd* respiratory oxygen reductases. *Biochim Biophys Acta* **1807**, 1398 (2011).
21. M. M. Bradford, A rapid and sensitive method for the quantitation of microgram quantities of protein utilizing the principle of protein-dye binding. *Anal Biochem* **72**, 248 (1976).
22. U. Brandt, Energy converting NADH:quinone oxidoreductase (complex I). *Annu Rev Biochem* **75**, 69 (2006).
23. C. Brochier-Armanet, E. Talla, S. Gribaldo, The multiple evolutionary histories of dioxygen reductases: Implications for the origin and evolution of aerobic respiration. *Mol Biol Evol* **26**, 285 (2009).
24. E. Broda, G. A. Peschek, Did respiration or photosynthesis come first? *Journal of Theoretical Biology* **81**, 201 (1979).
25. P. Brzezinski, R. Gennis, Cytochrome *c* oxidase: exciting progress and remaining mysteries. *J Bioenerg Biomembr* **40**, 521 (2008).
26. K. Budiman, A. Kannt, S. Lyubenova, O. Richter, B. Ludwig, H. Michel, F. MacMillan, Tyrosine 167: the origin of the radical species observed in the reaction of cytochrome *c* oxidase with hydrogen peroxide in *Paracoccus denitrificans*. *Biochemistry* **43**, 11709 (2004).
27. D. Bühler, R. Rossmann, S. Landolt, S. Balsiger, H. M. Fischer, H. Hennecke, Disparate pathways for the biogenesis of cytochrome oxidases in *Bradyrhizobium japonicum*. *J Biol Chem* **285**, 15704 (2010).
28. S. Buschmann, E. Warkentin, H. Xie, J. Langer, U. Ermler, H. Michel, The structure of *cbb*₃ cytochrome oxidase provides insights into proton pumping. *Science* **329**, 327 (2010).
29. G. Buse, T. Soulimane, M. Dewor, H. E. Meyer, M. Bluggel, Evidence for a copper-coordinated histidine-tyrosine cross-link in the active site of cytochrome oxidase. *Protein Sci* **8**, 985 (1999).
30. C. Butler, E. Forte, F. Maria Scandurra, M. Arese, A. Giuffre, C. Greenwood, P. Sarti, Cytochrome *bo*₃ from *Escherichia coli*: the binding and turnover of nitric oxide. *Biochem Biophys Res Commun* **296**, 1272 (2002).
31. E. Campeau, V. E. Ruhl, F. Rodier, C. L. Smith, B. L. Rahmberg, J. O. Fuss, J. Campisi, P. Yaswen, P. K. Cooper, P. D. Kaufman, A versatile viral system for expression and depletion of proteins in mammalian cells. *PLoS ONE* **4**, e6529 (2009).
32. D. C. Carter, K. A. Melis, S. E. O'Donnell, B. K. Burgess, W. R. Furey, B. C. Wang, C. D. Stout, Crystal structure of *Azotobacter* cytochrome *c*₅ at 2.5 Å resolution. *J Mol Biol* **184**, 279 (1985).
33. J. Castresana, M. Lubben, M. Saraste, D. G. Higgins, Evolution of cytochrome oxidase, an enzyme older than atmospheric oxygen. *EMBO J* **13**, 2516 (1994).
34. J. Castresana, M. Lubben, M. Saraste, New archaeobacterial genes coding for redox proteins: implications for the evolution of aerobic metabolism. *J Mol Biol* **250**, 202 (1995).

35. J. Castresana, M. Saraste, Evolution of energetic metabolism: the respiration-early hypothesis. *Trends Biochem Sci* **20**, 443 (1995).
36. G. Cecchini, Function and structure of complex II of the respiratory chain. *Annu Rev Biochem* **72**, 77 (2003).
37. B. Chance, G. R. Williams, Respiratory enzymes in oxidative phosphorylation. III. The steady state. *J Biol Chem* **217**, 409 (1955).
38. B. Chance, C. Saronio, J. Leigh, Functional intermediates in reaction of cytochrome oxidase with oxygen. *Proc Natl Acad Sci U S A* **72**, 1635 (1975).
39. H. Chang, Y. Ahn, L. Pace, M. Lin, Y. Lin, R. Gennis, The diheme cytochrome c_4 from *Vibrio cholerae* is a natural electron donor to the respiratory cbb_3 oxygen reductase. *Biochemistry* **49**, 7494 (2010).
40. H.-Y. Chang, S. K. Choi, A. S. Vakkasoglu, Y. Chen, J. Hemp, J. A. Fee, R. B. Gennis, Exploring the proton pump and exit pathway for pumped protons in cytochrome ba_3 from *Thermus thermophilus*. *Proc Natl Acad Sci USA* **109**, 5259 (2012).
41. K. Choi, A. Kumar, H. Schweizer, A 10-min method for preparation of highly electrocompetent *Pseudomonas aeruginosa* cells: application for DNA fragment transfer between chromosomes and plasmid transformation. *J Microbiol Methods* **64**, 391 (2006).
42. K.-H. Choi, L. A. Trunck, A. Kumar, T. Mima, R. Karkhoff-Schweizer, H. P. Schweizer, Genetic tools for *Pseudomonas*. *Pseudomonas: genomics and molecular biology*, ed. P. Cornelis, 65 (2008).
43. G. T. Chung, J. S. Yoo, H. B. Oh, Y. S. Lee, S. H. Cha, S. J. Kim, C. K. Yoo, Complete genome sequence of *Neisseria gonorrhoeae* NCCP11945. *J Bacteriol* **190**, 6035 (2008).
44. J. Comolli, T. Donohue, Differences in two *Pseudomonas aeruginosa* cbb_3 cytochrome oxidases. *Mol Microbiol* **51**, 1193 (2004).
45. F. Corpet, Multiple sequence alignment with hierarchical clustering. *Nucleic Acids Res* **16**, 10881 (1988).
46. C. Cousseau, J. Batut, Genomics of the $ccoNOQP$ -encoded cbb_3 oxidase complex in bacteria. *Arch Microbiol* **181**, 89 (2004).
47. A. R. Crofts, The cytochrome bc_1 complex: function in the context of structure. *Annual review of physiology* **66**, 689 (2004).
48. E. L. D'Antonio, J. D'Antonio, V. de Serrano, H. Gracz, M. K. Thompson, R. A. Ghiladi, E. F. Bowden, S. Franzen, Functional consequences of the creation of an Asp-His-Fe triad in a 3/3 globin. *Biochemistry* **50**, 9664 (2011).
49. R. D'mello, S. Hill, R. K. Poole, The cytochrome bd quinol oxidase in *Escherichia coli* has an extremely high oxygen affinity and two oxygen-binding haems: implications for regulation of activity *in vivo* by oxygen inhibition. *Microbiology (Reading, England)* **142** (Pt 4), 755 (1996).
50. J. Davison, Genetic tools for pseudomonads, rhizobia, and other gram-negative bacteria. *Biotechniques* **32**, 386 (2002).
51. J. de Gier, M. Lubben, W. Reijnders, C. Tipker, D. Slotboom, R. van Spanning, A. Stouthamer, J. van der Oost, The terminal oxidases of *Paracoccus denitrificans*. *Mol Microbiol* **13**, 183 (1994).
52. M. Deedom, J. Rock, J. Moir, Organization of the respiratory chain of *Neisseria meningitidis*. *Biochem Soc Trans* **34**, 139 (2006).

53. M. Deeudom, M. Koomey, J. W. B. Moir, Roles of *c*-type cytochromes in respiration in *Neisseria meningitidis*. *Microbiology (Reading, Engl)* **154**, 2857 (2008).
54. R. E. Dickerson, R. Timkovich, R. J. Almassy, The cytochrome fold and the evolution of bacterial energy metabolism. *Journal of molecular biology* **100**, 473 (1976).
55. J. Diver, L. Bryan, P. Sokol, Transformation of *Pseudomonas aeruginosa* by electroporation. *Anal Biochem* **189**, 75 (1990).
56. A. Dolla, L. Blanchard, F. Guerlesquin, M. Bruschi, The protein moiety modulates the redox potential in cytochromes *c*. *Biochimie* **76**, 471 (1994).
57. V. Drosou, F. Malatesta, B. Ludwig, Mutations in the docking site for cytochrome *c* on the *Paracoccus* heme *aa*₃ oxidase. Electron entry and kinetic phases of the reaction. *Eur J Biochem* **269**, 2980 (2002).
58. A. Ducluzeau, S. Ouchane, W. Nitschke, The *cbb*₃ oxidases are an ancient innovation of the domain bacteria. *Mol Biol Evol* **25**, 1158 (2008).
59. A.-L. Ducluzeau, R. van Lis, S. Duval, B. Schoepp-Cothenet, M. J. Russell, W. Nitschke, Was nitric oxide the first deep electron sink? *Trends Biochem Sci* **34**, 9 (2009).
60. K. Dürr, J. Koepke, P. Hellwig, H. Muller, H. Angerer, G. Peng, E. Olkhova, O. Richter, B. Ludwig, H. Michel, A D-pathway mutation decouples the *Paracoccus denitrificans* cytochrome *c* oxidase by altering the side-chain orientation of a distant conserved glutamate. *J Mol Biol* **384**, 865 (2008).
61. R. G. Efremov, R. Baradaran, L. A. Sazanov, The architecture of respiratory complex I. *Nature* **465**, 441 (2010).
62. S. Ekici, G. Pawlik, E. Lohmeyer, H.-G. Koch, F. Daldal, Biogenesis of *cbb*₃-type cytochrome *c* oxidase in *Rhodobacter capsulatus*. *Biochim Biophys Acta* **1817**, 898 (2011).
63. S. Ekici, H. Yang, H.-G. Koch, F. Daldal, Novel transporter required for biogenesis of *cbb*₃-type cytochrome *c* oxidase in *Rhodobacter capsulatus*. *MBio* **3**, (2012).
64. S. Elsen, L. R. Swem, D. L. Swem, C. E. Bauer, RegB/RegA, a highly conserved redox-responding global two-component regulatory system. *Microbiol Mol Biol Rev* **68**, 263 (2004).
65. J. M. Eraso, S. Kaplan, From redox flow to gene regulation: role of the PrrC protein of *Rhodobacter sphaeroides* 2.4.1. *Biochemistry* **39**, 2052 (2000).
66. H. Eubel, J. Heinemeyer, S. Sunderhaus, H. P. Braun, Respiratory chain supercomplexes in plant mitochondria. *Plant physiology and biochemistry : PPB / Societe francaise de physiologie vegetale* **42**, 937 (2004).
67. O. Farver, O. Einarsdóttir, I. Pecht, Electron transfer rates and equilibrium within cytochrome *c* oxidase. *European journal of biochemistry / FEBS* **267**, 950 (2000).
68. J. Fetter, J. Qian, J. Shapleigh, J. Thomas, A. Garcia-Horsman, E. Schmidt, J. Hosler, G. Babcock, R. Gennis, S. Ferguson-Miller, Possible proton relay pathways in cytochrome *c* oxidase. *Proc Natl Acad Sci U S A* **92**, 1604 (1995).
69. H. M. Fischer, Environmental regulation of rhizobial symbiotic nitrogen fixation genes. *Trends in microbiology* **4**, 317 (1996).
70. E. Forte, A. Urbani, M. Saraste, P. Sarti, M. Brunori, A. Giuffrè, The cytochrome *cbb*₃ from *Pseudomonas stutzeri* displays nitric oxide reductase activity. *Eur J Biochem* **268**, 6486 (2001).

71. H. E. Garcia, L. I. Gordon, Oxygen solubility in seawater - Better fitting equations. *Limnol Oceanogr* **37**, 1307 (1992).
72. J. García-Horsman, B. Barquera, J. Rumbley, J. Ma, R. Gennis, The superfamily of heme-copper respiratory oxidases. *J Bacteriol* **176**, 5587 (1994).
73. J. A. García-Horsman, E. Berry, J. P. Shapleigh, J. O. Alben, R. B. Gennis, A novel cytochrome *c* oxidase from *Rhodobacter sphaeroides* that lacks Cu_A. *Biochemistry* **33**, 3113 (1994).
74. M. A. Gilles-Gonzalez, G. Gonzalez, Heme-based sensors: defining characteristics, recent developments, and regulatory hypotheses. *J Inorg Biochem* **99**, 1 (2005).
75. L. Girard, S. Brom, A. Davalos, O. Lopez, M. Soberon, D. Romero, Differential regulation of *fixN*-reiterated genes in *Rhizobium etli* by a novel *fixL*-*fixK* cascade. *Mol Plant Microbe Interact* **13**, 1283 (2000).
76. A. Giuffrè, G. Stubauer, P. Sarti, M. Brunori, W. Zumft, G. Buse, T. Soulimane, The heme-copper oxidases of *Thermus thermophilus* catalyze the reduction of nitric oxide: evolutionary implications. *Proc Natl Acad Sci U S A* **96**, 14718 (1999).
77. C. F. Goodhew, K. R. Brown, G. W. Pettigrew, Haem staining in gels, a useful tool in the study of bacterial *c*-type cytochromes. *Biochim Biophys Acta* **852**, 288 (1986).
78. D. B. Goodin, D. E. McRee, The Asp-His-Fe triad of cytochrome *c* peroxidase controls the reduction potential, electronic structure, and coupling of the tryptophan free radical to the heme. *Biochemistry* **32**, 3313 (1993).
79. M. J. Granados-Baeza, N. Gómez-Hernández, Y. Mora, M. J. Delgado, D. Romero, L. Girard, Novel reiterated Fnr-type proteins control the production of the symbiotic terminal oxidase *cbb₃* in *Rhizobium etli* CFN42. *Mol Plant Microbe Interact* **20**, 1241 (2007).
80. K. A. Gray, M. Grooms, H. Myllykallio, C. Moomaw, C. Slaughter, F. Daldal, *Rhodobacter capsulatus* contains a novel *cb*-type cytochrome *c* oxidase without a Cu_A center. *Biochemistry* **33**, 3120 (1994).
81. J. Green, M. S. Paget, Bacterial redox sensors. *Nature reviews. Microbiology* **2**, 954 (2004).
82. P. Greiner, A. Hannappel, C. Werner, B. Ludwig, Biogenesis of cytochrome *c* oxidase--in vitro approaches to study cofactor insertion into a bacterial subunit I. *Biochim Biophys Acta* **1777**, 904 (2008).
83. A. V. Grinberg, N. M. Gevondyan, N. V. Grinberg, V. Y. Grinberg, The thermal unfolding and domain structure of Na⁺/K⁺-exchanging ATPase. A scanning calorimetry study. *Eur J Biochem* **268**, 5027 (2001).
84. C. J. T. d. Grotthuss, Sur la décomposition de l'eau et des corps qu'elle tient en dissolution à l'aide de l'électricité galvanique (Theory of decomposition of liquids by electric currents). *Ann. Chim.* **58**, 54 (1806).
85. C. R. Hackenbrock, B. Chazotte, S. S. Gupte, The random collision model and a critical assessment of diffusion and collision in mitochondrial electron transport. *J Bioenerg Biomembr* **18**, 331 (1986).
86. T. Haltia, N. Semo, J. Arrondo, F. Goni, E. Freire, Thermodynamic and structural stability of cytochrome *c* oxidase from *Paracoccus denitrificans*. *Biochemistry* **33**, 9731 (1994).
87. T. Haltia, E. Freire, Forces and factors that contribute to the structural stability of membrane proteins. *Biochimica et Biophysica Acta (BBA) - Bioenergetics* **1228**, 1 (1995).
88. H. Han, J. Hemp, L. A. Pace, H. Ouyang, K. Ganesan, J. H. Roh, F. Daldal, S. R. Blanke,

- R. B. Gennis, Adaptation of aerobic respiration to low O₂ environments. *Proc Natl Acad Sci U S A* **108**, 14109 (2011).
89. S. H. Han, Y. C. Ching, D. L. Rousseau, Cytochrome *c* oxidase: decay of the primary oxygen intermediate involves direct electron transfer from cytochrome *a*. *Proc Natl Acad Sci U S A* **87**, 8408 (1990).
90. D. Hanahan, Studies on transformation of *Escherichia coli* with plasmids. *J Mol Biol* **166**, 557 (1983).
91. N. Hasegawa, H. Arai, Y. Igarashi, Two *c*-type cytochromes, NirM and NirC, encoded in the *nir* gene cluster of *Pseudomonas aeruginosa* act as electron donors for nitrite reductase. *Biochem Biophys Res Commun* **288**, 1223 (2001).
92. R. S. Haun, I. M. Serventi, J. Moss, Rapid, reliable ligation-independent cloning of PCR products using modified plasmid vectors. *Biotechniques* **13**, 515 (1992).
93. P. Hellwig, C. Ostermeier, H. Michel, B. Ludwig, W. Mantele, Electrochemically induced FT-IR difference spectra of the two- and four-subunit cytochrome *c* oxidase from *P. denitrificans* reveal identical conformational changes upon redox transitions. *Biochim Biophys Acta* **1409**, 107 (1998).
94. J. Hemp, C. Christian, B. Barquera, R. B. Gennis, T. J. Martínez, Helix switching of a key active-site residue in the cytochrome *cbb*₃ oxidases. *Biochemistry* **44**, 10766 (2005).
95. J. Hemp, D. E. Robinson, K. B. Ganesan, T. J. Martinez, N. L. Kelleher, R. B. Gennis, Evolutionary migration of a post-translationally modified active-site residue in the proton-pumping heme-copper oxygen reductases. *Biochemistry* **45**, 15405 (2006).
96. J. Hemp, H. Han, J. Roh, S. Kaplan, T. Martinez, R. Gennis, Comparative genomics and site-directed mutagenesis support the existence of only one input channel for protons in the C-family (*cbb*₃ oxidase) of heme-copper oxygen reductases. *Biochemistry* **46**, 9963 (2007).
97. J. Hemp, R. Gennis, Diversity of the heme-copper superfamily in archaea: insights from genomics and structural modeling. *Results Probl Cell Differ* **45**, 1 (2008).
98. E. H. Heuberger, L. M. Veenhoff, R. H. Duurkens, R. H. Friesen, B. Poolman, Oligomeric state of membrane transport proteins analyzed with blue native electrophoresis and analytical ultracentrifugation. *J Mol Biol* **317**, 591 (2002).
99. F. Hilbers, I. von der Hocht, B. Ludwig, H. Michel, True wild type and recombinant wild type cytochrome *c* oxidase from *Paracoccus denitrificans* show a 20-fold difference in their catalase activity. *Biochim Biophys Acta* **1827**, 319 (2013).
100. B. C. Hill, The reaction of the electrostatic cytochrome *c*-cytochrome oxidase complex with oxygen. *J Biol Chem* **266**, 2219 (1991).
101. P. C. Hinkle, M. A. Kumar, A. Resetar, D. L. Harris, Mechanistic stoichiometry of mitochondrial oxidative phosphorylation. *Biochemistry* **30**, 3576 (1991).
102. T. Hino, Y. Matsumoto, S. Nagano, H. Sugimoto, Y. Fukumori, T. Murata, S. Iwata, Y. Shiro, Structural basis of biological N₂O generation by bacterial nitric oxide reductase. *Science* **330**, 1666 (2010).
103. J. Hirst, J. Carroll, I. M. Fearnley, R. J. Shannon, J. E. Walker, The nuclear encoded subunits of complex I from bovine heart mitochondria. *Bba-Bioenergetics* **1604**, 135 (2003).
104. J. Hirst, Mitochondrial complex I. *Annual review of biochemistry* **82**, 551 (2013).
105. J. Hosler, J. Shapleigh, D. Mitchell, Y. Kim, M. Pressler, C. Georgiou, G. Babcock, J.

- Alben, S. Ferguson-Miller, R. Gennis, Polar residues in helix VIII of subunit I of cytochrome *c* oxidase influence the activity and the structure of the active site. *Biochemistry* **35**, 10776 (1996).
106. J. P. Hosler, S. Ferguson-Miller, M. W. Calhoun, J. W. Thomas, J. Hill, L. Lemieux, J. Ma, C. Georgiou, J. Fetter, J. Shapleigh, et al., Insight into the active-site structure and function of cytochrome oxidase by analysis of site-directed mutants of bacterial cytochrome *aa*₃ and cytochrome *bo*. *J Bioenerg Biomembr* **25**, 121 (1993).
107. Y. Huang, J. Reimann, H. Lepp, N. Drici, P. Ädelroth, Vectorial proton transfer coupled to reduction of O₂ and NO by a heme-copper oxidase. *Proc Natl Acad Sci U S A* **105**, 20257 (2008).
108. Y. Huang, J. Reimann, L. M. R. Singh, P. Ädelroth, Substrate binding and the catalytic reactions in *cbb*₃-type oxidases: the lipid membrane modulates ligand binding. *Biochim Biophys Acta* **1797**, 724 (2010).
109. C. Hunte, V. Zickermann, U. Brandt, Functional modules and structural basis of conformational coupling in mitochondrial complex I. *Science* **329**, 448 (2010).
110. D. J. Hunter, K. R. Brown, G. W. Pettigrew, The role of cytochrome *c*₄ in bacterial respiration. Cellular location and selective removal from membranes. *Biochem J* **262**, 233 (1989).
111. H. Inoue, H. Nojima, H. Okayama, High efficiency transformation of *Escherichia coli* with plasmids. *Gene* **96**, 23 (1990).
112. S. Iwata, C. Ostermeier, B. Ludwig, H. Michel, Structure at 2.8 Å resolution of cytochrome *c* oxidase from *Paracoccus denitrificans*. *Nature* **376**, 660 (1995).
113. S. Iwata, J. W. Lee, K. Okada, J. K. Lee, M. Iwata, B. Rasmussen, T. A. Link, S. Ramaswamy, B. K. Jap, Complete structure of the 11-subunit bovine mitochondrial cytochrome *bc*₁ complex. *Science* **281**, 64 (1998).
114. R. J. Jackson, K. T. Elvers, L. J. Lee, M. D. Gidley, L. M. Wainwright, J. Lightfoot, S. F. Park, R. K. Poole, Oxygen reactivity of both respiratory oxidases in *Campylobacter jejuni*: the *cydAB* genes encode a cyanide-resistant, low-affinity oxidase that is not of the cytochrome *bd* type. *Journal of bacteriology* **189**, 1604 (2007).
115. P. D. Josephy, T. Eling, R. P. Mason, The horseradish peroxidase-catalyzed oxidation of 3,5,3',5'-tetramethylbenzidine. Free radical and charge-transfer complex intermediates. *J Biol Chem* **257**, 3669 (1982).
116. A. Jüngst, S. Wakabayashi, H. Matsubara, W. G. Zumft, The *nirSTBM* region coding for cytochrome *cd*₁-dependent nitrite respiration of *Pseudomonas stutzeri* consists of a cluster of mono-, di-, and tetraheme proteins. *FEBS Lett* **279**, 205 (1991).
117. D. Kahn, M. David, O. Domergue, M. L. Daveran, J. Ghai, P. R. Hirsch, J. Batut, *Rhizobium meliloti fixGHI* sequence predicts involvement of a specific cation pump in symbiotic nitrogen fixation. *J Bacteriol* **171**, 929 (1989).
118. D. Kahn, J. Batut, M. Daveran, J. Fourment, Structure and regulation of the *fixNOQP* operon from *Rhizobium meliloti*. *New Horizons in Nitrogen Fixation*. R. Palacios, J. Mora, and WE Newton, eds. Kluwer Academic Pub., Dordrecht, The Netherlands, 474 (1993).
119. P. A. Kaminski, C. L. Kitts, Z. Zimmerman, R. A. Ludwig, *Azorhizobium caulinodans* uses both cytochrome *bd* (quinol) and cytochrome *cbb*₃ (cytochrome *c*) terminal oxidases for symbiotic N₂ fixation. *J Bacteriol* **178**, 5989 (1996).
120. A. Kannt, T. Soulimane, G. Buse, A. Becker, E. Bamberg, H. Michel, Electrical current generation and proton pumping catalyzed by the *ba*₃-type cytochrome *c* oxidase from

- Thermus thermophilus*. *FEBS Lett* **434**, 17 (1998).
121. T. Kawakami, M. Kuroki, M. Ishii, Y. Igarashi, H. Arai, Differential expression of multiple terminal oxidases for aerobic respiration in *Pseudomonas aeruginosa*. *Environ Microbiol* **12**, 1399 (2010).
 122. Y.-J. Kim, I.-J. Ko, J.-M. Lee, H.-Y. Kang, Y. M. Kim, S. Kaplan, J.-I. Oh, Dominant role of the *cbb₃* oxidase in regulation of photosynthesis gene expression through the PrrBA system in *Rhodobacter sphaeroides* 2.4.1. *Journal of bacteriology* **189**, 5617 (2007).
 123. K. Kobayashi, H. Une, K. Hayashi, Electron transfer process in cytochrome oxidase after pulse radiolysis. *The Journal of biological chemistry* **264**, 7976 (1989).
 124. H. Koch, C. Winterstein, A. Saribas, J. Alben, F. Daldal, Roles of the *ccoGHIS* gene products in the biogenesis of the *cbb₃*-type cytochrome *c* oxidase. *J Mol Biol* **297**, 49 (2000).
 125. J. Koepke, E. Olkhova, H. Angerer, H. Muller, G. Peng, H. Michel, High resolution crystal structure of *Paracoccus denitrificans* cytochrome *c* oxidase: new insights into the active site and the proton transfer pathways. *Biochim Biophys Acta* **1787**, 635 (2009).
 126. A. Konstantinov, S. Siletsky, D. Mitchell, A. Kaulen, R. Gennis, The roles of the two proton input channels in cytochrome *c* oxidase from *Rhodobacter sphaeroides* probed by the effects of site-directed mutations on time-resolved electrogenic intraprotein proton transfer. *Proc Natl Acad Sci U S A* **94**, 9085 (1997).
 127. H. Körner, H. J. Sofia, W. G. Zumft, Phylogeny of the bacterial superfamily of Crp-Fnr transcription regulators: exploiting the metabolic spectrum by controlling alternative gene programs. *FEMS Microbiol Rev* **27**, 559 (2003).
 128. M. Kovach, R. Phillips, P. Elzer, R. Roop, K. Peterson, pBBR1MCS: a broad-host-range cloning vector. *Biotechniques* **16**, 800 (1994).
 129. M. Kovach, P. Elzer, D. Hill, G. Robertson, M. Farris, R. Roop, K. Peterson, Four new derivatives of the broad-host-range cloning vector pBBR1MCS, carrying different antibiotic-resistance cassettes. *Gene* **166**, 175 (1995).
 130. S. Koyanagi, K. Nagata, T. Tamura, S. Tsukita, N. Sone, Purification and characterization of cytochrome *c*-553 from *Helicobacter pylori*. *J Biochem* **128**, 371 (2000).
 131. R. G. Kranz, C. Richard-Fogal, J. S. Taylor, E. R. Frawley, Cytochrome *c* biogenesis: mechanisms for covalent modifications and trafficking of heme and for heme-iron redox control. *Microbiol Mol Biol Rev* **73**, 510 (2009).
 132. C. Kulajta, J. Thumfart, S. Haid, F. Daldal, H. Koch, Multi-step assembly pathway of the *cbb₃*-type cytochrome *c* oxidase complex. *J Mol Biol* **355**, 989 (2006).
 133. S. H. Kung, A. C. Retchless, J. Y. Kwan, R. P. Almeida, Effects of DNA size on transformation and recombination efficiencies in *Xylella fastidiosa*. *Appl Environ Microbiol* **79**, 1712 (2013).
 134. U. K. Laemmli, Cleavage of structural proteins during the assembly of the head of bacteriophage T4. *Nature* **227**, 680 (1970).
 135. J. Lalucat, A. Bennasar, R. Bosch, E. Garcia-Valdes, N. Palleroni, Biology of *Pseudomonas stutzeri*. *Microbiol Mol Biol Rev* **70**, 510 (2006).
 136. C. Lange, C. Hunte, Crystal structure of the yeast cytochrome *bc₁* complex with its bound substrate cytochrome *c*. *Proc Natl Acad Sci U S A* **99**, 2800 (2002).
 137. A. Lee, A. Kirichenko, T. Vygodina, S. A. Siletsky, T. K. Das, D. L. Rousseau, R. Gennis, A. A. Konstantinov, Ca²⁺-binding site in *Rhodobacter sphaeroides* cytochrome *c* oxidase.

- Biochemistry* **41**, 8886 (2002).
138. H. J. Lee, R. B. Gennis, P. Ädelroth, Entrance of the proton pathway in *cbb*₃-type heme-copper oxidases. *Proc Natl Acad Sci USA* **108**, 17661 (2011).
 139. H. M. Lee, T. K. Das, D. L. Rousseau, D. Mills, S. Ferguson-Miller, R. B. Gennis, Mutations in the putative H-channel in the cytochrome *c* oxidase from *Rhodobacter sphaeroides* show that this channel is not important for proton conduction but reveal modulation of the properties of heme *a*. *Biochemistry* **39**, 2989 (2000).
 140. F. A. Leitch, K. R. Brown, G. W. Pettigrew, Complexity in the redox titration of the dihaem cytochrome *c*₄. *Biochim Biophys Acta* **808**, 213 (1985).
 141. C. Li, A. Wen, B. Shen, J. Lu, Y. Huang, Y. Chang, FastCloning: a highly simplified, purification-free, sequence- and ligation-independent PCR cloning method. *BMC biotechnology* **11**, 92 (2011).
 142. Y. Li, A. Hopper, T. Overton, D. J. Squire, J. Cole, N. Tovell, Organization of the electron transfer chain to oxygen in the obligate human pathogen *Neisseria gonorrhoeae*: roles for cytochromes *c*₄ and *c*₅, but not cytochrome *c*₂, in oxygen reduction. *J Bacteriol* **192**, 2395 (2010).
 143. M. C. Liu, H. D. Peck, W. J. Payne, J. L. Anderson, D. V. Dervartanian, J. Legall, Purification and properties of the diheme cytochrome (cytochrome *c*-552) from *Pseudomonas perfectomarinus*. *FEBS Lett* **129**, 155 (1981).
 144. M. C. Liu, W. J. Payne, H. D. Peck, J. Legall, Comparison of cytochromes from anaerobically and aerobically grown cells of *Pseudomonas perfectomarinus*. *J Bacteriol* **154**, 278 (1983).
 145. E. Lohmeyer, S. Schröder, G. Pawlik, P.-I. Trasnea, A. Peters, F. Daldal, H.-G. Koch, The ScoI homologue SenC is a copper binding protein that interacts directly with the *cbb*₃-type cytochrome oxidase in *Rhodobacter capsulatus*. *Biochim Biophys Acta* **1817**, 2005 (2012).
 146. Y. Y. Londer, Expression of recombinant cytochromes *c* in *E. coli*. *Methods Mol Biol* **705**, 123 (2011).
 147. M. Lubben, K. Morand, Novel prenylated hemes as cofactors of cytochrome oxidases. Archaea have modified hemes A and O. *The Journal of biological chemistry* **269**, 21473 (1994).
 148. B. Ludwig, E. Bender, S. Arnold, M. Huttemann, I. Lee, B. Kadenbach, Cytochrome *c* oxidase and the regulation of oxidative phosphorylation. *ChemBiochem : a European journal of chemical biology* **2**, 392 (2001).
 149. V. M. Luna, Y. Chen, J. A. Fee, C. D. Stout, Crystallographic studies of Xe and Kr binding within the large internal cavity of cytochrome *ba*₃ from *Thermus thermophilus*: structural analysis and role of oxygen transport channels in the heme-Cu oxidases. *Biochemistry* **47**, 4657 (2008).
 150. J. A. Lyons, D. Aragão, O. Slattery, A. V. Pisljakov, T. Soulimane, M. Caffrey, Structural insights into electron transfer in *caa*₃-type cytochrome oxidase. *Nature* **487**, 514 (2012).
 151. F. MacMillan, A. Kannt, J. Behr, T. Prisner, H. Michel, Direct evidence for a tyrosine radical in the reaction of cytochrome *c* oxidase with hydrogen peroxide. *Biochemistry* **38**, 9179 (1999).
 152. E. Maklashina, G. Cecchini, The quinone-binding and catalytic site of complex II. *Biochim Biophys Acta* **1797**, 1877 (2010).
 153. K. Mandon, P. A. Kaminski, C. Mougél, N. Desnoues, B. Dreyfus, C. Elmerich, Role of

- the *fixGHI* region of *Azorhizobium caulinodans* in free-living and symbiotic nitrogen fixation. *FEMS Microbiol Lett* **114**, 185 (1993).
154. K. Mandon, P. A. Kaminski, C. Elmerich, Functional analysis of the *fixNOQP* region of *Azorhizobium caulinodans*. *J Bacteriol* **176**, 2560 (1994).
155. O. Maneg, F. Malatesta, B. Ludwig, V. Drosou, Interaction of cytochrome *c* with cytochrome oxidase: two different docking scenarios. *Biochim Biophys Acta* **1655**, 274 (2004).
156. G. D. Manetto, C. La Rosa, D. M. Grasso, D. Milardi, Evaluation of thermodynamic properties of irreversible protein thermal unfolding measured by DSC. *J Therm Anal Calorim* **80**, 263 (2005).
157. C. J. Marx, Development of a broad-host-range *sacB*-based vector for unmarked allelic exchange. *BMC research notes* **1**, 1 (2008).
158. M. W. Mather, P. Springer, S. Hensel, G. Buse, J. A. Fee, Cytochrome oxidase genes from *Thermus thermophilus*. Nucleotide sequence of the fused gene and analysis of the deduced primary structures for subunits I and III of cytochrome *caa*₃. *The Journal of biological chemistry* **268**, 5395 (1993).
159. Y. Matsumoto, T. Tosha, A. V. Pislakov, T. Hino, H. Sugimoto, S. Nagano, Y. Sugita, Y. Shiro, Crystal structure of quinol-dependent nitric oxide reductase from *Geobacillus stearothermophilus*. *Nat Struct Mol Biol* **19**, 238 (2012).
160. T. Meyer, J. Gross, C. Blanck, M. Schmutz, B. Ludwig, P. Hellwig, F. Melin, Electrochemistry of cytochrome *c*₁, cytochrome *c*₅₅₂, and Cu_A from the respiratory chain of *Thermus thermophilus* immobilized on gold nanoparticles. *J Phys Chem B* **115**, 7165 (2011).
161. H. Michel, The mechanism of proton pumping by cytochrome *c* oxidase. *P Natl Acad Sci USA* **95**, 12819 (1998).
162. H. Michel, J. Behr, A. Harrenga, A. Kannt, Cytochrome *c* oxidase: structure and spectroscopy. *Annu Rev Biophys Biomol Struct* **27**, 329 (1998).
163. H. Michel, Cytochrome *c* oxidase: catalytic cycle and mechanisms of proton pumping-- A discussion. *Biochemistry* **38**, 15129 (1999).
164. G. Miller, D. Mackay, M. Standley, S. Fields, W. Clary, R. Timkovich, Expression of *Pseudomonas stutzeri* Zobell cytochrome *c*-551 and its H47A variant in *Escherichia coli*. *Protein Expr Purif* **29**, 244 (2003).
165. G. T. Miller, B. Zhang, J. K. Hardman, R. Timkovich, Converting a *c*-type to a *b*-type cytochrome: Met61 to His61 mutant of *Pseudomonas cytochrome c*-551. *Biochemistry* **39**, 9010 (2000).
166. P. Mitchell, Coupling of phosphorylation to electron and hydrogen transfer by a chemi-osmotic type of mechanism. *Nature* **191**, 144 (1961).
167. P. Mitchell, Possible molecular mechanisms of the protonmotive function of cytochrome systems. *J Theor Biol* **62**, 327 (1976).
168. R. Mitchell, P. R. Rich, Proton uptake by cytochrome *c* oxidase on reduction and on ligand binding. *Biochim Biophys Acta* **1186**, 19 (1994).
169. G. R. Moore, G. W. Pettigrew, *Cytochromes c: evolutionary, structural, and physicochemical aspects*. (Springer-Verlag, 1990).
170. P. E. Morin, D. Diggs, E. Freire, Thermal stability of membrane-reconstituted yeast cytochrome *c* oxidase. *Biochemistry* **29**, 781 (1990).

171. D. Moss, E. Navedryk, J. Breton, W. Mantele, Redox-linked conformational changes in proteins detected by a combination of infrared spectroscopy and protein electrochemistry. Evaluation of the technique with cytochrome *c*. *Eur J Biochem* **187**, 565 (1990).
172. N. J. Mouncey, S. Kaplan, Oxygen regulation of the *ccoN* gene encoding a component of the *cbb₃* oxidase in *Rhodobacter sphaeroides* 2.4.1T: involvement of the FnrL protein. *J Bacteriol* **180**, 2228 (1998).
173. H. Myllykallio, U. Liebl, Dual role for cytochrome *cbb₃* oxidase in clinically relevant proteobacteria? *Trends in microbiology* **8**, 542 (2000).
174. K. Nagata, S. Tsukita, T. Tamura, N. Sone, A *cb*-type cytochrome-*c* oxidase terminates the respiratory chain in *Helicobacter pylori*. *Microbiology (Reading, Engl)* **142** (Pt 7), 1757 (1996).
175. J. F. Nagle, S. Tristram-Nagle, Hydrogen bonded chain mechanisms for proton conduction and proton pumping. *The Journal of membrane biology* **74**, 1 (1983).
176. A. Namslauer, A. S. Pawate, R. B. Gennis, P. Brzezinski, Redox-coupled proton translocation in biological systems: proton shuttling in cytochrome *c* oxidase. *Proc Natl Acad Sci U S A* **100**, 15543 (2003).
177. K. Narayanan, Q. Chen, Bacterial artificial chromosome mutagenesis using recombineering. *Journal of biomedicine & biotechnology* **2011**, 971296 (2011).
178. E. L. Neidle, S. Kaplan, *Rhodobacter sphaeroides rdxA*, a homolog of *Rhizobium meliloti fixG*, encodes a membrane protein which may bind cytoplasmic [4Fe-4S] clusters. *J Bacteriol* **174**, 6444 (1992).
179. D. L. Nelson, M. M. Cox, Lehninger Principles of Biochemistry. *Worth Publishers*, (2000).
180. D. P. Nelson, L. A. Kiesow, Enthalpy of decomposition of hydrogen peroxide by catalase at 25 degrees C (with molar extinction coefficients of H₂O₂ solutions in the UV). *Anal Biochem* **49**, 474 (1972).
181. K. E. Nelson, C. Weinel, I. T. Paulsen, R. J. Dodson, H. Hilbert, V. A. Martins dos Santos, D. E. Fouts, S. R. Gill, M. Pop, M. Holmes, L. Brinkac, M. Beanan, R. T. DeBoy, S. Daugherty, J. Kolonay, R. Madupu, W. Nelson, O. White, J. Peterson, H. Khouri, I. Hance, P. Chris Lee, E. Holtzapple, D. Scanlan, K. Tran, A. Moazzez, T. Utterback, M. Rizzo, K. Lee, D. Kosack, D. Moestl, H. Wedler, J. Lauber, D. Stjepandic, J. Hoheisel, M. Straetz, S. Heim, C. Kiewitz, J. A. Eisen, K. N. Timmis, A. Dusterhoft, B. Tumber, C. M. Fraser, Complete genome sequence and comparative analysis of the metabolically versatile *Pseudomonas putida* KT2440. *Environ Microbiol* **4**, 799 (2002).
182. R. T. Nelson, B. A. Pryor, J. K. Lodge, Sequence length required for homologous recombination in *Cryptococcus neoformans*. *Fungal genetics and biology : FG & B* **38**, 1 (2003).
183. J. P. O'Gara, J. M. Eraso, S. Kaplan, A redox-responsive pathway for aerobic regulation of photosynthesis gene expression in *Rhodobacter sphaeroides* 2.4.1. *J Bacteriol* **180**, 4044 (1998).
184. K. Ogawa, T. Sonoyama, T. Takeda, S.-I. Ichiki, S. Nakamura, Y. Kobayashi, S. Uchiyama, K. Nakasone, S.-I. J. Takayama, H. Mita, Y. Yamamoto, Y. Sambongi, Roles of a short connecting disulfide bond in the stability and function of psychrophilic *Shewanella violacea* cytochrome *c₅*. *Extremophiles* **11**, 797 (2007).
185. J. Oh, S. Kaplan, Oxygen adaptation. The role of the CcoQ subunit of the *cbb₃* cytochrome *c* oxidase of *Rhodobacter sphaeroides* 2.4.1. *J Biol Chem* **277**, 16220 (2002).

186. J. I. Oh, S. Kaplan, The *cbb₃* terminal oxidase of *Rhodobacter sphaeroides* 2.4.1: structural and functional implications for the regulation of spectral complex formation. *Biochemistry* **38**, 2688 (1999).
187. M. Oliveberg, B. G. Malmström, Internal electron transfer in cytochrome *c* oxidase: evidence for a rapid equilibrium between cytochrome *a* and the bimetallic site. *Biochemistry* **30**, 7053 (1991).
188. Y. Orii, K. Okunuki, Studies on Cytochrome *a*. X. Effect of hydrogen peroxide on absorption spectra of cytochrome *a*. *J Biochem* **54**, 207 (1963).
189. I. Ortiz-Martín, A. P. Macho, L. Lambersten, C. Ramos, C. R. Beuzón, Suicide vectors for antibiotic marker exchange and rapid generation of multiple knockout mutants by allelic exchange in Gram-negative bacteria. *J Microbiol Methods* **67**, 395 (2006).
190. C. Ostermeier, A. Harrenga, U. Ermler, H. Michel, Structure at 2.7 Å resolution of the *Paracoccus denitrificans* two-subunit cytochrome *c* oxidase complexed with an antibody F_V fragment. *Proc Natl Acad Sci U S A* **94**, 10547 (1997).
191. M. F. Otten, J. van der Oost, W. N. Reijnders, H. V. Westerhoff, B. Ludwig, R. J. Van Spanning, Cytochromes *c*₅₅₀, *c*₅₅₂, and *c*₁ in the electron transport network of *Paracoccus denitrificans*: redundant or subtly different in function? *J Bacteriol* **183**, 7017 (2001).
192. A. Oubrie, S. Gemeinhardt, S. Field, S. Marritt, A. J. Thomson, M. Saraste, D. J. Richardson, Properties of a soluble domain of subunit C of a bacterial nitric oxide reductase. *Biochemistry* **41**, 10858 (2002).
193. H. Ouyang, H. Han, J. H. Roh, J. Hemp, J. P. Hosler, R. B. Gennis, The functional importance of a pair of conserved glutamic acid residues and of Ca²⁺ binding in the *cbb₃*-type oxygen reductases from *Rhodobacter sphaeroides* and *Vibrio cholerae*. *Biochemistry* **51**, 7290 (2012).
194. C. C. Page, C. C. Moser, X. Chen, P. L. Dutton, Natural engineering principles of electron tunnelling in biological oxidation-reduction. *Nature* **402**, 47 (1999).
195. B. R. Palmer, M. G. Marinus, The *dam* and *dcm* strains of *Escherichia coli*--a review. *Gene* **143**, 1 (1994).
196. J. Parkhill, B. W. Wren, K. Mungall, J. M. Ketley, C. Churcher, D. Basham, T. Chillingworth, R. M. Davies, T. Feltwell, S. Holroyd, K. Jagels, A. V. Karlyshev, S. Moule, M. J. Pallen, C. W. Penn, M. A. Quail, M.-A. Rajandream, K. M. Rutherford, A. H. van Vliet, S. Whitehead, B. G. Barrell, The genome sequence of the food-borne pathogen *Campylobacter jejuni* reveals hypervariable sequences. *Nature* **403**, 665 (2000).
197. G. Pawlik, C. Kulajta, I. Sachelaru, S. Schroder, B. Waidner, P. Hellwig, F. Daldal, H. Koch, The putative assembly factor CcoH is stably associated with the *cbb₃*-type cytochrome oxidase. *J Bacteriol* **192**, 6378 (2010).
198. A. Peña, A. Busquets, M. Gomila, R. Bosch, B. Nogales, E. Garcia-Valdes, J. Lalucat, A. Bennisar, Draft Genome of *Pseudomonas stutzeri* Strain ZoBell (CCUG 16156), a Marine Isolate and Model Organism for Denitrification Studies. *Journal of Bacteriology* **194**, 1277 (2012).
199. M. Pereira, M. Santana, M. Teixeira, A novel scenario for the evolution of haem-copper oxygen reductases. *Biochim Biophys Acta* **1505**, 185 (2001).
200. M. M. Pereira, J. N. Carita, R. Anglin, M. Saraste, M. Teixeira, Heme centers of *Rhodothermus marinus* respiratory chain. Characterization of its *cbb₃* oxidase. *J Bioenerg Biomembr* **32**, 143 (2000).
201. M. M. Pereira, M. L. Verkhovskaya, M. Teixeira, M. I. Verkhovsky, The *caa₃* terminal

- oxidase of *Rhodothermus marinus* lacking the key glutamate of the D-channel is a proton pump. *Biochemistry* **39**, 6336 (2000).
202. A. Peters, C. Kulajta, G. Pawlik, F. Daldal, H. Koch, Stability of the *cbb₃*-type cytochrome oxidase requires specific CcoQ-CcoP interactions. *J Bacteriol* **190**, 5576 (2008).
203. G. W. Pettigrew, K. R. Brown, Free and membrane-bound forms of bacterial cytochrome *c₄*. *Biochem J* **252**, 427 (1988).
204. U. Pfitzner, A. Odenwald, T. Ostermann, L. Weingard, B. Ludwig, O. Richter, Cytochrome *c* oxidase (heme *aa₃*) from *Paracoccus denitrificans*: analysis of mutations in putative proton channels of subunit I. *J Bioenerg Biomembr* **30**, 89 (1998).
205. U. Pfitzner, A. Kirichenko, A. Konstantinov, M. Mertens, A. Wittershagen, B. Kolbesen, G. Steffens, A. Harrenga, H. Michel, B. Ludwig, Mutations in the Ca²⁺ binding site of the *Paracoccus denitrificans* cytochrome *c* oxidase. *FEBS Lett* **456**, 365 (1999).
206. U. Pfitzner, K. Hoffmeier, A. Harrenga, A. Kannt, H. Michel, E. Bamberg, O. Richter, B. Ludwig, Tracing the D-pathway in reconstituted site-directed mutants of cytochrome *c* oxidase from *Paracoccus denitrificans*. *Biochemistry* **39**, 6756 (2000).
207. N. Philippe, J. Alcaraz, E. Coursange, J. Geiselmann, D. Schneider, Improvement of pCVD442, a suicide plasmid for gene allele exchange in bacteria. *Plasmid* **51**, 246 (2004).
208. E. Pilet, A. Jasaitis, U. Liebl, M. H. Vos, Electron transfer between hemes in mammalian cytochrome *c* oxidase. *P Natl Acad Sci USA* **101**, 16198 (2004).
209. E. Pinakoulaki, S. Stavrakis, A. Urbani, C. Varotsis, Resonance Raman detection of a ferrous five-coordinate nitrosylheme *b₃* complex in cytochrome *cbb₃* oxidase from *Pseudomonas stutzeri*. *J Am Chem Soc* **124**, 9378 (2002).
210. R. Pitcher, T. Brittain, N. Watmough, Cytochrome *cbb₃* oxidase and bacterial microaerobic metabolism. *Biochem Soc Trans* **30**, 653 (2002).
211. R. Pitcher, M. Cheesman, N. Watmough, Molecular and spectroscopic analysis of the cytochrome *cbb₃* oxidase from *Pseudomonas stutzeri*. *J Biol Chem* **277**, 31474 (2002).
212. R. Pitcher, T. Brittain, N. Watmough, Complex interactions of carbon monoxide with reduced cytochrome *cbb₃* oxidase from *Pseudomonas stutzeri*. *Biochemistry* **42**, 11263 (2003).
213. R. Pitcher, N. Watmough, The bacterial cytochrome *cbb₃* oxidases. *Biochim Biophys Acta* **1655**, 388 (2004).
214. R. K. Poole, S. Hill, Respiratory protection of nitrogenase activity in *Azotobacter vinelandii*--roles of the terminal oxidases. *Bioscience reports* **17**, 303 (1997).
215. O. Preisig, D. Anthamatten, H. Hennecke, Genes for a microaerobically induced oxidase complex in *Bradyrhizobium japonicum* are essential for a nitrogen-fixing endosymbiosis. *Proc Natl Acad Sci U S A* **90**, 3309 (1993).
216. O. Preisig, R. Zufferey, H. Hennecke, The *Bradyrhizobium japonicum* *fixGHIS* genes are required for the formation of the high-affinity *cbb₃*-type cytochrome oxidase. *Arch Microbiol* **165**, 297 (1996).
217. O. Preisig, R. Zufferey, L. Thöny-Meyer, C. A. Appleby, H. Hennecke, A high-affinity *cbb₃*-type cytochrome oxidase terminates the symbiosis-specific respiratory chain of *Bradyrhizobium japonicum*. *J Bacteriol* **178**, 1532 (1996).
218. P. Prentki, F. Karch, S. Iida, J. Meyer, The plasmid cloning vector pBR325 contains a 482 base-pair-long inverted duplication. *Gene* **14**, 289 (1981).

219. D. A. Proshlyakov, T. Ogura, K. Shinzawa-Itoh, S. Yoshikawa, T. Kitagawa, Resonance Raman/absorption characterization of the oxo intermediates of cytochrome *c* oxidase generated in its reaction with hydrogen peroxide: pH and H₂O₂ concentration dependence. *Biochemistry* **35**, 8580 (1996).
220. D. A. Proshlyakov, M. A. Pressler, G. T. Babcock, Dioxygen activation and bond cleavage by mixed-valence cytochrome *c* oxidase. *Proc Natl Acad Sci U S A* **95**, 8020 (1998).
221. J. Qian, D. Mills, L. Geren, K. Wang, C. Hoganson, B. Schmidt, C. Hiser, G. Babcock, B. Durham, F. Millett, S. Ferguson-Miller, Role of the conserved arginine pair in proton and electron transfer in cytochrome *c* oxidase. *Biochemistry* **43**, 5748 (2004).
222. L. Qin, C. Hiser, A. Mulichak, R. Garavito, S. Ferguson-Miller, Identification of conserved lipid/detergent-binding sites in a high-resolution structure of the membrane protein cytochrome *c* oxidase. *Proc Natl Acad Sci U S A* **103**, 16117 (2006).
223. L. Qin, M. Sharpe, R. Garavito, S. Ferguson-Miller, Conserved lipid-binding sites in membrane proteins: a focus on cytochrome *c* oxidase. *Curr Opin Struct Biol* **17**, 444 (2007).
224. T. Rabilloud, Mechanisms of protein silver staining in polyacrylamide gels: a 10-year synthesis. *Electrophoresis* **11**, 785 (1990).
225. V. Rauhamäki, M. Baumann, R. Soliymani, A. Puustinen, M. Wikström, Identification of a histidine-tyrosine cross-link in the active site of the *cbb*₃-type cytochrome *c* oxidase from *Rhodobacter sphaeroides*. *Proc Natl Acad Sci USA* **103**, 16135 (2006).
226. V. Rauhamäki, D. Bloch, M. Verkhovsky, M. Wikström, Active site of cytochrome *cbb*₃. *J Biol Chem* **284**, 11301 (2009).
227. V. Rauhamäki, D. A. Bloch, M. Wikström, Mechanistic stoichiometry of proton translocation by cytochrome *cbb*₃. *Proc Natl Acad Sci USA* **109**, 7286 (2012).
228. J. Reimann, U. Flock, H. Lepp, A. Honigmann, P. Ädelroth, A pathway for protons in nitric oxide reductase from *Paracoccus denitrificans*. *Biochim Biophys Acta* **1767**, 362 (2007).
229. B. Reincke, L. Thöny-Meyer, C. Dannehl, A. Odenwald, M. Aidim, H. Witt, H. Rüterjans, B. Ludwig, Heterologous expression of soluble fragments of cytochrome *c*₅₅₂ acting as electron donor to the *Paracoccus denitrificans* cytochrome *c* oxidase. *Biochim Biophys Acta* **1411**, 114 (1999).
230. N. P. Revsbech, An oxygen microsensor with a guard cathode. *Limnol Oceanogr* **34**, 474 (1989).
231. F. E. Rey, C. S. Harwood, FixK, a global regulator of microaerobic growth, controls photosynthesis in *Rhodospseudomonas palustris*. *Mol Microbiol* **75**, 1007 (2010).
232. L. Rey, R. J. Maier, Cytochrome *c* terminal oxidase pathways of *Azotobacter vinelandii*: analysis of cytochrome *c*₄ and *c*₅ mutants and up-regulation of cytochrome *c*-dependent pathways with N₂ fixation. *J Bacteriol* **179**, 7191 (1997).
233. P. Rich, Towards an understanding of the chemistry of oxygen reduction. *Functional Plant Biology* **22**, 479 (1995).
234. D. J. Richardson, Bacterial respiration: a flexible process for a changing environment. *Microbiology* **146** (Pt 3), 551 (2000).
235. O. Richter, B. Ludwig, Electron transfer and energy transduction in the terminal part of the respiratory chain - lessons from bacterial model systems. *Biochim Biophys Acta* **1787**, 626 (2009).

236. D. L. Rousseau, S. Han, Time-resolved resonance Raman spectroscopy of intermediates in cytochrome oxidase. *Methods Enzymol* **354**, 351 (2002).
237. M. Ruitenbergh, A. Kannt, E. Bamberg, B. Ludwig, H. Michel, K. Fendler, Single-electron reduction of the oxidized state is coupled to proton uptake via the K pathway in *Paracoccus denitrificans* cytochrome *c* oxidase. *Proc Natl Acad Sci U S A* **97**, 4632 (2000).
238. L. Salomonsson, J. Reimann, T. Tosha, N. Krause, N. Gonska, Y. Shiro, P. Ädelroth, Proton transfer in the quinol-dependent nitric oxide reductase from *Geobacillus stearothermophilus* during reduction of oxygen. *Biochim Biophys Acta* **1817**, 1914 (2012).
239. J. Sambrook, D. W. Russell, *Molecular cloning : a laboratory manual*. (Cold Spring Harbor Laboratory Press, Cold Spring Harbor, N.Y., ed. 3rd, 2001).
240. C. Sanders, S. Turkarslan, D. W. Lee, F. Daldal, Cytochrome *c* biogenesis: the Ccm system. *Trends in microbiology* **18**, 266 (2010).
241. M. Saraste, J. Castresana, Cytochrome oxidase evolved by tinkering with denitrification enzymes. *FEBS letters* **341**, 1 (1994).
242. M. Saraste, Oxidative phosphorylation at the fin de siècle. *Science (New York, NY)* **283**, 1488 (1999).
243. D. Sasser, N. Lo, S. Epis, G. D'Auria, M. Montagna, F. Comandatore, D. Horner, J. Peretó, A. M. Luciano, F. Franciosi, E. Ferri, E. Crotti, C. Bazzocchi, D. Daffonchio, L. Sacchi, A. Moya, A. Latorre, C. Bandi, Phylogenomic evidence for the presence of a flagellum and *cbb₃* oxidase in the free-living mitochondrial ancestor. *Mol Biol Evol* **28**, 3285 (2011).
244. A. Savitzky, M. J. E. Golay, Smoothing + Differentiation of data by simplified least squares procedures. *Analytical chemistry* **36**, 1627 (1964).
245. E. Schäfer, N. A. Dencher, J. Vonck, D. N. Parcej, Three-dimensional structure of the respiratory chain supercomplex I₁III₂IV₁ from bovine heart mitochondria. *Biochemistry* **46**, 12579 (2007).
246. H. Schagger, G. von Jagow, Blue native electrophoresis for isolation of membrane protein complexes in enzymatically active form. *Anal Biochem* **199**, 223 (1991).
247. H. Schagger, K. Pfeiffer, Supercomplexes in the respiratory chains of yeast and mammalian mitochondria. *EMBO J* **19**, 1777 (2000).
248. A. Schlüter, T. Patschkowski, J. Quandt, L. B. Selinger, S. Weidner, M. Kramer, L. Zhou, M. F. Hynes, U. B. Priefer, Functional and regulatory analysis of the two copies of the *fixNOQP* operon of *Rhizobium leguminosarum* strain VF39. *Mol Plant Microbe Interact* **10**, 605 (1997).
249. B. Schmidt, J. McCracken, S. Ferguson-Miller, A discrete water exit pathway in the membrane protein cytochrome *c* oxidase. *Proc Natl Acad Sci U S A* **100**, 15539 (2003).
250. R. A. Scott, A. G. Mauk, *Cytochrome c : a multidisciplinary approach*. (University Science Books, Sausalito, Calif., 1996).
251. E. Sedláková, M. Fabian, N. C. Robinson, A. Musatov, Ferricytochrome *c* protects mitochondrial cytochrome *c* oxidase against hydrogen peroxide-induced oxidative damage. *Free radical biology & medicine* **49**, 1574 (2010).
252. K. L. Seib, M. P. Jennings, A. G. McEwan, A Sco homologue plays a role in defence against oxidative stress in pathogenic *Neisseria*. *FEBS Lett* **546**, 411 (2003).
253. V. Sharma, A. Puustinen, M. Wikström, L. Laakkonen, Sequence analysis of the *cbb₃*

- oxidases and an atomic model for the *Rhodobacter sphaeroides* enzyme. *Biochemistry* **45**, 5754 (2006).
254. V. Sharma, M. Wikström, L. Laakkonen, Modeling the active-site structure of the *ccb*₃-type oxidase from *Rhodobacter sphaeroides*. *Biochemistry* **47**, 4221 (2008).
255. M. Sharpe, M. Krzyaniak, S. Xu, J. McCracken, S. Ferguson-Miller, EPR evidence of cyanide binding to the Mn(Mg) center of cytochrome *c* oxidase: support for Cu_A-Mg involvement in proton pumping. *Biochemistry* **48**, 328 (2009).
256. P. Shen, H. V. Huang, Homologous recombination in *Escherichia coli*: dependence on substrate length and homology. *Genetics* **112**, 441 (1986).
257. K. Shimokata, Y. Katayama, H. Murayama, M. Suematsu, T. Tsukihara, K. Muramoto, H. Aoyama, S. Yoshikawa, H. Shimada, The proton pumping pathway of bovine heart cytochrome *c* oxidase. *Proc Natl Acad Sci U S A* **104**, 4200 (2007).
258. J. Sikorski, J. Lalucat, W. Wackernagel, Genomovars 11 to 18 of *Pseudomonas stutzeri*, identified among isolates from soil and marine sediment. *Int J Syst Evol Microbiol* **55**, 1767 (2005).
259. M. W. Silby, A. M. Cerdeno-Tarraga, G. S. Vernikos, S. R. Giddens, R. W. Jackson, G. M. Preston, X. X. Zhang, C. D. Moon, S. M. Gehrig, S. A. Godfrey, C. G. Knight, J. G. Malone, Z. Robinson, A. J. Spiers, S. Harris, G. L. Challis, A. M. Yaxley, D. Harris, K. Seeger, L. Murphy, S. Rutter, R. Squares, M. A. Quail, E. Saunders, K. Mavromatis, T. S. Brettin, S. D. Bentley, J. Hotherhall, E. Stephens, C. M. Thomas, J. Parkhill, S. B. Levy, P. B. Rainey, N. R. Thomson, Genomic and genetic analyses of diversity and plant interactions of *Pseudomonas fluorescens*. *Genome biology* **10**, R51 (2009).
260. S. A. Siletsky, A. S. Pawate, K. Weiss, R. B. Gennis, A. A. Konstantinov, Transmembrane charge separation during the ferryl-oxo → oxidized transition in a nonpumping mutant of cytochrome *c* oxidase. *J Biol Chem* **279**, 52558 (2004).
261. A. Skerra, T. G. Schmidt, Use of the Strep-Tag and streptavidin for detection and purification of recombinant proteins. *Methods in enzymology* **326**, 271 (2000).
262. A. Smith, B. Iglewski, Transformation of *Pseudomonas aeruginosa* by electroporation. *Nucleic Acids Res* **17**, 10509 (1989).
263. P. K. Smith, R. I. Krohn, G. T. Hermanson, A. K. Mallia, F. H. Gartner, M. D. Provenzano, E. K. Fujimoto, N. M. Goeke, B. J. Olson, D. C. Klenk, Measurement of protein using bicinchoninic acid. *Analytical Biochemistry* **150**, 76 (1985).
264. Y. Song, T. Hahn, I. Thompson, T. Mason, G. Preston, G. Li, L. Paniwnyk, W. Huang, Ultrasound-mediated DNA transfer for bacteria. *Nucleic Acids Res* **35**, e129 (2007).
265. T. Soulimane, G. Buse, G. P. Bourenkov, H. D. Bartunik, R. Huber, M. E. Than, Structure and mechanism of the aberrant *ba*₃-cytochrome *c* oxidase from *Thermus thermophilus*. *EMBO J* **19**, 1766 (2000).
266. F. L. Sousa, R. J. Alves, J. B. Pereira-Leal, M. Teixeira, M. M. Pereira, A bioinformatics classifier and database for heme-copper oxygen reductases. *PLoS ONE* **6**, e19117 (2011).
267. F. L. Sousa, R. J. Alves, M. A. Ribeiro, J. B. Pereira-Leal, M. Teixeira, M. M. Pereira, The superfamily of heme-copper oxygen reductases: types and evolutionary considerations. *Biochim Biophys Acta* **1817**, 629 (2012).
268. V. Srinivasan, C. Rajendran, F. Sousa, A. Melo, L. Saraiva, M. Pereira, M. Santana, M. Teixeira, H. Michel, Structure at 1.3 Å resolution of *Rhodothermus marinus* *caa*₃ cytochrome *c* domain. *J Mol Biol* **345**, 1047 (2005).

269. C. K. Stover, X. Q. Pham, A. L. Erwin, S. D. Mizoguchi, P. Warrenner, M. J. Hickey, F. S. Brinkman, W. O. Hufnagle, D. J. Kowalik, M. Lagrou, R. L. Garber, L. Goltry, E. Tolentino, S. Westbrook-Wadman, Y. Yuan, L. L. Brody, S. N. Coulter, K. R. Folger, A. Kas, K. Larbig, R. Lim, K. Smith, D. Spencer, G. K. Wong, Z. Wu, I. T. Paulsen, J. Reizer, M. H. Saier, R. E. Hancock, S. Lory, M. V. Olson, Complete genome sequence of *Pseudomonas aeruginosa* PAO1, an opportunistic pathogen. *Nature* **406**, 959 (2000).
270. J. G. Sutcliffe, Complete nucleotide sequence of the *Escherichia coli* plasmid pBR322. *Cold Spring Harbor symposia on quantitative biology* **43 Pt 1**, 77 (1979).
271. M. Svensson-Ek, J. W. Thomas, R. B. Gennis, T. Nilsson, P. Brzezinski, Kinetics of electron and proton transfer during the reaction of wild type and helix VI mutants of cytochrome *bo*₃ with oxygen. *Biochemistry* **35**, 13673 (1996).
272. D. L. Swem, C. E. Bauer, Coordination of ubiquinol oxidase and cytochrome *cbb*₃ oxidase expression by multiple regulators in *Rhodobacter capsulatus*. *J Bacteriol* **184**, 2815 (2002).
273. D. L. Swem, L. R. Swem, A. Setterdahl, C. E. Bauer, Involvement of SenC in assembly of cytochrome *c* oxidase in *Rhodobacter capsulatus*. *J Bacteriol* **187**, 8081 (2005).
274. L. R. Swem, S. Elsen, T. H. Bird, D. L. Swem, H. G. Koch, H. Myllykallio, F. Daldal, C. E. Bauer, The RegB/RegA two-component regulatory system controls synthesis of photosynthesis and respiratory electron transfer components in *Rhodobacter capsulatus*. *J Mol Biol* **309**, 121 (2001).
275. R. C. Switzer, 3rd, C. R. Merrill, S. Shifrin, A highly sensitive silver stain for detecting proteins and peptides in polyacrylamide gels. *Anal Biochem* **98**, 231 (1979).
276. C. Talbi, C. Sánchez, A. Hidalgo-Garcia, E. M. González, C. Arrese-Igor, L. Girard, E. J. Bedmar, M. J. Delgado, Enhanced expression of *Rhizobium etli cbb*₃ oxidase improves drought tolerance of common bean symbiotic nitrogen fixation. *Journal of experimental botany* **63**, 5035 (2012).
277. K. Terpe, Overview of tag protein fusions: from molecular and biochemical fundamentals to commercial systems. *Appl Microbiol Biotechnol* **60**, 523 (2003).
278. Y. Thielmann, J. Koepke, H. Michel, The ESFRI Instruct Core Centre Frankfurt: automated high-throughput crystallization suited for membrane proteins and more. *Journal of structural and functional genomics* **13**, 63 (2012).
279. P. E. Thomas, D. Ryan, W. Levin, An improved staining procedure for the detection of the peroxidase activity of cytochrome P-450 on sodium dodecyl sulfate polyacrylamide gels. *Anal Biochem* **75**, 168 (1976).
280. J. D. Thompson, T. J. Gibson, F. Plewniak, F. Jeanmougin, D. G. Higgins, The CLUSTAL_X windows interface: flexible strategies for multiple sequence alignment aided by quality analysis tools. *Nucleic Acids Res* **25**, 4876 (1997).
281. L. Thöny-Meyer, C. Beck, O. Preisig, H. Hennecke, The *ccoNOQP* gene cluster codes for a *cb*-type cytochrome oxidase that functions in aerobic respiration of *Rhodobacter capsulatus*. *Molecular microbiology* **14**, 705 (1994).
282. L. Thöny-Meyer, F. Fischer, P. Künzler, D. Ritz, H. Hennecke, *Escherichia coli* genes required for cytochrome *c* maturation. *J Bacteriol* **177**, 4321 (1995).
283. L. Thöny-Meyer, Biogenesis of respiratory cytochromes in bacteria. *Microbiol Mol Biol Rev* **61**, 337 (1997).
284. T. Tiefenbrunn, W. Liu, Y. Chen, V. Katritch, C. D. Stout, J. A. Fee, V. Cherezov, High resolution structure of the *ba*₃ cytochrome *c* oxidase from *Thermus thermophilus* in a

- lipidic environment. *PLoS ONE* **6**, e22348 (2011).
285. S. Todorovic, A. Verissimo, N. Wisitruangsakul, I. Zebger, P. Hildebrandt, M. M. Pereira, M. Teixeira, D. H. Murgida, SERR-spectroelectrochemical study of a *cbb₃* oxygen reductase in a biomimetic construct. *J Phys Chem B* **112**, 16952 (2008).
286. M. Toledo-Cuevas, B. Barquera, R. Gennis, M. Wikström, J. Garcia-Horsman, The *cbb₃*-type cytochrome *c* oxidase from *Rhodobacter sphaeroides*, a proton-pumping heme-copper oxidase. *Biochim Biophys Acta* **1365**, 421 (1998).
287. J. F. Tomb, O. White, A. R. Kerlavage, R. A. Clayton, G. G. Sutton, R. D. Fleischmann, K. A. Ketchum, H. P. Klenk, S. Gill, B. A. Dougherty, K. Nelson, J. Quackenbush, L. Zhou, E. F. Kirkness, S. Peterson, B. Loftus, D. Richardson, R. Dodson, H. G. Khalak, A. Glodek, K. McKenney, L. M. Fitzegerald, N. Lee, M. D. Adams, E. K. Hickey, D. E. Berg, J. D. Gocayne, T. R. Utterback, J. D. Peterson, J. M. Kelley, M. D. Cotton, J. M. Weidman, C. Fujii, C. Bowman, L. Watthey, E. Wallin, W. S. Hayes, M. Borodovsky, P. D. Karp, H. O. Smith, C. M. Fraser, J. C. Venter, The complete genome sequence of the gastric pathogen *Helicobacter pylori*. *Nature* **388**, 539 (1997).
288. M. J. Torres, A. Hidalgo-Garcia, E. J. Bedmar, M. J. Delgado, Functional analysis of the copy 1 of the *fixNOQP* operon of *Ensifer meliloti* under free-living micro-oxic and symbiotic conditions. *Journal of applied microbiology* **114**, 1772 (2013).
289. B. L. Trumpower, in *Frontiers of Cellular Bioenergetics*, S. Papa, F. Guerrieri, J. Tager, Eds. (Springer US, 1999), pp. 233-261.
290. T. Tsukihara, H. Aoyama, E. Yamashita, T. Tomizaki, H. Yamaguchi, K. Shinzawa-Itoh, R. Nakashima, R. Yaono, S. Yoshikawa, Structures of metal sites of oxidized bovine heart cytochrome *c* oxidase at 2.8 Å. *Science* **269**, 1069 (1995).
291. T. Tsukihara, H. Aoyama, E. Yamashita, T. Tomizaki, H. Yamaguchi, K. Shinzawa-Itoh, R. Nakashima, R. Yaono, S. Yoshikawa, The whole structure of the 13-subunit oxidized cytochrome *c* oxidase at 2.8 Å. *Science* **272**, 1136 (1996).
292. T. Tsukihara, K. Shimokata, Y. Katayama, H. Shimada, K. Muramoto, H. Aoyama, M. Mochizuki, K. Shinzawa-Itoh, E. Yamashita, M. Yao, Y. Ishimura, S. Yoshikawa, The low-spin heme of cytochrome *c* oxidase as the driving element of the proton-pumping process. *Proc Natl Acad Sci U S A* **100**, 15304 (2003).
293. S. Tsukita, S. Koyanagi, K. Nagata, H. Koizuka, H. Akashi, T. Shimoyama, T. Tamura, N. Sone, Characterization of a *cb*-type cytochrome *c* oxidase from *Helicobacter pylori*. *Journal of biochemistry* **125**, 194 (1999).
294. A. Ugidos, G. Morales, E. Rial, H. D. Williams, F. Rojo, The coordinate regulation of multiple terminal oxidases by the *Pseudomonas putida* ANR global regulator. *Environ Microbiol* **10**, 1690 (2008).
295. G. Udden, J. Bongaerts, Alternative respiratory pathways of *Escherichia coli*: energetics and transcriptional regulation in response to electron acceptors. *Biochim Biophys Acta* **1320**, 217 (1997).
296. A. Urbani, S. Gemeinhardt, A. Warne, M. Saraste, Properties of the detergent solubilised cytochrome *c* oxidase (cytochrome *cbb₃*) purified from *Pseudomonas stutzeri*. *FEBS Lett* **508**, 29 (2001).
297. J. van der Oost, C. von Wachenfeld, L. Hederstedt, M. Saraste, *Bacillus subtilis* cytochrome oxidase mutants: biochemical analysis and genetic evidence for two *aa₃*-type oxidases. *Mol Microbiol* **5**, 2063 (1991).
298. J. van der Oost, A. de Boer, J. de Gier, W. Zumft, A. Stouthamer, R. van Spanning, The

- heme-copper oxidase family consists of three distinct types of terminal oxidases and is related to nitric oxide reductase. *FEMS Microbiol Lett* **121**, 1 (1994).
299. G. C. Vanlerberghe, L. McIntosh, ALTERNATIVE OXIDASE: From Gene to Function. *Annual review of plant physiology and plant molecular biology* **48**, 703 (1997).
300. C. Varotsis, G. T. Babcock, J. A. García-Horsman, R. B. Gennis, Resonance Raman spectroscopy of the heme groups of cytochrome *cbb₃* in *Rhodobacter sphaeroides*. *The Journal of Physical Chemistry* **99**, 16817 (1995).
301. A. F. Veríssimo, F. L. Sousa, A. M. Baptista, M. Teixeira, M. M. Pereira, Thermodynamic redox behavior of the heme centers of *cbb₃* heme-copper oxygen reductase from *Bradyrhizobium japonicum*. *Biochemistry* **46**, 13245 (2007).
302. M. L. Verkhovskaya, A. García-Horsman, A. Puustinen, J. L. Rigaud, J. E. Morgan, M. I. Verkhovsky, M. Wikström, Glutamic acid 286 in subunit I of cytochrome *bo₃* is involved in proton translocation. *Proc Natl Acad Sci USA* **94**, 10128 (1997).
303. M. I. Verkhovsky, J. E. Morgan, M. Wikström, Intramolecular electron transfer in cytochrome *c* oxidase: a cascade of equilibria. *Biochemistry* **31**, 11860 (1992).
304. M. I. Verkhovsky, J. E. Morgan, A. Puustinen, M. Wikström, Kinetic trapping of oxygen in cell respiration. *Nature* **380**, 268 (1996).
305. M. I. Verkhovsky, A. Jasaitis, M. Wikström, Ultrafast haem-haem electron transfer in cytochrome *c* oxidase. *Biochim Biophys Acta* **1506**, 143 (2001).
306. M. I. Verkhovsky, A. Tuukkanen, C. Backgren, A. Puustinen, M. Wikström, Charge translocation coupled to electron injection into oxidized cytochrome *c* oxidase from *Paracoccus denitrificans*. *Biochemistry* **40**, 7077 (2001).
307. K. U. Vollack, J. Xie, E. Hartig, U. Romling, W. G. Zumft, Localization of denitrification genes on the chromosomal map of *Pseudomonas aeruginosa*. *Microbiology* **144** (Pt 2), 441 (1998).
308. K. U. Vollack, E. Hartig, H. Korner, W. G. Zumft, Multiple transcription factors of the FNR family in denitrifying *Pseudomonas stutzeri*: characterization of four *fnr*-like genes, regulatory responses and cognate metabolic processes. *Mol Microbiol* **31**, 1681 (1999).
309. C. von Ballmoos, P. Ädelroth, R. B. Gennis, P. Brzezinski, Proton transfer in *ba₃* cytochrome *c* oxidase from *Thermus thermophilus*. *Biochim Biophys Acta*, (2011).
310. I. von der Hocht, J. H. van Wonderen, F. Hilbers, H. Angerer, F. MacMillan, H. Michel, Interconversions of P and F intermediates of cytochrome *c* oxidase from *Paracoccus denitrificans*. *Proc Natl Acad Sci USA* **108**, 3964 (2011).
311. A. M. Waterhouse, J. B. Procter, D. M. Martin, M. Clamp, G. J. Barton, Jalview Version 2--a multiple sequence alignment editor and analysis workbench. *Bioinformatics* **25**, 1189 (2009).
312. V. M. Watt, C. J. Ingles, M. S. Urdea, W. J. Rutter, Homology requirements for recombination in *Escherichia coli*. *Proc Natl Acad Sci U S A* **82**, 4768 (1985).
313. R. F. Weiss, The solubility of nitrogen, oxygen and argon in water and seawater. *Deep Sea Research and Oceanographic Abstracts* **17**, 721 (1970).
314. M. Wikström, Energy-dependent reversal of the cytochrome oxidase reaction. *Proc Natl Acad Sci U S A* **78**, 4051 (1981).
315. M. Wikström, Pumping of protons from the mitochondrial matrix by cytochrome oxidase. *Nature* **308**, 558 (1984).

316. M. Wikström, Identification of the electron transfers in cytochrome oxidase that are coupled to proton-pumping. *Nature* **338**, 776 (1989).
317. M. Wikström, M. Verkhovsky, G. Hummer, Water-gated mechanism of proton translocation by cytochrome *c* oxidase. *Biochim Biophys Acta* **1604**, 61 (2003).
318. M. Wikström, M. Verkhovsky, Mechanism and energetics of proton translocation by the respiratory heme-copper oxidases. *Biochim Biophys Acta* **1767**, 1200 (2007).
319. M. Wikström, G. Hummer, Stoichiometry of proton translocation by respiratory complex I and its mechanistic implications. *Proc Natl Acad Sci USA* **109**, 4431 (2012).
320. M. K. Wikström, Proton pump coupled to cytochrome *c* oxidase in mitochondria. *Nature* **266**, 271 (1977).
321. H. J. Wing, J. Green, J. R. Guest, S. J. Busby, Role of activating region 1 of *Escherichia coli* FNR protein in transcription activation at class II promoters. *J Biol Chem* **275**, 29061 (2000).
322. B. Witholt, M. Boekhout, M. Brock, J. Kingma, H. V. Heerikhuizen, L. D. Leij, An efficient and reproducible procedure for the formation of spheroplasts from variously grown *Escherichia coli*. *Anal Biochem* **74**, 160 (1976).
323. H. Witt, V. Zickermann, B. Ludwig, Site-directed mutagenesis of cytochrome *c* oxidase reveals two acidic residues involved in the binding of cytochrome *c*. *Biochim Biophys Acta* **1230**, 74 (1995).
324. H. Witt, B. Ludwig, Isolation, analysis, and deletion of the gene coding for subunit IV of cytochrome *c* oxidase in *Paracoccus denitrificans*. *J Biol Chem* **272**, 5514 (1997).
325. H. Witt, F. Malatesta, F. Nicoletti, M. Brunori, B. Ludwig, Tryptophan 121 of subunit II is the electron entry site to cytochrome-*c* oxidase in *Paracoccus denitrificans*. Involvement of a hydrophobic patch in the docking reaction. *J Biol Chem* **273**, 5132 (1998).
326. H. Witt, F. Malatesta, F. Nicoletti, M. Brunori, B. Ludwig, Cytochrome-*c*-binding site on cytochrome oxidase in *Paracoccus denitrificans*. *Eur J Biochem* **251**, 367 (1998).
327. C. R. Woese, Bacterial evolution. *Microbiological reviews* **51**, 221 (1987).
328. J. Wu, C. E. Bauer, RegB kinase activity is controlled in part by monitoring the ratio of oxidized to reduced ubiquinones in the ubiquinone pool. *mBio* **1**, (2010).
329. D. Xia, C. A. Yu, H. Kim, J. Z. Xia, A. M. Kachurin, L. Zhang, L. Yu, J. Deisenhofer, Crystal structure of the cytochrome *bc*₁ complex from bovine heart mitochondria. *Science* **277**, 60 (1997).
330. Y. Yan, J. Yang, Y. Dou, M. Chen, S. Ping, J. Peng, W. Lu, W. Zhang, Z. Yao, H. Li, W. Liu, S. He, L. Geng, X. Zhang, F. Yang, H. Yu, Y. Zhan, D. Li, Z. Lin, Y. Wang, C. Elmerich, M. Lin, Q. Jin, Nitrogen fixation island and rhizosphere competence traits in the genome of root-associated *Pseudomonas stutzeri* A1501. *Proc Natl Acad Sci U S A* **105**, 7564 (2008).
331. V. Yankovskaya, R. Horsefield, S. Tornroth, C. Luna-Chavez, H. Miyoshi, C. Leger, B. Byrne, G. Cecchini, S. Iwata, Architecture of succinate dehydrogenase and reactive oxygen species generation. *Science* **299**, 700 (2003).
332. T. Yonetani, G. S. Ray, Studies on cytochrome *c* peroxidase. I. Purification and some properties. *J Biol Chem* **240**, 4503 (1965).
333. S. Yoshikawa, K. Shinzawa-Itoh, R. Nakashima, R. Yaono, E. Yamashita, N. Inoue, M. Yao, M. Fei, C. Libeu, T. Mizushima, H. Yamaguchi, T. Tomizaki, T. Tsukihara, Redox-coupled crystal structural changes in bovine heart cytochrome *c* oxidase. *Science*

- 280**, 1723 (1998).
334. S. Yoshikawa, K. Muramoto, K. Shinzawa-Itoh, H. Aoyama, T. Tsukihara, K. Shimokata, Y. Katayama, H. Shimada, Proton pumping mechanism of bovine heart cytochrome *c* oxidase. *Biochim Biophys Acta* **1757**, 1110 (2006).
335. M. A. Yu, T. Egawa, K. Shinzawa-Itoh, S. Yoshikawa, S.-R. Yeh, D. L. Rousseau, G. J. Gerfen, Radical formation in cytochrome *c* oxidase. *Biochim Biophys Acta* **1807**, 1295 (2011).
336. D. Zannoni, *Respiration in Archaea and Bacteria: Diversity of prokaryotic respiratory systems*. (Springer, 2010).
337. D. Zaslavsky, R. Sadoski, K. Wang, B. Durham, R. Gennis, F. Millett, Single electron reduction of cytochrome *c* oxidase compound F: resolution of partial steps by transient spectroscopy. *Biochemistry* **37**, 14910 (1998).
338. Y. Zhen, C. W. Hoganson, G. T. Babcock, S. Ferguson-Miller, Definition of the interaction domain for cytochrome *c* on cytochrome *c* oxidase. I. Biochemical, spectral, and kinetic characterization of surface mutants in subunit ii of *Rhodobacter sphaeroides* cytochrome *aa*₃. *J Biol Chem* **274**, 38032 (1999).
339. G. Zhou, J. Yin, H. Chen, Y. Hua, L. Sun, H. Gao, Combined effect of loss of the *caa*₃ oxidase and Crp regulation drives *Shewanella* to thrive in redox-stratified environments. *The ISME journal* **7**, 1752 (2013).
340. A. Zimmermann, C. Reimann, M. Galimand, D. Haas, Anaerobic growth and cyanide synthesis of *Pseudomonas aeruginosa* depend on *anr*, a regulatory gene homologous with *fnr* of *Escherichia coli*. *Mol Microbiol* **5**, 1483 (1991).
341. C. E. ZoBell, H. C. Upham, A list of marine bacteria including descriptions of sixty new species. *Bull. Scripps Inst. Oceanogr.* **5**, 239 (1944).
342. R. Zufferey, O. Preisig, H. Hennecke, L. Thöny-Meyer, Assembly and function of the cytochrome *cbb*₃ oxidase subunits in *Bradyrhizobium japonicum*. *J Biol Chem* **271**, 9114 (1996).
343. W. G. Zumft, Cell biology and molecular basis of denitrification. *Microbiol Mol Biol Rev* **61**, 533 (1997).
344. W. G. Zumft, Nitric oxide reductases of prokaryotes with emphasis on the respiratory, heme-copper oxidase type. *J Inorg Biochem* **99**, 194 (2005).

6 Appendix

A. Oligonucleotide primers

The oligonucleotide primers designed and used in this work (Table 6-1) were purchased from Eurofins MWG Operon (Ebersberg, Germany). Lyophilized primers were dissolved in nuclease-free H₂O. The stock oligos are stored in aliquots at -20°C.

Table 6-1: List of oligonucleotide primers^a.

	Oligonucleotide	Sequence (5'-3')	Description
General sequencing primers for <i>ccoNOP-1</i>	1_Seq	CCTCGGGATCATGTACTACTTC	
	2_Seq	TCGGTGGTGCGATCTTCTTC	
	3_Seq	AGCCGTCAGGGACTTCAATCG	
	12_Seq	GCAAGGTCAAGCACATCTAC	
	2_Fw	TGCTCATTACCCGTGGATGGAAGCCCATAC	
	3_Fw	ACAGCAACCAGTACCGCTACAGTTACAAG	
	4_Fw	GCCATCGGCGAAGAAGGCGTGAAGAAC	
	8_Fw	AGATCGTCCCGCTGTTCTTCCAGGACTC	
	9_Fw	CCTGGAATCCCGTTACCGCGATGAAG	
9_Rev	TTCAACCGGCTCGTTGACGGAGTCCTGG		
General sequencing primers for <i>ccoNOQP-2</i>	5_Seq	TTCTTCGGCACCATCATGAAGC	
	6_Seq	GATCAATGCGCACTTCTGGCTG	
	7_Seq	GGTAACGCATGATGGAATCGG	
	8_Seq	GATGTGCTTGGCCTTGGCCTTC	
	9_Seq	TAGAACGCCAGCGATACCAC	
	10_Seq	CGCCTGCGTAGATCGAGTAG	
	11_Seq	GGAAAGACGTGATCGGCGAAGAAGG	
	4_Fw	GCCATCGGCGAAGAAGGCGTGAAGAAC	
	10_Fw	CAACGAAGACGGCACCCCTGACCTACTCC	
	11_Fw	TCGGTGGTTGCGCACTGTTTGCCACGTC	
	3_Rev	CGACGTTCTTACGCCTTCTTCGCCGATGG	
	5_Rev	TTGGCTCCGGTCCATGGCAGACTACAC	
	6_Rev	AAACGGCGGCAAGTATGGAGAAAGCAG	
	7_Rev	GATGGCGAATTGGCGAACCACCTTATAG	
8_Rev	TCTTACGCCTTCTTCGCCGATGGCTTG		
10_Rev	GGCCTTGTCATCTCACGCTGCCATTCC		
11_Rev	AACCGGCTCGTTCACTGCGTCTGAAAAG		
General sequencing primers	bla_789_Fw	GAGTCAGGCAACTATGGATG	ampicillin resistance gene
	bla_39_Rev	AAAGGAATAAGGGCGACAC	
	T7-pro	TAATACGACTCACTATAGGG	T7 promoter
	T7-term	CTAGTTATTGCTCAGCGGT	
	Seq1 pBBR	TACGAGCCGGAAGCATAAAG	pBBR-based plasmid
	Seq2 pBBR	GGGAGGCAGACAAGGTATAG	
	Km-N	TCTGGTAAGGTTGGGAAGCCCTGCAAAG	kanamycin resistance gene
	Km-C	AGAGTCCCGCTCAGAAGAACTCGTCAAG	
	lacZ α -N	CGCGCAATTAACCCTCACTAAAGGGAAC	<i>lacZ</i> alpha gene
lacZ α -N1	AGGTTTCCCGACTGGAAAAGC		
lacZ α -C	TACGACTCACTATAGGGCGAATTGGAGC		
lacZ α -C1	GCGGGCTCTTCGCTATTAC		

6. APPENDIX

	lacZ α _C2	TGTGCTGCAAGGCGATTAAG	
	pMB1_Fw	TCGCCACCTCTGACTTGAGC	pMB1 origin
Primers used for generation of pXH-B and pXH-R	1_Fw pBBR	CCGCCCTATACCTTGTCTGC	Kan ^r and EGFP from pBBR1MCS-2-EGFP
	1_Rev pBBR	GGAAGTCCAGCGCCAGAAAC	
	1_Fw 184 H2	TGGCGCTGGACTTCCGTGATGCTGCCAACTTACTG	p15A origin from pACYC184 (pXH-B)
	1_Rev 184 H1	CAAGGTATAGGGCGGGACGATGAGCGCATTGTTAG	
	1_Fw 184 H1	CAAGGTATAGGGCGGGTGTGCTGCCAACTTACTG	p15A origin from pACYC184
	1_Rev 184 H2	TGGCGCTGGACTTCCGACGATGAGCGCATTGTTAG	
Primers used for generation of pXH-B and pXH-R	1_Fw 322 H1	CAAGGTATAGGGCGGCTTGC GGAGA AACTGTGAATG	pMB1 origin from pBR322 (pXH-R)
	1_Rev 322 H2	TGGCGCTGGACTTCCAGGTGCCTCACTGATTAAGC	
	1_Fw 322 H2	TGGCGCTGGACTTCCCTTGC GGAGA AACTGTGAATG	pMB1 origin from pBR322
	1_Rev 322 H1	CAAGGTATAGGGCGGAGGTGCCTCACTGATTAAGC	
	3181 CCW	TGCCACCTGGGATGAATGTC	linearized pXH-B, 5' insertion site
	3228 CW	TGTTTCTGGCGCTGGACTTC	
Primers used for generation of pXH- Δ I, pXH- Δ II and pXH- Δ I+II	1969 CCW	TTCATGCTGGAGTCTTCG	linearized pXH-B, 3' insertion site
	2016 CW	CGAAGCCCAACCTTTCATAG	
	3228 CW/cbb3I-F	CCAGCGCCAGAAACACTTGCAGATGGGCCACTCG	H1-flanking arm, 5' homologous regions
	3181 CCW/cbb3I-R	TCATCCAGGTGGCATGTATGGGCTTCCATCCAC	
	3228 CW/cbb3II-F	CCAGCGCCAGAAACACTCGCCGCTATGTTTACAG	H2-flanking arm, 5' homologous regions
	3181 CCW/cbb3II-R	TCATCCAGGTGGCACAGGCCATCCCAATGATTC	
	2016 CW/cbb3II-F	AAAGGTTGGGCTTCGCTCGCCGCTATGTTTACAG	H2-flanking arm, 3' homologous regions
	1969 CCW/cbb3II-R	AACTCCAGCATGAGACAGGCCATCCCAATGATTC	
	2016 CW/cbb3III-F	AAAGGTTGGGCTTCGTGATGCCTGGCTGAAAGAC	H3-flanking arm, 3' homologous regions
	1969 CCW/cbb3III-R	AACTCCAGCATGAGAGATACGTGCCAACCAGGATC	
	Cm-C SacI	AGTGAGCTCGAGGCGTTTTCGTATTGGG	Cam ^R -based suicide plasmid
	Cm-N1 Bam	CTCGGATCCAGTGCCACCTGACGTCTAAG	
	Cm-N2 Bam	CTCAGGGATCCTTCAGGAGCTAAGGAAGC	
	sacB-C SacI	AGTGAGCTCTCCTTAGCTCCTGCCCTATG	sacB-based suicide plasmid
sacB-N BamHI	CTCGGATCCAAGAAGCAGACCGCTAACAC		
Primers used for generation of pXH21-24	7_Fw (M6263)	CTTGCGAGATGGGCCACTCGAGGCTTGTG	amplification of <i>ccoNOP-1</i>
	6_Rev (M6263)	AAACGGCGGCAAGTATGGAGAAAGCAG	
	1.N Strep Fw	GAAGCCCATACATGGCTAGCTGGAGCCACCCGCAGT TCGAAAAAGGCGCCAAACACAGCAACCAG	Strep-tag II at N-terminus of <i>ccoN-1</i> (pXH21)
	1.N Strep Rev	CTGGTTGCTGTGTTGGCGCCTTTTTCGAACTGCGGGT GGCTCCAGCTAGCCATGTATGGGCTTC	
	1.C Strep Fw	CGCGCAGATCGCCAGCGCTGGAGCCACCCGCAGTT CGAAAAATGAGGAGCCTAGG	Strep-tag II at C-terminus of <i>ccoN-1</i> (pXH22)
	1.C Strep Rev	CCTAGGCTCCTCATTTTTCGAACTGCGGGTGGCTCCA AGCGCTGGCGATCTGCGCG	
	1.N His Fw	GAAGCCCATACATGGCTAGCAGAGGATCGCATCACC ATCACCATCAGGCGCCAAACACAGCAACCAG	His ₆ -tag at N-terminus of <i>ccoN-1</i> (pXH23)
	1.N His Rev	CTGGTTGCTGTGTTGGCGCCGTGATGGTGATGGTGAT GCGATCCTCTGCTAGCCATGTATGGGCTTC	
	1.C His Fw	CGCGCAGATCGCCAGAGGATCGCATCACCATCACCA TCACTGAGGAGCCTAGG	His ₆ -tag at C-terminus of <i>ccoN-1</i> (pXH24)
	1.C His Rev	CCTAGGCTCCTCAGTGATGGTGATGGTGATGCGATCC TCTGGCGATCTGCGCG	
ccoN-1-N BamHI	AGTGGATCCCAAGGCGCTCAGCCATTTTCG	cloning of <i>ccoNOP-1</i> into pBBR1MCS	
ccoP-1-C HindIII	CGTAAGCTTTCGAGAGTAGCGGAAGTTG		
Primers used for generation of pXH25-28	5_Fw (PCR101)	CGGCCTGGGGCCAAGCCATCGGCGAAG	amplification of <i>ccoNOQP-2</i>
	4_Rev (PCR101)	AGTCATCGAGTGCCTACCACGGCGGAAG	
	2.N Strep Fw	GGAAGCCTTGCATGGCTAGCTGGAGCCACCCGCAGT TCGAAAAAGGCGCCAGCACAGCAATCAG	Strep-tag II at N-terminus of <i>ccoN-2</i> (pXH25)
2.N Strep Rev	CTGATTGCTGTGCTGGCGCCTTTTTCGAACTGCGGGT GGCTCCAGCTAGCCATGCAAGGCTTCC		

	2.C Strep Fw	CCGCGCAGATCGCTAGCGCTTGGAGCCACCCGAGT TCGAAAAATGAGGAACGGATAG	Strep-tag II at C-terminus of <i>ccoN</i> -2 (pXH26)
	2.C Strep Rev	CTATCCGTTCTCATTTTTCGAACTGCGGGTGGCTCC AAGCGCTAGCGATCTGCGCGG	
	2.N His Fw	GGAAGCCTTGCATGGCTAGCAGAGGATCGCATCACC ATCACCATCACGGCGCCAGCACAGCAATCAG	His ₆ -tag at N-terminus of <i>ccoN</i> -2 (pXH27)
	2.N His Rev	CTGATTGCTGTGCTGGCGCCGTGATGGTGATGGTGAT GCGATCCTCTGCTAGCCATGCAAGGCTTCC	
	2.C His Fw	CCGCGCAGATCGCTAGAGGATCGCATCACCATCACC ATCACTGAGGAACGGATAG	His ₆ -tag at C-terminus of <i>ccoN</i> -2 (pXH28)
	2.C His Rev	CTATCCGTTCTCAGTGATGGTGATGGTGATGCGATC CTTAGCGATCTGCGCGG	
	IF <i>ccoN</i> -2-N IF <i>ccoP</i> -2-C	TAGAACTAGTGGATCTCCGCTACTCTGCGACTATC CGGTATCGATAAGCTGTCCAGCTGCGAATGGTACG	cloning of <i>ccoNOQP</i> -2 into pBBR1MCS
Primers used for generation of pXH39, promoter exchange	pXH22-Pro-N pXH22-Pro-C	GTATGGGCTTCCATCCAC ATCGATACCGTCGACCTC	promoter region from <i>ccoNOP</i> -1 (pXH22)
	IF-Pro-N IF-Pro-C	GATGGAAGCCCATACATGAGCACAGCAATCAG GTCGACGGTATCGATGTCCAGCTGCGAATGGTACG	structural genes from <i>ccoNOQP</i> -2 (pXH26)
Primers used for promoter exchange	IF-Plac-cbb3I-Fw IF-Plac-cbb3I-Rev	GCAGCCCGGGGATCATGGAAGCCCATACATGAAC TGGCGGCCGCTCTAGGCCCTTTGGGGCTCACTG	<i>lac</i> promoter
	IF-Plac-cbb3II-Fw IF-Plac-cbb3II-Rev	GCAGCCCGGGGATCCGTGGAAGCCTTGCATGAG TGGCGGCCGCTCTAGCGACCTCGAGCAATCAC	
	PCR B PCR X	GATCCCCCGGGCTGCAGG CTAGAGCGGCCGCCAC	
	Del1 Del2 Del3 Del4	CACAGGAAACAGCTATGAGCACAGCAATC GATTGCTGTGCTCATAGCTGTTCTCTGTG ATGAGCACAGCAATCAGTGAGAC AGCTGTTTCTGTGTGAAATTG	
Primers used for generation of EGFP-fused <i>Cbb</i> ₃ -1 and <i>Cbb</i> ₃ -2	22-TEV-Fw 22-TEV-Rev	GCAGATCGCCGAAAACCTGTACTTTCAAGGTCAATTC AGCGTTGGAG CTCCAAGCGCTGAATTGACCTGAAAGTACAGGTTTT CGGCGATCTGC	insertion of TEV protease cleavage site
	IF1 IF2	TTCAAGGTCAATTCGTGAGCAAGGGCGAGGAGC GTGGCTCCAAGCGCTTGTACAGCTCGTCCATGC	
	TEV1 TEV2	GAATTGACCTTGAAGTACAGGTTTTCGGCGATCTGC AGCGTTGGAGCCACCCGAGTTGAAAAATG	
	22-TEV-Fw-2 22-TEV-Rev-2	CTGCCGCGCAGATCGCCGAAAACCTGTACTTTCAAG GTCAATTCAGCGCTTGGAGCCAC GTGGCTCCAAGCGCTGAATTGACCTTGAAGTACAG GTTTTCGGCGATCTGCGCGGAG	
	L22 L2226 L26	GGCGATCTGCGCGGCAGCTCGTACTC AGCGTTGGAGCCACCCGAGTTCCG AGCGATCTGCGCGCAGTGTC	insertion of EGFP into the <i>ccoN</i> gene
	IF3-22 IF4-26 IF5	GCCGCGCAGATCGCCGAAAACCTGTACTTTCAAGGT CAATTCGTGAGCAAGGGCGAGGAGC GCCGCGCAGATCGCTGAAAACCTGTACTTTCAAGGTC AATTCGTGAGCAAGGGCGAGGAGC GTGGCTCCAAGCGCTTGTACAGCTCGTCCATGCCG AGAGTG	
Primers used for amplification of cytochrome <i>c</i> genes	C4-Fw C4-Rev	CCAGATTGGCGTGGGTACGCGTGTTCAG GGCAGCCGCTTGAATCGACATCCTCCG	cytochrome <i>c</i> ₄
	C5-Fw C5-Rev	GAGACCTATCCGCCGGTTCCGATACTG CTCGTGAGCGGTGGAGTGGTAGTGATGG	cytochrome <i>c</i> ₅
	C551-C552-Fw C551-C552-Rev	CGCACAAGATGGTGCGAAGGTAGAAGC TCGCCGAACAGCCCGCAATGTAGTAAC	cytochrome <i>c</i> ₅₅₁ + <i>c</i> ₅₅₂

6. APPENDIX

Primers used for generation of expression vectors of cytochrome <i>c</i>	C4-IF-N C4-IF-C	CCGGCGATGGCCATGGCTGGAGACGCCGAAG GCTCGAATTCGGATCACGCCCTACTGCTCAGAC	cytochrome <i>c</i> ₄
	C5-NcoI C5-BamHI	ATACCATGGCGACCGACGATGCAATC ATAGGATCCTCGACGCTCGATCAGAG	cytochrome <i>c</i> ₅
	C551-IF-N C551-IF-C	CCGGCGATGGCCATGCAAGACGGTGAAGCGCTGTTC GCTCGAATTCGGATCTCCGGAGCAGCTTACTTGAG	cytochrome <i>c</i> ₅₅₁
	C552-NcoI C552-BamHI	ATACCATGGCCGCGCCTGCCGATTGG ATAGGATCCCGGCCCGTTGCTTGCC	cytochrome <i>c</i> ₅₅₂
Primers used for mutagenesis studies of Cbb ₃ -I	E323A-Fw E323A-Rev	CATGTCGACCTTC <u>CGCG</u> GGTCCGATGATGG CCATCATCGGACC <u>CGC</u> GGAAGGTGCACATG	E323A
	E323D-Fw E323D-Rev	CATGTCGACCTTC <u>CGAC</u> GGTCCGATGATGG CCATCATCGGACC <u>GTC</u> GGAAGGTGCACATG	E323D
	E323Q-Fw E323Q-Rev	CATGTCGACCTTC <u>CCAG</u> GGTCCGATGATGG CCATCATCGGACC <u>CTG</u> GGAAGGTGCACATG	E323Q
	G211Y-Fw G211Y-Rev	CACAACGCCGTG <u>TACT</u> TCTTCCACCG CGGTGAGGAAGAA <u>GTAC</u> ACGGCGTTGTG	G211Y
	H337I-Fw H337I-Rev	CAACGCCCTGTCC <u>ATCT</u> TACACCGACTGG CCAGTCGGTGTAG <u>AT</u> TGGACAGGGCGTTG	H337I
	H337V-Fw H337V-Rev	CAACGCCCTGTCC <u>GTC</u> TACACCGACTGG CCAGTCGGTGTAG <u>AC</u> GGACAGGGCGTTG	H337V
	N333D-Fw N333D-Rev	GATCAAGACCGT <u>CGAT</u> GCCCTGTCCCAC GTGGGACAGGGC <u>ATC</u> GACGGTCTTGATC	N333D
	N333L-Fw N333L-Rev	GATCAAGACCGT <u>CTG</u> GCCCTGTCCCAC GTGGGACAGGGC <u>CAG</u> GACGGTCTTGATC	N333L
	T215V-Fw T215V-Rev	GGGCTTCTTCC <u>CTCGTC</u> GCCGGCTTCTC GAGGAAGCCGGC <u>GAC</u> GAGGAAGAAGCCC	T215V
	Y251A-Fw Y251A-Rev	CTGATCACCGT <u>CGCA</u> ATCTGGGCCG CGGCCAGAT <u>TGCG</u> ACGGTGATCAG	Y251A
	Y251F-Fw Y251F-Rev	CTGATCACCGT <u>TTC</u> ATCTGGGCCG CGGCCAGAT <u>GAA</u> GACGGTGATCAG	Y251F
	Y251G-Fw Y251G-Rev	CTGATCACCGT <u>GGT</u> ATCTGGGCCG CGGCCAGAT <u>ACC</u> GACGGTGATCAG	Y251G
	Y317F-Fw Y317F-Rev	CGCTGGCGTT <u>TTC</u> GGCATGTCGACC GGTCGACATGCC <u>GAA</u> GAACGCCAGCG	Y317F
	Y251A-I252Y-Fw Y251A-I252Y-Rev	CTGATCACCGT <u>GCATACT</u> TGGGCCGGCCCGCAC GTGCGGGCCGGCC <u>AGTATGCG</u> ACGGTGATCAG	Y251A/I252Y
	Y251G-I252Y-Fw Y251G-I252Y-Rev	CTGATCACCGT <u>GGTACT</u> TGGGCCGGCCCGCAC GTGCGGGCCGGCC <u>AGTAA</u> CCGACGGTGATCAG	Y251G/I252Y

^a The nucleotide sequence encoding the Strep-tag II (with a two amino acid linker) is shown in blue. Restriction enzymes sites are underlined. Point mutations are shown in red.

B. Predicted cytochromes *c* of *P. stutzeri*

The published genome sequences of *P. stutzeri* ZoBell were analyzed for the existence of the heme-binding motif (CXXCH). A total of 63 matches were found in 45 proteins. Of these, 16 proteins were predicted to be cytochromes *c* based on homology analyses (Table 6-2).

Table 6-2: Predicted cytochromes *c* of *P. stutzeri*^a.

Protein	Gene	UniProt ID	Location	No. of heme	MW of gene product (Da)	Protein existence
Cyt. <i>c</i> ₄	<i>cycA</i>	H7EVH9	PP, IM	2	21,718	Evidence at protein level
Cyt. <i>c</i> ₅	<i>cycB</i>	H7EWL8	PP, IM	1	13,900	Evidence at protein level
Cyt. <i>c</i> ₅₅₁	<i>nirM</i>	H7EQG5	PP	1	10,797	Evidence at protein level
Cyt. <i>c</i> ₅₅₂	<i>nirB</i>	H7EQG6	PP	2	30,426	Evidence at protein level
Cyt. <i>c</i> _{55X}	<i>nirC</i>	H7EQG4	PP	1	11,924	Inferred by homology
Tetra heme cytochrome	<i>nirT</i>	H7EQG7	IM	4	22,825	Evidence at transcript level
Cyt. <i>c</i> ?	<i>nirN</i>	H7EQH4	PP	1	55,483	Predicted
Cyt. <i>c</i> ₄	PstZobell_01147	H7EQK4	PP	2	25,175	Inferred by homology
Cyt. <i>c</i> ?	PstZobell_01752	H7EQX1	PP	2	22,448	Inferred by homology
Cyt. <i>c</i> ?	PstZobell_01757	H7EQX2	PP	2	33,487	Predicted
Cyt. <i>c</i> ?	PstZobell_08092	H7EUF9	PP	1	15,809	Predicted
Cyt. <i>c</i> ?	PstZobell_08245	H7EUI8	IM	2	30,557	Predicted
Cyt. <i>c</i> _{550?}	PstZobell_08596	H7EUQ5	PP	1	15,920	Predicted
Cyt. <i>c</i> ?	PstZobell_09337	H7EV52	?	1	16,456	Predicted
Cyt. <i>c</i> ?	PstZobell_11344	H7EW95	IM	1	28,084	Predicted
Cyt. <i>c</i> ?	PstZobell_13446	H7EXF9	IM	1	24,231	Predicted

^a Cyt, cytochrome; MW, molecular weight; IM, inner membrane; PP, periplasm.

C. Multiple sequence alignment of the central subunit of CcOs

<i>P. stutzeri</i> - cbb ₃	- - - - -	- - - - - M N	T A T S T A Y S Y K	V V R Q F A I M T V	22
<i>P. denitrificans</i> - aa ₃	M A D A A V H G H G	D H H D T R G F F T	R W F M S T N H K D	I G I L Y L F T A G	24
Bovine heart - aa ₃	- - - - -	- - - - - M F I N	R W L F S T N H K D	I G T L Y L L F G A	24
<i>T. thermophilus</i> - ba ₃	- - - - -	- M A V R A S E I S	R V Y E A Y P E K K	A T L Y F L V L G F	29
α1					
<i>P. stutzeri</i> - cbb ₃	V W G I V G M G L G	V F I A A Q - - L A	W P F L N F D - - -	- - - - -	47
<i>P. denitrificans</i> - aa ₃	I V G L I S V C F T	V Y M R M E L Q H P	G V Q Y M C L E G A	R L I A D A S A E C	80
Bovine heart - aa ₃	W A G M V G T A L S	L L I R A E L G Q P	- G T L L G D - - -	- - - - -	50
<i>T. thermophilus</i> - ba ₃	L A L I V G S L F G	P F Q A L N Y G N V	D A Y P L L K R L L	- - - - -	59
α2					
<i>P. stutzeri</i> - cbb ₃	- - L P W T S F G R	L R P L H T N A V I	F A F G G C A L F A	T S Y - Y S V Q R T	84
<i>P. denitrificans</i> - aa ₃	T P N G H L - W N V	M I T Y H G V L M M	F F V V I P A L F G	G F G N Y F M P L H	119
Bovine heart - aa ₃	- - D Q I - - Y N V	V V T A H A F V M I	F F M V M P I M I G	G F G N W L V P L M	86
<i>T. thermophilus</i> - ba ₃	- - P F V Q S Y Y Q	G L T L H G V L N A	I V F T Q L F A Q A	I M V - Y L P A R E	96
α3					
<i>P. stutzeri</i> - cbb ₃	C Q T - T L F A P K	L A A F T F W G W Q	L V I L L A A I S L	P - - - - - L G	116
<i>P. denitrificans</i> - aa ₃	I G A P D M A F P R	L N N L S Y W M Y V	C G V A L G V A S L	L A P G G N D Q M G	159
Bovine heart - aa ₃	I G A P D M A F P R	M N N M S F W L L P	P S F L L L L A S S	M V E A - - - - - G	121
<i>T. thermophilus</i> - ba ₃	L N M R - P - N M G	L M W L S W M A F	I G L V V A A L P L	L A N - - - - -	127
α4					
<i>P. stutzeri</i> - cbb ₃	F T S S K E Y A E -	- - - - -	- - - - - L - - - -	- - - - - E W P I D I	132
<i>P. denitrificans</i> - aa ₃	S G V - - G W V L Y	P P L S - - T T E A	G Y S M D L - - - -	- - - - - A I F A V H	187
Bovine heart - aa ₃	A G T - - G W T V Y	P P L A G N L A H A	G A S V D L - - - -	- - - - - T I F S L H	151
<i>T. thermophilus</i> - ba ₃	E A T V - L Y T F -	- - - - -	- - - - - Y P P L K	G H W A F Y L G A S	150
α5					
<i>P. stutzeri</i> - cbb ₃	L I T I V W V A Y A	V V F F G T L - A K	R K V - - - - K H	I Y V G N W F F G A	166
<i>P. denitrificans</i> - aa ₃	V S G A S S I L G A	I N I I T T F L N -	M R A P G M T L F K	V P L F A W S V F I	226
Bovine heart - aa ₃	L A G V S S I L G A	I N F I T T I I N -	M K P P A M S Q Y Q	T P L F V W S V M I	190
<i>T. thermophilus</i> - ba ₃	V F V L S T W V S I	Y I V L D L W - R R	W K A A - N P G K V	T P L V T Y M A V V	188
α6					
<i>P. stutzeri</i> - cbb ₃	F I L T V A I L H V	V N N L - - - E - -	I P V T A M K S Y S	L Y - - - - A G A T	197
<i>P. denitrificans</i> - aa ₃	T A W L I L L S L P	V L A G A I T M L L	M D R N F G T Q F F	D P A G G G D P V L	266
Bovine heart - aa ₃	T A V L L L L S L P	V L A A G I T M L L	T D R N L N T T F F	D P A G G G D P I L	230
<i>T. thermophilus</i> - ba ₃	F W L M W F L A S L	G L V L E A V L F L	L P W S F G L V E G	V - - - - - D P L V	223
α7					
<i>P. stutzeri</i> - cbb ₃	D A M V Q W W Y G H	N A V G F F L T A G	F L G I M Y Y F V P	K Q A - E R P V Y S	236
<i>P. denitrificans</i> - aa ₃	Y Q H I L W F F G H	P E V - Y I I I L P	G F G I I S H V I S	T F A - K K P I F G	304
Bovine heart - aa ₃	Y Q H L F W F F G H	P E V - Y I L I L P	G F G M I S H I V T	Y Y S G K K E P F G	269
<i>T. thermophilus</i> - ba ₃	A R T L F W W T G H	P I V - Y F W L L P	A Y A I I Y T I L P	K Q A - G G K L V S	261
α8					
<i>P. stutzeri</i> - cbb ₃	Y R L S I V H F W A	L I T V Y I W A G P	H H L H Y T A - L P	D W A Q S L G M V M	275
<i>P. denitrificans</i> - aa ₃	Y L P M V L A M A A	I G I L G F V V W A	H H M Y T A G - M S	L T Q Q A Y F M L A	343
Bovine heart - aa ₃	Y M G M V W A M M S	I G F L G F I V W A	H H M F T V G - M D	V D T R A Y F T S A	308
<i>T. thermophilus</i> - ba ₃	D P M A R L A F L L	F L L L S T P V G F	H H Q F A D P G I D	P T W K M I H S V L	301
α9					
<i>P. stutzeri</i> - cbb ₃	S L I L L A P S W G	G M I N G M M T L S	G A W H K L R - - -	- - - - -	302
<i>P. denitrificans</i> - aa ₃	T M T I A V P T G I	K V F S W I A T M W	G G S I E F K - - -	- - - - -	370
Bovine heart - aa ₃	T M I I A I P T G V	K V F S W L A T L H	G G N I K W S - - -	- - - - -	335
<i>T. thermophilus</i> - ba ₃	T L F V A V P S L M	T A F T V A A S L E	F A G R L R G R G	L F G W I R A L P W	341

<i>P. stutzeri</i> - cbb ₃	S D P I L R F L V V	S L A F Y G M S T F	E G P M M A I K T V	N A L S H Y T D W T	342
<i>P. denitrificans</i> - aa ₃	- - T P M L W A F G	F L F L F T V G G V	T G V V L S Q A P L	D R V Y H D T Y Y V	408
Bovine heart - aa ₃	- - P A M M W A L G	F I F L F T V G G L	T G I V L A N S S L	D I V L H D T Y Y V	373
<i>T. thermophilus</i> - ba ₃	D N P A F V A P V L	G L L G F I P G G A	G G I V N A S F T L	D Y V V H N T A W V	381
	α9			α10	
<i>P. stutzeri</i> - cbb ₃	I G H V H A G A L G	W V A M V S I G A L	Y H L V P K V F G R	- - E Q M H S I G L	380
<i>P. denitrificans</i> - aa ₃	V A H F H Y V M S L	G A V F G I F A G V	Y Y W I G K M S G R	- - - Q Y - P E W A	444
Bovine heart - aa ₃	V A H F H Y V L S M	G A V F A I M G G F	V H W F P L F S G Y	- - - T L - N D T W	409
<i>T. thermophilus</i> - ba ₃	P G H F H L Q V A S	L V T L T A M G S L	Y W L L P N L T G K	P I S D A - Q R R L	420
	α11				
<i>P. stutzeri</i> - cbb ₃	I N T H F W L A T I	G T V L Y I A S M W	V N G I A Q G L M W	R A I N D D G T L T	420
<i>P. denitrificans</i> - aa ₃	G Q L H F W M M F I	G S N L I F F P Q H	F L G R Q - G M P R	R Y I D Y P V - - -	480
Bovine heart - aa ₃	A K I H F A I M F V	G V N M T F F P Q H	F L G L S - G M P R	R Y S D Y P D - - -	445
<i>T. thermophilus</i> - ba ₃	G L A V V W L W F L	G M M I M A V G L H	W A G L L - N V P R	R A Y I A Q V P - -	457
<i>P. stutzeri</i> - cbb ₃	Y S F V E S L E A S	H P G F V V R M I G	G A I F F A G M L V	M A Y N T W R T V Q	460
<i>P. denitrificans</i> - aa ₃	- - - - - E F A Y	W N N I S S I G A Y	I S F A S F L F F I	G I V F Y T L F A G	514
Bovine heart - aa ₃	- - - - - A Y T M	W N T I S S M G S F	I S L T A V M L M V	- F I I W E A F A S	478
<i>T. thermophilus</i> - ba ₃	- - - - - D A Y P	H A A V P M V F N V	L A G I V L L V A L	L L F I Y G L F S V	491
	α12				
<i>P. stutzeri</i> - cbb ₃	A A K - - - - -	- - - - -	- - - P A E Y D A A	A Q I A - - - - -	474
<i>P. denitrificans</i> - aa ₃	K R V N V P N Y W N	E H A D T L E W T L	P S P P P E H T F E	T L P K R E D W D R	554
Bovine heart - aa ₃	K R E V L T - - V D	L T T T N L E W L N	G C P P P Y H T F E	E P - - - - - T Y	510
<i>T. thermophilus</i> - ba ₃	L L S R E R K P E -	- - - - -	- - - - - L A E A P	L P F A E V I S G P	515
<i>P. stutzeri</i> - cbb ₃	- - - - -	- - - - -	- - - - -	- - - - -	
<i>P. denitrificans</i> - aa ₃	A H A H - - - - -	- - - - -	- - - - -	- - - - -	558
Bovine heart - aa ₃	V N L K - - - - -	- - - - -	- - - - -	- - - - -	514
<i>T. thermophilus</i> - ba ₃	E D R R L V L A M D	R I G F W F A V A A	I L V V L A Y G P T	L V Q L F G H L N P	555
<i>P. stutzeri</i> - cbb ₃	- - - - -	- - - - -	- - - - -	- - - - -	
<i>P. denitrificans</i> - aa ₃	- - - - -	- - - - -	- - - - -	- - - - -	
Bovine heart - aa ₃	- - - - -	- - - - -	- - - - -	- - - - -	
<i>T. thermophilus</i> - ba ₃	V P G W R L W	- - - - -	- - - - -	- - - - -	

Figure 6-1: Multiple sequence alignment of the central subunit of the cytochrome *c* oxidases. The sequences of the central subunit of the *aa*₃-CcO from *Paracoccus denitrificans*, *aa*₃-CcO from bovine heart mitochondria, *ba*₃-CcO from *Thermus thermophilus* and *cbb*₃-CcO from *Pseudomonas stutzeri* are compared based on a structural alignment. The positions of helices α1-α12 are marked with a black line. The alignment of the connecting loops and the termini are ambiguous because of structural differences. Residues conserved in all aligned HCOs are highlight in yellow. Highly conserved residues are colored dark grey Alignments were constructed using MacVector and manually adjusted.

6. APPENDIX

		140	150	160	170	180	190	200																																																									
<i>BraJa_CcoN</i>	124	VLI	GTSLYVVGK	SCRVR	LAGD---	LAPWFV	VIGYNFF	LIAGTGYLL	GVTSK	EYAE	PEWYADLWLT	187																																																					
<i>BruSu_CcoN</i>	127	ALIC	SSFYVVRT	CRARL	FGG---	DLAWFV	FWGYQLF	IVMAATGYLL	GIQSR	EYAE	PEWYVDIWL	190																																																					
<i>ParDe_CcoN</i>	134	ALI	ATSFYVVRT	SAARL	WGG---	NAAWFV	FWGYQLF	IVLAATGYLL	GATQSK	EYAE	PEWYVDWWT	197																																																					
<i>RhoCa_CcoN</i>	126	ALI	ASAFYVVRT	SAARL	FGGT---	ALGWV	FWGWL	IVTAATSYLL	GGSQK	EYAE	PEWYLDLWLT	190																																																					
<i>RhoSp_CcoN</i>	130	ALI	ATSFYVVRT	SAARL	WGG---	NLGWV	FWGYQLF	IVLVAQSYLL	GATQSK	EYAE	PEWYLDLWLT	193																																																					
<i>NeiGo_CcoN</i>	75	GLI	GTSLYVVRT	CNTRL	FGG---	WLP	FTFWGQ	AVIVA	AVVS	FPMGW	TQK	EYAE	LEWPI	138																																																			
<i>NeiMe_CcoN</i>	75	GLI	GTSLYVVRT	CNTRL	FGG---	WLP	FTFWGQ	AVIVA	AVVS	FPMGW	TQK	EYAE	LEWPI	138																																																			
<i>CamJe_CcoN</i>	73	GIW	ATWYI	IGQR	VLVKS	MAESR	FLMAV	GLHFWL	HLVLA	IVISL	FMGV	TTSK	EYAE	LEWPL	140																																																		
<i>HelPy_CcoN</i>	73	GIW	ASWYI	IGQR	VLVKIT	YHQHP	FLKIV	GLHFWL	WILLL	ILGVI	S	L	FAGL	TQSK	EYAE	LEWPL	140																																																
<i>AzoVi_CcoN</i>	73	ALF	ATS	YVVRT	TCHTR	LISD---	SLAT	FTFWGQ	AVIVL	AVITL	PL	LGVT	TTSK	EYAE	LEWPI	136																																																	
<i>PseAe_CcoN1</i>	73	ALF	ATS	YVVRT	SQARL	LISD---	T	LAA	FTFWGQ	AVIVG	AVL	TLP	QGF	TTSK	EYAE	LEWPL	136																																																
<i>PseAe_CcoN2</i>	73	ALF	ATS	YAV	QRT	CQVRL	LFSD---	T	LAS	FTFWGQ	LVILL	LAAIS	LP	LG	T	S	SK	EYAE	LEWPI	136																																													
<i>PseFl_CcoN1</i>	72	ALF	ASS	FYSV	QRT	CQQLF	FAP---	K	I	A	FC	FWGQ	LVILL	LAAIS	LP	LG	T	S	SK	EYAE	LEWPI	135																																											
<i>PseFl_CcoN2</i>	73	ALF	ATS	YVVRT	CQTRL	LISD---	S	LAA	FTFWGQ	AVIVG	AVITL	PL	LG	T	T	S	SK	EYAE	LEWPL	136																																													
<i>PsePu_CcoN1</i>	72	ALF	ATS	YSV	QRT	CQTL	LISD---	G	LAA	FTFWGQ	LVILL	LAAIS	LP	LG	T	S	SK	EYAE	LEWPI	135																																													
<i>PsePu_CcoN2</i>	73	ALF	GT	SYVVRT	CQTRL	LISD---	S	M	A	A	FTFWGQ	AVIVG	AVITL	PL	PM	G	T	T	S	SK	EYAE	LEWPL	136																																										
<i>PseSt_CcoN1</i>	72	ALF	ATS	YSV	QRT	CQTL	LISD---	K	L	A	A	FTFWGQ	LVILL	LAAIS	LP	LG	T	S	SK	EYAE	LEWPI	135																																											
<i>PseSt_CcoN2</i>	73	ALF	ATS	YVVRT	CQARL	LFSD---	G	LAA	FTFWGQ	AVIVL	AVITL	PL	PM	G	T	T	S	SK	EYAE	LEWPI	136																																												
<i>PseSy_CcoN</i>	73	ALF	ATS	YVVRT	CQTRL	LISD---	G	LAA	FTFWGQ	AVIVG	AVITL	PL	PM	G	T	T	S	SK	EYAE	LEWPI	136																																												
<i>VibCh_CcoN</i>	76	ALF	ATS	YVVRT	CQTRL	FGG---	P	L	V	P	FTFWGQ	AVIVS	AAITL	PL	LG	T	S	G	K	EYAE	LEWPI	139																																											
		210	220	230	240	250	260	270																																																									
<i>BraJa_CcoN</i>	188	I	VWV	VYLLV	FLATI	I	K	K	E	P	H	I	F	V	A	N	W	F	L	A	F	I	V	T	I	A	V	L	H	L	G	N	N	P	A	L	P	V	S	V	F	G	---	---	S	K	S	Y	V	A	V	G	G	I	250										
<i>BruSu_CcoN</i>	191	I	VWV	YLLV	VFM	G	T	L	L	R	K	E	P	H	I	Y	V	A	N	W	F	L	S	F	I	T	I	A	M	L	H	I	N	N	L	A	I	P	V	S	F	L	G	---	---	S	K	S	V	L	F	S	G	V	253										
<i>ParDe_CcoN</i>	198	V	W	V	V	L	A	V	L	F	G	T	I	L	K	K	E	P	H	I	Y	V	A	N	W	F	L	S	F	I	V	T	I	A	M	L	H	I	N	N	L	A	I	P	V	S	F	L	G	---	---	S	K	S	V	L	F	S	G	V	260				
<i>RhoCa_CcoN</i>	191	I	VWV	YLLI	A	F	L	G	T	I	F	K	K	E	P	H	I	Y	V	A	N	W	F	L	S	F	I	V	T	I	A	M	L	H	I	N	N	L	A	I	P	V	S	I	F	G	---	---	T	S	V	L	Q	L	M	A	G	V	253						
<i>RhoSp_CcoN</i>	194	I	VWV	CYLA	A	F	L	G	T	I	K	K	E	P	H	I	Y	V	A	N	W	F	L	S	F	I	V	T	V	A	M	L	H	I	N	N	L	A	I	P	V	S	F	F	G	---	---	S	K	S	V	Q	V	F	S	G	V	256							
<i>NeiGo_CcoN</i>	139	L	V	W	V	A	I	A	I	V	F	G	T	I	A	K	K	V	K	H	I	Y	V	A	N	W	F	G	F	I	L	V	A	L	L	H	I	V	N	N	I	S	I	P	A	G	L	M	---	---	K	S	Y	P	V	S	G	A	199						
<i>NeiMe_CcoN</i>	139	L	V	W	V	A	I	A	I	V	F	G	T	I	A	K	K	I	K	H	I	Y	V	A	N	W	F	G	F	I	L	V	A	L	L	H	I	V	N	N	I	S	I	P	A	G	L	M	---	---	K	S	Y	P	V	S	G	A	199						
<i>CamJe_CcoN</i>	141	L	V	W	V	L	G	V	S	I	F	G	L	I	G	R	E	K	T	L	Y	I	S	L	W	Y	I	A	T	F	L	G	I	A	M	L	Y	L	F	N	M	V	E	P	T	Y	F	A	D	M	G	K	W	H	S	V	S	M	A	G	T	208			
<i>HelPy_CcoN</i>	141	V	A	W	V	L	G	V	N	M	F	G	S	M	S	V	R	R	E	N	T	I	Y	S	L	W	Y	I	A	T	V	G	I	A	V	M	Y	I	F	N	L	S	V	P	T	Y	F	A	D	M	G	S	V	H	S	I	S	M	S	G	S	208			
<i>AzoVi_CcoN</i>	137	V	W	V	I	T	A	V	V	F	G	T	V	I	K	K	T	K	H	I	Y	V	G	N	W	F	G	A	F	I	L	V	T	A	M	L	H	I	V	N	M	E	L	P	V	S	W	F	---	---	K	S	Y	S	L	S	G	A	197						
<i>PseAe_CcoN1</i>	137	I	V	W	I	T	A	I	V	F	G	T	I	V	K	K	V	K	H	I	Y	V	G	N	W	F	G	A	F	I	L	V	T	A	M	L	H	I	V	N	M	S	L	P	V	S	W	F	---	---	K	S	Y	S	A	S	G	A	197						
<i>PseAe_CcoN2</i>	137	V	W	V	A	A	V	V	F	G	T	L	V	K	K	V	K	H	I	Y	V	G	N	W	F	G	A	F	I	L	T	V	A	M	L	H	I	V	N	L	E	L	P	V	T	F	---	---	K	S	Y	S	L	Y	A	G	A	197							
<i>PseFl_CcoN1</i>	136	I	V	W	V	A	I	V	F	G	T	I	M	K	K	T	K	H	I	Y	V	G	N	W	F	G	A	F	I	T	V	A	L	H	I	V	N	L	E	L	P	V	S	F	---	---	K	S	Y	S	V	Y	A	G	A	196									
<i>PseFl_CcoN2</i>	137	I	V	W	V	T	G	L	V	F	G	T	I	T	K	K	T	K	H	I	Y	V	G	N	W	F	G	A	F	I	V	T	A	M	L	H	I	V	N	M	S	L	P	V	S	L	---	---	K	S	Y	S	A	S	G	A	197								
<i>PsePu_CcoN1</i>	136	I	V	W	V	G	A	I	V	F	G	T	L	M	K	N	T	K	H	I	Y	V	G	N	W	F	G	A	F	I	L	T	V	A	L	L	H	I	V	N	L	E	L	P	V	S	L	---	---	K	S	Y	S	V	Y	A	G	A	196						
<i>PsePu_CcoN2</i>	137	I	V	W	V	T	G	L	V	F	G	T	I	V	K	K	T	K	H	I	Y	V	G	N	W	F	G	A	F	I	V	T	A	M	L	H	I	V	N	H	I	S	L	P	V	S	L	---	---	K	S	Y	S	A	S	G	A	197							
<i>PseSt_CcoN1</i>	136	I	V	W	V	A	A	V	V	F	G	T	L	A	K	K	V	K	H	I	Y	V	G	N	W	F	G	A	F	I	L	T	V	A	L	H	V	N	L	E	L	P	V	T	A	M	---	---	K	S	Y	S	L	Y	A	G	A	196							
<i>PseSt_CcoN2</i>	137	L	V	W	V	S	I	A	V	F	G	T	I	M	K	K	A	K	H	I	Y	V	G	N	W	F	G	A	F	I	L	T	A	M	L	H	I	V	N	L	E	L	P	V	S	L	---	---	K	S	Y	S	I	Y	A	G	A	197							
<i>PseSy_CcoN</i>	137	I	V	W	A	A	A	V	V	F	G	T	I	V	K	R	T	R	H	I	Y	V	A	N	W	F	G	A	F	I	V	T	G	M	L	H	I	V	N	H	I	S	L	P	V	S	L	---	---	K	S	Y	S	A	Y	A	G	A	197						
<i>VibCh_CcoN</i>	140	A	V	W	V	A	A	V	V	F	G	T	L	V	K	K	T	S	H	I	Y	V	A	N	W	F	G	A	F	I	T	V	A	L	H	I	V	N	S	M	A	L	P	V	S	M	G	---	---	K	S	Y	S	I	Y	A	G	A	200						
		280	290	300	310	320	330																																																										
<i>BraJa_CcoN</i>	251	Q	D	A	M	F	W	W	Y	G	H	N	A	G	F	F	L	T	A	G	F	L	A	I	M	Y	F	I	P	K	R	A	E	R	P	I	Y	S	R	L	S	I	H	F	W	A	L	I	F	L	Y	I	W	A	G	P	H	H	L	H	Y	T	A	L	318
<i>BruSu_CcoN</i>	254	Q	D	A	V	T	Q	W	W	Y	G	H	N	A	V	F	F	L	T	V	P	F	L	A	M	Y	F	I	P	K	Q	A	N	R	P	V	Y	S	R	L	S	I	V	H	F	W	S	I	F	L	Y	I	W	A	G	P	H	H	L	H	Y	T	A	V	321
<i>ParDe_CcoN</i>	261	Q	D	A	M	T	Q	W	W	Y	G	H	N	A	V	F	F	L	T	A	G	F	L	G	M	Y	F	I	P	K	Q	A	E	R	P	V	Y																												

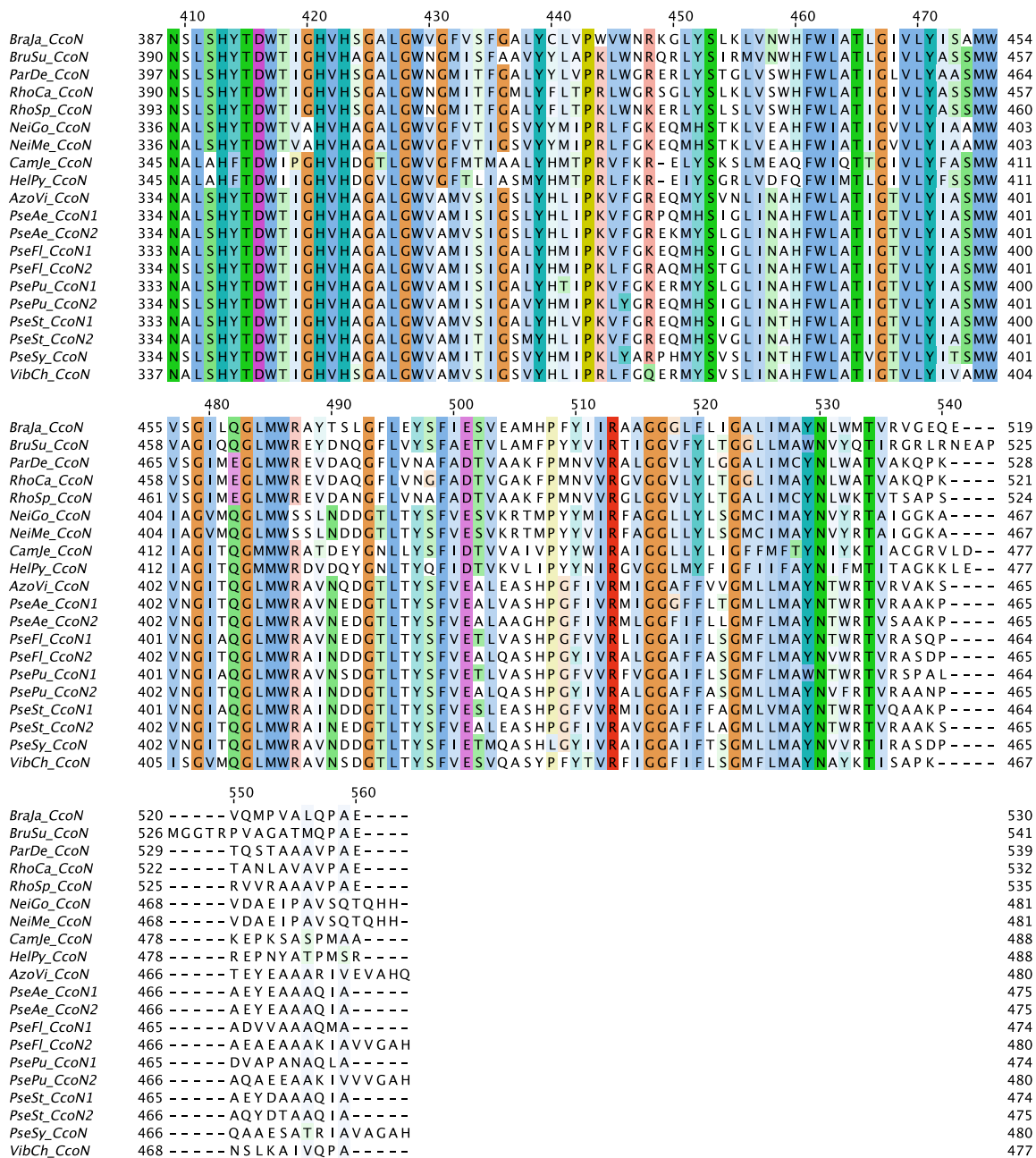


Figure 6-2: Multiple sequence alignment of the CcoN subunit of *cbb3*-CcOs. The alignment was generated using the ClustalW method with Jalview software. Amino acids are colored according to the standard Clustal color scheme. Color intensity reflects the degree of conservation at each position in the alignment.

E. Multiple sequence alignment of the CcoO subunit of *ccb₃*-CcoOs

Table 6-4: List of the sequences used for the multiple sequence alignment in Figure 6-3.

Phylum	Bacteria	Abbreviation CcoO subunit	Accession No.
α-Proteobacteria	<i>Bradyrhizobium japonicum</i> USDA 6	<i>BraJa_CcoO</i>	YP_005611847.1
	<i>Brucella suis</i> ATCC 23445	<i>BruSu_CcoO</i>	YP_001627053.1
	<i>Paracoccus denitrificans</i> PD1222	<i>ParDe_CcoO</i>	YP_915640.1
	<i>Rhodobacter capsulatus</i> SB 1003	<i>RhoCa_CcoO</i>	YP_003577323.1
	<i>Rhodobacter sphaeroides</i> 2.4.1	<i>RhoSp_CcoO</i>	YP_353772.1
β-Proteobacteria	<i>Neisseria gonorrhoeae</i> FA 1090	<i>NeiGo_CcoO</i>	YP_208433.1
	<i>Neisseria meningitidis</i> MC58	<i>NeiMe_CcoO</i>	NP_274727.1
ε-Proteobacteria	<i>Campylobacter jejuni</i> NCTC 11168	<i>CamJe_CcoO</i>	YP_002344869.1
	<i>Helicobacter pylori</i> 26695	<i>HelPy_CcoO</i>	NP_206944.1
γ-Proteobacteria	<i>Azotobacter vinelandii</i> DJ	<i>AzoVi_CcoO</i>	YP_002799182.1
	<i>Pseudomonas aeruginosa</i> PAO1	<i>PseAe_CcoO1</i>	NP_250244.1
		<i>PseAe_CcoO2</i>	NP_250247.1
	<i>Pseudomonas fluorescens</i> Pf0-1	<i>PseFl_CcoO1</i>	YP_347558.1
		<i>PseFl_CcoO2</i>	YP_347554.1
	<i>Pseudomonas putida</i> KT2440	<i>PsePu_CcoO1</i>	NP_746367.1
		<i>PsePu_CcoO2</i>	NP_746372.1
	<i>Pseudomonas stutzeri</i> ZoBell	<i>PseSt_CcoO1</i>	ADJ00001.1
		<i>PseSt_CcoO2</i>	ADJ00004.1
	<i>Pseudomonas syringae</i> pv. <i>syringae</i> B728a	<i>PseSy_CcoO</i>	YP_236484.1
	<i>Vibrio cholerae</i> O1 N16961	<i>VibCh_CcoO</i>	NP_231084.1

		10	20	30	40	50	60	
<i>BraJa_CcoO</i>	1	M S F W T R	-- H Q I F E K N S I V L I V G I L L V I A I	G G L V E I T P L F Y L K S T I E A V D G V R P Y T P L E L A G R N V Y V R E	66			
<i>BruSu_CcoO</i>	1	-----	----- M V T V G G L V E I A P L F Y L E N T I E K V E G M R P Y S P L E L A G R D I Y V R E	43				
<i>ParDe_CcoO</i>	1	M A I L E K	-- H K V L E K N A T L L L V F S F L V V T I G G I V E I A P L F Y L Q N T I E K V Q G M R P Y T P L E L K G R D I Y V R E	66				
<i>RhoCa_CcoO</i>	1	M S I M D K	-- H H V L E K N A T L L L I F A F L V V T I G G I V E I A P L F Y L E N T I E K V E G M R P Y T P L E L T G R D I Y I R E	66				
<i>RhoSp_CcoO</i>	1	M G I L A K	-- H K I L E T N A T L L L I F S F F V V T I G G L V Q I V P L F Y L E N T I E K V E G V R P Y T P L E L A G R D I Y I R E	66				
<i>NeiGo_CcoO</i>	1	M K L	---- Q Q L A E E K I G V L I V F T L L V V S V G L L I E V V P L A F T K A A T Q P A P G V K P Y N A L Q V A G R D I Y I R E	63				
<i>NeiMe_CcoO</i>	1	M K L	---- Q Q L A E E K I G V L I V F T L L V V S V G L L I E V V P L A F T K A A T Q P A P G V K P Y N A L Q V A G R D I Y I R E	63				
<i>CamJe_CcoO</i>	1	-----	M F S W L E K N P F F F A V A V F V V I A Y A G I V E V L P N F A E N A R -- P I E G K K P Y T V L Q L A G R A V Y I K D	59				
<i>HelPy_CcoO</i>	1	-----	M F S F L E K N P F F F T L A F I F V F A I A G L V E I L P N F F K S A R -- P I E G L R P Y T V L E T A G R Q I Y I Q E	59				
<i>AzoVi_CcoO</i>	1	M K	---- H E T L E K N I G L L G L F M V A A V S I G G L T Q I V P L F F Q D V N E P V E G M K P Y T A L Q L E G R D I Y I K E	62				
<i>PseAe_CcoO1</i>	1	M K N	---- H E I L E K N V G L L A I F M V I A V S I G G L T Q I V P L F F Q D V T N T P V E G M K P R T A L E L E G R D I Y I R E	63				
<i>PseAe_CcoO2</i>	1	M K	---- H E I L E K N V G L L A L C M A V A V S I G G L T Q I V P L F F Q D V T N T P V E G M K P Y T A L Q L E G R D I Y I R E	62				
<i>PseFl_CcoO1</i>	1	M K	---- H E T I E K N V G L L M L L M V F A V S I G G L T Q I V P L F F Q D V T N K P V E G M K P Y T A L Q L E G R D I Y I R E	62				
<i>PseFl_CcoO2</i>	1	M K	---- H E A V E K N I G L L A F F M V I A V S V G G L T Q I V P L F F Q D V T N K P V E G M K P R T A L E L E G R D V Y I A N	62				
<i>PsePu_CcoO1</i>	1	M K	---- H E V I E K N V G L M L L M V F A V S I G G L T Q I V P L F F Q D V T N K P V E G M K P Y T A L Q L E G R D I Y I R E	62				
<i>PsePu_CcoO2</i>	1	M K	---- H E A V E K N I G L L A F F M V I A V S V G G L T Q I V P L F F Q D V T N K P V E G M K P R T A L E V E G R D I Y I R E	62				
<i>PseSt_CcoO1</i>	1	M K S	---- H E K L E K N V G L L T L F M I L A V S I G G L T Q I V P L F F Q D S V N E P V E G M K P Y T A L Q L E G R D L Y I R E	63				
<i>PseSt_CcoO2</i>	1	M K N	---- H E I L E K N I G L L T L F M I L A V S I G G L T Q I V P L F F Q D A V N E P V E G M K P Y T A L Q L E G R D L Y I R E	63				
<i>PseSy_CcoO</i>	1	M K	---- H D A L E K N I G L L A V F M V I A V S I G G L T Q I V P L F F Q D V T N Q P V E G M K P R S A L E V E G R D V F I A N	62				
<i>VibCh_CcoO</i>	1	M S S N S N N R H E L L E R N V G L L A I F I V F A I S W G A L V E I T P L I F Q K Q T T E V Q N L K P Y T A L Q L E G R D I Y I R E	68					
		70	80	90	100	110	120	130
<i>BraJa_CcoO</i>	67	G C Y L C H S Q M I R P L R D E V E R Y G H F S L A A E S M Y D H P F Q W G S K R T G P D L A R V G A K Y S D D W H V T H L T N P R A I	134					
<i>BruSu_CcoO</i>	44	G C Y L C H S Q M I R P F R D E V E R Y G H Y S L A A E S M Y D H S F Q W G S K R T G P D L A R V G G R Y S N E W H V Q H L V R P R D V	111					
<i>ParDe_CcoO</i>	67	G C Y V C H S Q M I R P M R D E V E R Y G H Y S L A A E S M Y D H P F Q W G S K R T G P D L A R V G G R Y S D E W H L D H L V D P Q A V	134					
<i>RhoCa_CcoO</i>	67	G C Y V C H S Q M I R P M R D E V E R Y G H Y S L A A E S M Y D H P F Q W G S K R T G P D L A R V G G R Y S D A W H V E H L S N P Q S V	134					
<i>RhoSp_CcoO</i>	67	G C Y V C H S Q M I R P M R D E T E R Y G H Y S L A A E S M Y D H P F Q W G S K R T G P D L A R V G E R Y S D E W H V D H L T N P Q S V	134					
<i>NeiGo_CcoO</i>	64	G C Y N C H S Q M I R P F R A E T E R Y G H Y S V A G E S V Y D H P F Q W G S K R T G P D L A R V G G R Y S D E W H R I H L L N P R D V	131					
<i>NeiMe_CcoO</i>	64	G C Y N C H S Q M I R P F R A E T E R Y G H Y S V A G E S V Y D H P F Q W G S K R T G P D L A R V G G R Y S D E W H R I H L L N P R D V	131					
<i>CamJe_CcoO</i>	60	S N A C H S Q L I R P F K S E T D R Y G M Y S V G E F A Y D R P F L W G S K R T G P D L A R V G N Y R T A D W H E N H M W D P T S V	127					
<i>HelPy_CcoO</i>	60	G C Y H C H S Q L I R P F Q A E V D R Y G A Y S L S G E Y A Y D R P F L W G S K R I G P D L H R V G D Y R T D W H E K H M F D P K S V	127					
<i>AzoVi_CcoO</i>	63	G C V S C H S Q M V R P F R A E T E R Y G H Y S V A G E S V W D H P F L W G S K R T G P D L A R V G G R Y S D D W H R A H L Y N P R N V	130					
<i>PseAe_CcoO1</i>	64	G C V G C H S Q M V R P F R A E T E R Y G H Y S V A G E S V W D H P F L W G S K R T G P D L A R V G G R Y S D D W H R A H L Y N P R N V	131					
<i>PseAe_CcoO2</i>	63	G C V G C H S Q M I R P F R A E T E R Y G H Y S V A G E S V W D H P F L W G S K R T G P D L A R V G S R Y S D D W H R A H L F N P R N V	130					
<i>PseFl_CcoO1</i>	63	G C V G C H S Q M I R P F R A E T E R Y G H Y S V A G E S V W D H P F L W G S K R T G P D L A R V G A R Y S D D W H R A H L Y N P R N V	130					
<i>PseFl_CcoO2</i>	63	G C V G C H S Q M I R P F R A E T E R Y G H Y S V A G E S V W D H P F L W G S K R T G P D L A R V G G R Y S D D W Q R A H L Y N P R N V	130					
<i>PsePu_CcoO1</i>	63	G C V G C H S Q M I R P F R A E T E R Y G H Y S V A G E S V W D H P F L W G S K R T G P D L A R V G G R Y S D D W H R A H L Y N P R N V	130					
<i>PsePu_CcoO2</i>	63	G C V G C H S Q M I R P F R A E T E R Y G H Y S V A G E S V W D H P F L W G S K R T G P D L A R V G G R Y S D D W H R A H L Y N P R N V	130					
<i>PseSt_CcoO1</i>	64	G C V G C H S Q M I R P F R A E T E R Y G H Y S V A G E S V Y D H P F L W G S K R T G P D L A R V G G R Y S D D W H R A H L Y N P R N V	131					
<i>PseSt_CcoO2</i>	64	G C V G C H S Q M I R P F R A E T E R Y G H Y S V A G E S V Y D H P F L W G S K R T G P D L A R V G G R Y S D D W H R A H L Y N P R N V	131					
<i>PseSy_CcoO</i>	63	G C V G C H S Q M I R P L R A E T E R Y G H Y S V A G E S V W D H P F L W G S K R T G P D L A R I G G R Y S D E W H R V H L N N P R D L	130					
<i>VibCh_CcoO</i>	69	G C N V C H S Q M V R P F R S E T E R Y G H Y S V A G E S V W E H P F L W G S K R T G P D L A R V G G R Y S D E W H R V H L L N P R E L	136					

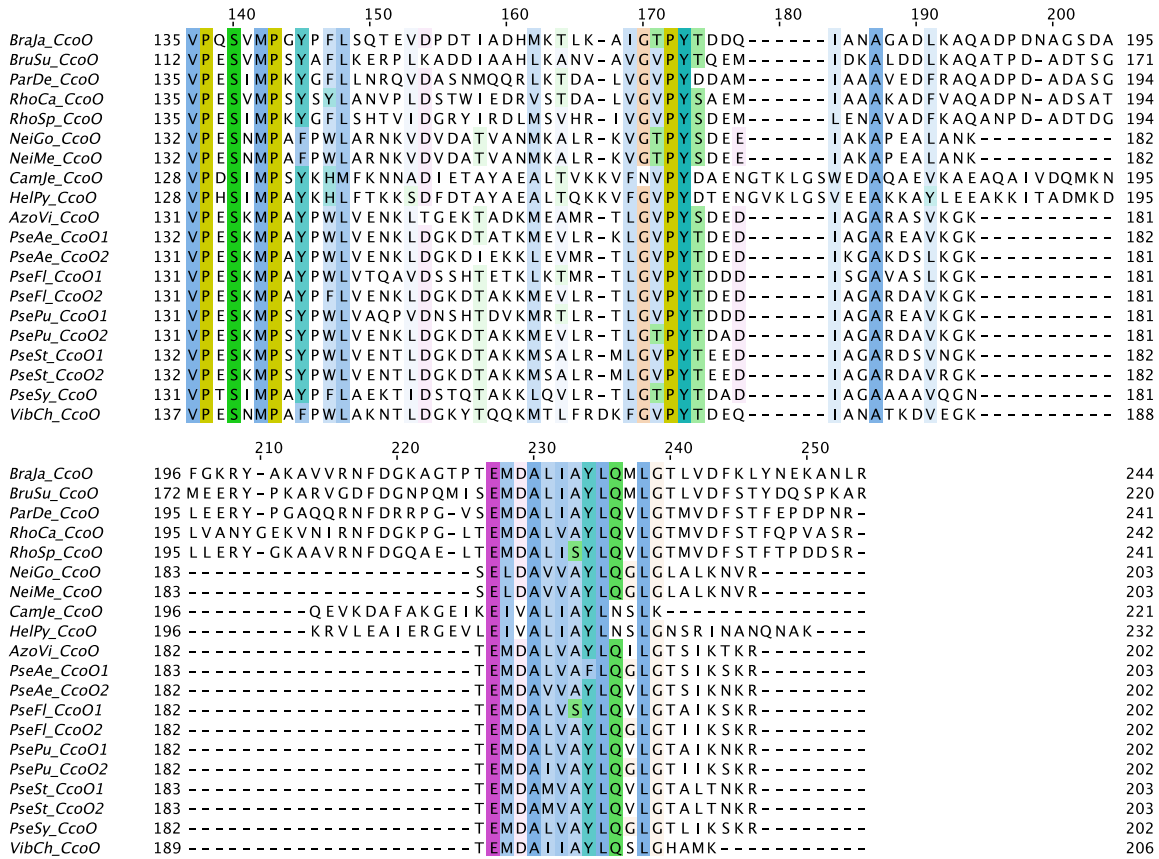


Figure 6-3: Multiple sequence alignment of the CcoO subunit of *cbb3*-CcOs. The alignment was generated using the ClustalW method with Jalview software. Amino acids are colored according to the standard Clustal color scheme. Color intensity reflects the degree of conservation at each position in the alignment.

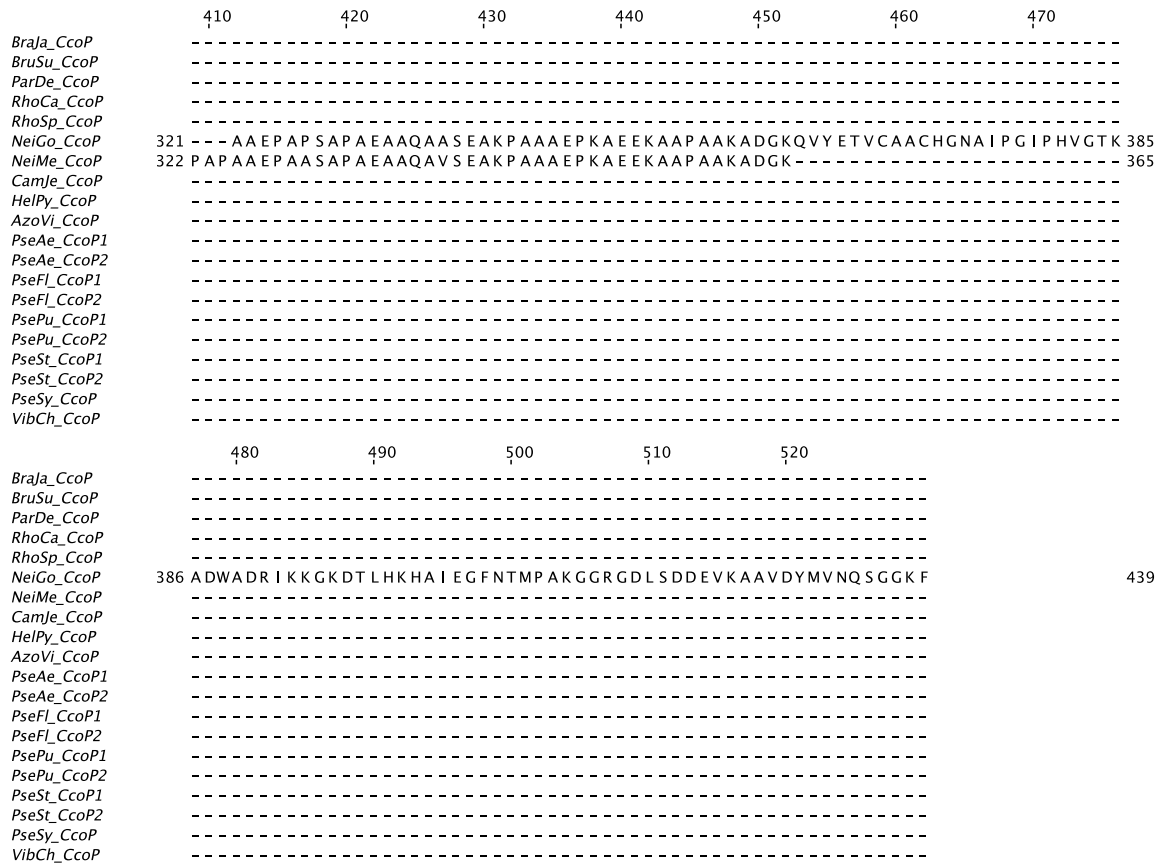


Figure 6-4: Multiple sequence alignment of the CcoP subunit of *cbb*₃-CcOs. The alignment was generated using the ClustalW method with Jalview software. Amino acids are colored according to the standard Clustal color scheme. Color intensity reflects the degree of conservation at each position in the alignment.

G. Multiple sequence alignment of the CcoQ subunit of *cbb₃*-CcOs

Table 6-6: List of the sequences used for the multiple sequence alignment in Figure 6-5.

Phylum	Bacteria	Abbreviation CcoP subunit	Accession No.
α-Proteobacteria	<i>Bradyrhizobium japonicum</i> USDA 6	<i>BraJa_CcoQ</i>	YP_005611846.1
	<i>Brucella suis</i> ATCC 23445	<i>BruSu_CcoQ</i>	YP_001627052.1
	<i>Paracoccus denitrificans</i> PD1222	<i>ParDe_CcoQ</i>	YP_915639.1
	<i>Rhodobacter capsulatus</i> SB 1003	<i>RhoCa_CcoQ</i>	YP_003577324.1
	<i>Rhodobacter sphaeroides</i> 2.4.1	<i>RhoSp_CcoQ</i>	YP_353771.1
β-Proteobacteria	<i>Neisseria gonorrhoeae</i> FA 1090	<i>NeiGo_CcoQ</i>	YP_208432.1
	<i>Neisseria meningitidis</i> 053442	<i>NeiMe_CcoQ</i>	YP_001599742.1
ε-Proteobacteria	<i>Helicobacter pylori</i> 26695	<i>HelPy_CcoQ</i>	NP_206945.1
γ-Proteobacteria	<i>Azotobacter vinelandii</i> DJ	<i>AzoVi_CcoQ</i>	YP_002799181.1
	<i>Pseudomonas aeruginosa</i> PAO1	<i>PseAe_CcoQ1</i>	YP_003933610.1
		<i>PseAe_CcoQ2</i>	YP_003933611.1
	<i>Pseudomonas fluorescens</i> Pf0-1	<i>PseFl_CcoQ1</i>	YP_347557.1
		<i>PseFl_CcoQ2</i>	YP_347553.1
	<i>Pseudomonas putida</i> KT2440	<i>PsePu_CcoQ1</i>	NP_746368.1
		<i>PsePu_CcoQ2</i>	NP_746373.1
	<i>Pseudomonas stutzeri</i> ZoBell	<i>PseSt_CcoQ</i>	ADJ00005.1
	<i>Pseudomonas syringae</i> pv. <i>syringae</i> B728a	<i>PseSy_CcoQ</i>	YP_236485.1
	<i>Vibrio cholerae</i> O1 N16961	<i>VibCh_CcoQ</i>	NP_231083.1

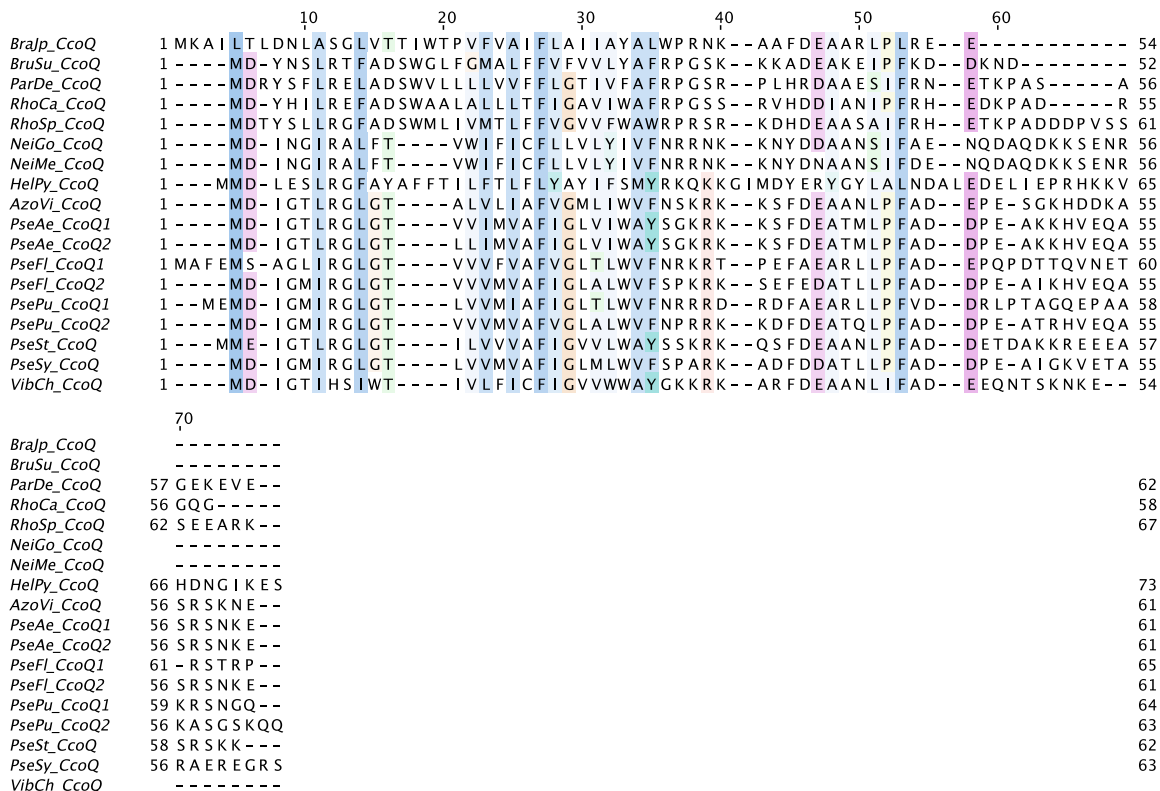


Figure 6-5: Multiple sequence alignment of the CcoQ subunit of *cbb₃*-CcOs. The alignment was generated using the ClustalW method with Jalview software. Amino acids are colored according to the standard Clustal color scheme. Color intensity reflects the degree of conservation at each position in the alignment.

H. Suppliers

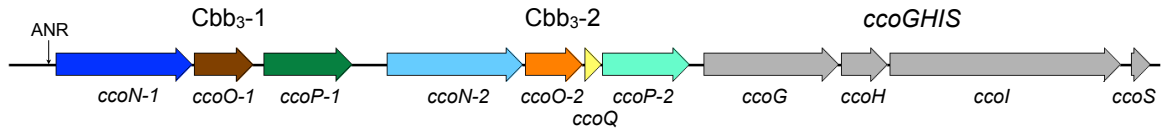
All suppliers and their products and services are listed in Table 6-7.

Table 6-7: List of suppliers and their products and services.

Supplier	Product / Service	Location
Adolf Kühner (Kühner AG)	Lab-Shaker, Lab-Therm	Birsfelden, CH
Agilent Technologies	Molecular biology products	Böblingen, DE
Alfa Aesar	Research chemicals	Karlsruhe, DE
AppliChem	Research chemicals	Darmstadt, DE
Bandelin Sonorex	Sonification bath RK 255 S	Mörfelden-Walldorf, DE
Beckman Coulter	Centrifuge Avanti J-26XP, Ultracentrifuge Optima L-90K, Ultracentrifuge L8-70M	Krefeld, DE
Berthold Technologies	Microplate multimode reader Trista LB 941	Bad Wildbad, DE
Biohit (Sartorius)	mLINE 8-channel pipettor (m300, m10)	Helsinki, FI
Biometra	Membrane vacuum pump MP40, Geldryer Mididry D62, T11 transilluminator, T-Gradient thermocycler	Göttingen, DE
Biomol	Cytochrome <i>c</i> (quine heart)	Hamburg, DE
Bio-Rad	Power supply (PowerPac HC, PowerPac Basic), Gel Doc system	München, DE
BRAND	Laboratory glassware, UV-Cuvette micro	Wertheim, DE
Bruker	Mass spectrometer maXis, Mass spectrometer micrOTOF-Q-II, FTIR spectrometer Vertex 70	Billerica, MA, US
Carl Roth	General laboratory consumables and chemicals	Karlsruhe, DE
Clontech	In-Fusion Cloning Kit	Mountain View, CA, US
Du Pont Instruments	Refrigerated superspeed centrifuge Sorvall RC-5B	Bad Homburg v. d. Höhe, DE
Epicentre	Molecular biology products	Madison, WI, US
Eppendorf	Centrifuge (5415D, 5424, 5417R), Thermomixer (comfort, compact), Multipette plus	Hamburg, DE
Eurofins MWG Operon	DNA sequencing, Oligonucleotide synthesis	Ebersberg, DE
Fermentas (Thermo Fisher Scientific)	Molecular biology products	Vilnius, LT
Finnzymes (Thermo Fisher Scientific)	Molecular biology products	Schwerte, DE
Fluka (Sigma-Aldrich)	Research chemicals	Seelze, DE
GE Healthcare Life Sciences (Formerly Amersham Biosciences)	ÄKTA Prime chromatography system, ÄKTA Purifier chromatography system, Chelating Sepharose Fast Flow resin, PBE 94, PD-10 desalting column, Q Sepharose High Performance resin	München, DE
GERBU Biotechnik GmbH	Research chemicals	Heidelberg, DE
GFL	Orbital-Rocking shaker 3011	Burgwedel, DE
Gilson	Pipetman pipettes, Microman pipettes	Middleton, WI, US
GLYCON Biochemicals	Detergents	Luckenwalde, DE
Hamilton	Precision syringes, Gastight syringes	Bonaduz, CH
Hansatech	Oxygraph oxygen electrode system	King's Lynn, UK
Heidolph	Magnetic stirrer (MR Hei-mix L, MR3000)	Schwabach, DE
Hellma Analytics	Cuvettes	Müllheim, DE

Heraeus (Thermo Fisher Scientific)	Incubator BK-600	Schwerte, DE
Hirschmann-Laborgeräte	Pipetus	Eberstadt, DE
IBA	Strep-Tactin Superflow high capacity resin	Göttingen, DE
IKA	Magnetic stirrer IKAMAG RCT basic, Homogenizer Ultra-Turrax T25 basic	Staufen, DE
Infors-HT	Shaker CH-4103	Bottmingen, CH
Invitrogen	i-Blot Blotting system, Novex Semi-Dry Blotter, Novex gel system (NuPAGE and NativePAGE)	Karlsruhe, DE
iNtRON	Genomic DNA Extraction Kit	Jungwon-gu, KR (South)
Julabo	Incubator Biotherm 37	Seelbach, DE
Jasco	Jasco J-810 spectropolarimeter	Gross-Umstadt, DE
Knick	pH-Meter 766 Calimatic	Berlin, DE
Merck	Research chemicals	Darmstadt, DE
Mettler Toledo	pH-Meter S20 SevenEasy	Giessen, DE
MicroCal (GE Healthcare Life Sciences)	VP-Capillary DSC system	München, DE
Microfluidics	High pressure homogenizer 110LA	Westwood, MA, US
Millipore (Merck Millipore)	Immobilon-P membrane, SNAP I.d system, Concentrators (Amicon and Centriprep), Ultrafree centrifugal devices	Schwalbach am Taunus, DE
NanoDrop Technologies	NanoDrop ND-1000 spectrophotometer	Wilmington, DE, US
New England Biolabs	Molecular biology products	Ipswich, MA, US
Novagen (EMD Millipore)	Molecular biology products	Darmstadt, DE
Pharmacia Biotech (GE Healthcare Life Sciences)	Power supply LKB ECPS 3000/150	München, DE
Perkin-Elmer	UV/Vis Spectrophotometer LAMBDA 35	Waltham, MA, US
PEQLAB	Molecular biology products	Erlangen, DE
Pierce (Thermo Fisher Scientific)	Protein assay	Rockford, IL, US
Qiagen	Molecular biology products, Research chemicals	Hilden, DE
Rigaku	CrystalMation system	Tokyo, JP
Roche	Research chemicals	Mannheim, DE
Sarstedt	General laboratory consumables	Nümbrecht, DE
Sartorius	Laboratory balance Cubis (individual), Analytical balance R180D	Göttingen, DE
SEQLAB	DNA sequencing	Göttingen, DE
Sigma	Centrifuge 4K10 and 4K15	Osterode am Harz, DE
Sigma-Aldrich	Research chemicals	Seelze, DE
Stratagene (Agilent Technologies)	Site-Directed Mutagenesis Kit	Waldbronn, DE
Thermo Scientific	Spectrophotometer Spectronic BioMate 3	Bonn, DE
Unisense	OX-MR oxygen microsensors	Aarhus, DK
Varian (Agilent Technologies)	UV/Vis Spectrophotometer Cary 100 and Cary 300	Böblingen, DE
Vivaproducts	Concentrators (Vivaspin)	Littleton, MA, US
VWR	General laboratory consumables and chemicals	Darmstadt, DE
Whatman	Chromatography paper 0.34 mm 3MM Chr	Dassel, DE
Zymo Research	Molecular biology products	Irvine, CA, US

I. The nucleotide sequences of the two *ccoNO(Q)P* operons and the *ccoGHIS* operon of wild-type *P. stutzeri* ZoBell



```

1  cgaggetttg cctgcttggc agcaggatgg aacggatagc ccaggcagac cagcgcaccc acccctgttt catcggccaa aaggctggcc atgcggccgc
   gctccgaaca ggacgaacgg tcgtctacc  ttgctatcgc ggtccgtctg gtccgctagg tggggacaaa gtacgcggtt ttccgaccgg tacgcccggc

101  ccacgcactt gccgccaacg gccaaaagcc ctgtggcctg ctgtgcgacc agagcatgga tttcgcgaca ttgcgcaagc agatgcccct gtgggctggg
   ggtagctgaa cggcgggttc cgtttttcgg gacaccggac gacagcgtgg tctcgtacct aaagcgcgtg aacgcgttgc tctacgcca caccggacc

201  cggccgctta cggccttcgg tacgacgccc agccatgtag gagaactcga agcgcacac  cgcaatacca cgcgccgcaa ggcgctcagc cattedgttc
   gccggcgaat gccggaagcg atgctgcgcg tcggtacatc ctcttgagct tcgctgtgtg cgtttatggt cggggggcgt cgcgagctg gtaaaagcaag

301  atgaacggac tgtccattgg cgcaccgcca ccattggcca ggatcagcgt ggcccaggta tcgacctgcg gttggttcca gctgacgaga tgtcctttgt
   tacttgctcg acaggtaac  gcgtggcgtg ggtaccgggt cctagtcgca ccgggtccat agctggacgc caaccaaggt cgaactgctc acaggaaca

401  cactttgtgt gtattgatcc gtgtcaatac cggcagattg ccctttcccc atccttgcct cgttttctat tagaagaaa aaaactgctc attaccctgt
   gtgaaacaca cataactagg cacagttatg gccgtctaac gggaaagggg taggaaacgga gcgaaagata atctttcttt tttgacgag taatgggca

501  gatggaagcc catacatgaa cacagcaacc agtaccgctc acagttacaa ggtggctccg caattcgcca tcactgacgt ggtgtgggga atcgtcggga
   ctaccttcgg gtatgtactt gtgtcgtttg tcattggcga tgtcaatggt ccaccagcgg gtaaaagcgt agtactgcca ccacaccctc tagcaccctc
   >>.....ccoN-1.....>
1  M N T A T S T A Y S Y K V V R Q F A I M T V V W G I V G

601  tggggctcgg cgttttcac  gcagcacaat tggcctggcc atttctgaac ttgcacctcc cgtggaccag tttcgttcca ctactgccat tgcacaccaa
   accccgaccg gcaaaagtag cgtcgtgtta accggaccgg taaagacttg aagctggagg gcacctggtc aaagccagct gatgcaggtc acgtgtggtt
   >.....ccoN-1.....>
29  M G L G V F I A A Q L A W P F L N F D L P W T S F G R L R P L H T

701  cgcggtgatt ttgcctttg cggcgtgtgc actgttcgca acgtctact actcggttca gcgcacctgc cagaccacc  tgttcgcgcc gaagctggcc
   gcgccactaa aagcggaaac cgcgcgacac tgacaagcgt tcagagatga tgagccaaat cgcgtggacg gtctggtggg acaagcggcg cttgcaccgg
   >.....ccoN-1.....>
62  N A V I F A F G G C A L F A T S Y Y S V Q R T C Q T T L F A P K L A

801  gcgttaccct tctggggttg gcagttggtc atcctgctcg ccgcaatc  cctgccctcg ggtttcacca gtcaccaagga gtatgcggaa ctggagtgcc
   cgcaggtgga agaccaccaac cgtcaaccag taggacgagc ggcgttatag ggacggcgac ccaaagtggt cgaggttcc  catacgcctt gaactaccg
   >.....ccoN-1.....>
96  A F T F W G W Q L V I L L A A I S L P L G F T S S K E Y A E L E W

901  cgatgcacat cctgatcacc atcgtctggg tggcctatgc ggtcgtcttt ttccgggacgc tggtaagcg caaggtcaag cacatctacg tcgtaactg
   gctagctgta ggaactagtg tagcagacc  accggatacg ccagcagaaa aagccctgcg accgattcgc gttccagttc gttagatgc agccattgac
   >.....ccoN-1.....>
129  P I D I L I T I V W V A Y A V V F F G T L A K R K V K H I Y V G N

1001  gttctctcgt gccctcacc  tgaccgtgac gatcctgcat gtcgcaaca acctggaaat ccggttacc gcgatgaagt cctattcgtg gtatgcgggt
   caagaagcca cggaaagtag actggcaccg ctaggacgta cagcagttgt tggaccttta gggccaatgg cgtacttcca ggataagcga catacggcca
   >.....ccoN-1.....>
162  W F F G A F I L T V A I L H V V N N L E I P V T A M K S Y S L Y A G

1101  gcgaccgatg cgatggtgca atggtgttac ggccacaacg ccgtgggctt cttctcacc gccggcttcc togggatcat gtaactctto gtgctaagc
   cgtcgtctac gctaccacgt taccaccatg ccggtgttgc ggcaccgcaa gaaggagtg  cggccgaagg agccctagta catgatgaag caccgattcg
   >.....ccoN-1.....>
196  A T D A M V Q W W Y G H N A V G F F L T A G F L G I M Y Y F V P K

1201  aggcggagcg cccggtgtat tcgtatcggc tgtcgtcgt  tcactctcgg gcactgatca ccgtctacat ctgggccgcg ccgaccacc  tgcactacac
   tccggctcgc gggccacata agcatagcgg acagctagca agtgaagacc cgtgactagt ggcagatgta gaccggccc  ggcgtggtag acgtgatgtg
   >.....ccoN-1.....>
229  Q A E R P V Y S Y R L S I V H F W A L I T V Y I W A G P H H L H Y

1301  cgcgctgcca gattgggca  agacccggg catggtgatg tcctgatc  tgctggctcc gagctgggg  ggcgatgata accgcatgat gacgtgtgc
   gcgcagcgtt ctaaccctgt tctcggacc  gtaccactac agcactaag acgaccgagg ctcgaccctg ccgtactagt tgcgtaacta ctgcgacgc
   >.....ccoN-1.....>
262  T A L P D W A Q S L G M V M S L I L L A P S W G G M I N G M M T L S

1401  ggtcctcggc acaaaactcg tagcaccgg atcctcgcct tctcgtggtt ttctcggcg ttctacggca tctgacctt  cgaaggtccg atgatggca
   ccacggaccg tgtttgacgc atcctcgggc taggacgcga aggaccacca aagcaccgc  aagatgccg acagctggaa gcttccagc  tactaccct
   >.....ccoN-1.....>
296  G A W H K L R S D P I L R F L V V S L A F Y G M S T F E G P M M A

1501  tcaagaccgt caagccctg  tccactaca ccgactggac catcggccac gtacacgctg gcgcccctcg ctgggttcca atggtctcca tcggcgcgt
   agttctggca gttgcgggac aggtgatgt  ggtgacctg gtagccggtg catgtgcgac ccggggagcc gaccacaact taccagaggt agccgcgca
   >.....ccoN-1.....>
329  I K T V N A L S H Y T D W T I G H V H A G A L G W V A M V S I G A

```

6. APPENDIX

```

1601 gtatcaactg gtcccgaag tgtteggccg cgagcagatg cacagtatcg gtotgatcaa caccoacttc tggctagcca ccatcgccac cgtgctctac
catagtgga cagggtcttc acaagccgcg gctcgtctac gtgtcatagc cagactagtt gtgggtgaag accgatcggt ggtagccgtg gcacagatg
>.....ccoN-1.....>
362 L Y H L V P K V F G R E Q M H S I G L I N T H F W L A T I G T V L Y

1701 atcgcttoga tgtgggtcaa cggtatocgg cagggcctga tgtggcgtgc aatcaacgac gacggcagcg tgacctattc cttcgtcgaa tegctggaag
tagcgaagct acacccagtt gccatagcgc gtcccggact acaccgcaag ttagttgctg ctgccgtgcg actggataag gaagcagctt agcgacotc
>.....ccoN-1.....>
396 I A S M W V N G I A Q G L M W R A I N D D G T L T Y S F V E S L E

1801 ccagccacc cggcttcgta gtgcgaatga togggtgtgc gatctcttc gccgcgatgc tgggtatggc ctacaacacc tggcgaccg tgcaggctgc
ggtcgggtgg gccgaagcat cacgcttact agccaccacg ctagaagaag cggccgtacg accactaccg gatgtgtggg accgctggc acgtccgagc
>.....ccoN-1.....>
429 A S H P G F V V R M I G G A I F F A G M L V M A Y N T W R T V Q A

1901 caagcccgc gagtacgagc ctgcccgcga gatcgcctga ggagcctagg taaatgaaat cgcacgagaa actagaaaag aacgtaggtc tgttgaccct
gttcggggcg ctcatgctgc gacggcgcgt ctagcggact cctcggatcc atttacttta gcgtgctctt tgatcttttc ttgatccagc acaactggga
>.....ccoN-1.....>
462 A K P A E Y D A A A Q I A -
>>.....ccoO-1.....>
1 M K S H E K L E K N V G L L T

2001 gttcatgac ctggcggtaa gcctggcggc tctgaccag atcgtcccgc tgtttctcca ggactccgtc aacgagccgg ttgaaggcat gaagccttac
caagtactag gaccgcatt cgtatgcccgc agactgggtc tagcaggggc acaagaaggt cctgagcag ttgctcgcc aactcccgta cttcggaaatg
>.....ccoO-1.....>
16 L F M I L A V S I G G L T Q I V P L F F Q D S V N E P V E G M K P Y

2101 accgctgctc agctcgaag cgggacotg tacatccgg agggctcgtg ttgctgcccac togcagatga tccgccctt cgcgctgag accgagcgt
tggcgcgagc tocgacttcc ggcctggac atgtaggcgc tcccagcga accgagcgtg agcgtctact aggggggaa ggcgcgactc tggctcgcga
>.....ccoO-1.....>
50 T A L Q L E G R D L Y I R E G C V G C H S Q M I R P F R A E T E R

2201 acggccaact cctcgtggcc ggtgaaagcg tctacgacca tccgttctcg tgggctcca agcgtaccgg accgatctg gccctgtgct gggcccgta
tgccggtgat gaggcaccgg ccactttcgc agatgctggt aggcaagag accccgaggt tgcgatggcc tggcctagac cgggcacagc cgccggcgtg
>.....ccoO-1.....>
83 Y G H Y S V A G E S V Y D H P F L W G S K R T G P D L A R V G G R

2301 ctccgatgac tggcaccgtg cgcactgta caaccgcgc aacgtagttc ctgagtcgaa gatccgctc tatccgtggc tggctgagaa caccctcgc
gaggctactg accgtggcac gcgtggacat gttggggcgc ttgatcaag gactcagctt ctacggcagc ataggcaccg accagctctt gtgggagctg
>.....ccoO-1.....>
116 Y S D D W H R A H L Y N P R N V V P E S K M P S Y P W L V E N T L D

2401 ggcaaggaca ctgccaagaa gatgtcggct ctgcccgcgc ttggcgttcc ttacaccgaa gaggacatcg cggcgcctcg ggactccgtc aacggcaaaa
cgtttctctg gacggttctt ctacagccga gacgcgtacg aaccgcaagc aatgtggctt ctccctgtag gcccgcgagc cctgagcagc ttccgcttt
>.....ccoO-1.....>
150 G K D T A K K M S A L R M L G V P Y T E E D I A G A R D S V N G K

2501 ccgagatgga tgcgatgggt gcttacctgc aggtactcgg cacagctctg accaataagc gctgagctg actgaccaag aaaaaatgac cggctggcaa
ggctctacct acgctaccac cgaatggagc tccatgagcc gtgtcgagac tggttattcg cgaactcagc tgactggctc tttttactg gccgaccgtt
>.....ccoO-1.....>
183 T E M D A M V A Y L Q V L G T A L T N K R -

2601 atcagccgctc agggacttca atcgcggaca gccagagttg ctccggctgt ccaggagtag cacatgagca ctttctggag tggataacac gccctcgtga
tagtcggcag tccctgaagt tagcgcctgt cggctcacc gagcccgaca ggtcctcacc >>.....ccoP-1.....>
1 M S T F W S G Y I A L L

2701 cgtgggac catcgtcgt ctgttctggt tgatcttcgc caccgcaag ggcgaatccg ccggcaactc ggatcaaac atgggacatg ccttcgatgg
gcgaccctg gtatgacgca gacaagacca actagaagcg gtggcgcttc ccgcttaggc ggccgtgatg cctagtttgc taccctgtac ggaagctacc
>.....ccoP-1.....>
13 T L G T I V A L F W L I F A T R K G E S A G T T D Q T M G H A F D

2801 catcagggaa tacgacaacc cgtgcccgc ctgggtgttc ctgctcttca ttggcaccct ggtgttcgca atcctgtact tggctctca ccccgccctg
tgactcctt atgctgttg gcgacggcgc gaccaccaag gacgagaagt aaccgtggga ccacaagcgg taggacatga accacgagat gggccggagc
>.....ccoP-1.....>
46 G I E E Y D N P L P R W W F L L F I G T L V F G I L Y L V L Y P G L

2901 ggtaactgga agggcgttct gccaggtac gaggggtgct ggactcaaga gaagcagtg gaacgcaag ttgctcaggc cgtgaaaaa tacggtccga
ccattgacct tcccgaaga cggctcgatg ctcccaccga cctgagttct cttcgtcacc cttgcgcttc aacgagtcgg gctacttttc atgccagct
>.....ccoP-1.....>
80 G N W K G V L P G Y E G G W T Q E K Q W E R E V A Q A D E K Y G P

3001 ttttgcgcaa gtacgtgccc atgtcagtg aagaagtggc acaggaccgg caagccgtga aaatgggccc tgcctgttc gccaaactact gctccatctg
aaaagcgtt catgcaagc tacagtcacc tttctcacc tgtcctgggc ttccggaact tttaccggc agcggacaag cggttgatga cgaagtagac
>.....ccoP-1.....>
113 I F A K Y A A M S V E E V A Q D P Q A V K M G A R L F A N Y C S I

3101 ccaggttcc gatgcaaac gttcgttagg tttccgaac ctgcccgcac aagaetggcg ctggggtggt gatgcccgtt cgataaaaa cagcactcc
ggtgcaagc ctacggttcc caagcgtacc aaagggctg gagcggctg ttctgaccgc gacccacca ctacggcgaa gctagttttg gtctgtagg
>.....ccoP-1.....>
146 C H G S D A K G S L G F P N L A D Q D W R W G G D A A S I K T S I L
3201 aacggagcta tgcagcaat gccgcctgg ggccaagcca tggcgaaga aggcgtgaag aacgtcgcag cgttcgtccg caagcacctc gcggcgttcg
ttgctcgcac agcgtcgtta cggccggacc cgggttcggt agccgttct tccgcacttc ttgagcgtc gcaagcaggc gttcctggag cgcccgaac
>.....ccoP-1.....>
180 N G R I A A M P A W G Q A I G E E G V K N V A A F V R K D L A G L

```


6. APPENDIX

```

3301 cgctgcccga aggcaccgat gccgacctca gcgaggcaca gaacgtotac gcacagacct gcgcccgtctg ccacggctcag ggtggcgaag gtatggccgc
    gcgagggcct tccgtggcta cggtgggagt cgcgtccgtt cttgcagatg cgtgtcttga cggcgagac ggtgcccagc ccaccgcttc caccagccgc
    >.....ccoP-1.....>
213 P L P E G T D A D L S A G K N V Y A Q T C A V C H G Q G G E G M A

3401 gctgggtgag cotaagotca acagcgccgc cggctggatc tatggctega gctcggcca actgcaacag accattogcc atggtogcaa tggccagatg
    cgaccacgc ggattogagt tctcggcgc gccgacctag ataccagcct cggagccggt tgacgtttgc ttgtaagcgg taccagcgtt accggtctac
    >.....ccoP-1.....>
246 A L G A P K L N S A A G W I Y G S S L G Q L Q Q T I R H G R N G Q M

3501 cctgctcagc agcaatatct gggcgacgac aaggttcacc tgcctcgcgc ctatgtttac agcctgtcgc aaaaaccgga acaactcgtt aaccagttag
    ggacgagtc tctttataga cccgctcgtg ttccaagtgg acgagccgcg gatacaaatg tccgacagcg tttttggcct tgttagcgga ttggtcactc
    >.....ccoP-1.....>
280 P A Q Q Q Y L G D D K V H L L A A Y V Y S L S Q K P E Q L A N Q -

3601 ccccaaaagg gcggtacact cgtaccgcc ttctcgcctt gtccccagc aacttccgct actctcgcac tatctgtcgc atcgcaaaact gaccaacgct
    ggggttttcc cgccatgtga gcatggcggg aagagcggaa cagggggtcc ttgaagcgga tgagacgctg atagacagcg tagcgtttga ctggttgacg

3701 ttcccccttc cgcgtagca cttetaagct gtgcttcoga ttcgccatcc cgcctagaac cataaggcgc aatcgttaatt tcttacgca cgcggtgtg
    gaagggggag cgcgtagcgt gaagattcga cacgaaggct aagcggtagg cgggatcttg gtattccgcg ttagcattaa aggatgcgct gccgcaccac

3801 cgatacctcc ctgcacagca caccgaaaac gctttaaact agggttttg ccagcaaaga cagcccggcg gcggtttgca ttgccccctt gctttctcca
    gctatggagg gacgtgtcgt gtgcctttg cgaattttag tccaaaacc ggtcgtttct gtcgggcccg cgcaaacgtt aacgggggga cgaaagaggt

3901 taactgcccg cgtttttgct ttcgaaaatg ctattagcgt ggaagccttg catgagcaca gcaatcagtg agactgotta taactataag gtggttcgc
    atgaacggcg gcaaaaacgg aagcttttac gataatcgca ccttcggaac gtactcgtgt cgttagtcac tctgacgaat attgatattc caccagcgg
    >>.....ccoN-2.....>
1 M S T A I S E T A Y N Y K V V R

4001 aattcggcat catgacggtg gtgtggggaa tcattgggat gggcctgggt gttttcatcg ccgcgaatt ggtgtggccc tgcctcaatt tggacctgcc
    ttaagcggta gtaactgccac cacaccctt agtaacccta ccggagacca caaaagtagc ggcgcgttaa ccacaccggg agcgagttaa acctggacg
    >.....ccoN-2.....>
17 Q F A I M T V V W G I I G M G L G V F I A A Q L V W P S L N L D L

4101 ttggagcagc ttcggccgct tgcgccatt gcacaccaat cgggtgatct tgcggtcgg ttggttgcga ctgtttgcca cgtctacta cgtggttcag
    cacctcctcg aagccggcag acgcggttaa cgtgtgggta cgcactaga agcgaacgc accaacgcgt gacaaacggt gcaggatgat gcaccaagtc
    >.....ccoN-2.....>
50 P W T S F G R L R P L H T N A V I F A F G G C A L F A T S Y Y V V Q

4201 cgcacctgcc aggcccgctt gttctcgcg gactcgcgg cttcacctt ctggggttgg caggctgtga tctgtcttc ggtcaccag cttccgatgg
    gcgtgacgag tccgggcaga caagaggctg cctgagcgcg gaaagtgaaa gaccccaacc gtcgcacct agcacaagc ccagtagtgc gaaggtacc
    >.....ccoN-2.....>
84 R T C Q A R L F S D G L A A F T F W G W Q A V I V L A V I T L P M

4301 gctacaccag ctccaaggag tatcggaac tggagtggcc gattgatata ctgacaccc ttggttgggt gtcgtatata gccgtgttct tcggaccat
    cgatgtggtc gaggttcttc atacgccttg acctcaccgg ctaactatag gactagtggt accagacca cagcatatag cggcacaaga agcgtgtgta
    >.....ccoN-2.....>
117 G Y T S S K E Y A E L E W P I D I L I T L V W V S Y I A V F F G T

4401 catgaagcgc aaggccaagc acatctatgt aggtaactgg ttctcgggt cttcactcct ggtgacggcg atgtgcaca tcttaacaa cctggaat
    tgaactcgcg ttccgggtcg ttagatata tccattgacc aagaagcacc gaaagtagga ccaactgccc tagcagctgt agcaattgtt ggaccttaa
    >.....ccoN-2.....>
150 I M K R K A K H I Y V G N W F F G A F I L V T A M L H I V N N L E I

4501 ccggtcagcc tgttaagtc ctactcgcg tacgcaggcg ctaccgatgc gatggtgcaa ttggtgtacg gccacaacc cgtgggcttc ttctgacca
    ggccagtcgg acaagttcag gatgagtag atgcctcgc gatggctacg ctaccacgtt accaccatgc cgtgtttgcg gcaccogaag aaggactggt
    >.....ccoN-2.....>
184 P V S L F K S Y S I Y A G A T D A M V Q W W Y G H N A V G F F L T

4601 ccggttctct cggcatgat tactacttgc tgcotaagca ggcagcgtc ccggtgtact cctatgcct gtcgatcgc cacttotggg cactgatcac
    ggcogaagga gccgtactac atgatgaagc acggattcgt ccgctcgcga ggccacatga ggatagcggg cagtagcag gtgaagacc gtgactagt
    >.....ccoN-2.....>
217 T G F L G M M Y Y F V P K Q A E R P V Y S Y R L S I V H F W A L I

4701 cctctatata tggcgccgcc cgcaccact gcactacacc gccctgccc attggcgca gagcctggc atggtgatgt cgtatcctt cgtgctccg
    ggagatatag acccggccgg cgtgtgtgga cgtgatgtg cgggacgct taaccgcgt ctcggaccg taccactaca gctagtagga cgaccagggc
    >.....ccoN-2.....>
250 T L Y I W A G P H H L H Y T A L P D W A Q S L G M V M S I I L L A P

4801 agctggggcg gcatgatcaa cggcatgat accctgtcgg gtgcctggca taagtgcgc accgatccga tctcgcctt cctggtggtg tctgtggcgt
    tgcaccgcc cgtactagt gccgtactac tgggacagcc cacggacctt attcagcgcg ttgctaggct aggacgcgaa gaccaccat agcagccga
    >.....ccoN-2.....>
284 S W G G M I N G M M T L S G A W H K L R T D P I L R F L V V S L A

4901 tctacggcat gtcgacctc gaaggtccga tgatggcgt caagaccgct aacgactgt ccaactacac cgaactgact atcgccacg tacaccggc
    agatgccga cagctggaag ctccaggct actaccgcta gttctggcag ttgctgaca ggtgatgtg gctgacctga tagccggtgc atgtcggcc
    >.....ccoN-2.....>
317 F Y G M S T F E G P M M A I K T V N A L S H Y T D W T I G H V H A

5001 agcctcgtt tgggtagcga tgatcaetat cggctcgtg taccacctga ttccgaaagt gttcggggcg gagcagatgc acagcgtcgg cctgatcaat
    tccggagcca acccatcgt actagtata gccgagctac atggtggact aagccttca caagcccgcg ctgctctacg tctcgcagcc ggactagtta
    >.....ccoN-2.....>
350 G A L G W V A M I T I G S M Y H L I P K V F G R E Q M H S V G L I N

```

6. APPENDIX

```

5101 ggcgaacttct ggctggcccac catcggcacc gtgctttaca tgcctcgcgat gtgggtcaaac ggcatoacco aaggcctgat gtggcgcgcg atcaacgaag
cgcgtgaaga ccgaccgggtg gtgaccgtgg cacgaaatgt agcggagata caccocagttg ccgtagtggg ttccgggacta caccgcgcgc tagttgtctc
>.....ccoN-2.....>
384 A H F W L A T I G T V L Y I A S M W V N G I T Q G L M W R A I N E

5201 acggcaccct gacactactc ttctgogaag cgtggaagc cagtcacccc ggcttcacgc tccgcgcagt cggcggcgcg ttcttctcgc ctggcatgct
tgccgtggga ctggatgagg aagcagcttc gcgaccttcg gtcagtaggg ccgaagttagc aggcgcgctca gccgcgcgcg aagaaggagc gaccgtacga
>.....ccoN-2.....>
417 D G T L T Y S F V E A L E A S H P G F I V R A V G G A F F L A G M

5301 gttgatggca tacaacacct ggcgcaccgt acgggcccgc aagtacgccc agtacgacac tgccgcgcag atcgcttgag gaacggatag atgaagaacc
caactaccgt atgttggga ccgctgggca tgcccggcgg ttcagctggg tcatgctgtg acggcgcgctc tagcgaactc cttgctctac tacttctgtg
>.....ccoN-2.....>
450 L L M A Y N T W R T V R A A K S A Q Y D T A A Q I A -
>>cco0-2.>
1 M K N

5401 acgaaatact cgaaaagaac attggtctgc tgacctgtt catgatcctg gcagtgagca tggcggctct gaccagatc gtcccgcgtg tctttcagga
tgctttatga gctttctctg taaccagacg actgggacaa gtaactaggc cgtcactcgt agccgcgaca ctgggtctag caggggcaca agaaagtctc
>.....cco0-2.....>
4 H E I L E K N I G L L T L F M I L A V S I G G L T Q I V P L F F Q

5501 cgcagtgaac gagccgggtg aaggcatgaa gccttacacc gcgctgcagc tcgaaggctg ggatctgtac atccgcgagg gctgcgttgg ctgccactcg
cgtcactctg ctccgccaac ttccgtactt cggaatgtgg ccgcagctcg agcttccagc cctagacatg taggcgctcc gcagcacaac gacggtgagc
>.....cco0-2.....>
37 D A V N E P V E G M K P Y T A L Q L E G R D L Y I R E G C V G C H S

5601 cagatgatcc gcccttccgc cgtgagacc gagcgtacg gccactactc cgtggcgggt gaaagcgtct acgaccatcc gttcctgtgg ggtcccaagc
gtctactagg cggggaaggc gcgactctgg ctccgcgatc cgggtgatg gcaccggcca ctttcgcaga tgctgtagg caaggacacc ccgaggtctg
>.....cco0-2.....>
71 Q M I R P F R A E T E R Y G H Y S V A G E S V Y D H P F L W G S K

5701 gtaccggacc ggatctggcc cgtgtcggcg gccctactc cgtgactgac caccgtgcgc acctgtacaa cccgcgcaac gtgattcctg agtcgaagat
catggcctgg cctagaccgg gcacagccgc cggcgtatg gtaactgacc gtggcacgcg tggacatggt gggcgcgttg catcaaggca tcagcttcta
>.....cco0-2.....>
104 R T G P D L A R V G G R Y S D D W H R A H L Y N P R N V V P E S K

5801 gccctctat ccgtgcttg tcgagaacac cctcgaccgc aaggacactg ccaagaagat gtcgctctg ccgatgctg gcgttccgta caccgaagaa
ggcagagata ggcaccgacc agctcttctg ggagctgccc ttctctgac ggttcttcta cagccgagac gcgtacgaac cgcaaggcat gtggcttctt
>.....cco0-2.....>
137 M P S Y P W L V E N T L D G K D T A K K M S A L R M L G V P Y T E E

5901 gacatgcggc ggcggctgta tgccgtcctg ggcaagacc agatggatgc catggtggcc tacctgcaag tgctcggcac tgcttaacc aacaaacggt
ctgtagcggc ccggggcact acggcagcca ccgttctggc tctacctacg gtaccaccgg atggacgttc acgagccgtg acgagatgg ttgtttgcca
>.....cco0-2.....>
171 D I A G A R D A V R G K T E M D A M V A Y L Q V L G T A L T N K R

6001 aacgcatgat gaaatcggt actcttcggc gctggggcac aattctggta gtcgtccctc tcatcgccgt agtgcctctg gctacagca gcaaacgcaa
ttgcgtacta cctttagcca tgagaagcgc cggaccctgt ttaagaccat cagcagcgga agtagccgca tcacgagacc cggatgctgt cgtttgcgtt
>> cco0-2
204 -
>>.....ccoQ-2.....>
1 M M E I G T L R G L G T I L V V V A F I G V V L W A Y S S K R

6101 gcaagcttc gacgaagcag ccaactgcc cttcgcagac gacgagaccg acgccaagaa cgtgaagaa gaagcttcca ggagtaagaa ataaatgacc
cgtttcgaag ctgctctgct ggttggacgg gaagcgtctg ctgctctggc tgccggttctt cgcacttctt cttcgaaggt cctcattctt tatttactgg
>.....ccoQ-2.....>
32 K Q S F D E A A N L P F A D D E T D A K K R E E E A S R S K K -
>>.....ccoP-2 >>...>
1 M T

6201 tcttttggg gttgtaactg caccctgctg agcctgggca caattggcgc gctggtatgg ctgctactgg caacgcgcaa gggacaacc cccgacagca
agcaaaacct caaccatgca gtgggacgac tcggaccctg gtaaacggcg ccaccatacc gacgatgacc gttgcgcgtt cctctgttgc gggctgtcgt
>.....ccoP-2.....>
3 S F W S W Y V T L L S L G T I A A L V W L L L A T R K G Q R P D S

6301 ccgaagaac cgtcgggcat tcctatgacg gcctcgagga gtacgacaac ccgctaccgc gctggtggtt catgctgttc gtgggtaccg tgatctttg
ggcttctttg gcagcccgta aggatactgc cgtagctcct catgctgttg ggcgatggcg cgaccaacaa gtacgacaag caccatgac actgaaaacg
>.....ccoP-2.....>
36 T E E T V G H S Y D G I E E Y D N P L P R W W F M L F V G T V I F

6401 tcttggatac ctggtgctgt atccggcct aggcaactgg aaggcattc tgcccggta cgaaggtggc tggaccagg tcaaggaatg gcagcgtgag
agaacctatg gaccacgaca tagggccgga tccgttgacc ttcccgaag acgggccaat gcttccaccg acctgggtcc agttccttac cgtgcactc
>.....ccoP-2.....>
69 A L G Y L V L Y P G L G N W K G I L P G Y E G G W T Q V K E W Q R E

6501 atggacaagg ccaatgagca atacggcccg ctgtatgcca agtacgctgc catgcccgta gaagaggtg ccaagatcc gcaagccctg aagatgggtg
taactgttcc ggttactcgt tatgcccggc gacatacggc tcatgagcgc gtaaccgcat cttctocacc gtttctagc cgttcgggac ttctaccacc
>.....ccoP-2.....>
103 M D K A N E Q Y G P L Y A K Y A A M P V E E V A K D P Q A L K M G

6601 gacgtctgtt cgcatacaac tgctcgtctt gccatggctc tgatgcaaaa ggcctctatg gcttccgaa tctgaccgac gacgactgac tgtggggcg
ctgcagacaa cgttaggttg acgagccaga cggtagccg actacgggtt ccgcccgtac cgaagggctt agactggctg ctgctgaccg acacccccgc
>.....ccoP-2.....>
136 G R L F A S N C S V C H G S D A K G A Y G F P N L T D D D W L W G

```

6. APPENDIX

```

6701 cgagcctgaa accatcaaga ccaccatcct gcaacggcgc caggccgtga tgcctggctg gaaagacgtg atcggcgaag aagcoatccg caacgtagct
gctcggactt tggtagttct ggtggtagga cgtgcccgcg gtcocggcact accgaccgac ctttctgcac tagccgcttc ttccgtagcg gttgcatoga
>.....ccoP-2.....>
169 G E P E T I K T T I L H G R Q A V M P G W K D V I G E E G I R N V A

6801 ggctatgttc goagcctgtc cggacgtgat accocagagg gtattagcgt cgacattgag cagggtcaaa aaatcttcgc ggccaactgt gtagtctgcc
cggatacaag cgtcggacag gctcgcacta tggggctotcc cataatcgca cgtgtaactc gtcocagttt tttagaagcg ccggttgaca catcagacgg
>.....ccoP-2.....>
203 G Y V R S L S G R D T P E G I S V D I E Q G Q K I F A A N C V V C

6901 atggaccgga agccaagggc gttacagcca tgggcgcgcg gaacctgacc gacaatgtct ggctgtatgg ttcagcttcg gctcagatcc agcaaacct
tacctggcct tccgttcccg caatgtcggg acccgcgcgc cttggactgg ctgttacaga ccgacatacc aagctcgaag cgagtctaag tctgttggga
>.....ccoP-2.....>
236 H G P E A K G V T A M G A P N L T D N V W L Y G S S F A Q I Q Q T

7001 gcgctacggt cgcaatggcc gcctgcctgc tcaggaagcg atccttggta atgacaaggt tcacctgctg gcggcctacg tctacagcct gtcgcagcaa
cgcgatgcca gcgttaccgg cgtacggacg agtcccttcg taggaacct tactgttcca agtggacgac ccocggatcg agatgtcgga cagcgtcgtt
>.....ccoP-2.....>
269 L R Y G R N G R M P A Q E A I L G N D K V H L L A A Y V Y S L S Q Q

7101 ccggagcagt gattgctcga ggtgggggt gacgtcctgt cgcaccgcac ctcaaaactc cgggcgtacc attcgcagct ggacagaaaa ttgatcctgg
ggcctcgtca ctaacgagct ccagccccc ctgcaggaca gctggggctg gagttttgag gccccgatgg taagcgtcga cctgtctttt aactaggacc
>..ccoP-2..>>
303 P E Q -

7201 ttggcaagta tccgcccggg caccacactt ccgcccgtgt acgcactcga tgactgagca gattcccgtt cgtgatgtaa cccccctgc caaggccgga
aacctgtcat agccggcccc gtgggtggaa ggcggcacca tgcgtgagct actgactcgt ctaagggcaa gcaactacat gggggggcag gttccggctt
>>.....ccoG.....>
1 M T E Q I P V R D V T P P S K A G

7301 gcgctacggt acctctacgc cgcgctgtaa aaaatttaca ccagagcctt cagcggcttg tttcgtaatc tgcagcgcgt agcggcgcgc gtactcttca
cgcagctcag tggagatgcg gcgcgcactt ttttaaatgt gggctcggaa gtcgccgaac aaagcattag acgtcgcgca tcccgcgcgc catgagaagt
>.....ccoG.....>
18 A S A D L Y A A R E K I Y T R A F S G L F R N L R R V G G A V L F

7401 tctcttctt cggaaccgtc tggctcaact ggaacggcgc tcaggctgct tgggtggacc tgcgggatcg caagtccac atcttcgggg cgcagttctg
aggagaagaa gccttggcag accgagttag ccttgcgcgc agtccgacag accaccctgg acggcctagc gttcaagttg tagaagcccc gctgcaagac
>.....ccoG.....>
51 I L F F G T V W L N W N G R Q A V W W D L P D R K F H I F G A T F

7501 gcccccagat ttcctatgct tctcgtggct gctaatacat tgcgccttcg gctgttctt catcaaccgc ttcctgtgcc gcgtctggcg ccgtatcacg
cggggctccta aagtagcagc acagcaccga cgattagtag acgcggaagc cggacaagaa gtatgtggcag aagcagcccg cgcagaccac gccgatgtgc
>.....ccoG.....>
84 W P Q D F M L L S W L L I I C A F G L F F I T V F A G R V W C G Y T

7601 tgcccgcaga gcgtgtttac ttgggtgttc atgtgggcgc agaagatcac caggggtgat cgcaaccagc gaatgaagct cgacaaggcg ccaatgagcg
acggcgtctc cgcaacaatg aaccacaaag taacaccgcgc tctctatagt gtcococacta gcgttggctcg cttactctga gctgttcccg ggttactcgc
>.....ccoG.....>
118 C P Q S V F T W V F M W A E K I T E G D R N Q R M K L D K A P M S

7701 ccaacaagtt ccttcgcaaa ctggccaagc acgcccctct gctcgcggtt ggcatcctcg tggcaatcac cttcgtcggc tacttccacc ccattcgcga
ggttgttcaa ggaagcgttt gaccggttcc tgcggtagac cgagcgcaca ccgttaggagc accgttagtg gaagcagccg atgaagtgcg ggtaagcgtc
>.....ccoG.....>
151 A N K F L R K L A K H A I W L A V G I L V A I T F V G Y F T P I R

7801 gctgttccc gacctgctca ccttgaactg caacggctgg gcggcgttct ggatcggctt ctttaccctc gccacctacg gcagtgtctg ctacctgct
cgaccaaggg ctggacagat ggaacttga gttgcccgacc cgcgcgaaga ctagccgcaa gaaatgggag ccgtggatgc cgtcacgacc gatggagca
>.....ccoG.....>
184 E L V P D L L T L N V N G W A A F W I G F F T L A T Y G S A G Y L R

7901 gacgaggtgt gcattatcat gtgccgttac gcgcgcttcc agagcgtgat gttcgacaag gacacgctga tcttttcta cgaccgcgc cgtggcgaga
ctctccaca cgtatagta cacgggcatg cgcgcgaagg tctgcactca caagctgto ctgtgcgact agcaaaagat gctgggcgcg gcaaccctc
>.....ccoG.....>
218 E Q V C I Y M C P Y A R F Q S V M F D K D T L I V S Y D P R R G E

8001 agcgcggccc gcggaagaaa gataccgact acaaggccat gggacttggc gactgtatcg actgcaccat gtcggtccag gctcgcctca ccggtatcga
tcgcgcggcg cgccttcttt ctatggctga tgttccggta ccctgaaccg ctgacatagc tgacgtggta cacgcagctc cagacgggtt ggccatagct
>.....ccoG.....>
251 K R G P R K K D T D Y K A M G L G D C I D C T M C V Q V C P T G I

8101 catccgcagc ggtctgcaga tggatgcat tggctgcgca gcctgcctcg atgcctcgga tgcgatcag gacaagatga actatccacg cgggttgatc
gtaggcctg ccagacgtct agctcacta accgacgcgt cggactgagc tacggacgct acgctagtac ctgttctact tgataggtgc gcccaactag
>.....ccoG.....>
284 D I R D G L Q I E C I G C A A C I D A C D A I M D K M N Y P R G L I

8201 agctacacca ccagcacaa cctgtctggc cagaagacgc acctgatgct tcccgcctg atcggttatg ccgtgcctct ggcggccatg atgggtctg
tcgatgtgtt ggctcgtgtt ggacagaccg gtcttctcgc tggactacgc agggggcgac tagccaatac ggacgcggga ccgcgcgtac taccagaca
>.....ccoG.....>
318 S Y T T E H N L S G Q K T H L M R P R L I G Y A V A L A A M M G L

8301 ttgcgtacgc cgtttacgat cgcocgctgg tcaagctgga cgtactcaag gatcgcgtgc tctatcgca gaacagcagc ggcaacatcg agaacttta
aacgcatgcg gcaaatgcta gcgggcgacc agttcgaact gcattgcttc ctagcgcacg agatagcct cttgctcgc ccgtttagc tcttgcfaat
>.....ccoG.....>
351 F A Y A V Y D R P L V K L D V L K D R V L Y R E N E Q G N I E N V

```

6. APPENDIX

```

8401 tacgttgaag gtcataaaca aggetcaaca cgagcgcacc ttctgatcgc aggcacccgg tctcgatggc ctggtctaac aaggccgcag cgagattcgc
atgcaacttc cagtaactgt tccgagtcgt gctcgcgtgg aagcactaga tccgtaggcc agagctaccg gaccagatgc ttccggcgctc gctctaagcg
>.....ccCG.....>
384 Y T L K V M N K A Q H E R T F V I E A S G L D G L V Y E G R S E I R

8501 gccgaagccg gcgagctcgt taccatcccg gtcgagctgt ccatcgcgcc tgaaaagctt cctcaagca ccaacgaaat cgttttccac gttcgcctcg
cggcttcggc cgctcgagca atggttaggc cagctcgaca ggtagcgcgc acttttcgaa gggagttcgt ggttgcttta gcagaaggtg caagcgagcc
>.....ccCG.....>
418 A E A G E L V T I P V E L S I A P E K L P S S T N E I V F H V R S

8601 tagacgacga ttcaattaac gatgatgcag acagccgctt catcggccca agcattcctc aagcaaggtg atacatgcgc tctgataacg aacaaacgcg
atctgctgct aagttaattg ctactacgct tctcggcgaa gtacccgggt tcgtaagcga ttctgtccat tatgtacgcg agactattgc ttgtttgcgc
>.....ccCG.....>>
451 V D D D S I N D D A D S R F I G P S I R -
1 >>.....ccoH.....>
M R S D N E Q T

8701 ttggtacacc cagttctggg cotggtttgt cattgcaatc ctggttagct cgggtggtct ggggctgca ctggttagca tccgcatcgc aaactccgac
aacatctggg gtaacagacc ggacaaaaca gtaacgttag gacaactcga gccaccaaga ccccgacagt gacaactggt agcgctaagc ttgaggtcg
>.....ccOH.....>
9 R W Y T Q F W A W F V I A I L L S S V V L G L S L L T I A I R N S D

8801 tgcgtggttg cggacaacta ctacgacgcc ggcaagggca tcaaccagtc actggaactg gagaagctag ccgaaagcct gaaatgcgcg gctcagctcg
agcgaccaac gcctgttgat gatcgtcggc cgtttccctg agttggtcag tgacctgca ctcttcgata ggctttcgga ctttaactcg cgagtcgagc
>.....ccOH.....>
43 S L V A D N Y Y D A G K G I N Q S L E R E K L A E S L E M R A Q L

8901 tgcctaacga cgagcgcggc ctggccgaag tgcagctgag cggtgccagt cgcctcccaag agctggtgct caacctgctc tctcccacc aacctgagcg
acgagttgct gctcgcgcgc gaccggcttc acgtcgcact gccaccgtca cggggggtcg tccaccagca gttggacgag agaggggtgg ttggactcgc
>.....ccOH.....>
76 V L N D E R G L A E V Q L S G A S R P Q Q L V L N L L S P T Q P E

9001 tgaccgcgcg gtcattctgc agcctcaggg cgacggcttg tatcagggac aaatgcaaga gccggctcgt gcccgccctc tcattgaact gatcgtcgc
actggcggcg cagtaagacg tccgagctcc gctgcccgaac atagtcctcg tttaacttct cgccagctca ccggcccgca agtaacttga ctagccagcg
>.....ccOH.....>
109 R D R R V I L Q P Q G D G L Y Q G Q M Q E P V S G R R F I E L I G R

9101 gaggcgcaac aggactggcg tctgtacgaa gaaaaaaca tcgaaaccgg ccatcgcctc gaactgacgc cttgaccccc tgatggcaaa gcccttccc
ctcccgttg tcttgaccgc agacatgctt cttttttgtt agctttggcc ggtacgcgag cttgactcgc gaactggggg actaccgttt cggggaaggg
>.....ccOH.....>>
143 E G E Q D W R L Y E E K T I E T G H A L E L T P -
1 >>.....ccoI.....>
M A K P L P

9201 tgctaccact ttggcctgcc ggtacctgcc ggcagcccct ttacggcccg cgtgctgggt gaggcgcggg ctttgtgctg tccgggtgct caggcggtcg
acgatggtga caccggacgg ccatggacgg ccgtcgggga aagtccgggc gcacgaccca ctccgcgcc gaaacacgac aggcaccgac gtcgccacc
>.....ccOI.....>
7 C Y H C G L P V P A G S P F Q A R V L G E A R A L C C P G C Q A V

9301 cggaggcgat cgtcaacgcg gggctggaaa gttactacct gcaccgcagc gacacggcaa tcaatcctca gccgctcccc caggagctcg gcgaggagat
gcctccgcta gcagttgcgc ccgaccttt caatgatgga cgtggcgtcg ctgtgccgtt agttaggagt ccgcgagggg gtcctcagac cgctccctca
>.....ccOI.....>
40 A E A I V N G G L E S Y Y L H R S D T A I N P Q A L P Q E L G E E

9401 ggccctttac gatcgtaaag acgtacagga gcccttcgct cagcatcaag gggagctggc gagcaatcg ctgatgatgc agggcatcag ctgcgcggcc
ccgggaaatg ctacgattcc tgcattgctt cgggaagcag gctcgtagtc cctcgcagcc ctctgtgagc gactactagc tccctgagtc gacgcgcgg
>.....ccOI.....>
73 M A L Y D R K D V Q E P F V Q H Q G E L A S T S L M I E G I S C A A

9501 tgtggtggc tgatcgaacg tcactcgcgc aacctcagcg gttgcccga gccagccctg aacctatcca accaccgctt gaatgtgccc tggagcgacg
acaccgaccg actagcttgc agtagacgcg ttggatgctc cacagcggct ccggtcggac ttgataggtg tggtagggga cttacacgcg acctcgcgc
>.....ccOI.....>
107 C G W L I E R H L R N L S G V A E A S L N L S N H R L N V R W S D

9601 cccagctacc gctgagcgag ctgctagctg agctcggcgg gattgctat gcagcacacc cctatcaagc cgatcaggca gccagcgcct tggccagcga
gggtcagatg gcactcgcct gacgatcgc tcgacgcgcc ctaaccgata cgtcgtgtgg gtagatgctg gctagtcctg ccgctcgcgc accggtcctt
>.....ccOI.....>
140 A Q L P L S E L L A E L R R I G Y A A H P Y Q A D Q A A E R L A S

9701 gaaccggcgc tgcctcgcgc aactagcgtg agccgggctc ctgtgtagc aggtgatgat gccaccatg gcgacttggc ccgagttcaa cctggattg
ctggcccgcg agcgcgcggg ttgatccgca tccgcccag gacacctacg tccaacta cgggtggtac gcctgaaccg ggctcaagt ggacctaac
>.....ccOI.....>
173 E N R R S L R Q L G V A G L L W M Q V M M A T M A T W P E F N L D L

9801 tccgagagct tctctgttac cctgcctgg actgcttctg tctgaccac gccaatcctc ttctactcct gcacggactt cttcaaaagg gcctacgcg
agcctctcga agaagcaatg ggacgcgacc tgacggaaca acgactggtg cggttagcag aagatgagga cgtgctgaa gaagtctcc cgctagcgc
>.....ccOI.....>
207 S E S F F V T L R W T A L L L T T P I V F Y S C T D F F K G A L R

9901 atttgcgcac acgcccctg accatggacg tctcgggtgc gctggcgatt ggtggtgctt atgtcgcggc catctggtct acgatcacc gtcagggtga
taaaccgctg tgcggtggac ttgtacctgc acagcccag cgaccgctaa ccaccacgga tacagcggcc gtgaccaga tgcctagtcg cagtcaccat
>.....ccOI.....>
240 D L R T R H L T M D V S V S L A I G G A Y V A G I W S T I T G Q G

```

6. APPENDIX

```

10001 gctgtacttc gatgaggtag gcatgttcgc ccttttcctg ctggccggtc gttatctgga acgaaggcgc cgagagcgta ctggggctgc cacagcgcaa
cgacatgaag ctacgccatc cgtacaagcg ggaaaaggac gaccggcccg caatagacct tgcttcccgc gctctcgcgt gacgccgcag gtgtcgcggtt
>.....ccoI.....>
273 E L Y F D A V G M F A L F L L A G R Y L E R R A R E R T A A A T A Q

10101 ctggteaate tgctcccgc ctctgctcg aagctcgaag cagagggcca cagcaaccgt attctgtca acgagctgca gctagccgac cgcgtgcttg
gaccagttag acgagggcgc gaggacggac ttcgagctgc gtctcccggg gtcggttgca taagacgagt tgctcgcagt cgatcgcttg gccgcagaac
>.....ccoI.....>
307 L V N L L P A S C L K L D A E G H S N R I L L N E L Q L A D R V L

10201 tccagcccgc cggattgatt cctgcagatg cgtcctatc cagcggccaa tccagcgtcg acgagtcagt gcttaccggg gagtacatgc ctttgctctg
aggtcggggc gcctaactaa ggaagctctac cgcagtagta gtcgcccgtt aggtcgcagc tgctcagta cgaatggccc ctcatgtacg gaaacggagc
>.....ccoI.....>
340 V Q P G G L I P A D G V I I S G Q S S V D E S V L T G E Y M P L P

10301 cggcgtcgc gatgcgctca ctgcccgcac actgaacgtg gaaggtccct tgacgcttga agtgcaagcc ctgggtgacg aaactcgtct gtcggccatc
gccgcagccg ctacggcagt gacggcgtg tgacttgca cttccaggga actgcgaact tcacgttccg gaccactgc tttgagcaga cagccggtag
>.....ccoI.....>
373 R G V G D A V T A G T L N V E G P L T L E V Q A L G D E T R L S A I

10401 gtccgctgc tcgagcgcgc gacggcggac aaacaaagc tggccgagct ggctgaccgg gtcgcgcagt ggtttttgct gatagttctg gtgtggcgcg
cagccgcagc agctcgcgcg cgtccgcctg tttgtttctg accgctcga cgcagtggcc cagcgcgtca ccaaaaaaga ctatcaagac caccaccggc
>.....ccoI.....>
407 V R L L E R A Q A D K P K L A E L A D R V A Q W F L L I V L V V A

10501 ctatcgttgg cctggcttgg tggcagatcg accgcacaag cgcattctgg atcgtctctg ccttctgtgt cgcaccctgc cctcgcgcc tgccttggc
gatagaacc ggaccagacc accgtctagc tggcgcttgc gcgtaagacc tagcagacc ggaacgacca gcggtggacg gggacgcggg acaggaaccg
>.....ccoI.....>
440 A I V G L V W W Q I D P Q R A F W I V L A L L V A T C P C A L S L

10601 gaccctacc gcgctcaaga cagcagcagg cacgctgcac aagctcgggc tgttctgac ccgaggacac gtgctggaag gtctcaatca gatgcacacc
ctggggatgg cgcgagtgct gtcgctgtcc gtcgcagctg ttcgagcccc acaacgactg ggctcctgtg cacgacctc cagagttagt ctagctgtgg
>.....ccoI.....>
473 A T P T A L T T A T G T L H K L G L L L T R G H V L E G L N Q I D T

10701 gtatattcgc acaagaccgc caccctgacc gagggtgcac tgacgctcag cgcctgcat ccgctgggcg cgtctgatgc cgatacctgc ctggcgttg
catcataagc tgttctggcc tggggactgc ctcccagctg actgcgagtc gcggcaagta ggcgaccgc gcgagctacg gctatggacg gaccgcgacc
>.....ccoI.....>
507 V V F D K T G T L T E G R L T L S A V H P L G A L D A D T C L A L

10801 cggcagccct cgaaaaccgc tccagcacc cgatcgcgcg tcttttggc cgggcgccac aagctctgga atcggctgag accgttccag cccttgggt
ccgctcggga gcttttggc aggtcctgtg gctagcgcgc acgaaagccg cccgcggctg ttcgacgact tagccagctc tggcaaggtc cggaaaccga
>.....ccoI.....>
540 A A A L E N R S E H P I A R A F G R A P Q A A E S V E T V P G L G

10901 tcatggcagg gtcgacgggc gaaacctgcg aatcgcccaa ccaatttgc ttcgggaggg tttctccaa ccagccccta ccattcccgc cgaacagggg
agtaccgtcc cagctgcgcc cgttggacg ttacggcgtt ggggtaaagc aagcctccc aaagaggggt ggtcggggat ggaagggccc gcttctcccc
>.....ccoI.....>
573 L H G R V D G R N L R I G Q P N F V A E G F S Q P A P T I P G E Q G

11001 cagtgctgtg tgctgggtga cgaacagggc ccgctggcct ggctgtgtct ggaagaccgt cttcgtgacg acgccccgc cctgctgac ccctgtgcc
gtcaccgaca acgaccact gcttgtccc ggcgaccgga ccgaccaga cctgctggca gaagcactgc tgcggggcgc ggaagctg cggacagcgg
>.....ccoI.....>
607 Q W L L L G D E Q G P L A W L V L D D R L R D D A P A L L D A C R

11101 gtcgcgctg gcagacactt ctactgtctg gcgatagctc acccatggtc agccagatcg ccaacgaact gggcatgat caggctgagg gcggtatgac
cagcgcagc cgtctgtgaa gatgacagac cgtatcgag tggtaaccag cgttcttagc ggttcttga cccgtagcta gtcgactcc cgcatactg
>.....ccoI.....>
640 R R G W Q T L L L S G D S S P M V S Q I A N E L G I D Q A E G G M

11201 gcctcggctt aaactatcca gactgcagc cttgcaggct caggggcac cgttctgat gcttgggat ggcctoaacg acgttcccgt gcttccgtg
cggacgcoga tttgataggt ctgaogtccg gaacgtccga gtccccttag cgcaagacta cgaacctota ccgagttgc tgcaagcca cgaacggcac
>.....ccoI.....>
673 T P A A K L S R L Q A L Q A Q G H R V L M L G D G V N D V P V L A V

11301 gccgacatca gctgctgat gggctctgag accgatctcg ccaagaccag tgcagatgca gctgctgtg ccaatcact ggcagctctt gccgagcat
cggctgtagt cacagccta cccgagacg tgcctagagc ggttctgttc acgtctact cagcagaca ggttagctga ccgctcagaa ccgctcctga
>.....ccoI.....>
707 A D I S V A M G S A T D L A K T S A D A V L L S N R L A S L A Q A

11401 tcgatgttc acgcccgcgc cggcgcata tcactgaaaa cctgacttgg gcaagcctgt acaatggcct cattcttccc tttgctgca ttggttgggt
agctacaacg tgcgctgctg gccgctagt agtagctttt ggactgaacc cgttgggaca tgttacggga gtaagaaggg aaacgagcct acccaacca
>.....ccoI.....>
740 F D V A R R S R R I I I E N L T W A S L Y N G L I L P F A A I G W

11501 caocccgctt tggccgcac tgggatgct tatcagctcg ctgctctgtg tattgaatgc gctgcgactg acccggcaac caagcagccg caactgaatg
gtcggcgcaa acccggcgtg agccctacag atagctgagc gacgagacc ataactacg cgacgctgac tggcggttgg gttcgtgccc gttgacttac
>.....ccoI.....>>
773 V T P L W A A L G M S I S S L L V V L N A L R L T R Q P S S R N -

11601 cttcgcgca atgcccgcag ttgtggctcc gctccgttgg cgcattggca cgaacaatg gcagctgaag cttctgtctt cagaccctgg aggtctctgat
gaagcggcgt tacgctgctc aacaccgagg cgaggcaaac gcgtaccggt gctttgttac cgtcacttc gaagaacgaa gttcgggacc tccaggacta
ccoS >>

```

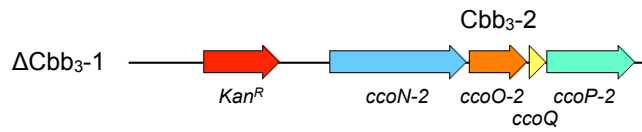
```

11701  ggccgctctg tatactctga ttctctgtgc tgtagtctg gtggccctgg ctatatgggt tttttctgg gcagtgata ggggtcaatt cgatgacctg
      cggcgagac atataggact aaggacagcg acatcacgac caccgggacc gatataccca aaaaaagacc cgtcacctat cgccagttaa gctactggac
      >.....ccoS.....>
      1  M A A L Y I L I P V A V V L V A L A I W V F F W A V D S G Q F D D L

11801  gacggcccgg cacacagcat cotgttogac gacgacgagc cgcagcgccc ggcagaagac aagcaaccgg agaaaattga agagccgag gagcagcgca
      ctgcccggcc gtgtgtogta ggacaagctg ctgctgctcg gcgtcggcgg cegtcttctg ttogttggcc tcttttaact tctcggctc ctgctcgctg
      >.....ccoS.....>
      35  D G P A H S I L F D D D E P Q R P A E D K Q P E K I E E P Q E Q R

11901  aagtgattg agctgttgc cctcctgtg tetgcottcg tgttggcct actcgttggc ggtcattgoc tgggcatgtg tggcggttg atgggcgat
      ttccactaac tcgacaacgg ggaggaccac agacggaagc acaaccggga tgagccaccg ccagtaacgg acccgtacac accgcccgaac taccgcgcta
      >...ccoS...>
      68  K G D -
    
```

J. The Nucleotide sequences of Δ Cbb₃-1



```

1  cgaggcttgt cctgcttgcc agcaggatgg aacggatagc ccaggcagac cagcgcattcc acccctgttt catcggccaa aaggctggcc atcgcgccgc
      gctccgaaca ggacgaacgg tcgtctacc ttgcctatcg ggtccgtctg tgcgctagg tggggacaaa gtacccggtt ttccgaccgg tacgcccggc

101  ccactgactt gccgccaacg gccaaaagcc ctgtggcctg ctgtcgcacc agagcatgga tttcgcgaca ttgcgcaagc agatgcgcct gtgggctggg
      ggtagctgaa cggcggttgc cggttttcgg gacaccggac gacagcgttg tctcgtacct aaagcgtgt aacgcgttcc tctacgcgga cacccgacc

201  cggccgctta cggccttcg tacgacgcgc agccatgtag gagaactcga agcgcacacac cgcataacca cccccgcaa ggcgctcagc catttcttc
      ccgcgcaat gccggaagcg atgctcgcgc tcggtacatc ctcttgagct tcgctgtgtg gcgttatggt gcggggcgct ccgcgagtcg gtaaagcaag

301  atgaacggac tgtccattgg cgcaccgcga ccattggcca ggatcaggct ggcocaggta tcgacctcgc gttggttcca gctgacgaga tgcctttgt
      tacttgcctg acagtaacc cgttggcgct ggtaccggct cctagtccga ccgggtccat agctggacgc caaccaaggt cgactgctct acaggaaca

401  cactttgtgt gtattgatcc gtgtcaatac cggcagattg ccttttcccc atccttgctc cgttttctat tagaaagaaa aaaactgctc attaccctg
      gtgaaacaca cataactagg cacagttagt gccgtcctaac gggaaagggg taggaacgga gcgaaagata atctttcttt tttgacgag taatggggcac

501  gatggaagcc catacatgcc acctgggatg aatgtcagct actggcctat ctggacaagc gaaaacgcaa gcgcaaagag aaagcaggta gcttgacgtg
      ctaccttggg gtatgtaacg tggaccctac ttacagtcca tgaccggata gacctgttcc cttttgcggt ccgctttctc tttcgtccat cgaaegtcac
      ccoN-1 >

601  ggcttcatgt gcgatagcta gactggcgcg ttttatggac agcaagcgaa ccggaattgc cagctggggc gccctctggt aaggttggga agccctgcaa
      ccgaatgtac cgctatcgat ctgaccgcgc aaaatacctg tcgttcgctt ggccttaacg gtcgaccccg cgggagacca ttccaacctc tcgggacggt
      >>.....PKm.....>>

701  agtaaaactg atggctttct tgccgccaag gatctgatgg cgcaggggat caagatctga tcaagagaca ggtatgagat cgtttcgcac gattgaacaa
      tcatttgacc taaccgaaga accgcggttc ctgactacc ggtccoccta gttctagact agttctctgt cctactccta gcaaaagcgt ctaactgtgt
      >>...Km....>

1  M I E Q

801  gatggattgc acgaggttc tcggcccgct tgggtggaga ggctattcgg ctatgactgg gcacaacaga caatcgctg ctctgatgcc gccgtgtcc
      ctacctaac tgcgtccaag aggcggcgga acccaacctc ccgataagcc gatactgacc cgtgtgtgct gttagccgac gagactacgg cggcacaag
      >.....Km.....>
      5  D G L H A G S P A A W V E R L F G Y D W A Q Q T I G C S D A A V F

901  ggctgtcagc gcagggcgcc cgggttcttt ttgtcaagac cgaactgtcc ggtgcctcga atgaactgca ggaagggca gcgcggctat cgtggctggc
      ccgacagctg cgtcccgcgc ggccaagaaa aacagttctg gctggacagc ccacgggact tacttgacgt cctgctccgt ccgcccgata gcaccgacc
      >.....Km.....>
      38  R L S A Q G R P V L F V K T D L S G A L N E L Q D E A A R L S W L

1001  cagcagggc gttccttgcg cagctgtgct cgacgttgc actgaagcgg gaagggactg gotgctattg ggcaagtgc cggggcagga tctcctgtca
      gtgctgccc caaggaacgc gtcgacacga gctgcaacag tgaactcgc cttccctgac cgacgataac ccgcttcacg gccccgtcct agaggacagt
      >.....Km.....>
      71  A T T G V P C A A V L D V V T E A G R D W L L L G E V P G Q D L L S

1101  tctcaacttg ctctgcgca gaaagtatcc atcatggctg atgcaatgca gcgctgcat acgcttgatc cggtaactc cccattogac cacaagcga
      agagtgaac gaggaacgct ctttcatagg tagtaaccgac tacgttaacg ccacgacgta tcgcaactag gccgatggac ggtaagctg gtggttcgct
      >.....Km.....>
      105  S H L A P A E K V S I M A D A M R R L H T L D P A T C P F D H Q A

1201  aacatcgcat cgagcgagca cgtactcggg tggaaagcgg ttttgcgat caggatgac tggaagaa gcatcagggg ctccgcccag ccgaactgtt
      ttgtagccta gctcgtcgt gcatgagcct accttcggcc agaacagcta gtctactag acctcctctc cgtagtcccc gagcgggctc ggcttgaca
      >.....Km.....>
      138  K H R I E R A R T R M E A G L V D Q D D L D E E H Q G L A P A E L
    
```

6. APPENDIX

```

1301 cgccaggctc aaggcgcgca tgcccgaagg cgaggatctc gtctgtaacc atggcgatgc ctgcttcccg aatatcatgg tggaaaatgg cgcgtttct
cgggtccgag ttccgcgcgt acgggctgcc gctcctagag cagcactggg taccgctacg gacgaaccgc ttatagtacc accttttacc ggcaaaaaga
>.....Km.....>
171 F A R L K A R M P D G E D L V V T H G D A C L P N I M V E N G R F S

1401 ggattcatcg actgtggcgc gctgggtgtg ggggaccgct atcaggacat agcgttggct acccgtgata ttgctgaaga gottggggcg gaatgggctg
cctaagtagc tgacacgcgc cgaccacac cgcctggcga tagtctgtga tcgcaaccga tgggcactat aacgacttct cgaaccgcgc cttaccgcgc
>.....Km.....>
205 G F I D C G R L G V A D R Y Q D I A L A T R D I A E E L G G E W A

1501 accgcttctc cgtgctttac ggtatcgccg ctcccgatcc gcagcgcata gccttctatc gccttcttga cgagtctctc tgacggggac tctggggctc
tggcgaagga gcacgaatg ccatagcggc gagggctaag cgtcgcgtag cggagaatag cggagaact gctcaagaag actcgcctcg agaccccaag
>.....Km.....>>
238 D R F L V L Y G I A A P D S Q R I A F Y R L L D E F F -

1601 gaaatgaccg accaagcgcg gcccaacctg ccatcacgag atttcgattc caccgccgcc ttctatgaaa ggttgggctt cgtcgcgcgc ctatgtttac
ctttactggc tggttcgctg cgggttggac ggtatgctc taaagctaag gtggcggcgg aagatacttt ccaaccgcga >>....ccoP-1.....>
1 L A A Y V Y

1701 agcctgtcgc aaaaaccgga acaactcgct aaccagttag ccccaaaagg gcggtacact cgtaccgccc ttctcgcctt gteccacggc aacttccgct
tcggacagcg tttttggcct tgttgagcga ttggtcactc ggggttttcc cgccatgtga gcatggcggg aagacgggaa caggggctcc ttgaagcggc
>.....ccoP-1.....>>
7 S L S Q K P E Q L A N Q -

1801 actctgcgac tatctgtcgc atcgaaact gaccaacgtc ctccccctc cgcgctagca cttctaagct gtgcttccga ttccgcatcc cgcctagaac
tgagacgctg atagacagcg tagcgtttga ctggttcgag gaagggggag gcgcgatcgt gaagattcga cacgaaggct aagcggtagg gcggtacttg

1901 cataaggcgc aatcgtaatt tcctacgca cggcgtggty cgatacctcc ctgcacagca caccgaaaac gctttaaatc agggtttttg ccagcaaaaga
gtattccgcy tttagcattaa aggatgcgty gccgcaccac gctatggagg gacgtgtcgt gtgccttttg cgaattttag tcccaaaaac ggtcgtttct

2001 cagccccggc cgggtttgca ttgccccctc gttttctcca taactgcgcg cgtttttgcc ttcgaaaatg ctattagcgt ggaagccttg catgagcaca
gtcggggccc gcgcaaacgt aacgggggga cgaagaggt atgaacggcg gcaaaaaccg aagcttttac gataatcgca ccttcggaac gtactcgtgt
>>.....ccoN-2 >>.....>
1 M S T

2101 gcaatcagty agactgctta taactataag gtggttcgcc aattcccat catgacggtg gtgtggggaa tcattgggat gggcctgggt gttttcatcg
cgttagtcac tctgacgaat attgatattc caccaagcgg ttaagcggtg gtactgccac cacaccctt agtaacccta ccggcaccga caaaagtagc
>.....ccoN-2.....>
4 A I S E T A Y N Y K V V R Q F A I M T V V W G I I G M G L G V F I

2201 ccgcgcaatt ggtgtggccc tcgctcaatt tggacctgcc gtggacgagc ttccggcctc tgcgccatt gcacaccaat cgggtgatct tcgcttcgg
ggcgcgttaa ccacacggg agcagattaa acctggaagg caoctcctc aagccggcag acgcggttaa cgtgtggtta cgcactaga agcgaagcc
>.....ccoN-2.....>
37 A A Q L V W P S L N L D L P W T S F G R L R P L H T N A V I F A F

2301 tgggtgcgca ctgtttgcca cgtcctacta cgtggttcag cgcacctgcc aggcctctct gttctccgac ggactcgcgc ccttaccctt ctggggtttg
accaacgctg gacaaacggt gcaggatgat gcaccaagtc gcgtggacgg tccgggcaga caagagctg cctgagcgcg ggaagtggaa gacccaacc
>.....ccoN-2.....>
70 G G C A L F A T S Y Y V V Q R T C Q A R L F S D G L A A F T F W G W

2401 caggctgtga tctgtcttgc ggtcatcagc ctccgatgg gctacaccag ctccaaggag tatgcggaac tggagtggcc gattgatate ctgatcccc
tcccgactac agcagcaagc ccagtagtgc gaaggtacc cgtgtggctc gagttctctc atacgccttg acctaccggc ctaactatag gactagtggg
>.....ccoN-2.....>
104 Q A V I V L A V I T L P M G Y T S S K E Y A E L E W P I D I L I T

2501 tggctgggtg gtctgatate gccgtgttct tggcaccat catgaagcgc aaggccaagc acatctatgt aggtaactgg ttcttggtg ccttcatcct
accagacca cagcatatag cggcacaaga agccgtggta gtactcggcg ttccgggtcg ttagatata tccattgacc aagaagcac ggaagttaga
>.....ccoN-2.....>
137 L V W V S Y I A V F F G T I M K R K A K H I Y V G N W F F G A F I

2601 ggtgacggcg atgctgaca tcttaacaa cctggaatc ccggtcagc tgttcaagtc ctactgata taocgagggc ctaccgatgc gatggtgcaa
ccaactgcgc tacgacgtgt agcaattggt ggacctttaa gccagtcgg acaagttcag gatgagctag atgctcgcg gatggtcag ctaccacgtt
>.....ccoN-2.....>
170 L V T A M L H I V N N L E I P V S L F K S Y S I Y A G A T D A M V Q

2701 tgggtgtaag gccacaacgc cgtgggcttc ttctgacca ccggttctct cggcatgatg tactacttgc tgcctaagca ggccgagcgt ccggttact
accacatgc cgggtgttgc gcaccgaag aaggactggt ggccgaagga gcgtaactac atgatgaagc acggattcgt ccggtcgcga ggccacatga
>.....ccoN-2.....>
204 W W Y G H N A V G F F L T T G F L G M M Y Y F V P K Q A E R P V Y

2801 cctatgcctt gtgatcgtc cacttctggg cactgatcac cctctatate tggccggccc cgcaccacct gcactacacc gcctgcgac attggggcga
ggatagcgga cagctagcag gtgaagaccc gtgactagtg ggagatata acccggcggc gcgtggttga cgtgatgtgg cgggacggtc taaccgcgt
>.....ccoN-2.....>
237 S Y R L S I V H F W A L I T L Y I W A G P H H L H Y T A L P D W A

2901 gagcctgggc atggtgatgt cgtatcctc gctggctccg agctggggcg gcatgatcaa cggcatgatg accctcgcgc gtcctggca taagtgcgc
ctcggaccgc taacctata gctagttaga cgaccgagc tcgaccocgc cgtactagt gctgactac tgggacagcc caccgacctg attcgcgcgc
>.....ccoN-2.....>
270 Q S L G M V M S I I L L A P S W G G M I N G M M T L S G A W H K L R

3001 accgatcga tctcgcgctt cctggttggta tctgtgctg tctaccgcat gtcacacttc gaagttcga tgatggcgat caagaccgct aacgcactgt
tggctaggct aggacggaa ggaccacct agcgcaccga agatgcgta cagctggaag ctccaggct actaccgcta gttctggcag ttgctgaca
>.....ccoN-2.....>
304 T D P I L R F L V V S L A F Y G M S T F E G P M M A I K T V N A L

```

6. APPENDIX

```

3101 cccactaac cgactggact atcggccacg tacacgcggg agccctcggg tgggtagcga tgatactat cggctcgatg taccacctga ttccgaaagt
>.....ccoN-2.....>
337 S H Y T D W T I G H V H A G A L G W V A M I T I G S M Y H L I P K

3201 gttcgggcg gagcagatgc acagcgtogg cotgatcaat ggcacttctt ggotggccac catcggcacc gtgctttaca tgcctcgatg gtgggtoaac
caagcccgcg ctgctctaac tgcctcagcc ggactagtta cgcgtgaaga cgcaccgggtg gtacggcgtg caccgaaatg agcggagcta caccagttg
>.....ccoN-2.....>
370 V F G R E Q M H S V G L I N A H F W L A T I G T V L Y I A S M W V N

3301 ggcacacccc aaggcctgat ttggcgcgcg atcaacgaag acggcaccct gacctactcc ttctggaag cgtggaagc cagtcatccc ggcttcatcg
ccgtagtggg ttccggacta caccgcgcgc tagttgcttc tgccgtggga ctggatgagg aagcagcttc gcgaccttcg gtcagtaggg ccgaagtagc
>.....ccoN-2.....>
404 G I T Q G L M W R A I N E D G T L T Y S F V E A L E A S H P G F I

3401 tccgcgcagt cggcggcgcg ttcttctcgc ctggcatgct gttgatggca tacaacacct ggcgcaccgt acgggcccgc aagtacgccc agtacgacac
agggcgcgca gccgcgcgcg aagaaggagc gacctgacga caactaccgt atgtttgga cgcgtggca tgcccggcgg ttcagtcggg tcatgctgtg
>.....ccoN-2.....>
437 V R A V G G A F F L A G M L L M A Y N T W R T V R A A K S A Q Y D

3501 tgccgcgacg atcgttgtag gaacgatag atgaagaacc acgaaatact cgaagaagc attggtctgc tgacctgtt catgatcctg gcagttagca
acggcgcgct tagcgaactc cttgcctatc tactcttggg tgctttatga gctttcttgg taaccagacg actgggaca gtaactaggac cgtcactcgt
>.....ccoN-2.....>
470 T A A Q I A -
>>.....cco0-2.....>
1 M K N H E I L E K N I G L L T L F M I L A V S

3601 tcggcgctc gccaccagatc gtcccgtgtg tcttccagga cgcagtgaac gagccggttg aaggcatgaa gccttacacc gcgctcagc tcgaaggtcg
agcccaccga ctgggtctag caggcgaca agaaagtctc gctcacttg ctccggcaac ttccgtactt cggaatgtgg cgcgacgctc agcttccacc
>.....cco0-2.....>
24 I G G L T Q I V P L F F Q D A V N E P V E G M K P Y T A L Q L E G

3701 ggatctgtac atccgcgag gctcgtgttg ctgccactcg cagatgacc gcccttccg cgtgagacc gagcgtacg gccactactc cgtggccggt
cctagacatg taggcgctcc cgcgcgaacc gacggtgagc gtctacttag cggggaagc gcgactctgg ctccgcatgc cggatgatg gcaccggcca
>.....cco0-2.....>
57 R D L Y I R E G C V G C H S Q M I R P F R A E T E R Y G H Y S V A G

3801 gaaagcgtct acgaccatcc gttcctgttg ggtccaaagc gtaccggacc ggatctggcc cgtgtcggcg gccctactc cgatgactgg caccgtgcgc
ctttccgaga tgctgttagg caaggacacc ccgaggttcc catggcctgg cctagaccgg gcacagccgc cggcgtatg gctactgacc gtggcaccgc
>.....cco0-2.....>
91 E S V Y D H P F L W G S K R T G P D L A R V G G R Y S D D W H R A

3901 acctgtacaa cccgcgaac gtatgtctg agtccaagat gccctctat cgtggtctg tcgagaacac cctcagcgc aaggacactg ccaagaagat
tgacatggtt gggcgcgtg catcaaggac tcagcttcta cgcaggata ggcaccgacc agctctgtg ggagctgcc ttctctgtgac gtttcttcta
>.....cco0-2.....>
124 H L Y N P R N V V P E S K M P S Y P W L V E N T L D G K D T A K K

4001 gtcgctctg cgcattctg cgttccgta caccgaagaa gacatcggc cgcgccgtga tgcctcctg ggcaagacc agatggatgc catggtggcc
cagccgagac gcgtacgaac ccgaaggcat gtgcttctt ctgtagcgc cgcgggcaat acggcagca ccgttctgct tctacctagc gtaccaccgg
>.....cco0-2.....>
157 M S A L R M L G V P Y T E E D I A G A R D A V R G K T E M D A M V A

4101 tacctgcaag tgctcggcac tgcttaaac acaaacggtt aacgatgat ggaatcggg actctctcgc gctggggcac aattctggtg gtcgtcgtc
atggacgttc acgagccgtg acgagattgg ttggttgcca ttgcgtaata cctttagcca tgagaagcgc cggaccctgt taaagccat cagcagcgga
>.....cco0-2.....>
191 Y L Q V L G T A L T N K R -
>>.....ccoQ-2.....>
1 M M E I G T L R G L G T I L V V V A

4201 tcactggcgt agtgccttg gcctacagca gcaaacgcaa gcaagcttc gacgaagcag ccaacctgcc cttccgagac gacgagacc acgccaagaa
agttagccga tcacgagacc cggatgtcgt cgtttgcgtt cgtttcgaag ctgctctgc ggttgagcgg gaagcgtctg ctgctctgac tgcggttctt
>.....ccoQ-2.....>
19 F I G V V L W A Y S S K R K Q S F D E A A N L P F A D D E T D A K

4301 gcgtgaagaa gaagctcca ggagtaagaa ataatgacc tcttttggg gttggtactg caccctcgtg agcctgggca caattgccg gctggtatgg
cgcacttctt ctccaaggt cctcattctt tattactagg agcaaacct caaccatgca gtgggacgac tcggaccctg gtaaacggcg cgaccatacc
>.....ccoQ-2.....>
52 K R E E E A S R S K K -
>>.....ccoP-2.....>
1 M T S F W S W Y V T L L S L G T I A A L V W

4401 ctgctactgg caacgcgcaa gggacaacgc cccgacgca cgaagaaac cgtcgggcat tctatgacg gcctcagga gtaacgacac ccgctaccgc
gacgatgacc gttgcggtt ccctgttgcg gggctgctg gcttctttg gcagccgta aggatactgc cgtagctcct catgctgttg ggcgatggcg
>.....ccoP-2.....>
23 L L L A T R K G Q R P D S T E E T V G H S Y D G I E E Y D N P L P

4501 gctggtggtt catgctgtc ttgggtaccg tgatctttgc tcttgatc ctggtctgt atcccggcct aggcactgg aaggcattc tgcggggtta
cgaccacca gtaacgaaag caaccatgac actagaaagc agaactatg gaccagcaca tagggccgga tccgttgacc ttcccgtaaag acggcccaat
>.....ccoP-2.....>
56 R W W F M L F V G T V I F A L G Y L V L Y P G L G N W K G I L P G

4601 cgaaggtggc tggaccagc tcaaggaatg gcagcgtgag atggacaag ccaatgagca ataccggcc ctgtatgcca agtacctgc catgcccgtg
gcttccaccg acctgggtcc agttccttac cgtcgcactc tactgttcc gtttactcgt tatgcccggc gacatacgtt tcatgagacg gtaccggcat
>.....ccoP-2.....>
89 Y E G G W T Q V K E W Q R E M D K A N E Q Y G P L Y A K Y A A M P V

```



```

4701 gaagagggtg ccaagatgc gaaagccctg aagatgggtg gacgtctgtt cgcacccaac tgctcgtctt gccatggctc tgatgcaaaa ggcgcctatg
ctttccaac ggttccatag cgttcgggac ttctaccacc ctcgacagaa gcgtagggtt acgagccaga cggtaaccgag actacgggtt cgcgggatac
>.....ccoP-2.....>
123 E E V A K D P Q A L K M G G R L F A S N C S V C H G S D A K G A Y

4801 gcttcccga tctgacgc gacgactggc tgtggggcgg cgaagcctgaa accatcaaga ccaccatcct gcaagccgcg caggccgtga tgcctggctg
cgaagggctt agactggctg ctgctgacgc acaccgccgc gctcggactt tggtagttct ggtggttaga cgtgccggcg gtcggcgcact acggaccgac
>.....ccoP-2.....>
156 G F P N L T D D D W L W G G E P E T I K T T I L H G R Q A V M P G

4901 gaaagacgtg atcggcgaag aaggcatccg caacgtagct ggctatgttc gcagcctgtc cggacgtgat accccagagg gtattagcgt cgaattgag
ctttctgcac tagccgcttc ttccgtagge gttgcatcga ccgatacaag cgtcgggacg gcctgcacta tggggtctcc cataatcgca gctgtaactc
>.....ccoP-2.....>
189 W K D V I G E E G I R N V A G Y V R S L S G R D T P E G I S V D I E

5001 cagggtaaaa aaatcttcgc ggccaactgt gtagtctgcc atggaccgga agccaagggc gttacagcca tgggcccgcg gaacctgacc gacaatgtct
gtcccagttt tttagaagcg ccggttgaca catcagacgg tacctggcct cggttcccgc caatgctcgt accccggcgg cttggactgg ctgttacaga
>.....ccoP-2.....>
223 Q G Q K I F A A N C V V C H G P E A K G V T A M G A P N L T D N V

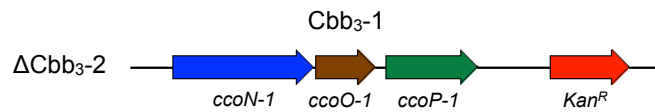
5101 ggctgtatgg ttcgagcttc gtcagatcc agcaaacct cgcgtacggt cgcgaatgcc gcattgcctgc tcaggaagcg atccttgcta atgacaaggt
cgcacatacc aagctcgaag cgagtctaag tctttggga cgcgatgcca gcgttacccg cgtacggacg agtccttcgc taggaacctt tactgttcca
>.....ccoP-2.....>
256 W L Y G S S F A Q I Q Q T L R Y G R N G R M P A Q E A I L G N D K

5201 tcactgctg cggccttacg tctacagcct gtcgcagcaa ccggagcagt gattgctcga ggtcgggggt gacgtcctgt cgcaccgccg ctcaaaactc
agtggagcac cgcgggatgc agatgtcga cagcgtcgtt ggcctcgtca ctaacgagct ccagccccca ctgcaggaca gcgtgggctg gagttttgag
>.....ccoP-2.....>
289 V H L L A A Y V Y S L S Q Q P E Q -

5301 cggcgttacc attcgcagct ggacagaaaa ttgatcctgg ttggcagcta tcggccgggg caccacctt ccgcccgtgt acgactcga tgact
gcccgcattg taagcgtcga cctgtctttt aactaggacc aacctgcat agcccggccc gtgggtggaa ggccgcacca tgcgtgagct actga

```

K. The Nucleotide sequences of Δ Cbb₃-2



```

1 cgaggtctgt cctgcttgc agcaggatgg aacggatagc ccaggcagac cagcgcctcc acccctgttt catcggccaa aaggttgccc atcggccgcg
gctccgaaca ggacgaacgg tctctctacc ttgctatcgg ggtccgtctg gtcgcgttagg tggggacaaa gtacggcgtt ttccgaccgg tacgccggcg

101 ccactgcact gcgcaccaag gccaaaagcc ctgtggcctg ctgtcgcacc agagcatgga tttcgcgaca ttgcgcaagc agatgcgcct gttgggtggg
ggtagctgaa cggcggttgc cggttttcgg gacaccggac gacagcgtgg tctcgtacct aaagcgtgtg aacgcgttcc tctacgggga caccgaccc

201 cggccgttta cggccttccg tacgacgcgc agccatgtag gagaactcga agcgaacac cgaataacca gcgcccgcaa ggcgcctcag catttcgttc
gcccgcgaat gccggaaggc atgctgcgcg tcggtaacatc ctcttgagct tcgctgtgtg gcgttatggt gcggggcgtt ccgagatgct gtaaaagcaag

301 atgaacggac tgtccattgg cgcaccgccg ccatgggcca ggatcaggct ggcccaghta tcgacctgcg gttggttcca gotgacgaga tgtcctttgt
tacttgctg acaggaatac gcgtgggctg gttaccgggt cctagtcoga ccgggtccat agctggacgc caaccaaggt cgactgctct acaggaaaaa

401 cactttgtgt gtattgatcc gtgtcaatac cggcagattg ccctttcccc atccttgctc cgttttctat tagaaagaaa aaaactgctc attaccgtg
gtgaaacaca cataactagg cacagttatg gccgtctaac gggaaagggg taggaacgga gcgaaagata atctttcttt tttgacagc taatgggac

501 gatggaagcc catacatgaa cacagcaacc agtaccgcct acagttacaa ggtggtcgcg caattcgcga tcatgacggt ggtgtgggga atcgtcggga
ctacctcgg gtatgtaact gtgtcgttgg tcatggcgga tgtcaatggt ccaccagcgc gttaaagcgt agtactgcca ccacaccctt tagcagccct
>>.....ccoN-1.....>
1 M N T A T S T A Y S Y K V V R Q F A I M T V V W G I V G

601 tggggtcgg cgttttccat gcagcacaat tggcctggcc atttctgaac ttcgacctcc cgtggaccag tttcgttoga ctactgcat tgcacaccaa
accocagacc gcaaaagtag cgtcgtgtta accgagccgg taaagacttg aagctggagg gcacctggtc aaagccagct gatgcaghta acgtgtggtt
>.....ccoN-1.....>
29 M G L G V F I A A Q L A W P F L N F D L P W T S F G R L R P L H T

701 cgcggtgatt ttcgccttgg gcggctgtgc actgttgcga acgtctact actcgggtca gcgcacctgc cagaccacc cgttgcgcc gaagctggcc
cgcaccaata aagcggaaac cgcgcacacg tgacaagcgt tgcagatga tgcgcaagt cgcgtggacg gttcgtgggg acaagcggcg cttcagaccg
>.....ccoN-1.....>
62 N A V I F A F G G C A L F A T S Y Y S V Q R T C Q T T L F A P K L A

801 gcgttacct tctggggttg gcagttggtc atcctgctcg ccgcaatc cctgccgctg ggtttacca gtcaccaaga gtatcgggaa ctggagtgcc
gcgaagtgga agaccacca cgtcaaccag taggacgagc ggcgttatg ggacggcgac ccaagtggt cgaggttctc catacgcctt gacctcaccg
>.....ccoN-1.....>
96 A F T F W G W Q L V I L L A A I S L P L G F T S S K E Y A E L E W

```

6. APPENDIX

```

901 cgatcgacat cctgatacacc atcgtctggg tggcctatgc ggtgcttctt ttccgggaacg tggetaagcg caaggtcaag cacatctacg tcggtaactg
gctagctgta ggactagtgg tagcagacc accggatacg ccagcagaaa aagccctgcg accgattcgc gttccagctc gtgtagatgc agccattgac
>.....ccON-1.....>
129 P I D I L I T I V W V A Y A V V F F G T L A K R K V K H I Y V G N

1001 gttcttcggg gcttcatcc tgaccgtggc gatcctgcat gtcgtcaaca acctggaat cccggttacc gcgatgaagt cctattcgct gtatgcoggt
caagaagcca cggaagttag actggcaccg ctaggacgta cagcagttgt tggacctta gggccaatgg cgtacttca ggataagcga catacggcca
>.....ccON-1.....>
162 W F F G A F I L T V A I L H V V N N L E I P V T A M K S Y S L Y A G

1101 ggcaccgatg cgtatgggca atggtggtac ggccacaacg ccgtgggctt ctctctcacc gccggcttcc tgggatcat gtaactcttc gtgcctaagc
cgctggctac gctaccacgt taccaccatg ccggtgttgc ggcaccggaa gaaggtgtgg cggccaaggg agccctagta catgatgaag cacggattcg
>.....ccON-1.....>
196 A T D A M V Q W W Y G H N A V G F F L T A G F L G I M Y Y F V P K

1201 aggcggagcg cccggtgat tcgtatcgcc tgcgtatcgt tcacttctgg gcactgatca ccgtctacat ctgggcccgc ccgaccacc tcgaactaac
tccggctcgc gggccacata agcatagcgg acagctagca agtgaagacc cgtgactagt ggcagatgta gaccggccg ggcgtggtgg acgtgatgtg
>.....ccON-1.....>
229 Q A E R P V Y S Y R L S I V H F W A L I T V Y I W A G P H H L H Y

1301 cgcgctgcca gattgggca acagcctggg catggtgatg tgcgtatcgc tgcgtgctcc gagctggggc ggcagatgta accgcatgat gacgctgctg
gcgagcaggt ctaaccctgt tctcggaccg gtaccactac agcgactaag acgaccggag ctcgaccgcc ccgtactagt tgcctgacta ctgcgacagc
>.....ccON-1.....>
262 T A L P D W A Q S L G M V M S L I L L A P S W G G M I N G M M T L S

1401 ggtgctcggc aaaaactgcg tagcagcccg atcctgcgct tctgtggtgt ttctgctggc ttctacggca tgcgtacctt cgaaggtccg atgatggcga
ccagggcagc tgtttgacgc atcgtctggc taggacgcga aggaccacca aagcagccgc aagatggcct accagctgga gcttccagcg tactaccctg
>.....ccON-1.....>
296 G A W H K L R S D P I L R F L V V S L A F Y G M S T F E G P M M A

1501 tcaagaccgt caagcctctg tcccactaca ccgactggac catcgccac gtacacgctg gcgcccctgg ctgggttga atggtctcca tcggcgctg
agtcttgcca gttcggggac aggtgatgtg gctgacctg gtacccgggt catgtgctgc gcggggagcc gaccacaagt taccagaggt agcccgccga
>.....ccON-1.....>
329 I K T V N A L S H Y T D W T I G H V H A G A L G W V A M V S I G A

1601 gtatccctg gtcocgaaag tgttcggcgc ccagcagatg cacagtagt gctgatcaa caccoacttc tggctagcca ccactcggac cgtgctctac
catagtggac cagggcttcc acaagccgcg gctcgtctac gtgctcatcg cacactagt gtgggtgaag accgatcggg ggtagccctg gcacgagatg
>.....ccON-1.....>
362 L Y H L V P K V F G R E Q M H S I G L I N T H F W L A T I G T V L Y

1701 atcgtctga tgtgggcaa cggtatcgcg caggccctga tgtggcgtgc aatcaacgac gacggcagc tgacctatc ctctcgtcaa tcgctggaa
tagcgaagct acaccagtt gccatagcgc gtcocggact acaccgacg ttagtgtctg ctgcccgtgc actggataag gaagcagctt agcgaccctc
>.....ccON-1.....>
396 I A S M W V N G I A Q G L M W R A I N D D G T L T Y S F V E S L E

1801 ccagccacc cggcttctga gtgcgaatga tcgggtgctg gatctcttc gccggcatgc tgggtgatgg ctacaacacc tggcgcaccg tgcaggctgc
ggtcgggtgg gccgaagcat cacgcttact agccaccacg ctagaagaag ccgcccgtac accactaccg gatgttggg accgctggc acgtccgacg
>.....ccON-1.....>
429 A S H P G F V V R M I G G A I F F A G M L V M A Y N T W R T V Q A

1901 caagccccc gagtacgacg ctgcccgcga gatccctga ggagcctagg taaatgaaat ccgacgagaa actagaaaag aacgtaggtc tgttgacct
gttcggggcg ctcagctgct gacggcgcgt ctacgggact cctcggatcc attacttcta gctgctctt tgatcttctc ttgctaccag acaactggga
>.....ccON-1.....>
462 A K P A E Y D A A A Q I A -
1 >>.....ccO-1.....>
M K S H E K L E K N V G L L T

2001 gttcatgat ctggcggtaa gcactcggcg tctgaccag atcgtcccgc tgttcttcca ggaactccgc aacgagccg ttgaaggcat gaagccttac
caagctactg gaccgccatt cgtagccgcg agactgggct tagcagggcg acaagaaggt cctgaggcag ttgctcggcc aacttccgta ctctggaatg
>.....ccO-1.....>
16 L F M I L A V S I G G L T Q I V P L F F Q D S V N E P V E G M K P Y

2101 accgctgctg agctcgaagg ccgggacctg tacatccgcg agggctcgtg tggctgccac tcgcagatga tccgccctt ccgctgctg accgagcct
tggcgcagc tcgagcttcc ggccttggac atgtaggcgc tcccagcga accgagcgtg agctctact aggcggggaa ggcgcgactc tggctcgcga
>.....ccO-1.....>
50 T A L Q L E G R D L Y I R E G C V G C H S Q M I R P F R A E T E R

2201 accgccaact ctccgtggcc ggtgaaagcg tctacgacca tccgttctg tggggtcca agcgtaccg accgatctg gccctgtctg gcggccgta
tgccgggtgat gaggcaccg ccaacttctc agatgctggt aggcaaggac accccgaggt tcgcatggcc tggcctagac cgggcacagc gcggcgcat
>.....ccO-1.....>
83 Y G H Y S V A G E S V Y D H P F L W G S K R T G P D L A R V G G R

2301 ctccgatgac tggcaccgtg ccgacctgta caaccgcgc aacgtagttc ctgagtcgaa gatccctcc tatccgtggc tggctogaaa caccctgac
gaggctactg accgtggcac gcgtgacat atgtggcgcg ttgcatcaag gactcagctt ctacggcagg ataggcaccg accagctctt gtgggagctg
>.....ccO-1.....>
116 Y S D D W H R A H L Y N P R N V V P E S K M P S Y P W L V E N T L D

2401 ggcaaggaca ctgcaagaa gatgtggct ctgcgatgc ttggcgttcc ttacaaccgaa gaggacatcg ccggcctcg ggaactccgc aacgcaaaa
ccgttctctg gacggtctt ctacagccga gacggtacg aaccgaaag aatgtggtt ctctgtagc ggccggcagc cctgaggcag ttgcgtttt
>.....ccO-1.....>
150 G K D T A K K M S A L R M L G V P Y T E E D I A G A R D S V N G K
2501 ccgagatgga tgcgatggtg gcttacctgc aggtactcgg cacagctctg accaataagc gotgatctg actgaccaag aaaaaatgac ccgctggcaa
ggctctacct acgctaccac cgaatggacg tccatgacg gtgctgagac tggttattcg cgaactcaga tgaactggtc tttttactg gccgaccgtt
>.....ccO-1.....>
183 T E M D A M V A Y L Q V L G T A L T N K R -

```

6. APPENDIX

```

2601 atcagccgtc agggacttca atcgcggaca gccagagttg ctcgggctgt coaggagtag cacatgagca cttttcggag tggataacac gccctgctga
tagtcggcag tccctgaagt tagcgcctgt cggctcaca gagcccgaca ggtcctcacc >>.....ccoP-1.....>
1 M S T F W S G Y I A L L

2701 cgctgggca ccatcgtcgt ctgtttcgtg tgatcttcgc caccgcgaag ggcgaatccg ccggcactac ggatcaaacg atgggacatg ccttcgatgg
gcgaccctgt gtagcagcga gacaagacca actagaagcg gtggcgcttc ccgcttaggc ggccgtgatg cctagtttgc taccctgtac ggaagctacc
>.....ccoP-1.....>
13 T L G T I V A L F W L I F A T R K G E S A G T T D Q T M G H A F D

2801 ccatcaggaa tacgacaacc cgtcgcgcg ctggtggttc ctgctcttca ttggcaacct ggtgttcggc atcctgtact tgggtcctca ccccgccgtg
gtagctcctt atgctgttgg gcgacggcgc gaccaccaag gacgagaagt aaccgtggga ccacaagccg taggacatga accacagatg ggggccggac
>.....ccoP-1.....>
46 G I E E Y D N P L P R W W F L L F I G T L V F G I L Y L V L Y P G L

2901 ggtaactgga agggcgttct gccaggtacc gaggggtggt ggactcaaga gaagcagtgg gaacgcgaag ttgctcagcg cgtagaaaag tacggtccga
ccattgacct tccgcgaaga cggctcagatg ctcccaccga cctgagttct cctcgtcacc cttgcgcttc aacgagtcgc gctacttttc atgcccaggt
>.....ccoP-1.....>
80 G N W K G V L P G Y E G G W T Q E K Q W E R E V A Q A D E K Y G P

3001 ttttcgcaa gtacgtcgc atgctagtg aagaagtggc acaggaccgc caagccgtga aaatggggcg tcgctgttc gccaaactact gctccatctg
aaaagcgggt catgcagcgg tacagtcacc ttcttcaccg tgcctcgggc gttcggcact tttaccgcg acgcgacaag cggttgatga cgaggtagac
>.....ccoP-1.....>
113 I F A K Y A A M S V E E V A Q D P Q A V K M G A R L F A N Y C S I

3101 ccacggttcc gatgccaaag gttcgtcagg ttcccgcaac ctcgcgcacc aagactggcg ctgggggtgt gatgccgctt cgtacaaaac cagcatctc
ggcgccaag ctacggttcc caagcagacc aaaggccttg gagcggcttg ttctgaccgc gaccccacca ctacgcgcaa gctagttttg gtcgtaggag
>.....ccoP-1.....>
146 C H G S D A K G S L G F P N L A D Q D W R W G G D A A S I K T S I L

3201 aacggacgta tcgcagcaat gccgcctcgg ggccaagcca tcgcgcaaga agcgtgaag aacgtcgcag cgttcgtccg caaggacctc gcgggcttgc
ttgctcgtat agcgtcgtta cggccggacc ccggttcggt agccgcttct tccgcacttc ttgcagcgtc gcaagcagcg gttcctggag cgcggcaag
>.....ccoP-1.....>
180 N G R I A A M P A W G Q A I G E E G V K N V A A F V R K D L A G L

3301 cgctcgcgga aggcacgat gccgaacctc gcgcaggcaa gaacgtctac gcacagacct gcgcgctctg ccaaggtcag ggtggcgaag gtatggccgc
gcgaccgctt tccgtggcta cggctggagt cgcgtccggt cttgcagatg cgtgctcgtga cgcggcagac ggtgccagtc ccaccgcttc cataccggcg
>.....ccoP-1.....>
213 P L P E G T D A D L S A G K N V Y A Q T C A V C H G Q G G E G M A

3401 gctgggtgcg cctaagctca acagcgcgc cggctggatc tatggtctga cctcgggcca actgcaacag accattcgc atggtgcaa tggccagatg
cgaccacgc ggattcagat tgcgcggcgg gccgacctag ataccagctt cggagccggt tgacgttctg ttgtaagcgg taccagcgtt accggtctac
>.....ccoP-1.....>
246 A L G A P K L N S A A G W I Y G S S L G Q L Q Q T I R H G R N G Q M

3501 cctcctcagc agcaatatct gggcgacgac aaggttcacc tgcctcgcgc ctatgtttac agcctgtcgc aaaaaccgga acaactcgtt aaccagtgag
gacagagtcg tcgttataga cccgctcgtg ttccaagtgg acgagcggcg gatacaaatg tcggacagcg tttttggcct tgttgagcga ttgctcactc
>.....ccoP-1.....>
280 P A Q Q Q Y L G D D K V H L L A A Y V Y S L S Q K P E Q L A N Q -

3601 ccccaaaag gcggtacact cgtaccgcgc ttctcgcctt gtcccagcg aacttcgcct actctgcgac tatctgtcgc atcgcaaac gaccaacgct
ggggttttcc gcctatgta gcatggcggg aagagcggaa cagggttcgg ttgaaggcga tgagacgctg atagacagcg tagcgtttga ctggttgca

3701 cttccccctc cgcgctagca cttctaagct gtgcttcgga ttcgccatcc cgcctagaac cataaggcgc aatcgttaatt tcctacgca cggcgtggtg
gaagggggag gcgcgctcgt gaagattcga cacgaaggct aagcgttagg gcgcatcttg gtattccgcg ttacgattaa aggatcgtg gcgcgaccac

3801 cgatacctcc ctgcacagca caggaaaac gtttaaatc agggtttttg ccagcaaaag cagcccgggc gcggtttgca ttgccccctt gttttctcca
gctatggagg gacgtgtcgt gtgccttttg cgaatttag tcccaaaacc ggtcgtttct gtcgggcccc gcgcaaacgt aacgggggga cgaagaggt

3901 tacttgccgc cgtttttgcc ttgaaaatg ctattagcgt ggaagccttg catgagcaca gcaatcagtg agactcgtta taactataag gtggttcgcc
atgaacggcg gcaaaaacgg aagcttttac gataatgcga ccttcggaac gtactcgtgt cgttagtca cttgacgaat attgatattc caccagcggc
>>.....ccoN-2.....>
1 M S T A I S E T A Y N Y K V V R

4001 aattcgcct catgacgggt gtgtgggaa tcaatgggat gggcctgtgc caactgggat gaatgtcagc tactgggcta tctggacaag gaaaaacgca
ttaagcggta gtactgccac cacaccctt agtaacctca cccggacagc gtggacccta cttacagtcg atgaccgatg agacctgttc cttttgctg
>.....ccoN-2.....>
17 Q F A I M T V V W G I I G M G L

4101 agcgcacaag gaaagcaggt agcttcagct gggcttacat ggcgatagct agactggcg gttttatgga cagcaagcga accggaattg ccagctgggg
tcgcgtttct ctttctgcca tcgaacgcca cccgaagtga ccgctatcga tctgaccgcg caaaaacct gtcgttcgct tggcctaac ggtgcacccc
>>.....PKm.....>

4201 gcctcctcgt taaggttggg aagcctgca aagtaaacgt gatgcttctc ttgcccga ggatctgatg gcgagggga tcaagatctg atcaagagac
gcgggagacc attccaacc ttccggagct tcatattgac ctaccgaaag aacggcggtt ctagactac cgcgtccctc agttctagac tagttctctg
>.....PKm.....>

4301 aggatgagga tcgtttogca tgattgaaca agatggattg caagcaggtt ctcgcgcgc ttgggtggag aggtattcgt gctatgactg ggcacaacag
tctactcct agcaaacgt actaacctgt tctacctaac gtgcgtccaa gaggcggcg aaccacctc tccgataagc cgatactgac ccgtgttctc
>>.....Km.....>
1 M I E Q D G L H A G S P A A W V E R L F G Y D W A Q Q

4401 acaatcggct gctctgatc cgcctgttc cggctcag cgcagggcg ccggttctt ttgtcaaga ccgacctgct cgggtccctg aatgaactgc
tgtagccga cgagactac gcggcacaag gccgacagtc cgtccccgc gggccaagaa aaacagttct ggctggacag gccacgggac ttacttgac
>.....Km.....>
28 T I G C S D A A V F R L S A Q G R P V L F V K T D L S G A L N E L

```

6. APPENDIX

```

4501 aggcagaggc agcgcggcta tcgtggctgg coacgacggg cgttccttgc gcagetgtgc tcgacgttgc cactgaagcg ggaagggact ggctgctatt
    tccgtctccg tcgcgcgat agcaccggacc ggtgtgtccc gcaaggaacg cgtcgcacag agctgcaaca gtgacttcgc ccttccctga cgcagataa
    >.....Km.....>
61 Q D E A A R L S W L A T T G V P C A A V L D V V T E A G R D W L L

4601 gggcgaagtg cggggcagc atctcctgtc atctcacctt gctcctgccc agaaagtatc catcatggct gatgcaatgc ggcggctgca tacgcttgat
    cccgtttcac ggccccgtcc tagaggacag tagagtgtaa cgaggacggc tctttcatag gtagtaccga ctacgttacg ccgcccagct atgcgaacta
    >.....Km.....>
94 L G E V P G Q D L L S S H L A P A E K V S I M A D A M R R L H T L D

4701 cgggtacct gccattcga ccaccaagcg aaacatcgca tcgagcgagc acgtactcgg atggaagccc gtcttgcga tcaggatgat ctggacgaag
    ggccgatgga cgggtaagct ggtgttctgc tttgtagcgt agctcgcctc tgcctgagcc taccttccgc cagaacagct agtcctacta gacctgtctc
    >.....Km.....>
128 P A T C P F D H Q A K H R I E R A R T R M E A G L V D Q D D L D E

4801 agcatcaggg gctcgcgca gccgaactgt tcgccagct caagcgcgcc atgcccagc ggcaggatct cgtcgtgacc catggcgatg cctgcttccc
    tcgtagtccc cgagcgggt cggcttgaca agcggtcgca gttccgcccg tacgggctgc cgtcctctaga gcagcactg gtaccgctac ggacgaacgg
    >.....Km.....>
161 E H Q G L A P A E L F A R L K A R M P D G E D L V V T H G D A C L

4901 gaatatcatg gtgaaaaatg gcccttttcc tggattcacc gactgtggcc ggctgggtgt ggcgagccc tatcaggaca tagcgttggc tacccgtgat
    cttatagtac caccttttac cggcgaaaag acctaagtag ctgacaccgg ccgaccaca ccgctggcg atagctcctgt atcgcaaccg atgggcaacta
    >.....Km.....>
194 P N I M V E N G R F S G F I D C G R L G V A D R Y Q D I A L A T R D

5001 attgctgaag agcttggcgg cgaatgggct gaccgcttcc tcgtgttcta cggtatcgcc gctcccatt cgcagcgcac cgccttctat cgccttcttg
    taagacttc tcgaaccgcc gcttaccgca ctggcgaagg agcacgaat gccatagcgg cgagggttaa gcgtcgcgta gcggaagata gcggaagaa
    >.....Km.....>
228 I A E E L G G E W A D R F L V L Y G I A A P D S Q R I A F Y R L L

5101 acgagtcttt ctgagcggga ctctggggtt cgaatgacc gaccaagcga gcgccaacct gccatcagca gatttcgatt ccaccggcg cttctatgaa
    tgctcaagaa gactcgcct gagaccocaa gctttactgg ctggttcgct cggggttggc cggtagtgc cttaaagctaa ggtgcgcgcg gaagatactt
    >.....Km.....>
261 D E F F -

5201 aggttgggct tcgtgatgcc tggctggaaa gacgtgatcg gcgaagaagg catccgcaac gtatgtggct atgttcgag cctgtccgga cgtgataccc
    tccaaccgca agcactacgg accgaccttt ctgcactagc cgtcttctcc gtaggcgttg catcgaccga tacaagcgtc ggacaggcct gcaactatgg
    >>.....ccoP-2.....>
1 - C L A G K T - S A K K A S A T - L A M F A A C P D V I P

5301 cagagggat tagcgtgac attgagcagg gtcaaaaaat cttcgcggcc aactgtgtag totgcoatgg accggaagcc aaggcgctta cagccatggg
    gttcccata atcgacgtg taactcgtcc cagtitttta gaagcgcgg ttgacacatc agacggtacc tggcctcgg tcccgcgat gtcggtacc
    >.....ccoP-2.....>
30 Q R V L A S T L S R V K K S S R P T V - S A M D R K P R A L Q P W

5401 cgcgcgcaac ctgaccgaca atgtctggct gtaggttgc agcttcgctc agatcagca aaccctgcgc tacggtcga atggccgat gctcgtcag
    gcgcggttg gactggctgt tacagaccga cataccaagc tcgaagcgag tctaagtcgt ttgggacgcg atgccagcgt taaccgctga cggacgagtc
    >.....ccoP-2.....>
63 A R R T - P T M S G C M V R A S L R F S K P C A T V A M A A C L L

5501 gaagcgatcc ttgtaataga caaggttacc ctgctggcgg cctacgtcta cagcctgtcg cagcaaccgg agcagtgatt gctcagagtc gggggtgacg
    cttcgttagg aaccattact gttccaagtg gacgaccgcc ggatgcagat ctgagacagc gtcgttggcc tcgtactaa cgagctccag cccccactgc
    >.....ccoP-2.....>
96 R K R S L V M T R F T C W R P T S T A C R S N R S S

5601 tcctgtcga ccgacctca aaactcggg cgtaccattc gcagctggac agaaaattga tcctggttgg cagtatcgg ccggggcacc caccttccgc
    aggacagct gggctggagt tttgaggccc gcatggtaag cgtcgacctg tcttttaact aggaccaacc gtgcatagcc ggccccgtgg gtggaagggc

5701 cgtggtacgc actcgatgac t
    gcaccatgcy tgactactg a

```